PhD Thesis

Analysis of Power Distribution Systems Using a Multicore Environment

Luis Gerardo Guerra Sánchez

Barcelona, March 2016

Analysis of Power Distribution Systems Using a Multicore Environment

Luis Gerardo Guerra Sánchez

Dissertation submitted to the Doctorate Office
of the Universitat Politècnica de Catalunya in
partial fulfillment of the requirements for the
degree of Doctor of Philosophy by the

UNIVERSIDAD DE MALAGA
UNIVERSIDAD DE SEVILLA
UNIVERSIDAD DEL PAÍS VASCO/EUSKAL ERRIKO UNIBERTSITATEA
UNIVERSITAT POLITÈCNICA DE CATALUNYA

Joint Doctoral Programme in
Electric Energy Systems

Barcelona, March 2016

Analysis of Power Distribution Systems Using a Multicore Environment

Printed by the UPC
Barcelona, March 2016

ISBN: --
Research Project: --

UNIVERSITAT POLITÈCNICA DE CATALUNYA
Escola de Doctorat
Edifici Vertex. Pl. Eusebi Güell, 6
08034 Barcelona
Web: http://www.upc.edu

UNIVERSIDAD DE MALAGA
Escuela de Doctorado
Pabellón de Gobierno - Plaza el Ejido s/n
(29013) Málaga.
Web: http://www.uma.es

UNIVERSIDAD DE SEVILLA
Escuela Internacional de Doctorado
Pabellón de México - Paseo de las Delicias, s/n
41013 Sevilla
Web: http://www.us.es

UNIVERSIDAD DEL PAÍS VASCO/EUSKAL ERRIKO UNIBERTSITATEA
Escuela de Master y Doctorado
Edificio Aulario II - Barrio Sarriena, s/n
48940- Leioa (Bizkaia) Spain.
Web: http://www.ehu.eus/es

Acknowledgments

I have never been a good writer; I always related more to numbers and equations than I ever did to words, which is probably why I became an engineer. However, as I finish this chapter of my life, I would like to take a moment to express my appreciation and gratitude towards everyone who has helped or supported me in any way during this time.

I have always seen myself as a man of faith and this faith has been one of the main driving forces in my adult life. The comfort and solace I find in God has given me the strength to pursue my goals and the peace of mind to overcome difficult times; His love makes everything possible.

The completion of this Thesis has required an enormous amount of work and effort from my part; however none of it would have been possible without the support and guidance from Professor Juan Antonio Martínez Velasco. It has been a real pleasure and honor to work with someone so dedicated and committed to his work. I am truly grateful to him for giving me the opportunity to pursue this path and prove myself.

I would also like to thank those whose help has directly contributed to the development of my work, Víctor Fuses, Gabriel Verdejo, and everybody at RDLab. Víctor's help was invaluable during the early stages when we were trying to acquire our own computer cluster and RDLab provided the much needed technical support to set it up. Their hard work is one of the reasons behind this Thesis' success.

I cannot see myself being here without my family; I have been blessed with the unconditional love and support of my parents, Mauricio and Betty. They have always encouraged me to be the best person I can be and to look for new horizons; words fail me to express the gratitude and love I feel for them. Many people go through their lives without really getting to know their siblings, to them they are just strangers who live in the same house; to me Carlos is not only my brother, he is my best friend and I am really thankful for having him in my life. Of course I cannot forget my sister-in-law Samantha, who soon will bless us with the greatest gift of all, my soon-to-be-born nephew Carlos Fernando.

For a long time my life revolved primarily around my work and I couldn't help feeling that something was missing; that emptiness was filled when a very special person entered my life, my girlfriend Canan. Her love has been a constant source of inspiration and I can only hope to be there for her as she has been there for me; the uncertainties of the future do not scare me if she is with me.

No man's life is complete without friends; as a kid I grew up surrounded by a small group of friends and along the way I was lucky enough to be able to keep them and meet new persons whom now I am proud to call my friends. The following names are meant to be a small recognition to the persons I consider true friends and whose support has helped me get where I am now: Javier Corea, Víctor Renderos, Carlos Quintanilla, Luis Márquez, Verónica Quintanilla, Isabel Duarte, Gloria Hernández, Wendy Flamenco, Víctor Romero, José Segovia, José Quintanilla, Yuri Linares, Rodrigo

Torres, Javier Portillo, Violeta Pastore, Javier Saade, René González, Walter Leiva, Laura Di Raimondo, Alejandra García, Jorge Acevedo, Alberto Canales, and Manolo López.

Finally, as I embark myself on a new adventure, I cannot help but to feel excited about what is to come; for I know this is not the beginning of the end but the end of the beginning.

¡Gracias, totales!

“It’s a magical world,
Hobbes, ol’ buddy,
Let’s go exploring!”
Bill Watterson

List of Publications

Journal Publications:

J.A. Martinez and **G. Guerra**, "A Parallel Monte Carlo method for optimum allocation of distributed generation," *IEEE Trans. on Power Systems*, vol. 29, no. 6, pp. 2926-2933, November 2014.

J.A. Martinez and **G. Guerra**, "A Parallel Monte Carlo approach for distribution reliability assessment", *IET Gener., Transm. Distrib.*, vol. 8, no. 11, pp. 1810-1819, November 2014.

J.A. Martinez-Velasco and **G. Guerra**, "Analysis of large distribution networks with distributed energy resources", *Ingeniare*, vol. 23, no. 4, pp. 594-608, October 2015.

G. Guerra and J.A. Martinez, "Optimum allocation of distributed generation in multi-feeder systems using long term evaluation and assuming voltage-dependent loads," *Sustainable Energy, Grids and Networks*, vol. 5, pp. 13-26, March 2016.

J.A. Martinez and **G. Guerra**, "Reliability Assessment of Distribution Systems with Distributed Generation Using a Power Flow Simulator and a Parallel Monte Carlo Approach," Submitted for publication in *Sustainable Energy, Grids and Networks*.

Conference Publications:

J.A. Martinez and **G. Guerra**, "Optimum placement of distributed generation in three-phase distribution systems with time varying load using a Monte Carlo approach," *IEEE PES General Meeting*, San Diego, July 2012.

J.A. Martinez and **G. Guerra**, "A Monte Carlo approach for distribution reliability assessment considering time varying loads and system reconfiguration," *IEEE PES General Meeting*, Vancouver, July 2013.

G. Guerra and J.A. Martinez, "A Monte Carlo method for optimum placement of photovoltaic generation using a multicore computing environment," *IEEE PES General Meeting*, National Harbor, USA, July 2014.

G. Guerra, J.A. Corea-Araujo, J.A. Martinez, and F. Gonzalez-Molina, "Generation of bifurcation diagrams for ferroresonance characterization using parallel computing," *EEUG Conf.*, Grenoble (France), September 2015.

Book Chapters:

J.A. Martinez-Velasco and **G. Guerra**, "Allocation of Distributed Generation for Maximum Reduction of Energy Losses in Distribution Systems," Chapter 12 of *Energy Management of Distributed Generation Systems*, InTech, In editing process.

Table of Contents

List of Tables

List of Figures

Chapter 1

Introduction

1.1. Problem Formulation

Currently it is widely accepted that the construction of large generation centers is no longer the best option to supply the increment of electric load. High costs related to the construction of new generation centers, state policies aimed at reducing the production of greenhouse gases, and legal issues, such as obtaining environmental permits for the construction of new transmission lines, are some of the main reasons that have driven the growth of small scale generation located close to actual load consumption, also known as Distributed Generation (DG). Distributed generation can also be encompassed within a much larger scope, the Distributed Energy Resources (DER) concept. DER refers to a variety of small, modular electricity-generating or storage technologies that can be aggregated to provide power necessary to meet regular demand and are installed at distribution level; distributed energy resources also includes demand-side management (i.e. energy efficiency and demand response) [1.1].

The introduction of distributed energy resources can provide great benefits for system operation. However, construction and connection of distributed generators cannot be made without considering the impact they will have on the system. Different planning studies must be carried out in order to ensure maximum benefits, normal operation, and foresee any eventual issues. The connection of distributed generation under non-optimal circumstances can have a negative impact on the system conditions and put normal operation at risk.

The optimum allocation of distributed generation will depend on the target function used to evaluate the different options. The target function can comprehend both technical and economic aspects. It is typically not possible to find a solution that can optimize all factors considered in the evaluation; it is the target function that must balance the benefits obtained from every single option and determine the best solution.

In recent years many new methodologies have been developed to determine the optimum allocation of distributed generation [1.2]. Some of these methodologies rely on analytical approaches and assume many model simplifications [1.3]-[1.5], whereas others apply highly complex optimization algorithms [1.6]-[1.8]. The accuracy of these methods will depend on the solution approach and also the model used for representation of the distribution system.

Most current methods pursue the optimum allocation of distributed generators that constantly operate at rated capacity; therefore generation based on renewable resources (such as photovoltaic or wind generation) cannot be evaluated using these methodologies. Moreover, these methods fail to take into account the temporal nature of electric load (i.e. load behavior over time); consequently the optimum allocation of distributed generation is performed for one specific moment in time, rather than contemplating a larger evaluation period (e.g. one year). These are some of the aspects that need to be considered when developing new methods for the optimum allocation of distributed generation; furthermore, these new methodologies must be accurate, with a straightforward implementation, and time-efficient.

One aspect that can be improved with the introduction of distributed generation is the reliability of the distribution system. Distribution reliability is assessed through the estimation of system and load-point reliability indices [1.9]. Reliability indices can be calculated in a predictive or statistical manner; a predictive approach allows the validation of the reliability of a system design, whereas the statistical method can be used to monitor system performance over a determined period of time.

It is important for reliability methods to be able to cope with the possibility of system reconfiguration; that is, modifying the system topology in order to restore service to affected customers in the shortest time possible. The introduction of distribution generation further complicates the evaluation of reliability indices. Moreover, random nature of system failure causes reliability indices to show a varying behavior (i.e. they do not present constant values); therefore a proper analysis must be carried out in order to estimate this variation. The use of detailed system element models allows a more accurate calculation of reliability indices.

As a conclusion, it is clear that new methods for the evaluation of distribution reliability must be developed. These new methods must take into account the random nature of system failure, reconfiguration processes, the presence of distributed generation, and the response of system protection devices. Additionally, the new methods must be able to estimate the probability density function of reliability indices.

This Chapter is summarized as follows. Section 1.2 details the common structure of distribution systems and lists some of the most common elements found in them. Section 1.3 makes a brief introduction to distributed generation and the main technologies, and analyzes the impact DG can have on system losses. In Section 1.4 a summary of reliability evaluation of power distribution systems is presented. Section 1.5 presents the main accomplishments achieved as a result of the work carried out for this Thesis. Finally, Section 1.6 presents the structure of the Thesis and provides a short description of the following Chapters.

1.2. Power Distribution Systems

1.2.1. Power Systems General Structure

Power delivery systems are designed to collect electrical energy produced in large generation centers and transport it to the final load points where costumers demand it. Power delivery systems are comprised by other subsystems; in a deregulated market each subsystem is owned by a different company and free competition is permitted in each of them. The main subsystems in the power delivery system are presented in this sub-Section. Figure 1.1 shows the general structure of power systems [1.10]-[1.13].

Large Generation Centers

The great majority of electrical energy is produced using large generation units clustered in remote sites, far from final consumption points. Different technologies have traditionally been used to produce electrical energy in a large scale, such as nuclear, natural gas, coal, hydro, etc. Many of these plants were constructed in the past when the entire power system was owned by one company; lower costs and economies of scale allowed these companies to construct large yet still profitable plants.

Transmission System

The transmission system consists of a set of lines, substations, and equipment designed to connect large generation plants and consumption centers, power consumption is mainly carried out in cities and industrial areas. Lines belonging to the transmission system span over long distances and transport large quantities of energy; therefore, these lines operate at high-voltage levels (e.g. 400 and 220 kV).

Subtransmission System

The subtransmission system is an intermediary link between the transmission and the distribution system. The lines that compose the subtransmission system cover shorter distances than those in the transmission system; for that reason they operate at lower voltage levels (e.g. 132, 66, and 45 kV). An initial voltage reduction is required due to the difference in voltage level with respect to the transmission system. Large loads (such as big factories and other high consumption facilities) can be directly connected to the subtransmission system.

Primary Distribution System

The first component of the primary distribution system is the distribution substation, where the energy delivered by the transmission and subtransmission system is received and a new voltage reduction is performed. From the distribution substation one or more medium-voltage distribution lines (e.g. 25 and 11 kV) take this energy one step closer to

the final customers. As in the subtransmission system, large loads can be connected to the primary distribution system.

Secondary Distribution System

The secondary distribution system consists of step-down (MV/LV) distribution transformers and low-voltage lines (e.g. 400 and 230 V) that deliver the energy to low power customers, such as commercial and residential loads.

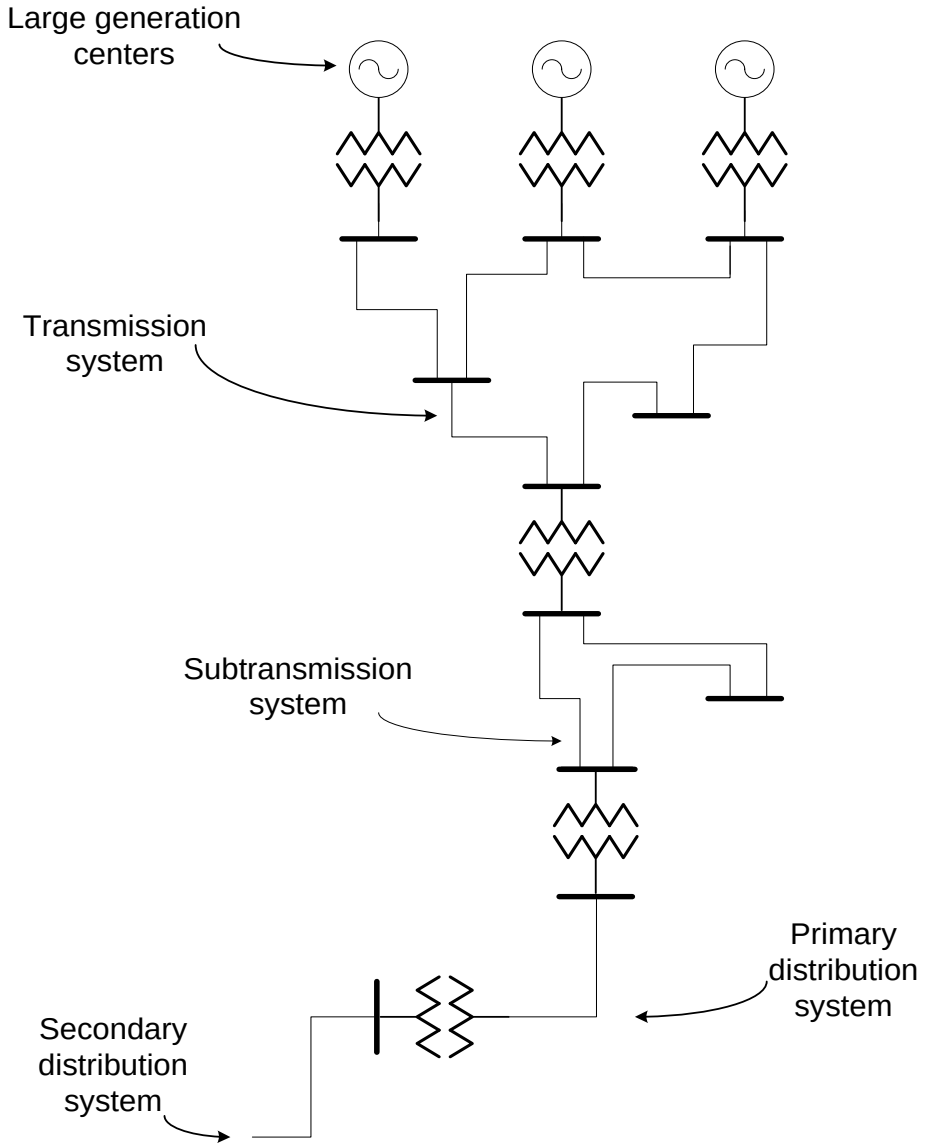

Figure 1.1. Power delivery system structure [1.10].

1.2.2. Distribution System Structure

The distribution substation is the interconnection element between the distribution system and the upstream power delivery system. At the substation the step-down (HV/MV) transformer reduces the subtransmission voltage level to an appropriate value

for primary distribution lines. Different protection, switching, and measurement equipment is installed at the substation to ensure a safe operation. The primary distribution lines spread across the consumption area served by the substation, these primary distributions lines are also known as feeders. One or more lateral lines (or laterals) branch from distribution feeders and extend until they reach the step-down (MV/LV) distribution transformers, which are responsible for performing the final voltage reduction in order to obtain a voltage level adequate for customer use (e.g. 400 and 230 V). The secondary distribution lines operating at a low-voltage level transport the energy to the customer's interconnection point; these lines are usually one-phase but there can also exist three-phase circuits. Overhead lines are primarily used in rural circuits, whereas in urban circuits distribution lines are mostly underground; in suburban areas there can be a mixture of overhead and underground circuits. Big industrial zones are usually served by dedicated circuits as they represent large loads that can affect the service of other loads. Figure 1.2 presents the typical configuration of a power distribution system, including the substation and the layout of one distribution feeder.

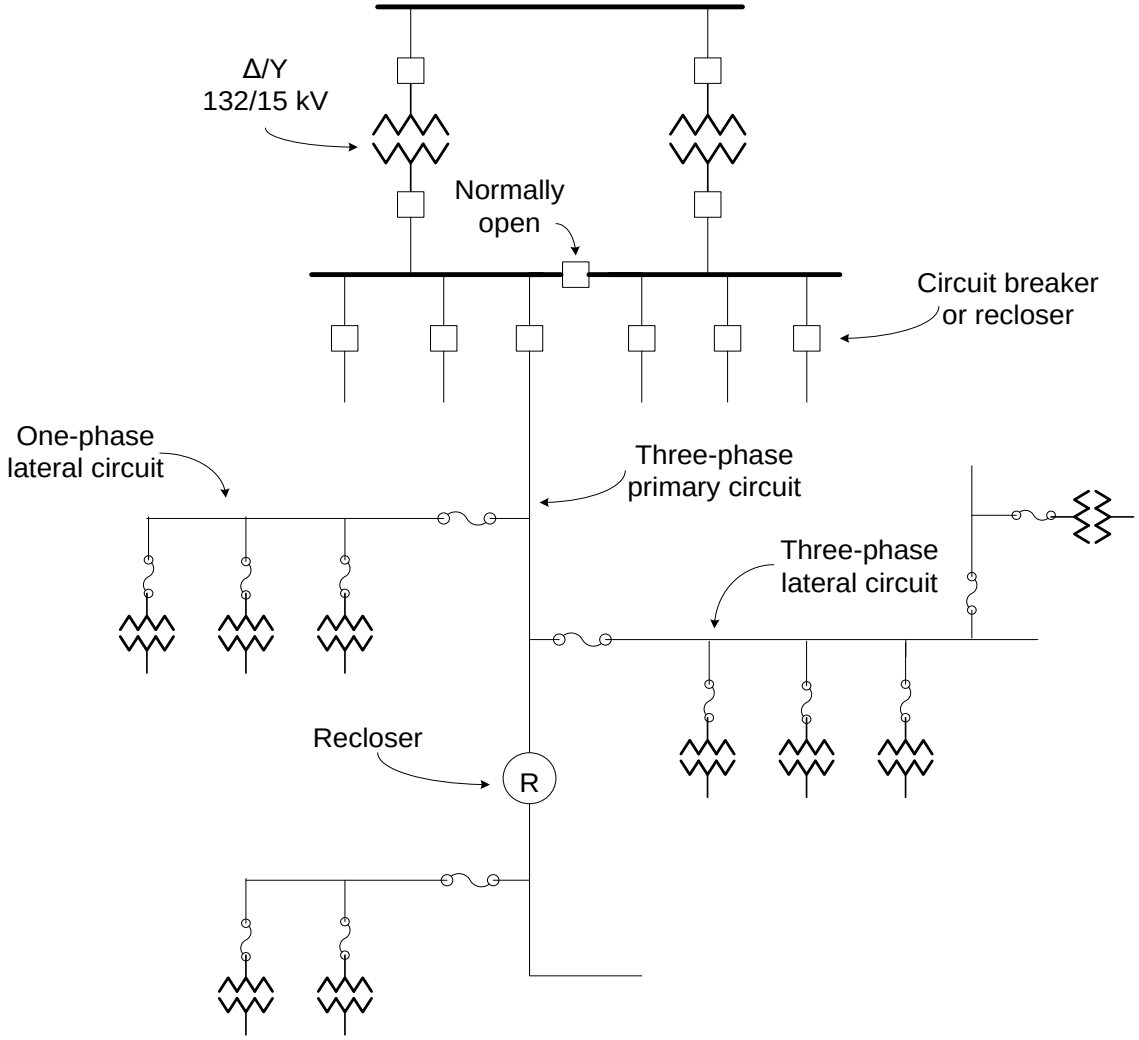

Figure 1.2. Typical distribution system configuration [1.10].

1.2.3. Distribution System Primary Circuits

Primary distribution circuits are generally radial in design, unlike transmission systems where circuit designs are meshed. In comparison to meshed circuits, radial designs present certain advantages for power distribution: (1) protection is basically overcurrent, (2) lower fault currents, (3) voltage regulation and power flow control are easier to implement, and (4) system design is less expensive. The general radial circuit design can present different variations, such as the single feeder and open-loop configurations [1.11].

Single Feeder Configuration

Under this configuration all power demanded by laterals and secondary circuits is served by a single primary line; in case of failure or any other event that forces the feeder to be out of service (e.g. maintenance), all loads will experience a service interruption. The single feeder layout can also present a branched-configuration, where several branches stem from the original feeder in order to cover a larger area. These branches are not to be confused with laterals; laterals present a much lower current capacity, whereas the branches have the same (or similar) capacity as the main feeder. Figure 1.3 shows two examples of the single feeder configuration.

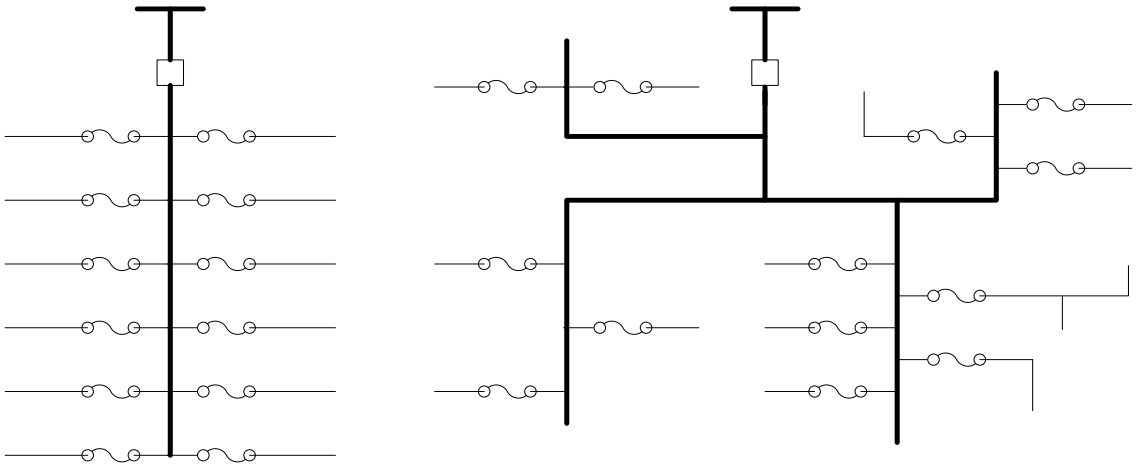

a) Simple feeder b) Branched-configuration

Figure 1.3. Single feeder configuration [1.11].

Open-loop Configuration

In the open-loop configuration two feeders parting from the same substation are connected at their end terminals through a normally-open tie-switch. Under normal conditions each feeder serves a different number of lateral circuits but has the capacity to provide the necessary power to all circuits connected to both feeders. Load transfer between feeders is possible by closing the normally-open tie-switch (either manually or automatically). This configuration presents a greater reliability level than the single feeder configuration but requires that each feeder have the capacity to carry the load corresponding to both feeders; additionally, extra equipment is needed (e.g. the tie-switch). Figure 1.4 presents a typical open-loop configuration.

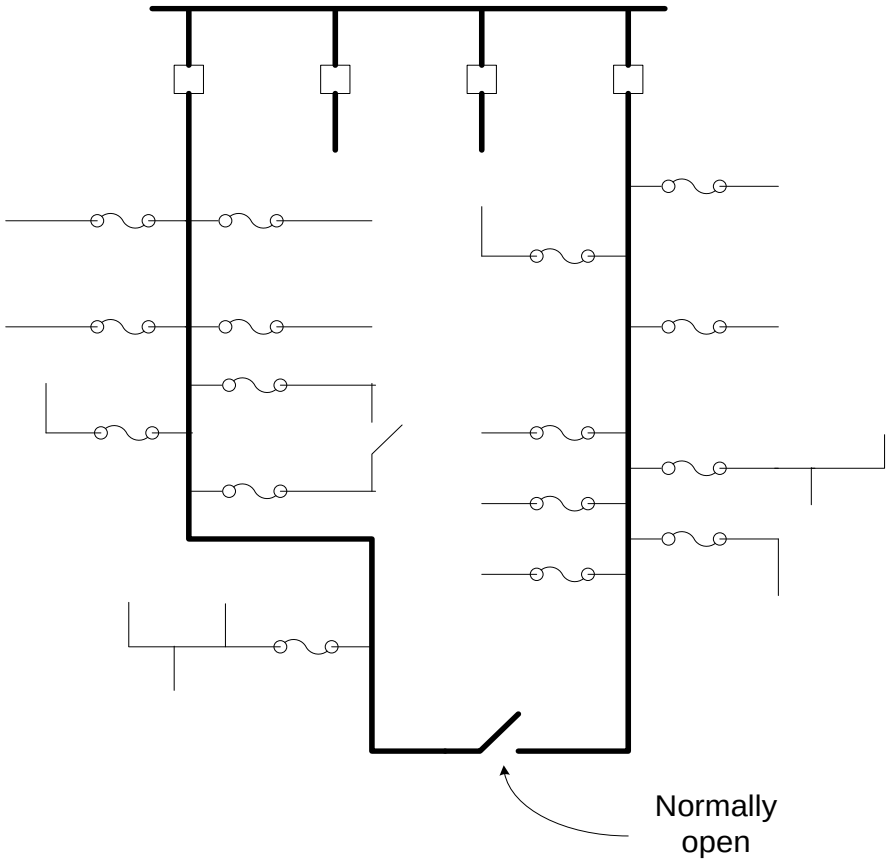

Figure 1.4. Open-loop configuration [1.11].

1.2.4. Distribution System Secondary Circuits

In rural and suburban areas a radial configuration is the most common design in secondary circuits; however, in urban circuits different configurations can be used depending on the type of load to be served. The spot configuration is used for large loads concentrated in one point (e.g. factories and large buildings), whereas the network configuration is used to serve a great number of loads distributed over a large area [1.11].

Radial Configuration

The radial design in distribution secondary circuits is equivalent to the configuration used in primary circuits. A secondary circuit parts from the step-down (MV/LV) distribution transformer and it spreads over the area where the customers are located; due to the size of the covered areas, the secondary circuits normally present a branched-configuration, see Figure 1.5a.

Spot Configuration

The spot configuration is used for loads that require dedicated circuits due to their high power demand; typically three or five feeders deliver the power demanded by the load, system design allows normal operation with the loss of one or two of the primary circuits. Each feeder arrives at a step-down (MV/LV) distribution transformer that serves part of the total load; all transformers are equipped with a protection device installed on its secondary side. A spot configuration is shown in Figure 1.5b.

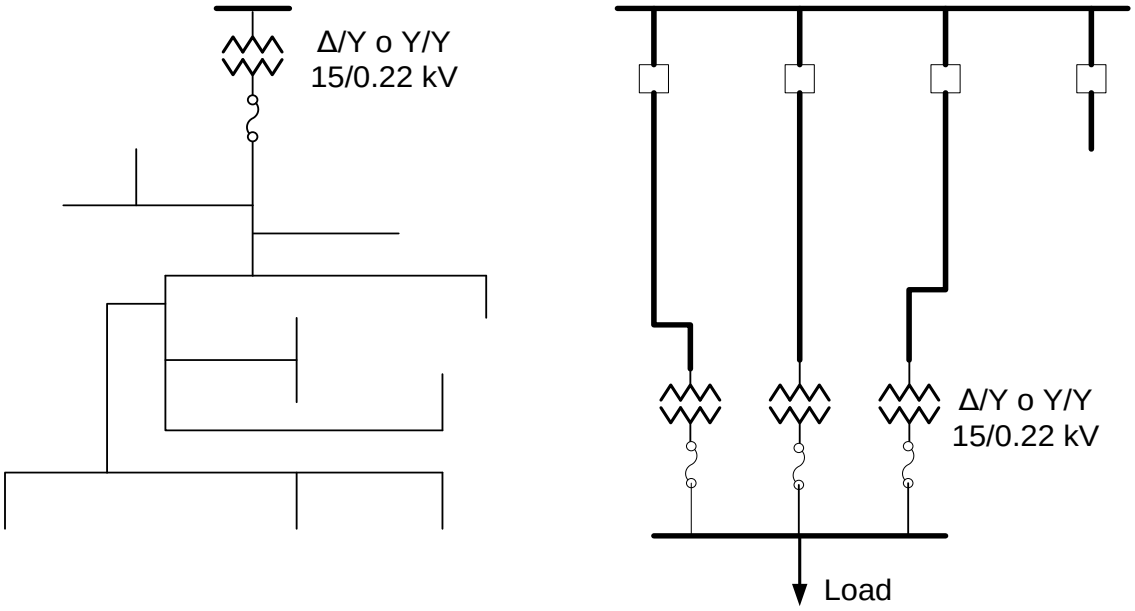

a) Radial configuration b) Spot configuration [1.11]

Figure 1.5. Distribution secondary circuit configuration.

Network Configuration

In the network configuration several primary circuit lines feed the secondary network from multiple step-down (MV/LV) distribution transformers. The secondary circuits connected at the low-voltage side of the distribution transformers form a meshed network, from which the load power is provided. This configuration is used to serve commercial and residential loads (both three and one-phase). An example of a network configuration is presented in Figure 1.6.

1.2.5. Distribution System Substations

The configuration of a distribution substation will depend on the type of system served (urban, suburban, or rural); load level and desired reliability will affect the substation's design and auxiliary equipment required [1.11].

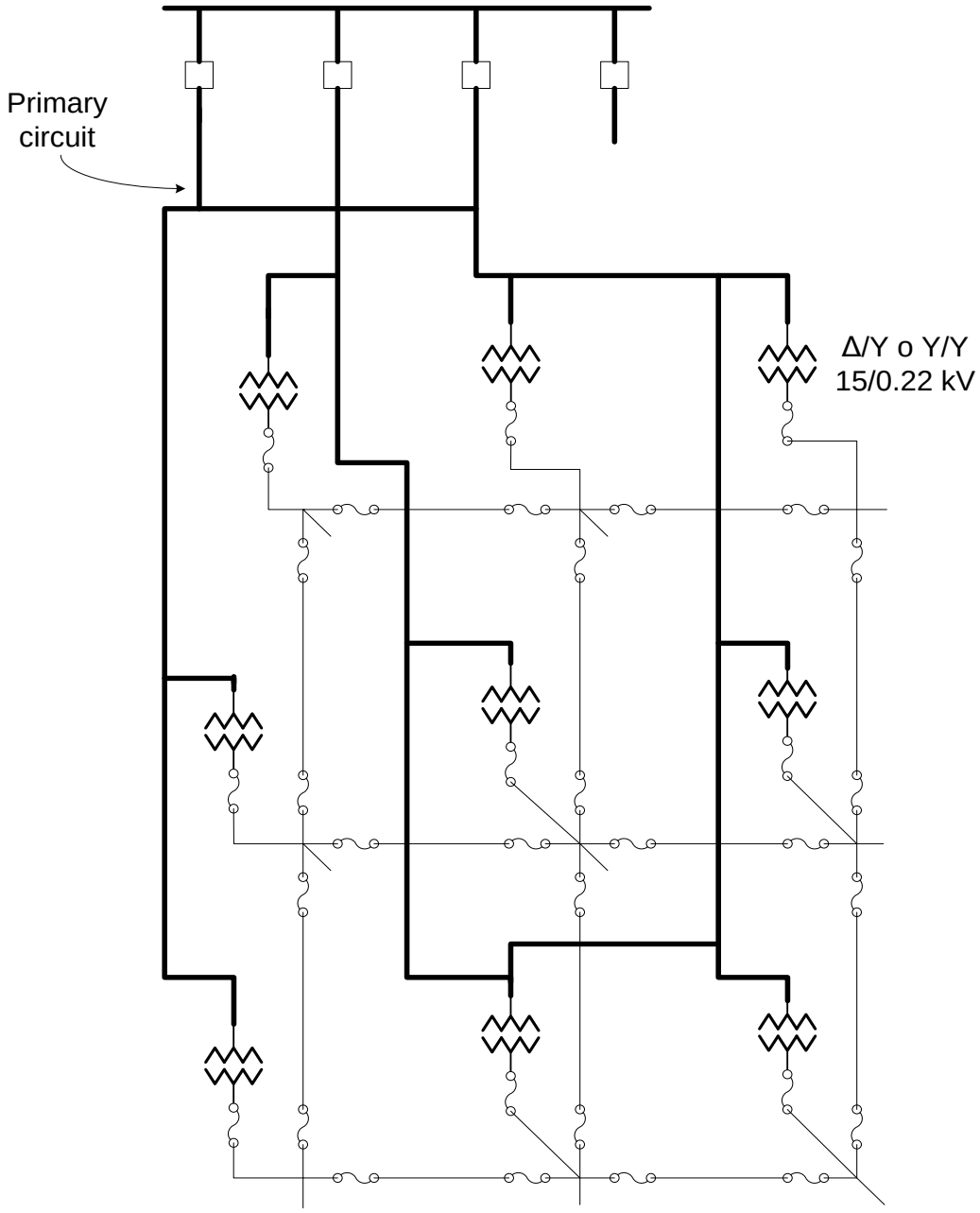

Figure 1.6. Network configuration [1.11].

Rural Substation

Substations designed for rural systems present a simple configuration; they consist of a single high-voltage and medium-voltage bus. Due to low load levels, a single transformer is enough to supply the entire power demand; transformer protection will depend on the transformer's rated power. Primary distribution lines are connected to the medium-voltage bus and are protected by reclosers or overcurrent relays. Figure 1.7a presents the diagram of a rural substation.

Suburban Substation

Suburban systems present higher load levels than rural systems; therefore more than one transformer will be necessary to serve the total system load. Suburban substations have a single bus on the high-voltage side, whereas each substation transformer has its own medium-voltage bus; medium-voltage buses are connected to each other through a normally-open tie-switch (see Figure 1.7b). In case of transformer failure, the tie-switch can be operated and the load corresponding to the failed transformer will be served by the remaining in-service transformers. This configuration known as *split bus* reduces fault levels, facilitates voltage control, and prevents the presence of circulating currents among transformers. Some utilities prefer to use a single medium-voltage bus for all substation transformers, which allows a more uniform load distribution among transformers.

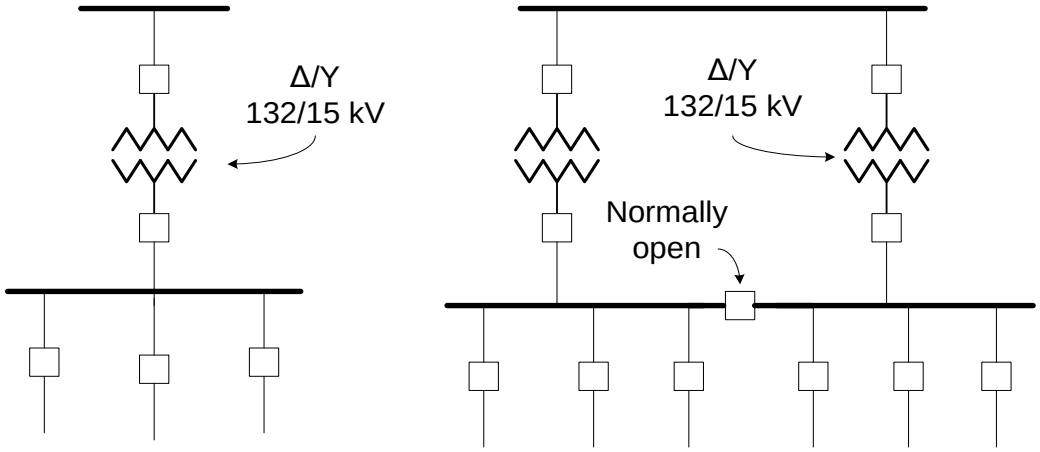

a) Rural substation b) Suburban substation

Figure 1.7. Distribution substation configuration [1.11].

Urban Substation

The configurations in urban substations are more complex than those used for rural and suburban systems; two of the most common substation designs are the ring-bus and breaker-and-a-half configuration. In the ring-bus configuration, the medium-voltage buses form a closed loop with each section separated by a circuit breaker; distribution feeders and the secondary side of the substation transformers can be connected to the mid-point of any section, between two circuit breakers [1.14]. The breaker-and-a-half configuration consists of one or more branches connected between two medium-voltage buses, where each branch is made up of three circuit breakers. The secondary side of a substation transformer or primary distribution lines can be connected between any two adjacent circuit breakers [1.14]. Both configurations can be readily modified in order to carry out load transfer or perform maintenance on one of the circuit breakers. Figure 1.8 shows the diagram of two urban substations following the ring-bus and breaker-and-a-half configuration, respectively.

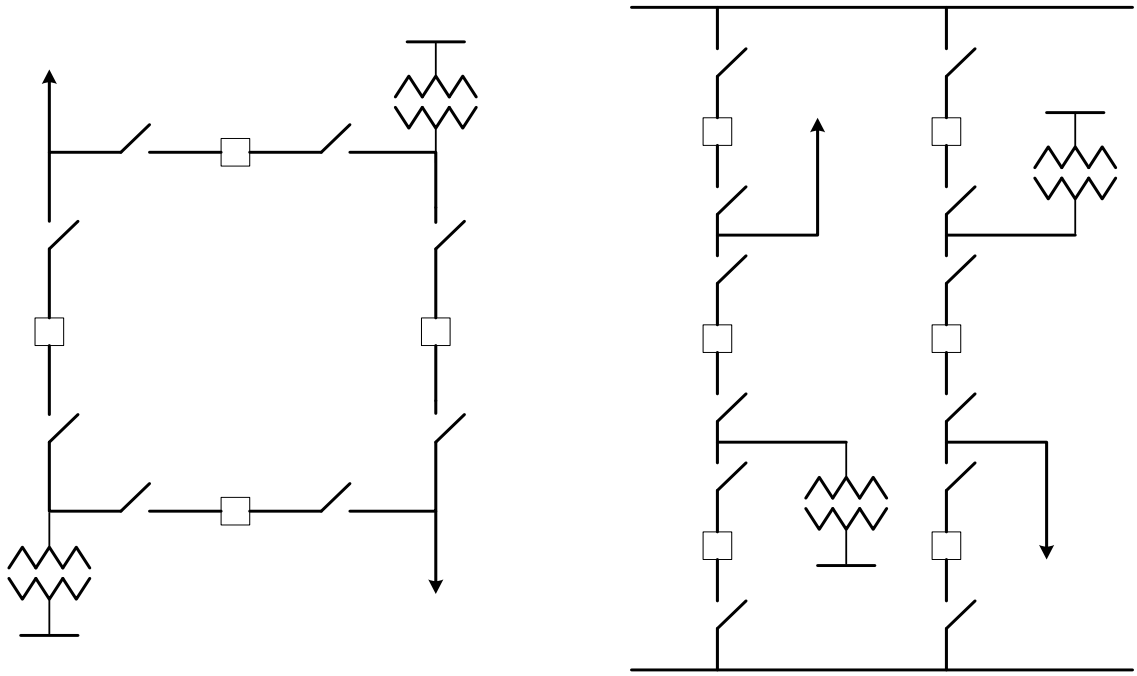

a) Ring-bus b) Breaker-and-a-half

Figure 1.8. Urban substation configuration.

1.2.6. Distribution System Elements

The safe operation of a power distribution system requires much dedicated equipment; this equipment is installed throughout the distribution system and it includes elements, such as power transformers, circuit breakers, and control and monitoring apparatuses. The most important elements and a brief definition are presented as follows.

Lines

Lines are responsible for transporting electrical energy between two distant points; overhead lines are typically made of bare aluminum (being ACSR a commonly used type), whereas underground lines commonly use cables with polymer-insulation, such as XLPE and EPR. Cables and conductors used for distribution lines are characterized by their current capacity and rated voltage [1.10].

Transformer

A transformer is an electric device that consists of two or more windings coupled by their electromagnetic fields; it transfers power from one winding to another without changing the frequency and is capable of performing voltage level transformation (reduction or increment). Transformers are used to perform successive voltage reductions along the distribution system in order to adjust the voltage level to an adequate value for every system section.

Circuit Breaker

A circuit breaker is a switching device designed to open and close a circuit by non-automatic means and to open the circuit automatically on a predetermined overcurrent in order to avoid damage to itself and other equipment [1.15].

Potential Transformer

A potential transformer is a conventional transformer with primary and secondary windings on a common core. Standard potential transformers are single-phase units designed and constructed so that the secondary voltage maintains a fixed relationship with primary voltage [1.15]. They are used to reduce the primary circuit voltage to a safe value (120 V), so it can be used as an input signal for monitoring and protection devices; these transformers only have the capacity to serve low rating meters and relays.

Current Transformer

A current transformer transforms line current into values suitable for standard protective and monitoring devices, and isolates the relays from line voltages. A current transformer has two windings, designated as primary and secondary, which are insulated from each other. The primary winding is connected in series with the circuit carrying the line current to be measured, and the secondary winding is connected to protective devices, instruments, meters, or control devices. The secondary winding supplies a current in direct proportion and at a fixed relationship to the primary current [1.15].

Relay

A relay is an electronic, low-powered device used to activate a high-powered device [1.16]. In distribution systems, relays protect feeders and system equipment from damage in the event of a fault by issuing tripping commands to the corresponding circuit breakers in order to interrupt the current produced by the fault.

Recloser

The automatic circuit recloser is a protective device with the necessary intelligence to sense overcurrents and interrupt fault currents, and to re-energize the line by reclosing automatically. In case of a permanent fault, the recloser locks open after a preset number of operations (usually three or four), isolating the faulted section from the main part of the system [1.17].

Fuse

A fuse is a protective device used in distribution systems to protect laterals, secondary circuits, and low power transformers; it consists of a strip of wire that melts and clears an electric circuit when an overcurrent or short-circuit current passes through it. Melting

and clearing times depend on the fuse's time-current curves. The most commonly used fuses are the types *K* and *T*.

Sectionalizer

The sectionalizer is a circuit-opening device used in conjunction with source-side protective devices, such as reclosers or circuit breakers, to automatically isolate faulted sections of electrical distribution systems. The sectionalizer senses current flow above a preset level, and when the source-side protective device opens to de-energize the circuit, the sectionalizer counts the overcurrent interruption [1.17].

Switch

A switch is a switching device used to isolate a system element for repair or maintenance. It must be capable of carrying and breaking currents during normal operating conditions; a switch may include specified operating overload conditions and also carrying for a specified time currents under specified abnormal circuit conditions such as those of a short circuit. A switch, therefore, is not expected to break fault current, although it is normal for a switch to have a fault making capacity.

Voltage regulator

A voltage regulator is transformer with a 1:1 nominal transformation ratio equipped with an on-load tap changer; this device allows the transformer to vary its transformation ratio to react to voltage variations at the primary side. Voltage regulators are installed at intermediate points of long primary lines in order to compensate the voltage drop produced along the circuit; voltage control will impact the voltage profile of all loads downstream from the voltage regulator.

Capacitor Bank

A capacitor bank is a local source of reactive power. By correcting power factor it can perform voltage regulation and reduce system losses. Capacitor banks are generally three-phase and are installed within the distribution substation or at intermediate points of a primary circuit line.

SCADA

SCADA (System Control and Data Acquisition) is a communication system that allows real-time monitoring of the distribution system; it collects information from equipment installed throughout the system and stores it in a database accessible to different users and applications. The measured values reflect different time varying quantities, such as bus voltages, line currents and tap changer positions [1.18]. SCADA also has the capability to remotely operate circuit breakers and switches, which provides a greater flexibility for system operation and reduces response times for switching actions.

1.3. Distributed Generation

Distributed generation (DG) or embedded generation refers to generation applied at the distribution level [1.10]; DG units can be directly connected at the distribution substation or dispersed throughout the power distribution system. Due to their small size distributed generators can be placed close to load consumption, typically DG present sizes of up to 5 MW [1.10] (IEEE STD 1547 [1.19] applies for generators under 10 MW); however, utilities can limit the rated power of generation units according to their own operation policies [1.20].

The origins of distributed generation can be found in the "cogeneration" practiced by some industries; these generators serve a portion of the load at these industrial facilities and inject any excess of generation into the utility system; they also provide emergency power to the industrial facility during utility outages [1.21]. This is a common practice in industries such as pulp and paper, steel mills, and petrochemical facilities that had internal generation within their electrical facilities that operated in parallel with the utility system.

Costs reduction and efficiency improvement in small-size generators have turned distributed generation into an attractive option for utilities and independent producers. While the independent producer seeks to maximize its profits, utilities are concerned with exploiting the benefits of DG and improving system performance. The connection of distributed generation to the distribution system can be used for supporting voltage, reducing losses, providing backup power, providing ancillary services, or deferring distribution system upgrade [1.22]. Aspects to be considered when embedding DG into a distribution system are the great variety of generating technologies, or the intermittent nature of some renewable sources.

It is also important to remark the challenges and negative impacts that the connection of distributed generation can carry. Power distribution systems were not designed to host local generation; as a consequence of this design limitation, distributed generation can disrupt normal system operation. One of the most important concerns is the formation of undesired islands within the system [1.10]; under this condition an isolated section of the circuit is continued to be served by a local generator. Islanding (or island operation) can cause damage to distribution equipment and poses safety hazard for customers and utility personnel. In general, DG can cause miscoordination of protection devices and, if not properly handled, reduce reliability and power quality.

1.3.1. Distributed Generation Technologies

Distributed generation does not make reference to a specific technology; different types of technologies are used to drive DG depending on the selected primary energy source. In recent years there has been a great effort to develop and improve technologies based on renewable energy sources; much of this effort has been oriented to work on small-size generators that can have an application in distributed generation; however, classical combustion engines remain a cost-effective option for the small scale generation of electrical energy. Common types of technologies used in distributed generation are

microturbines, fuel cells, Stirling engines, internal combustion engines, photovoltaic, and wind [1.23].

Microturbines

Microturbines are scaled down turbine engines with integrated generators and power electronics [1.23]. They operate at high speeds (about 100,000 rpm) and generate high-frequency AC power that is rectified by means of power electronics to comply with utility operating conditions. Microturbines can operate on a wide variety of gaseous and liquid fuels, and have extremely low emissions of nitrogen oxides. Electrical efficiency of microturbines is in the 25-30 percent range. Ancillary heat from microturbines can be used for water and space heating, process drying, food processing and absorption chilling.

Fuel Cells

A fuel cell is an electromechanical engine with no moving parts that collects the energy released from the combination of hydrogen and oxygen [1.23]. This reaction generates electricity, heat and water, while it produces almost no pollutants. In principle, a fuel cell operates like a battery; however, a fuel cell does not decay or require recharging; it will produce energy as long as fuel is supplied. The hydrogen needed for reaction in a fuel cell is typically produced from hydrogen rich fuels such as natural gas, propane, or methane from biogas recovery.

Stirling Engines

The Stirling engine is also known as an "external combustion engine”; it derives its power from heating and cooling a gas inside a sealed chamber with a piston. When the gas is heated, it will expand and build pressure within the sealed chamber; thus pushing a piston out [1.23]. When the gas cools, it will contract and pull the piston in. The Stirling engine runs cleaner and more efficiently than an internal combustion engine.

Internal Combustion Engines

The purpose of internal combustion engines is the production of mechanical power from the chemical energy contained in the fuel [1.24]. The expansion of hot gases produced during the combustion causes movement by acting on mechanical elements, such as pistons or rotors; the mechanical energy contained in this movement can be transferred to a generator, which transforms it into electrical energy. The most common internal combustion engine is the piston-type.

Photovoltaic

Photovoltaic generators are made up of two main parts [1.25]: The solar modules and the balance of system (BOS), a collection of different auxiliary components. The solar module consists of several interconnected solar cells that convert solar radiation into a

direct electric current. The key component of the BOS is the inverter; it is a power electronics device that converts the direct current generated by the solar cells into an alternating current. The Energy output of a PV generator depends on the amount of global radiation received and the generator's technical specifications.

Wind

Modern wind energy systems consist of three basic components [1.23]: a tower (where the wind turbine is mounted), a rotor with blades, and the nacelle. The nacelle is a capsule-shaped component which contains auxiliary and electric equipment, including the generator. Wind turbines convert the wind's kinetic energy transferred to their rotor into mechanical energy; a generator converts this mechanical energy into electricity. Actual power generation is mainly dependent on wind speed and the area covered by the turbine's blades.

1.3.2. Distributed Generation and Loss Reduction

Distributed generation is operated according to its role in the system; two main modes of DG connection can be distinguished: (1) operating as a backup source within a microgrid; (2) operating in parallel with the distribution system.

Customers that require uninterrupted and highly reliable service may rely on internal generation to supply load demand in case of service interruption, i.e. they can operate as an island. This type of application can be found in critical loads (e.g. hospitals) and represents the operational core of a microgrid. Microgrids are defined as a small energy system capable of balancing captive supply and demand resources to maintain stable service within a defined boundary [1.26]; hence the presence of local generation is an essential element to the microgrid operation.

The operation of DG in parallel with the distribution system can contribute to relieve overburdened transmission and distribution facilities as well as reduce losses and voltage drop [1.10]. Distributed generation helps to reduce losses as it locally generates power demanded by loads, rather than producing it in large generation centers and forcing it to travel great distances to consumption points; the reduction achieved will depend on the generator's rated power and location.

The optimum allocation of a generator injecting only active power in a radial feeder serving a uniformly distributed load is presented in [1.27]; according to this study, the maximum loss reduction is achieved by a generator of a rated capacity equal to 2/3 of the total load active power and located at 2/3 of the total feeder length (this is known as the 2/3 rule), this result is derived from the optimum allocation of capacitor banks presented in [1.10]. Although the 2/3 rule has limited practical application (system design is not realistic, and loads and DG are represented as constant current sources), the analysis carried out to obtain it can help to explain how DG helps to reduce system losses. Figure 1.9 presents the feeder current profile with and without DG; where I_1 is the total load current, I_{dg} is the current injected by DG, and x is the distance from the feeder origin at which DG is located. It is clear how the current profile is affected by the presence of DG; loss reduction is produced by the decreased current in the feeder

segment between the origin and DG location. A similar behavior can be found in other systems with a more complex design; however it will not be as easy to demonstrate the effect of DG, which is why this simple example is important to understand the way distributed generation influences system losses.

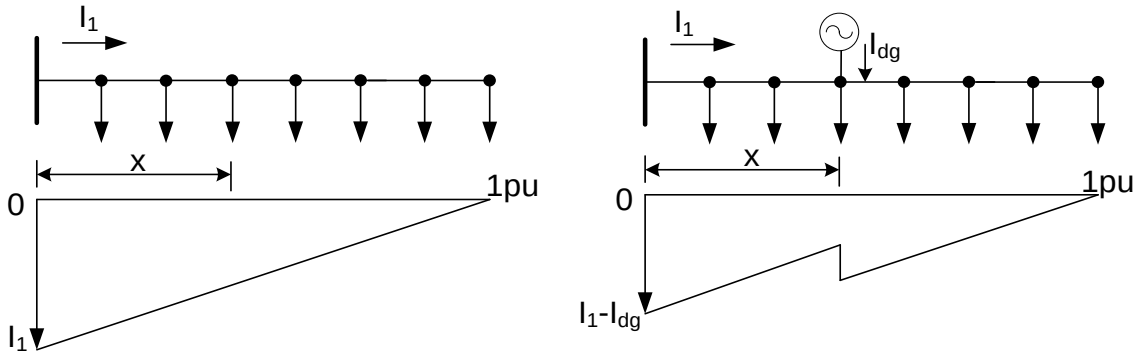

a) Without DG b) With DG

Figure 1.9. Feeder current profile.

1.4. Power Distribution Reliability

1.4.1. Introduction to Power Distribution Reliability

Reliability refers to a system's ability to perform its required function under given conditions for a stated time interval [1.28]. From a power distribution system's point of view, its function is to supply electrical energy to final customers without interruptions and within accepted tolerance margins (i.e. acceptable values for voltage and frequency) [1.29].

Power distribution systems are responsible for approximately 90% of all service interruptions experienced by customers [1.29]. Therefore, it is important to understand how the distribution system behaves and the effect that every element that composes it has in terms of system reliability; an accurate evaluation of power distribution reliability is essential to identify design weaknesses and areas within the system that require special attention.

A distribution system is composed by a great number of elements (see Section 1.2); a failure in one of these elements will affect the continuity of service provided to customers. The impact of element failure will depend on the element's statistical parameters and system design [1.29]. The most important statistical parameters are the failure rate and the repair time. A failure rate is defined as the number of expected failures per element in a given time interval; while the repair time is the time required to restore service, whether by repairing or replacing the failed element [1.30]. The area affected by an element failure will depend on system design; a reliability-based design will include protection and switching devices, whose main task is to reduce the number of customers affected by a service interruption.

The analysis of power distribution reliability is performed by following either a predictive or a statistical approach. These two approaches are not mutually exclusive as they both have different purposes and are carried out at different stages, but are equally relevant to the reliability evaluation of a power distribution system.

1.4.2. Predictive Analysis

Predictive analysis of power distribution system reliability can be used to validate system design as well as ensure that the reliability level provided meets utility policies and customer requirements. A great variety of methods have been developed for the predictive analysis of power distribution reliability, which can be classified into several categories; according to [1.31], these methods can be classified as: analytical and simulation-based methods.

Analytical methods

In analytical methods all system elements are represented by means of mathematical models. These methods use analytical equations in order to estimate system reliability indices; due to the complexity of real distribution systems, analytical methods generally rely on assumptions and simplification techniques. The evaluation of the analytical equations is rather straightforward and results can be found in a short period of time; however, developing the equations that model the system behavior can be a complex task, especially when considering reconfiguration processes and distributed generation.

The basic concepts of the analytical evaluation of power distribution systems are presented in [1.32]. The elements and segments that compose a distribution system are defined as follows:

1. General lateral section: it refers to lateral circuits branching from a feeder. It may include distribution transformers, line segments, and fuses.
2. General main section: it represents a main segment in a primary feeder or branch.
3. General series element: it is the series equivalent of any component, assumed for the purpose of easy calculation.
4. General feeder: a general feeder is a simple distribution system containing general main sections, general lateral sections and a general series component.

The following equations can be used to estimate the load point reliability indices when using the general feeder model.

Load point failure rate:

$$\lambda_j = \lambda_s + \sum_{i=1}^{n} \lambda_i + \sum_{k=1}^{m} p_k \lambda_k \qquad (1.1)$$

Average outage duration:

$$U_j = \lambda_s r_s + \sum_{i=1}^{n} \lambda_i r_i + \sum_{k=1}^{m} p_k \lambda_k r_k \quad (1.2)$$

Average annual outage time:

$$r_j = \frac{U_j}{\lambda_j} \quad (1.3)$$

where p_k are the lateral section control parameters that depend on the fuse operation mode; it can be 0, 1, and 2 corresponding to 100% reliable fuse, not fuse and a fuse operating not successfully with p_k probability; λ_i, λ_k, and λ_s are the failure rate of the main section, lateral section, and series element; r_i, r_k, and r_s are the failure duration of the three elements respectively. Failure duration times may vary depending on one of the following scenarios: (1) there is no alternate power supply; (2) the alternate power supply is 100% reliable; and (3) the alternate power supply is not 100% reliable, successful load transfer will depend on the availability probability p_a.

Simulation-based methods

As the name implies, simulation-based methods rely on system simulation in order to analyze the reliability of the system under evaluation. The Monte Carlo method has been extensively used in power system reliability evaluation due to the random behavior presented by system failure [1.31]; this approach can be used in either sequential or non-sequential manner. In the application of the Monte Carlo method, random variables are generated to represent the state of system elements and times related to fault duration and service restoration. Simulation-based methods present a main disadvantage; that is, they require large computational efforts and long simulation times to obtain accurate results.

[1.31] presents a procedure for the evaluation of power distribution reliability based on a sequential Monte Carlo method; in this procedure each element is represented by a two-state model (Up and Down); the transition between these two states is defined by the parameters TTF and TTR. The time during which the element remains in the Up state is called the time to failure (TTF), whereas the time during which the element is in the down state is called the time to repair (TTR). Both TTF and TTR are random numbers defined by means of a probability density function (PDF).

In this procedure an artificial history that shows the Up and Down times of the system elements is generated in chronological order using random number generators and the probability distributions of the element failure and restoration parameters; see Figure 1.10.

In order to carry out the reliability evaluation of a distribution system it is necessary to determine which loads will be affected by an element failure; this information is required in order to estimate load point reliability indices. The main indices to be calculated for a load point using the load point UP-Down history are defined as follows.

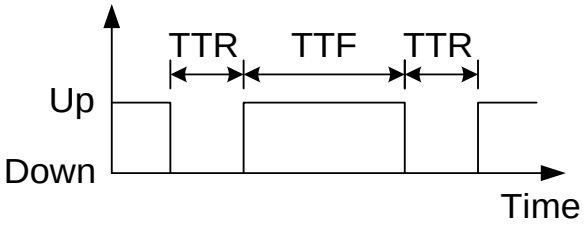

Figure 1.10. Element Up/Down history [1.31].

Average failure rate:

$$\lambda_j = \frac{N_j}{\sum T_{uj}} \qquad (1.4)$$

Average outage time:

$$r_j = \frac{\sum T_{dj}}{N_j} \qquad (1.5)$$

Average annual outage time:

$$U_j = \frac{\sum T_{dj}}{\sum T_{uj} + \sum T_{dj}} \qquad (1.6)$$

where j is the load point index, $\sum T_u$ and $\sum T_d$ are the summations of all Up times (T_u) and all Down times (T_d) respectively, and N_j is the number of failures during the total sampled years.

1.4.3. Statistical Analysis

Statistical analysis allows monitoring system performance from a reliability point of view; it also provides information that can help validate predictive analysis as well as identify areas where reliability needs to be improved. Statistical approaches require historical data of all service interruptions experienced by customers over a defined evaluation period. System reliability will be quantified by means of the customer interruption indices; the main indices are calculated according to the following equations [1.9].

System average interruption frequency index:

$$SAIFI = \frac{\sum_{i=1}^{n} N_i}{N_T} \qquad (1.7)$$

System average interruption duration index:

$$SAIDI = \frac{\sum_{i=1}^{n} N_i \cdot H_i}{N_T} \quad (1.8)$$

Customer average interruption duration index:

$$CAIDI = \frac{\sum_{i=1}^{n} N_i \cdot H_i}{\sum_{i=1}^{n} N_i} = \frac{SAIDI}{SAIFI} \quad (1.9)$$

Where k is the number of interruptions, N_i is the number of customer interrupted by a fault, N_T is the total number of customers in the system, and H_i is the duration of interruption to customers interrupted by a fault.

The need of much detailed data for calculation of reliability indices may represent an important drawback for certain utilities as they do not possess the necessary facilities to keep record of every interruption experienced in their systems or lack an application that allows a prompt and easy access to it, posing an obstacle for an accurate evaluation of the system reliability.

1.5. Accomplishments

The work in this Thesis has been oriented at developing a procedure for the optimum allocation of distributed generation and another procedure for reliability evaluation of distributed systems; both procedures are based on the Monte Carlo method.

The procedure for optimum allocation of distributed generation has been developed to determine the quasi-optimum rated power and location of one or more generation units when the objective is to achieve the maximum energy loss reduction; it is capable of evaluating any system regardless of its topology or model used for load representation. Energy system losses are calculated by simulating the system for the specified evaluation period; the procedure can cope with different evaluation periods, ranging from one year to up to 10 years or more. The general Monte Carlo procedure was refined in order to reduce the number of necessary executions; the new methods introduced as “Refined Monte Carlo” and “Divide and Conquer” were tested and proved to cause a reduction in total simulation times without loss in the results accuracy.

The reliability evaluation of distribution systems is carried out by simulating the effects of element failure in the continuity of service. Failed elements and repair times are randomly generated to replicate the stochastic nature of system failure. The procedure has been developed to cope with system reconfiguration processes and the presence of distributed generation in the system. The system under evaluation is simulated during consecutive runs (varying the number and characteristics of failed elements) in order to obtain the probability density functions of reliability indices.

Due to their Monte Carlo nature both developed methods are time consuming and require a large number of runs/samples to obtain accurate results. As a result it was necessary to introduce new techniques in order to reduce total simulation times; parallel computing was the tool chosen to achieve this goal. Thanks to the application of parallel computing it was possible to execute both methods in affordable times without any loss in accuracy. Additionally, these methods require information regarding the load and generation behavior over the evaluation period; therefore, three algorithms were implemented in order to obtain node load profiles, and solar and wind generation curves. These three algorithms allow the user to generate the necessary information without having to rely on external tools (e.g. HOMER [1.33]).

As a result of the research work carried out for this Thesis, several technical papers have been submitted to different conferences and journals. The complete list of accepted and submitted papers is as follows:

1. J.A. Martinez and G. Guerra, "Optimum placement of distributed generation in three-phase distribution systems with time varying load using a Monte Carlo approach," *IEEE PES General Meeting*, San Diego, July 2012.
2. J.A. Martinez and G. Guerra, "A Monte Carlo approach for distribution reliability assessment considering time varying loads and system reconfiguration," *IEEE PES General Meeting*, Vancouver, July 2013.
3. J.A. Martinez and G. Guerra, "A Parallel Monte Carlo method for optimum allocation of distributed generation," *IEEE Trans. on Power Systems*, vol. 29, no. 6, pp. 2926-2933, November 2014.
4. G. Guerra and J.A. Martinez, "A Monte Carlo method for optimum placement of photovoltaic generation using a multicore computing environment," *IEEE PES General Meeting*, National Harbor, USA, July 2014.
5. J.A. Martinez and G. Guerra, "A Parallel Monte Carlo approach for distribution reliability assessment", *IET Gener., Transm. Distrib.*, vol. 8, no. 11, pp. 1810-1819, November 2014.
6. J.A. Martinez-Velasco and G. Guerra, "Analysis of large distribution networks with distributed energy resources", *Ingeniare*, vol. 23, no. 4, pp. 594-608, October 2015.
7. G. Guerra, J.A. Corea-Araujo, J.A. Martinez, and F. Gonzalez-Molina, "Generation of bifurcation diagrams for ferroresonance characterization using parallel computing," *EEUG Conf.*, Grenoble (France), September 2015.
8. G. Guerra and J.A. Martinez, "Optimum allocation of distributed generation in multi-feeder systems using long term evaluation and assuming voltage-dependent loads," *Sustainable Energy, Grids and Networks*, vol. 5, pp. 13-26, March 2016.
9. J.A. Martinez and G. Guerra, "Reliability Assessment of Distribution Systems with Distributed Generation Using a Power Flow Simulator and a Parallel Monte Carlo Approach," Submitted for publication in *Sustainable Energy, Grids and Networks*.
10. J.A. Martinez-Velasco and G. Guerra, "Allocation of Distributed Generation for Maximum Reduction of Energy Losses in Distribution Systems," Chapter 12 of *Energy Management of Distributed Generation Systems*, InTech, In editing process.

1.6. Document Structure

The remainder of this Thesis is divided into five subsequent Chapters and one Appendix. The Chapters will present the procedures developed for the Thesis as well as detail case studies used to prove the usefulness of the proposed methods. The following Chapters are organized as follows.

Second Chapter

The Second Chapter makes a brief introduction of the main concepts of parallel computing. It also introduces the "Multicore for MATLAB" library, which is the tool chosen for individually accessing system cores and implementing multicore computing. Finally, it presents how the "Multicore for MATLAB" library can be used in conjunction with OpenDSS for the application of parallel computing to the simulation of power distribution systems.

Third Chapter

The Third Chapter presents the three algorithms implemented for the generation of node load profiles, and PV and wind generation curves. A short example is presented to demonstrate the information that can be generated with these three algorithms and how it can be used in different studies.

Fourth Chapter

The Fourth Chapter presents the developed procedure for the optimum allocation of distributed generation, including how this procedure was implemented to be executed in a multicore environment. Furthermore, two refinements of the proposed Monte Carlo approach aimed at reducing total execution times are presented. The implemented procedure is tested in different systems and the main results and conclusions are presented in this Chapter.

Fifth Chapter

In the Fifth Chapter the procedure for the reliability evaluation of distribution systems is detailed. The most important aspects of the procedure are presented as well as the criteria selected for reliability evaluation with presence of distributed generation. Additionally, the application of parallel computing using the "Multicore for MATLAB" library is also presented. The probability density functions of the reliability indices of a test system (with and without DG) are obtained by means of the developed method and presented in this Chapter.

Sixth Chapter

The Sixth Chapter summarizes the main conclusions derived from the work developed for this Thesis.

Appendix A

The Appendix A presents the software for simulation of power distribution systems, OpenDSS; it also introduces the main features and capabilities present in the Stand-alone and COM DLL versions. Two test cases are used to show the main solution modes and the information that can be generated from the solution of a circuit under evaluation.

1.7. References

[1.1] New York Independent System Operator, *A Review of Distributed Energy Resources*, September 2014.

[1.2] P.S. Georgilakis and N.D. Hatziargyriou, "Optimal distributed generation placement in power distribution networks: Models, methods, and future research," *IEEE Trans. on Power Systems*, vol. 28, no. 3, pp. 3420-3428, August 2013.

[1.3] C. Wang and M.H. Nehir, "Analytical approaches for optimal placement of distributed generation in power systems," *IEEE Trans. on Power Systems*, vol. 19, no. 4, pp. 2068-2076, November 2004.

[1.4] N. Acharya, P. Mahat, and N. Mithulananthan, "An analytical approach for DG allocation in primary distribution networks," *International Journal of Electrical Power & Energy Systems*, vol. 28, no. 10, pp. 669-678, December 2006.

[1.5] T. Gözel and M.H. Hocaoglu, "An analytical method for the sizing and siting of distributed generator in radial systems," *Electric Power Systems Research*, vol. 79, no. 6, pp. 912-918, June 2009.

[1.6] G. Celli, E. Ghiani, S. Mocci, and F. Pilo, "A multiobjective evolutionary algorithm for the sizing and siting of distributed generation," *IEEE Trans. on Power Systems*, vol. 20, no. 2, pp. 750-757, May 2005.

[1.7] C.L.T. Borges and D.M. Falcao, "Optimal distributed generation allocation for reliability, losses, and voltage improvement," *International Journal of Electrical Power & Energy Systems*, vol. 28, no. 6, pp. 413-420, July 2006.

[1.8] A.A. Abou El-Ela, S.M. Allam, M. Shatla, "Maximal optimal benefits of distributed generation using genetic algorithms," *Electric Power Systems Research*, vol. 8, no. 7, pp. 869-877, July 2010.

[1.9] IEEE 1366: "IEEE Guide for Electric Power Distribution Reliability Indices", 2012.

[1.10] T.A. Short, *Electric Power Distribution Handbook*, 2nd Edition, CRC Press, 2004.

[1.11] T.A. Short, *Electric Power Distribution Equipment and Systems*, CRC Press, 2005.

[1.12] T. Gönen, *Electric Power Distribution System Engineering*, 2nd Edition, CRC Press, 2008.

[1.13] A.A. Salam and O.P. Malik, *Electric Distribution Systems*, John Wiley & Sons, 2011.
[1.14] D. Nack, "Reliability of Substation Configurations", Iowa State University, 2005.
[1.15] IEED 242: "IEEE Recommended Practice for Protection and Coordination of Industrial and Commercial Power Systems", 2001.
[1.16] A.J. Pansini, *Guide to Electrical Power Distribution Systems*, 6th Edition, CRC Press, 2005.
[1.17] URL: http://www.cooperindustries.com/content/public/en/power_systems/products/overhead_distributionequipment.html
[1.18] J. Northcote-Green and R.G. Wilson, *Control and Automation of Electrical Power Distribution Systems*, CRC Press, 2006.
[1.19] IEEE 1547: "Standard for Interconnecting Distributed Resources with Electric Power Systems", 2003.
[1.20] The Regulatory Assistance Project, "Interconnection of Distributed Generation to Utility Systems," RAP report (Main author: P. Sheaffer), September 2011. Available at www.raponline.org.
[1.21] C.J. Mozina, "Interconnection Protection of Dispersed Generators", Beckwith Electric Co., Inc.
[1.22] H. Lee Willis and W.G. Scott, *Distributed Power Generation. Planning and Evaluation*, Marcel Dekker, 2000.
[1.23] "An Introduction to Distributed Generation Interconnection". Available at http://www.renewwisconsin.org.
[1.24] J. Heywood, *Internal Combustion Engine Fundamentals*, 1st Edition, McGraw-Hill, 1988.
[1.25] F. Wagner, *Renewables in Future Power Systems*, Springer, 2014.
[1.26] URL: http://www.microgridinstitute.org/about-microgrids.html
[1.27] H.L. Willis, "Analytical Methods and Rules of Thumb for Modeling DG-Distribution Interaction," *Power Engineering Society Summer Meeting*, Seattle, Washington, USA, 2000.
[1.28] A. Birolini, *Reliability Engineering*, Springer, 2004.
[1.29] R.E. Brown, *Electric Power Distribution Reliability*, 2nd Edition, CRC Press, 2009.
[1.30] A. Chowdhury and D. Koval, *Power Distribution System Reliability: Practical Methods and Applications*, Wiley-IEEE Press, 2009.
[1.31] R. Billinton and P. Wang, "Teaching Distribution System Reliability Evaluation Using Monte Carlo Simulation," ," *IEEE Trans. on Power Systems*, vol. 14, no. 2, pp. 7397-403, August 2002.
[1.32] R. Billinton and P. Wang, "A Generalized Method for Distribution System Reliability Evaluation," *IEEE WESCANEX Conference Proceedings*, pp. 349-354, 1995.
[1.33] HOMER Software, National Renewable Energy Laboratory (NREL), 2003. Available at http://www.nrel.gov/homer.

Chapter 2

Application of Parallel Computing to Distribution Systems Analysis

2.1. Introduction

Parallel computing can be defined as the task carried out by a group of independent processing units working collaboratively to perform many calculations simultaneously. Large computational problems can be partitioned into smaller sub-problems and these can be distributed among available processing units; the objective is to reduce total execution time and utilize larger memory/storage resources [2.1], [2.2].

In recent times there has been a major advance in semiconductor technology which has led to a reduction in market prices; during this period multicore processors in PCs and workstations have become a standard feature; easier access to multicore equipment has facilitated the development of parallel-oriented software tools. The progress in both areas (hardware and software) has pushed forward the growth of parallel computing applications.

Parallel computing has had a significant impact on a variety of fields ranging from computational simulations for scientific and engineering applications to commercial applications in data mining and transaction processing. Performance improvement and affordability of multicore platforms is turning parallel computing into a cost-effective solution for large and data-intensive problems [2.3].

The use of multicore computing in studies related to power distribution systems is a natural approach given the capabilities of the software tools used in the simulation of power systems and the nature of the analyzed problems. In recent years many important works have been carried out on the application of parallel computing to power systems analysis; see [2.4] and [2.5].

This Chapter has been organized as follows. The basic concepts of parallel computing are introduced in the remainder of Section 2.1. In Section 2.2 the main features of the "Multicore for MATLAB" library are detailed. Section 2.3 presents the implementation developed to apply parallel computing to the simulation of power distribution systems using OpenDSS; this Section also presents the details of the multicore installation used to perform all the studies carried out for this Thesis. In Section 2.4 a case study that demonstrates the application and reduction simulation times of parallel computing in the simulation of power distribution systems is presented and Section 2.5 summarizes the main conclusions derived from the Chapter are summarized.

2.1.1. Serial vs. Parallel Computing

Traditional software has been written to be run on a single computer using a single central processing unit (CPU) for its execution. When solving a problem, this is broken into a discrete set of functions; each instruction is executed in a serial manner by the CPU; see Figure 2.1 [2.6]. The time needed to solve the problem is proportional to the number of instructions in which it is divided.

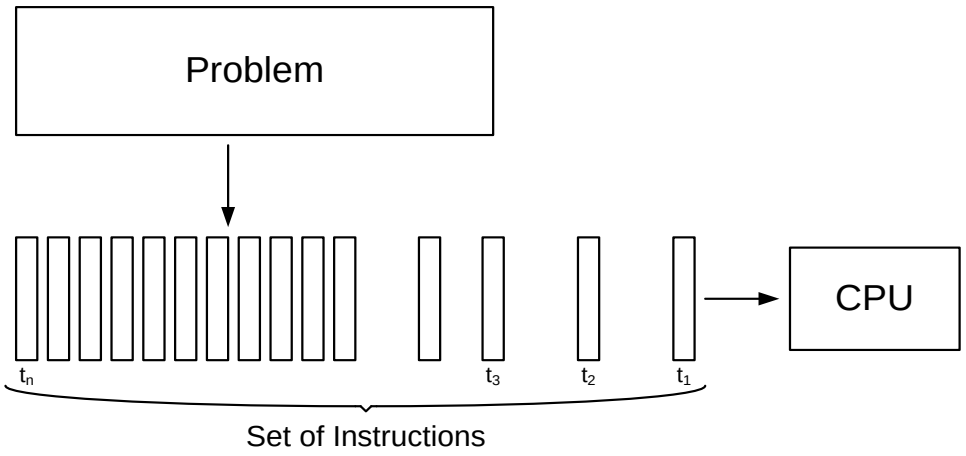

Figure 2.1. Serial execution [2.6].

Parallel oriented software is designed to exploit multiple computer resources (multiple CPUs). The solution of a computational problem requires partitioning it into discrete parts that can be solved simultaneously. Each part is then broken into a set of instructions. Instructions for a specific part are executed concurrently on the available CPUs (see Figure 2.2) [2.6]. The simultaneous solution of multiple instructions allows a reduction in total execution times when compared to serial execution, which is proportional to the number of available CPUs.

2.1.2. Hardware Configuration

Systems with multiple CPUs can have different hardware configurations; from a memory point of view they can be placed in two categories: systems with shared memory and systems with distributed memory [2.1], [2.6].

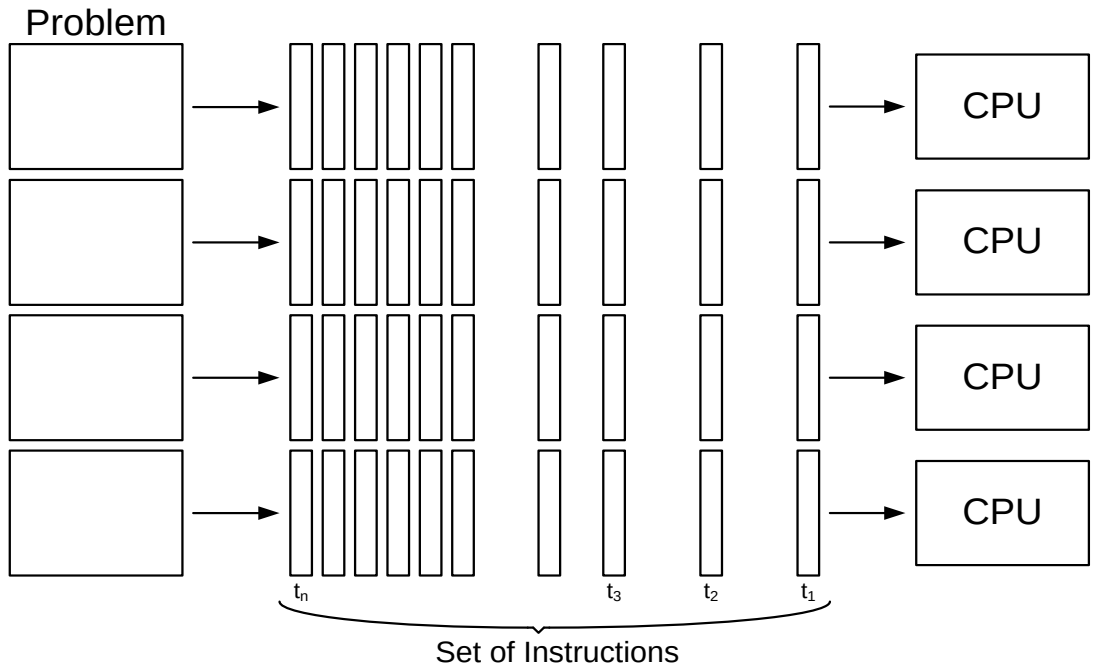

Figure 2.2. Parallel execution [2.6].

In shared memory systems all CPUs have access to a common system memory (see Figure 2.3); the common memory can be realized at hardware or software level. This configuration allows a better communication among CPUs as changes made in local memory can be seen by all CPUs. The principal disadvantage of this configuration is the lack of scalability, adding more CPUs can increase traffic in system on the shared memory-CPU path.

The main characteristic of distributed memory systems is that every CPU has an independent local memory (Figure 2.4). Any local changes are not reflected on the memory of other CPUs, therefore communication among CPUs is done through an interconnection network. Unlike shared memory systems, this configuration presents no problems with scalability; however communication among CPUs can become rather complex and the programmer is in charge of handling most implementation details.

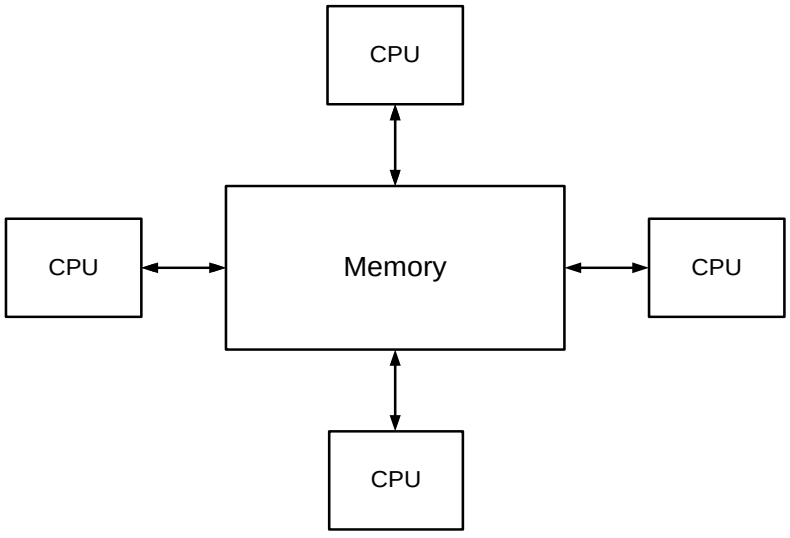

Figure 2.3. Shared memory configuration [2.6].

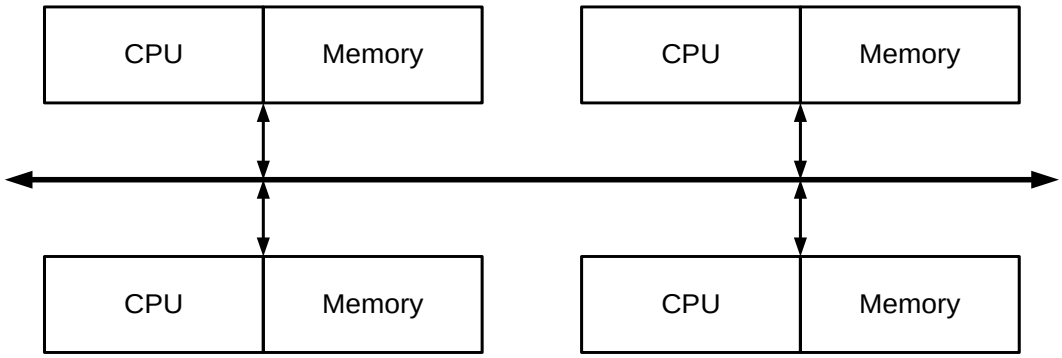

Figure 2.4. Distributed memory configuration [2.6].

On a bigger scale there can also be a distinction in multicore systems between computers with multiple processors and computer clusters [2.6]. A computer cluster is a group of computers working together as one; each computer (or node) can have one or more processors and has its own operative system (OS); nodes must be connected to a communication network in order to interact with each other. A cluster requires special software to distribute tasks among system nodes. In a computer with multiple processors (each processor has one or more cores) all computational resources are contained within a single system and communication among processors is internal; the maximum number of processors will depend on hardware restrictions. The decision to choose one of these configurations will depend on whether the configuration is suited for the specific application and is cost-effective or not.

2.1.3. Types of Parallel Jobs

Different types of problems (or jobs) can be solved using parallel computing; the nature of the problem under consideration will determine how the resources of a multicore installation can be exploited to solve it. In general, these jobs can be categorized as follows [2.3], [2.7]:

- Task-parallel jobs
- Data-parallel jobs
- Job Scheduling.

Task-Parallel Jobs

In task-parallel jobs the same task must be executed many times with only small variations (usually input values). Each task can be executed independently and the order of execution does not affect the outcome results. These types of jobs are also known as distributed or embarrassingly parallel jobs. Examples of task-parallel jobs are Monte Carlo simulations and image processing.

Data-Parallel Jobs

In these types of jobs a single task is concurrently run on multiple CPUs; each CPU works on a specific part of the task and communication among CPUs may be required.

They are also known simply as parallel jobs. Examples of a parallel job include many linear algebra applications: matrix multiply, linear system of equation solvers, or eigen solvers.

Job Scheduling

The computational resources of a computer cluster or multiprocessor computers can be shared by multiple users. Through a job scheduling software different tasks can be assigned to the system CPUs; assigned tasks are executed simultaneously but are independent from each other, they are submitted by different users. This type of application allows a better use of the resources at hand.

2.2. Multicore for MATLAB Library

MATLAB's native capabilities can be used to execute parallel jobs in a multicore installation [2.8]-[2.10]; however this usually requires purchasing special toolbox licenses. The "Multicore for MATLAB" library (developed by M. Buehren [2.11]) consists of a set of *.m* files which allow the user access to all cores in a multicore installation. This library can be used to execute embarrassingly parallel jobs by distributing task executions among system cores in an equivalent manner to MATLAB's *parfor* function. In order to access all available cores one MATLAB session must be run for each parallel execution; one session will serve as master, whereas the rest will work as slave sessions. The maximum number of concurrent MATLAB sessions must be equal to the number of cores at the user's disposal.

The "Multicore for MATLAB" library may exhibit a lower efficiency than MATLAB's native capabilities in terms of task distribution and information gathering times; however it does not require a special toolbox license and can be readily expanded for its use with a computer cluster.

As the name implies, the "Multicore for MATLAB" library runs entirely on MATLAB (i.e. it requires no additional software tool to access the available cores in the multicore installation). This Section describes in detail the master function and the main parameters that control the library execution; it also presents how the task chosen for execution must be defined in the MATLAB environment. Additionally, some comments on the execution of the "Multicore for MATLAB" library in a computer cluster are made.

2.2.1. Job-Task and Input Data

The task to be executed must be defined as a function within the MATLAB environment. The input parameters will be stored in a cell structure and the output parameters will also be returned as a cell. Input and output parameters may contain any type of variable format (double, matrix, string, cells, etc.).

The *testfun* function has been defined to be used as an example of how the library works:

```
[Out1,Out2]=testfun(Param1,Param2,Param3);
```

Input parameters are stored in a cell structure using the code lines shown in Figure 2.5.

```
paramCell = cell(1,N);
for k = 1:N
    paramCell{1,k} = {Param1(k),Param2(k),Param3(k)};
end
```

Figure 2.5. Library input parameters.

where *N* is the total number of executions.

The task-function is a standard MATLAB function, namely it only has access to locally defined variables and only returns the variables predefined as outputs; however the function can make use of auxiliary scripts saved as *.m* files.

2.2.2. Master Function and Main Parameters

As it was previously mentioned, one MATLAB session must serve as master; it is in the master session that the main script must be run. The main script must include the so-called *startmulticoremaster* function, which will be in charge for creating a set of *.mat* files containing the information required for the tasks to be executed. The master session is also in charge of collecting information produced by slave sessions.

Continuing with the *testfun* example, the following line presents the command to be executed in order to run the master function:

```
resultCell=startmulticoremaster(@testfun,paramCell,settings);
```

`testfun`: task-function to be executed
`paramCell`: cell structure with input data
`settings`: library settings, overwrite default values.
`resultCell`: cell structure with output data

In this scenario *testfun* outputs are assumed to be single values using double format; *Out1* and *Out2* are retrieved using the code presented in Figure 2.6.

```
for n=1:N
    resu=resultCell{n};
    Out1(n)=cell2mat(resu(1));
    Out2(n)=cell2mat(resu(2));
end
```

Figure 2.6. Output variables collection.

The library execution is controlled by a group of settings that can be overwritten to adapt to the user's needs. Settings must be defined before the *startmulticoremaster* function is executed. The main settings are:

settings.nrOfEvalsAtOnce

The *.mat* files generated by the library contain the information related to the tasks to be executed. Slave sessions read these *.mat* files and execute the tasks defined in them. This field determines the number of tasks that will be included in a single *.mat* file, thus the number of consecutive executions performed by a slave session.

settings.maxEvalTimeSingle

It is the maximum expected time for each individual execution. If the individual execution time expires and the master session has not received the output information from the slave session, it will assumed there has been an error and will execute the task itself.

settings.multicoreDir

This setting specifies the folder where the *.mat* files will be created. All slave sessions must have access to this directory.

settings.masterIsWorker

Defines whether the master session will be used to perform task executions or stay idle, waiting to gather information produced by slave sessions ("1" master sessions will perform some task executions, "0" master session will not perform any tasks).

2.2.3. Slave Function

The so-called *startmulticoreslave* function must be executed in every slave session; this function will load the *.mat* files created by the master function and execute the task-function with information contained in those files. While it is being executed, it will continuously read the specified folder searching for *.mat* files and execute the tasks contained in those files.

The slave function will be run executing the following command:

```
startmulticoreslave('C:\testdir')
```

`testdir`: folder where the slave function will search for *.mat* files; it must match the folder specified in *settings.multicoreDir*

2.2.4. Library Execution in a Computer Cluster

The use of the "Multicore for MATLAB" library is not constrained to a single multicore computer; its capabilities can also be used to control a group of computers (i.e. a computer cluster); this possibility will grant the user access to larger computational

resources. A computer cluster can be easily expanded by adding more nodes to its original structure, thus increasing the number of available cores for task executions. This increment in available cores will allow the user to achieve a greater reduction in execution times, since to number of task executions per core will be drastically reduced.

The implementation of the "Multicore for MATLAB" library in a cluster requires access to a folder that can be reached by all nodes that are scheduled to take part in the job execution. The *.mat* files and other files related to each task execution (e.g. task-function file and other auxiliary files) must be placed in this folder, so all slave sessions can reach them. The target folder must be defined using the complete access path (including host's name or IP address); this is a requirement for the nodes that will remotely access the folder. No additional actions are required for the library's cluster implementation.

2.3. Simulation of Power Distribution Systems Using Parallel Computing

OpenDSS is a distribution system simulator whose capabilities allow users to represent the most important distribution components and perform multiphase calculations; its solution algorithm is capable of performing many calculations in a short period of time (see [2.12] and Appendix A). Planning studies may require simulating the same system many times with only small variations in certain design parameters; although individual OpenDSS execution times are relatively short, total simulation times can be rather long if the number of required simulations for a certain study is too high. In many of these studies each execution can be performed independently and is not affected by the results obtained from other executions; these characteristics fit the definition of a Task-parallel job.

The embarrassingly parallel nature of many planning studies implies that parallel computing can be applied to these studies with the goal of reducing total simulation times. Furthermore, it means that OpenDSS can be used in conjunction with the "Multicore for MATLAB" library [2.11] for developing an application that introduces parallel computing to the simulation of power distribution systems. Moreover, this application can be developed for its use in a computer cluster.

The studies presented in the following Chapters of this Thesis are carried out taking advantage of the application of parallel computing to the simulation of power distribution systems. The objective is to have access to a large computational capacity in order to achieve the greatest reduction possible in total simulation times; for this purpose, OpenDSS and the "Multicore for MATLAB" library will be executed in a high performance computer cluster. The details regarding the characteristics of the multicore installation and the most important aspects of the implementation that allows the joint execution of OpenDSS and the "Multicore for MATLAB" library are presented in this Section.

2.3.1. Cluster Description

Hardware and Operative System

The computer cluster used for this implementation consists of four high performance servers; each equipped with two 8-core processors. The main characteristics of the servers in the multicore installation are as follows:

- Model: Fujitsu PRIMERGY CX 250 S1
- Processor: 2 Intel Xeon E5-2660 (8 Cores, Clock frequency = 2.2-3 GHz)
- Hard disc memory: 500 GB
- RAM memory: 128 GB
- Communication: 2x Port Gigabit Ethernet LAN.

Cluster servers run Linux's distribution Ubuntu as operative system (OS). However OpenDSS is only compatible with Windows; therefore it was decided to use virtual machines running Windows 7 Professional as OS. The Linux implementation allows the user to launch several virtual machines in each server, with the possibility to adjust the number of cores and memory of the virtual machines. For standard working conditions it was decided to execute eight virtual machines, each with 8 cores and 16 GB RAM each (see Figure 2.7).

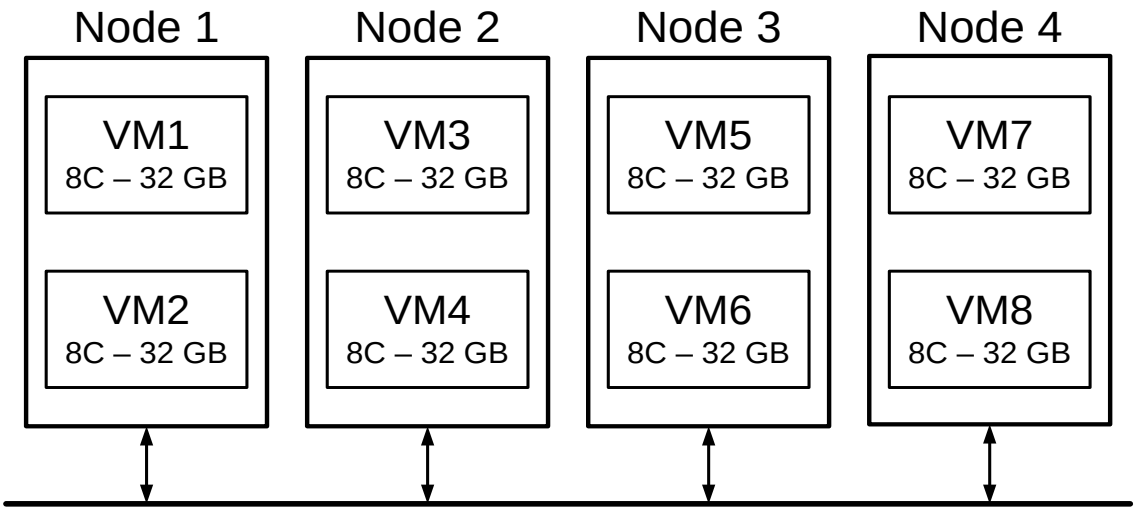

Figure 2.7. Virtual machines configuration.

Shared Folder

The first virtual machined launched is designated as the master; with the first virtual machine a shared folder (C:\Shared) that can be accessed by the rest of the virtual machines is created. This folder will appear as a local directory in all virtual machines; therefore it is not necessary to include the IP address or host's name as part of the access path. Additionally, this shared folder can be remotely accessed (from outside the cluster) to upload and download files from it.

A sub-folder has been created within the shared folder; this sub-folder will be used to contain the *.mat* files generated by the "Multicore for MATLAB" library. The complete sub-folder path is C:\Shared\files (Figure 2.8).

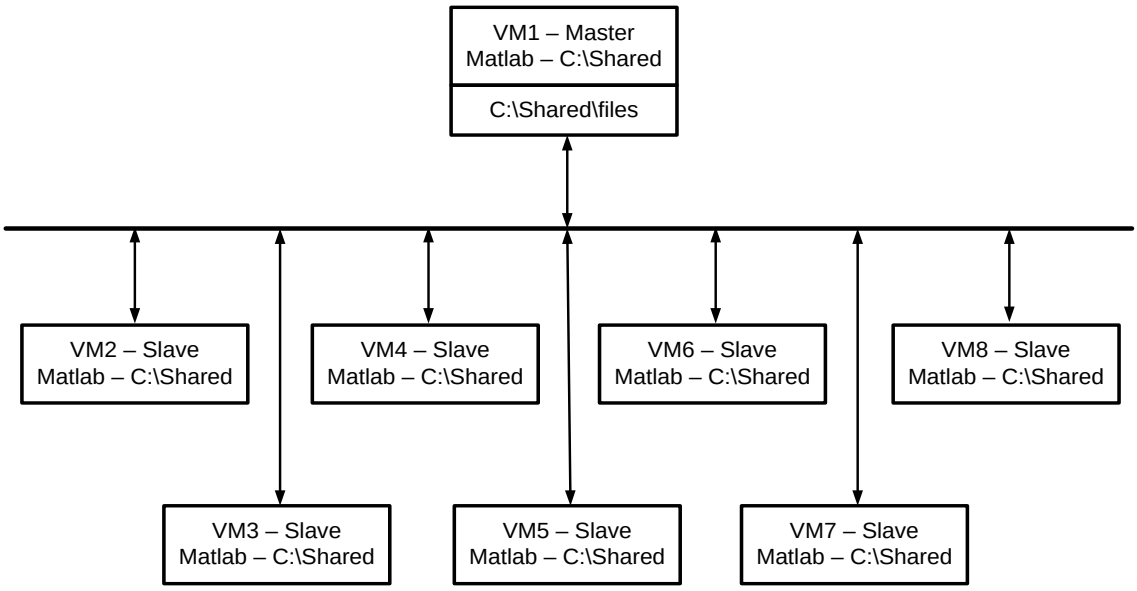

Figure 2.8. Shared folder and virtual machines.

2.3.2. MATLAB Sessions and OpenDSS

The number of concurrent MATLAB sessions must be equal to the desired number of parallel executions. The maximum number of concurrent sessions per virtual machine will be eight, as it is the number of cores assigned to each virtual machine (see Figure 2.7).

All MATLAB sessions must work with the same files to ensure the obtained results are correct. It has been decided that all *.m* and *.dss* files will be placed in the shared folder. C:\Shared will be the work folder for all MATLAB sessions.

An OpenDSS instance will be initiated in every MATLAB session; this will allow the parallel execution of the system to be simulated. OpenDSS instances will be started using the command:

```
[DSSStartOK, DSSObj, DSSText] = DSSStartup();
```

2.3.3. Slave Function Execution

All MATLAB slave sessions must run the *startmulticoreslave* function, as it was previously explained. When executing the slave function, the folder where the *.mat* files will be located must be specified; in this case the sub-folder created for containing the *.mat* files is used. The command to be run is:

```
startmulticoreslave('C:\Shared\files')
```

2.3.4. Master Function and Settings

The *startmulticoremaster* function must be included in the main *.m* file that will be executed in the MATLAB master session. The main library settings are specified as follows:

settings.nrOfEvalsAtOnce

The "Multicore for MATLAB" library does not possess a feature that allows it to balance the task distribution among available cores; therefore this option must be set to help distribute the required executions among the servers. If the total number of executions is relatively low compared to the total number of available cores, then one evaluation at once can be specified. If the number to executions is very large, then the number of evaluations at once can be defined as the rounded ratio between the total number of executions to the number of working sessions. This last option must be used with care, since the size of *.mat* files depend on the number of executions included and the information passed for every execution.

settings.maxEvalTimeSingle

This setting depends on the type of study and the test system to be analyzed.

settings.multicoreDir

This option must be set to generate the files in the sub-folder created for this purpose in the shared directory (C:\Shared\files).

settings.masterIsWorker

As a standard practice it has been decided that the master session will not perform any task execution; a consequence of this choice is that an extra slave session must be launched to obtain the desired number of concurrent executions.

2.3.5. Execution Overview

Figure 2.9 presents an overview of the interaction between OpenDSS and MATLAB in the application of parallel computing to the simulation of power distribution systems; it shows how the information is exchanged among the different tools present in the implementation. According to this diagram MATLAB is responsible for managing the complete process; it generates the input information required for the execution, passes information to OpenDSS via the COM Server, distributes the tasks among the available cores in the cluster, and collects and processes the information obtained from the simulations. Details related to input data generation and data handling will depend on the objective of the study, namely what information is necessary for individual task execution and how collected data have to be analyzed. The figure also shows how one

instance of OpenDSS is executed for every MATLAB slave session and system definition is loaded directly from *.dss* files; OpenDSS may require information generated by external tools (e.g. HOMER [2.13]) for specific solution modes, such as time-driven simulations. Finally, the "Multicore for MATLAB" library is embedded within MATLAB and is executed as part of the main script that controls the complete execution.

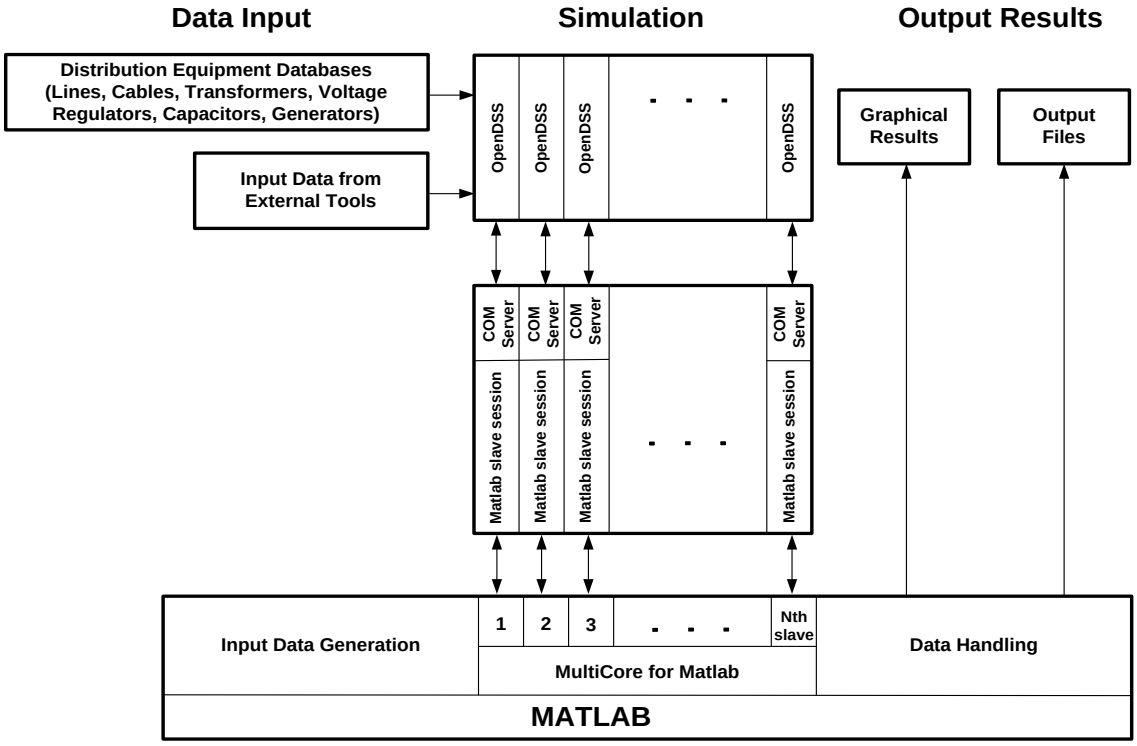

Figure 2.9. Block diagram of OpenDSS-MATLAB interaction.

2.3.6. Stand-Alone files

The configuration implemented requires one MATLAB license for every virtual machine running MATLAB sessions; for the present implementation floating campus licenses have been used for the virtual machines. This situation can become a problem when only a limited number of licenses is available, especially for certain toolboxes. Eight virtual machines will require eight MATLAB licenses and if a special toolbox is used (e.g. Statistics Toolbox), then eight licenses for the special toolbox will be needed. This inconvenient can be circumvented by using stand-alone files; these files will contain all files related to the task execution. Stand-alone files do not require MATLAB licenses as they interact directly with MATLAB installed libraries, thus only one MATLAB license will be needed, the one corresponding to the MATLAB master session.

Stand-alone File Structure

A main file must be created and added to the stand-alone file project; this file will contain the necessary commands to initiate an OpenDSS instance and execute the

library's slave function. The name *slavefun* will be used as example to create the main file in the MATLAB workspace.

```
function slavefun()
DSSStartOK, DSSObj, DSSText] = DSSStartup();
startmulticoreslave('C:\Shared\files')
```

Figure 2.10. *slavefun* function.

The stand-alone file project must also include all the necessary *.m* files related to the "Multicore for MATLAB" library and system simulation (task-function and auxiliary files). The file project will be compiled using MATLAB's *deploytool* (see Figure 2.11).

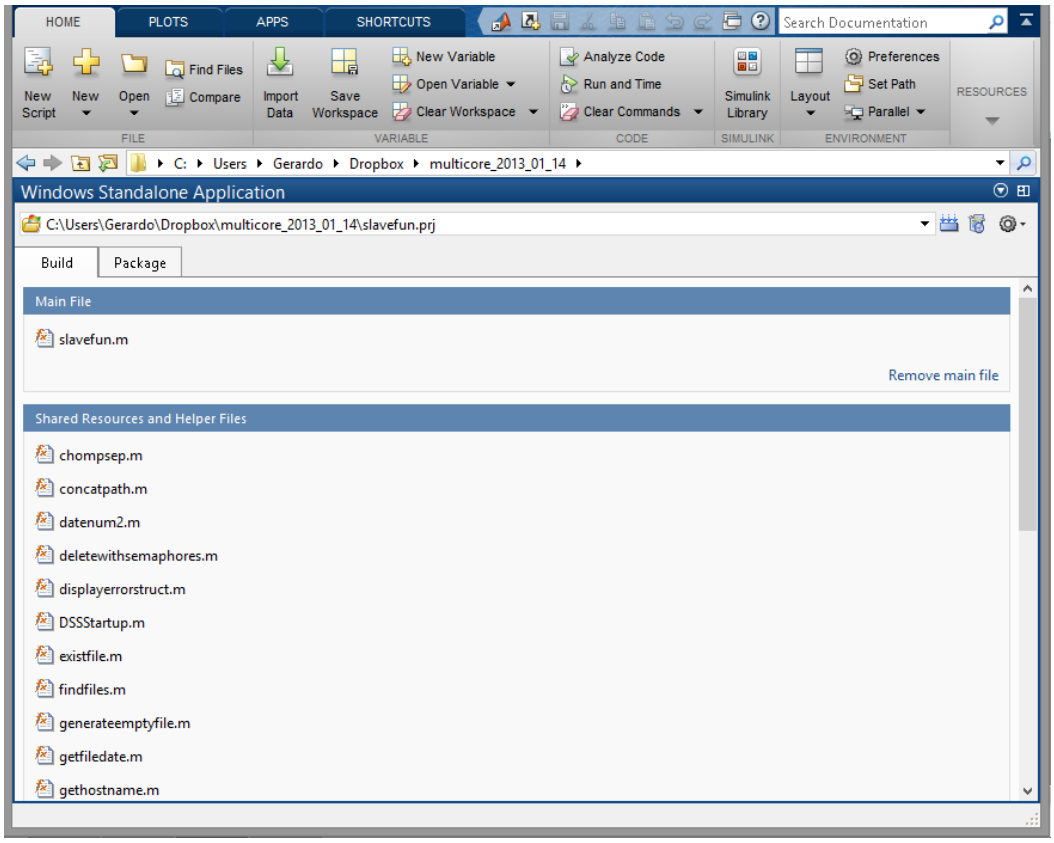

Figure 2.11. Deploytool user interface.

Each study will require a different stand-alone file, as the *.m* files needed for every task will be different. Once the stand-alone file has been created no changes to its internal structure can be made; if the project's *.m* files are modified or improved, a new stand-alone file must be generated.

Execution of Stand-alone Files

Stand-alone files will be uploaded into the shared folder, so they can be accessed from all virtual machines. The stand-alone files can be executed using the Windows prompt (see Figure 2.12) or by double-clicking on the *.exe* file. One instance of the stand-alone file must be executed for every desired slave session.

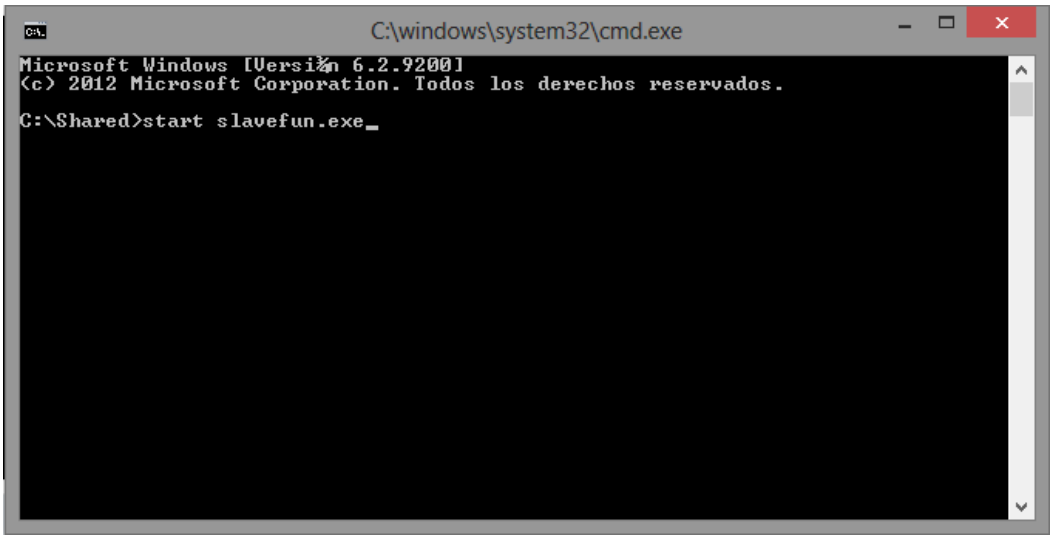

Figure 2.12. Execute stand-alone file from Windows prompt.

2.4. Case Study

A case study has been prepared in order to demonstrate the potential and the prospective reduction in total simulation times that can be achieved when applying parallel computing to the simulation of power distribution systems. The study presented in this Section is a parametric study; in it a distributed generator with a fixed rated power will be connected to all the available medium voltage nodes and different parameters will be monitored for every position to which the distributed generator is connected. Figure 2.13 shows the diagram of the test system used in this study; all loads are modeled using a constant power load model and the distributed generator will be modeled as a negative load. Some important numbers about the system are given below:

- Rated system voltage: 4.16 kV
- Rated power of substation transformer: 5000 kVA
- Number of medium-voltage nodes: 48
- Number of load nodes: 31
- Initial total load rated power: 2045 kW
- Overall line length: 18.52 km.

The evaluation period chosen for the study is 10 years, using a simulation time-step of one hour, and the monitored parameters are energy losses and minimum voltage in p.u. (among others); a MATLAB script has been developed to collect the necessary information needed to assess the impact of the distributed generator on the test system. Moreover, the study will be carried out using the multicore installation presented in the previous Sections, first using a single core and later using multiple slave sessions in order to determine the reduction in total simulation times.

The following Sections will present the MATLAB code used to control the “Multicore for MATLAB” library and to simulate the system for the specified evaluation period. Additionally, the results of the study will be presented and a comparison of total simulation times when using serial and parallel simulation of each execution will be made.

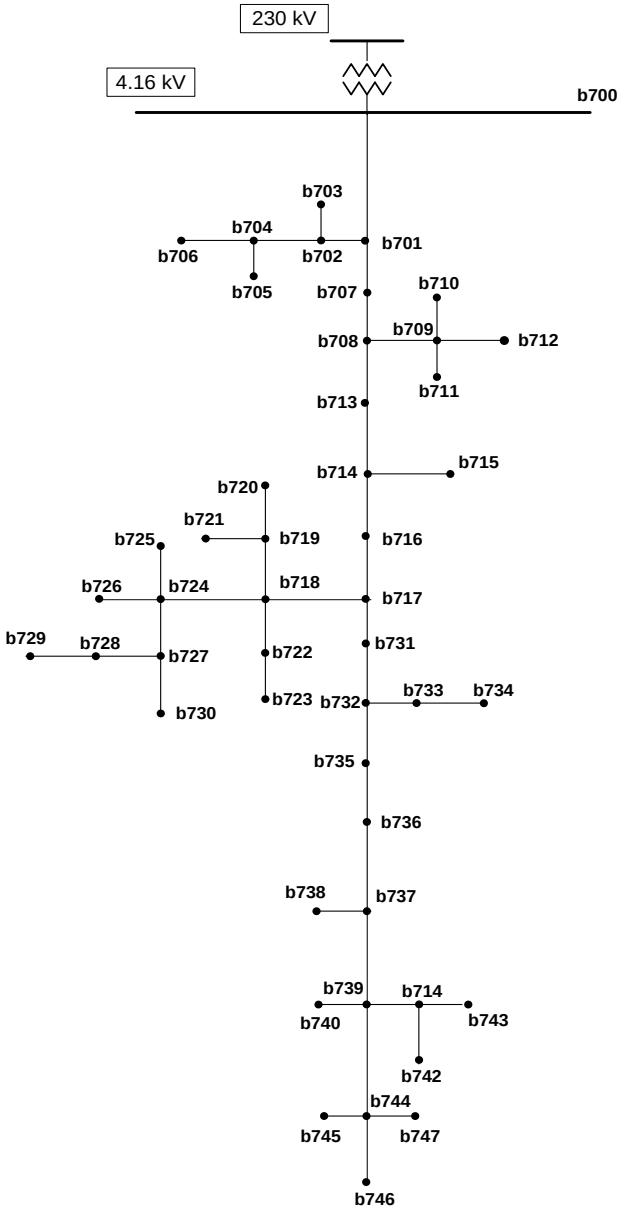

Figure 2.13. Diagram of the test system.

2.4.1. MATLAB Code

As it has been mentioned in the previous Sections of this Chapter the main settings of "Multicore for MATLAB" library must be set to accordingly to the study to be performed. Figure 2.14 presents the settings defined for the present study.

```
settings.nrOfEvalsAtOnce = 1;
settings.maxEvalTimeSingle = timeeval*2.5;
settings.multicoreDir='C:\Shared\files';
settings.masterIsWorker = 0;
parameterCell = cell(1,nb);
```

Figure 2.14. Settings for "Multicore for MATLAB" library.

where *nb* is the number of medium-voltage nodes and *timeeval* is the simulation time for a single execution; prior to the study execution the test system is simulated without distributed generation in order to estimate the execution time of the task-function.

The input data and execution of the master function is carried out using the code lines presented in Figure 2.15. The variables passed to the task-function are detailed in Table 2.1.

```
%Data input
for k = 1:nb
    paramCell{1,k} = {DSSObj,mydir,nomckt,k,kvckt,pu,hvstring,
                      trafnm,Busnames_Test(k),kvge,kW_DG,
                      yelshp,H,NA};
end
%Master function execution
resultCell = startmulticoremaster(@dg_fun,paramCell,settings);
```

Figure 2.15. Data input and master function execution.

Variable	Description
`DSSObj`	OpenDSS object interface
`mydir`	Folder that contains OpenDSS and MATLAB files
`nomckt`	Name of the master OpenDSS file
`k`	Execution index
`kvckt`	High-voltage system rated voltage
`pu`	Actual voltage in High-voltage system
`hvstring`	String with main parameters of High-voltage system
`trafnm`	Name of substation transformer
`Busnames_Test(k)`	Generator connection node
`kvge`	Generator rated voltage
`kW_DG`	Generator rated power
`yelshp`	Loadshape assigned to generator
`H`	Number of hours in one year
`NA`	Length of evaluation period

Table 2.1. Task-function input variables.

Figure 2.16 presents the main aspects of the *dg_fun* function, which is responsible for the simulation of every execution considered in the present study. All variable names presented in Table 2.1 have been preserved, with the exception of *Busnames_Test(k)* which has been renamed to *Bus*. In the *dg_fun* function the distributed generator is defined by creating a variable that contains a string with the generator definition, as one would use to define a generator in a *.dss* file. The remainder of the code is used to simulate the test system and collect the information required for the case study. Additionally, Figure 2.17 presents the MATLAB code used to retrieve the output variables generated by the *dg_fun* function; all output variables are stored in a matrix for further post-processing.

```
%Generator definition
DSSText.Command = ['New Generator.prueba',' bus1=',char(Bus),
                   ' phases=3 kv=',kvge,' kw=',num2str(kW_DG),
                   ' pf=1 yearly=',yelshp];
%System simulation
DSSCircuit.Solution.Number=1;
DSSSolution.Tolerance=1e-4;
%Power provided by HV system in kW
Power=zeros(H*NA,1);
%Total system losses in kW
Losses=zeros(H*NA,1);
%Minimum voltage in p.u.
Vmin=zeros(H*NA,1);
%Solution convergence
Convergence=zeros(H*NA,1);
%System overload
Overload=zeros(H*NA,1);
for nac=1:NA
    %Set Solution year
    DSSSolution.Year=nac;
    %Set solution hour
    DSSSolution.dblHour=H*(nac-1)+1;
    for n=1:H
        %Solve Circuit
        DSSSolution.Solve
        %Sample Emergy Meters
        DSSCircuit.Sample
        %Collect Power Provided by HV System
        Power(H*(nac-1)+n)=-DSSCircuit.TotalPower(1);
        %Collect Total System Losses
        Losses(H*(nac-1)+n)=DSSCircuit.Losses(1)/1000;
        %Collect All Node Voltages
        Vckt=DSSCircuit.AllBusVmagPu;
        %Obtain Minimum Voltage in p.u.
        Vmin(H*(nac-1)+n)=min(Vckt);
        %Collect Solution Convergence
        Convergence(H*(nac-1)+n)=DSSSolution.Converged;
        %Collect System Overload
        Overload(H*(nac-1)+n)=DSSEmeter.totals(9);
    end
end
%Total Active Energy
Energy_HV=sum(Power);
%Total Energy Losses
Losses_HV=sum(Losses);
%Minimum Yearly Voltage in p.u.
MinimumV=min(Vmin);
%Outout Cell
Output={Energy_HV,Losses_HV,MinimumV,Hour_overload,
        Total_convergence};
```

Figure 2.16. Task-function code.

```
%Total Active Energy
Energy_HV=zeros(nb,1);
%Total Energy Losses
Losses_HV=zeros(nb,1);
%Minimum Yearly Voltage in p.u.
MinimumV=zeros(nb,1);
%Circuit convergence
Circuit_convergence=zeros(nb,1);
%Number of hours with overload
Hour_overload=zeros(nb,1);
for n=1:nb
    resu=resultCell{n};
    Energy_HV(n)=cell2mat(resu(1));
    Losses_HV(n)=cell2mat(resu(2));
    MinimumV(n)=cell2mat(resu(3));
    Circuit_convergence=cell2mat(resu(4));
    Hour_overload=cell2mat(resu(5));
end
```

Figure 2.17. Output data retrieval.

2.4.2. Simulation results

The main results obtained from the simulations are presented in Figure 2.18 and Figure 2.19; from these results it is possible to observe that the impact the distributed generator has on the system will depend on the connection node, even though the same generation curves and rated power have been used in every execution. As expected, the active energy provided by the HV systems and energy losses present the same behavior pattern, although it is much harder to recognize on the active energy provided by the HV system due to scale differences.

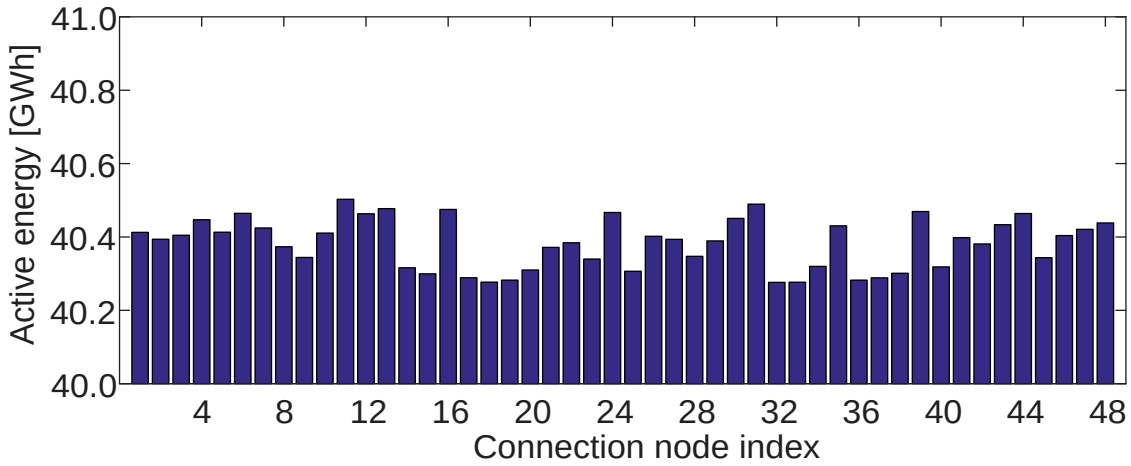

Figure 2.18. Energy required from the HV system.

The minimum energy losses and active energy are produced when the distributed generator is connected to node b730 (see Figure 2.13); however, several nodes present losses values similar to those achieved when the distributed generator is connected to node b730, in fact these differences can be below 0.1%. The minimum voltage during the evaluation period presents the same value regardless of the generator's connection node (0.9281 p.u.); this value is produced during the fifth year of the evaluation period

and it occurs at a moment when the power produced by the distributed generator is equal to zero; therefore, the presence of DG will have no impact on minimum system voltages.

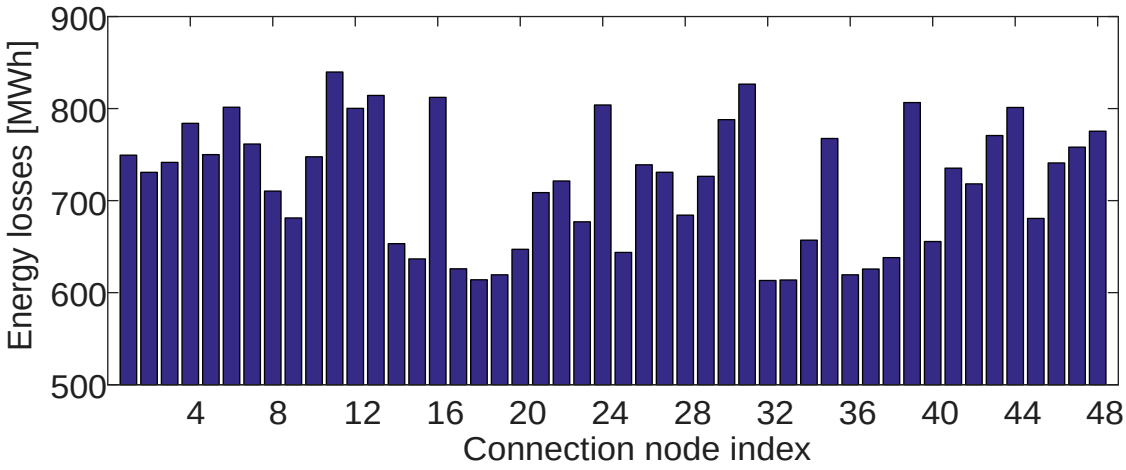

Figure 2.19. Energy losses.

The main objective of this case study is to determine the differences in evaluation times when using serial and parallel computing, total execution times are presented in Table 2.2. The approximate evaluation time of a single execution with serial computing is 58 seconds, whereas the total evaluation time using the multicore installation is approximately 69 seconds. For this study the total number of evaluations is smaller than the number of available cores, therefore all evaluations can be performed simultaneously. However, one can observe some differences between these evaluation times; these differences are partly produced by the overhead times caused by the tasks distribution among available cores. Moreover, the concurrent use of several cores on the same processor causes a reduction in performance, which leads to larger evaluation times.

Number of cores	Total Execution time
1	2788.3 s
60	69.6 s

Table 2.2. Simulation times comparison.

With the use of parallel computing the same study has been completed 40 times faster than with serial computing, which represents a time reduction of 97.5%. Although the execution time for the present case study is not too large, it allows assessing the time reduction that can be achieved with the multicore installation presented in the present Chapter; furthermore, the actual time reduction found in this case study (i.e. 97.5%) remains almost constant for all the studies carried out for this Thesis.

2.5. Conclusions

This Chapter makes a brief introduction of some of the main parallel computing concepts; the difference between serial and parallel computing was first presented, as well as different types of hardware configurations. Finally, a classification of parallel

jobs based on how the computational resources are used to solve the problem was summarized.

The Chapter also introduces the most important features of the "Multicore for MATLAB" library [2.11], and how it can be used to perform embarrassingly parallel jobs. A very interesting characteristic of this library is that it does not require any special license for its use; it is comprised by a set of *.m* files that interact with different MATLAB sessions in order to carry out the task at hand. Another key aspect is that it can be readily expanded to work with a computer cluster; the only requirement is to have a shared directory that can be accessed by all nodes that are part of the computer cluster. The "Multicore for MATLAB" library may exhibit a lower efficiency than MATLAB's native capabilities; however the extra overhead time caused by a less efficient task distribution and data collection does not pose a problem when individual execution times are larger than a few seconds, which is the case with most planning studies.

The introduction of parallel computing to the simulation of power distribution systems becomes a necessity when the user desires to perform a study that will require a large number of executions and the total simulation time is prohibitive when the executions are performed in a serial manner. The application presented in this Chapter uses the "Multicore for MATLAB" library in conjunction with OpenDSS for the execution of embarrassingly parallel jobs in a computer cluster; this implementation allows taking advantage of computational resources larger than those available in a single multicore computer. In this application, OpenDSS is in charge of carrying out the system simulation, while MATLAB (through the library) handles the task distribution among the available slave sessions. MATLAB is also responsible for collecting and processing the data produced by the slave sessions as a result of the task execution.

2.6. References

[2.1] X. Cai, E. Acklam, H.P. Langtangen, and A. Tveito, Parallel Computing, Chapter 1 of *Advanced Topics in Computational Partial Differential Equations*, H.P. Langtangen and A. Tveito (Eds.), Springer, 2003.

[2.2] M. Skuhersky, "Introduction to Parallel Computing". Available from http://web.mit.edu/vex/www/Parallel.pdf

[2.3] A. Grama, A. Gupta, G. Karypis, and V, Kumar, *Introduction to Parallel Computing*, 2nd Edition, Addison Wesley, 2003

[2.4] D.M. Falcao, C.L.T. Borges, and G.N. Taranto, "High Performance Computing in Electrical Energy Systems Applications," Chapter 1 of *High Performance Computing in Power and Energy Systems*, S. Kumar Khaitan and A. Gupta (Eds.), Springer, 2013.

[2.5] D.J. Tylavsky, A. Bose, F. Alvarado, R. Betancourt, K. Clements, G.T. Heydt, I.M. Huang, M. La Scala, and M.A. Pai, "Parallel processing in power systems computation," *IEEE Trans. on Power Systems*, vol. 7, no. 2, pp. 629–638, May 1992.

[2.6] P. Krastev, "Introduction to Parallel Computing". Available from http://www.physics.sdsu.edu/~johnson/phys580/Parallel_computing1.pdf

[2.7] Boston University, "MATLAB Parallel Computing Toolbox Tutorial". Available from http://www.bu.edu/tech/support/research/training-consulting/online-tutorials/matlab-pct

[2.8] J. Kepner, *Parallel MATLAB for Multicore and Multinode Computers*, SIAM, 2009.

[2.9] C. Moler, *Parallel MATLAB: Multiple processors and multiple cores*, TheMathWorksNews & Notes, 2007.

[2.10] P. Luszczek, "Enhancing multicore system performance using parallel computing with MATLAB," *MATLAB Digest*, 2008.

[2.11] M, Buehren, *MATLAB Library for Parallel Processing on Multiple Cores*, Copyright 2007. Available from http://www.mathworks.com.

[2.12] R. Dugan, T.E. McDermott, "An Open Source Platform for Collaborating on Smart Grid Research", *IEEE PES General Meeting*, Detroit, USA, July 2011.

[2.13] HOMER Software, National Renewable Energy Laboratory (NREL), 2003. Available at http://www.nrel.gov/homer.

Chapter 3

System Curves

3.1. Introduction

Continuous advance in software packages have resulted in the development of powerful simulation tools aimed at meeting the requirements of modern studies in power distribution systems. One of the most important features introduced in recent years is the capability to perform time-driven (or quasi-static) solutions; this characteristic allows the user to carry out simulations where system element behavior (e.g. load and generation) varies with time.

Although time-driven simulations permit a more realistic representation of power distribution systems, performing studies over an arbitrary period of time is no easy task; in addition to system equipment information (lines, cables, transformers, voltage regulators, loads, capacitors, generators, etc.) system performance over the evaluation period must also be defined. This performance will be described by a set of curves that will dictate the behavior of loads, generators, and other elements in the system. In [3.1] different load profiles and generation curves were estimated using HOMER capabilities [3.2].

Certain types of studies (such as feasibility studies) consider evaluation periods as long as 20 years; in such cases curves must be yearly updated taking into account randomness in both load and generation shapes and the load variation (usually an increase); the objective is to avoid repeating consumption and generation patterns during the study. For longer evaluation periods each element curve must define an individual value for every point in the curve; for example, if the study covers 10 years, each (load and generation) curve will have 87600 points, one for every hour of the evaluation period (assuming a 1-hour time-step).

Three different algorithms have been implemented in MATLAB in order to generate curves that dictate system element behavior, namely:

- Photovoltaic (PV) generation curves
- Wind generation curves
- Node load profiles

The curves resulting from the implemented algorithms will be used as input for studies/simulations that require this information to determine the behavior of loads and generators over the evaluation period. By default curves will be created for an evaluation period of one year using a 1-hour time-step; however, the algorithms must be able to generate curves for different evaluation periods.

The content in the present Chapter has been organized as follows. Section 3.2 presents the procedure developed for obtaining Photovoltaic generation curves. In Section 3.3 the algorithm implemented for the creation of Wind generation curves is detailed. Section 3.4 introduces the procedure for the generation of Node Load profiles. Section 3.5 presents a case study developed to demonstrate the usefulness of the implemented algorithms. Finally, the main conclusions of this Chapter are summarized in Section 3.6.

3.2. PV Generation Curves

PV generation is determined by the availability of the solar resource. Solar radiation varies throughout the year and also depends on the location of the evaluation site. Moreover, a model for the PV generator is needed to calculate the actual power injected into the grid; depending on the model's complexity more parameters can be required, such as ambient temperature, generator efficiency, inverter model, etc.

The rest of this section introduces the OpenDSS PV generator model, the generation of solar irradiance curves, and the generation of PV panel temperature.

3.2.1. Built-in OpenDSS PV System Element Model

The built-in PV model includes the array and the inverter into a single model adequate for distribution system impacts studies, and is useful for simulations with time steps greater than 1s. The model assumes the inverter is able to find the maximum power point (mpp), being the active power a function of the irradiance, temperature, rated power at the mpp (*Pmpp*) at a selected temperature and an irradiance of 1.0 kW/m^2, and the efficiency of the inverter at the operating power.

In addition to the rated voltage and power of the PV array and inverter, the data to be specified are: (i) an average *Pmpp* at 1 kW/m^2 irradiance and a constant panel temperature; (ii) the pu variation of *Pmpp* as a function of the cell temperature at 1 kW/m^2 irradiance, and (iii) the efficiency curve for the inverter (i.e., pu efficiency vs pu power). Reactive power is specified separately from the active power as either a fixed kvar values or a fixed power factor value. The model provides the active and reactive power injected to the distribution system. Figure 3.1 shows a simplified scheme of this model [3.3], [3.4]. Notice that the PV model uses the panel operating temperature, not the ambient temperature.

This model has been expanded to obtain a standalone representation without appealing to any external tool. Irradiance and Panel temperature have been incorporated using the procedures presented in the following Sections.

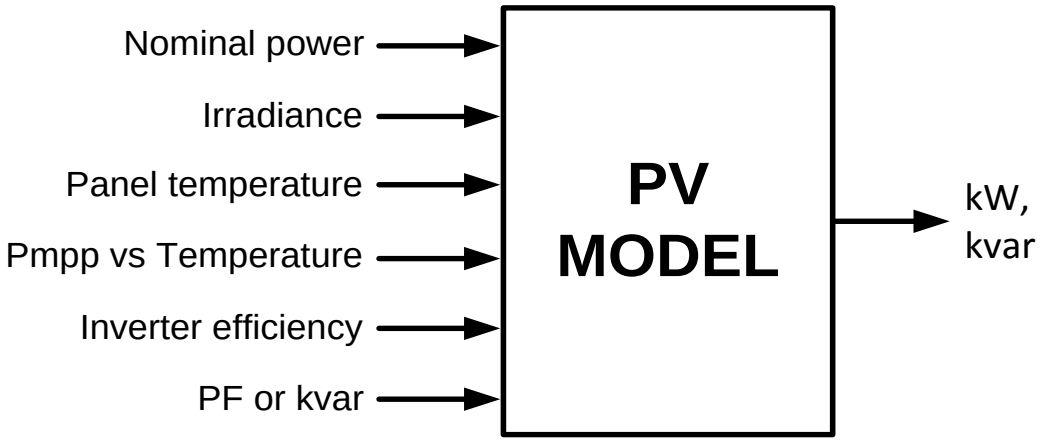

Figure 3.1. Scheme of the OpenDSS PV generator model.

3.2.2. Generation of the Yearly Curve of Solar Irradiance

The solar irradiance curves are derived by means of an algorithm that can obtain the hourly solar irradiance for a PV array from its slope angle (tilted surface), its geographical coordinates (latitude, altitude and hourly zone) and the average monthly values of the solar resource (i.e., average clearness index). The algorithm must take into account the randomness of the solar resource, namely include the possibility of a more or less clear sky and the intermittent presence of clouds.

The following steps have been implemented to generate hourly values of incident irradiance on a tilted surface:

- Calculation of the daily clearness index
- Calculation of the hourly clearness index for a given day
- Calculation of the hourly solar irradiance

Calculation of the Daily Clearness Index

The synthesis of time series of solar irradiance is made by using clearness indices [3.5]. The clearness index is the ratio of measured data to the extraterrestrial radiation. The method used in this work is that implemented in Hybrid2 [3.5] and provides a statistical distribution of the daily clearness index, K_t, as a function of the average monthly clearness index using the following probability density function (defined between K_{tmin} and K_{tmax}, which depend on the monthly average clearness index $\overline{K_T}$):

$$p(K_T) = \frac{\gamma \cdot e^{-\gamma \cdot K_T}}{e^{-\gamma \cdot K_{T,\min}} - e^{-\gamma \cdot K_{T,\max}}} \tag{3.1}$$

where

$$\gamma = -1.498 + \frac{1.184 \cdot \xi - 27.182 \cdot e^{-1.5\xi}}{K_{T,\max} - K_{T,\min}} \tag{3.2}$$

$$\xi = \frac{K_{T,\max} - K_{T,\min}}{K_{T,\max} - K_T} \tag{3.3}$$

$$K_{T,\max} = 0.6316 + 0.267 \cdot \overline{K_T} - 11.9 \cdot \left(\overline{K_T} - 0.75\right)^8 \tag{3.4}$$

$$K_{T,\min} = 0.05 \tag{3.5}$$

The estimation of the average clearness index is made independently for each month and uses average monthly clearness indices. These indices can be obtained from some data bases with information for a specific location [3.6].

Calculation of Hourly Clearness Index for a Given Day

For each day there exists an ordered set of values of the hourly clearness index, k_t. Given such values and the corresponding set of ordered extraterrestrial irradiation values, the daily clearness index K_t takes on a unique value. According to [3.7], the variation of k_t may consist of two components (a mean component and a random component):

$$k_t = k_{tm} + \alpha \tag{3.6}$$

The mean component k_{tm} represents the clearness index if the presence of radiation attenuators were uniformly distributed over the day:

$$k_{tm} = \lambda + \varepsilon \cdot e^{-k \cdot m} \tag{3.7}$$

where

$$\lambda\left(K_T\right) = K_T - 1.167 \cdot K_T^3 \cdot \left(1 - K_T\right) \tag{3.8}$$

$$\varepsilon\left(K_T\right) = 0.979 \cdot \left(1 - K_T\right) \tag{3.9}$$

$$k\left(K_T\right) = 1.141 \cdot \left(\frac{1 - K_T}{K_T}\right) \tag{3.10}$$

$$m = \frac{1}{\cos\left(\theta_Z\right)} \tag{3.11}$$

being θ_z the zenith angle.

The random component α incorporates the effect of random variations mainly caused by varying cloud cover, and can be approximated by a beta function:

$$\alpha(t) = \phi \cdot \alpha(t-1) + v(t) \tag{3.12}$$

$$\phi = 0.35 + 1.1 \cdot (1 - K_T) \tag{3.13}$$

The beta distribution is defined using the normalized variable defined below:

$$u = \frac{k_t - k_{tl}}{k_{tu} - k_{tl}} \tag{3.14}$$

The distribution parameters are calculated using the following equations:

$$\sigma_\alpha = 0.16 \cdot \sin\left(\pi \cdot \left(\frac{K_T}{0.9}\right)\right) \tag{3.15}$$

$$U = \frac{k_{tm} - k_{tl}}{k_{tu} - k_{tl}} \tag{3.16}$$

$$\sigma_u = \frac{\sigma_\alpha}{k_{tu} - k_{tl}} \tag{3.17}$$

$$k_{tl} = \max(0, k_{tm} - 4\sigma_\alpha) \tag{3.18}$$

$$k_{tu} = \min(0, k_{tm} + 4\sigma_\alpha) \tag{3.19}$$

$$A = \frac{U^2 \cdot (1-U)}{\sigma_u^2} - U \tag{3.20}$$

$$B = \frac{A \cdot (1-U)}{U} \tag{3.21}$$

where *A* and *B* are beta distribution shape parameters.

Calculation of Hourly Solar Irradiance

The following parameters are required to calculate the solar irradiance on a tilted surface [3.5]:

- Site latitude (ø)
- Site longitude (L)
- Ground's reflection coefficient, (ρ)
- GMT time zone (Zc)
- Panel's slope angle (β)
- Panel's azimuth angle (α)

For every day of the year the following parameters must be calculated:

- Solar declination angle

$$\delta = 23.45 \cdot \sin\left(2\pi\left(\frac{284+n}{365}\right)\right) \tag{3.22}$$

- Sunset angle

$$w_s = \cos^{-1}\left(\tan(L)\cdot\tan(\delta)\right) \tag{3.23}$$

- Equation of time

$$B = 2\pi\left(\frac{n-1}{365}\right) \tag{3.24}$$

$$E = 3.82 \cdot \begin{pmatrix} 0.000075 + 0.001868\cdot\cos(\mathrm{B}) - 0.032077\cdot\sin(\mathrm{B}) \\ - 0.014615\cdot\cos(2\mathrm{B}) - 0.04089\cdot\sin(2\mathrm{B}) \end{pmatrix} \tag{3.25}$$

where n is the day of the year (1-365).

For every hour of the day it is necessary to calculate the solar time:

$$w = \left(t_c + \frac{L}{15} - Z_c + E - 12\right)\cdot 15[^\circ] \tag{3.26}$$

where t_c is the civil time.

The clearness index is the ratio between the actual average hourly irradiance on the horizontal (G) to the average irradiance outside the earth's atmosphere (G_0) [3.5]:

$$G = k_t \cdot G_0 \tag{3.27}$$

where

$$G_0 = G_{sc}\left(1 + 0.33\cdot\cos\left(2\pi\cdot\left(\frac{n}{365}\right)\right)\right)\left[\cos(\phi)\cdot\cos(\delta)\cdot\cos(w) + \sin(\phi)\cdot\sin(\delta)\right] \tag{3.28}$$

$$k_t \le 0.22 \qquad G_d = (1 - 0.09\cdot k_t)\cdot G_0 \tag{3.29a}$$

$$0.22 < k_t \le 0.8 \qquad G_d = \begin{pmatrix} 0.9511 - 0.1604\cdot k_t + 4.388\cdot k_t^2 \\ -16.638\cdot k_t^3 + 12.336\cdot k_t^4 \end{pmatrix}\cdot G_0 \tag{3.29b}$$

$$k_t > 0.8 \qquad G_d = 0.165 \cdot G_0 \tag{3.29c}$$

$$G_b = G_0 - G_d \tag{3.30}$$

where G_{sc} is the solar constant (1.367 kW/m^2).

The equation used for calculating the irradiance on a tilted surface, given the irradiance on a horizontal surface, is as follows [3.5]:

$$\begin{aligned} G_T = & \left(G_b + G_d \cdot A_i\right) \cdot R_b \\ & + G_d \cdot (1 - A_i) \cdot \left(\frac{1+\cos(\beta)}{2}\right) \cdot \left(1 + f \cdot \sin^3\left(\frac{\beta}{2}\right)\right) \\ & + G \cdot \rho \cdot \left(\frac{1-\cos(\beta)}{2}\right) \end{aligned} \tag{3.31}$$

where

$$A_i = \frac{G_b}{G_0} \tag{3.32}$$

$$f = \sqrt{\frac{G_d}{G}} \tag{3.33}$$

$$R_b = \frac{\cos(\theta)}{\cos(\theta_Z)} \tag{3.34}$$

$$\begin{aligned} \cos(\theta) = & \sin(\delta) \cdot \sin(\phi) \cdot \cos(\beta) \\ & - \sin(\delta) \cdot \cos(\phi) \cdot \sin(\beta) \cdot \cos(\alpha) \\ & + \cos(\delta) \cdot \cos(\phi) \cdot \cos(\beta) \cdot \cos(w) \\ & - \cos(\delta) \cdot \sin(\phi) \cdot \sin(\beta) \cdot \cos(\alpha) \cdot \cos(w) \\ & + \cos(\delta) \cdot \sin(\beta) \cdot \sin(\alpha) \cdot \sin(w) \end{aligned} \tag{3.35}$$

$$\cos(\theta_Z) = \cos(\phi) \cdot \cos(\delta) \cdot \cos(w) + \sin(\phi) \cdot \sin(\delta) \tag{3.36}$$

3.2.3. Generation of the Yearly Curve of Panel Temperature

Panel temperature is used by the PV generator model to determine its operational efficiency; it is derived from ambient temperature and solar irradiance. Ambient temperature presents a random behavior which must be replicated by the implemented algorithm. The procedure implemented to obtain the panel temperature has been also divided into three steps:

- Calculation of minimum and maximum daily temperatures
- Calculation of hourly temperatures
- Calculation of average panel temperature

Calculation of Minimum and Maximum Daily Temperatures

The temperature is assumed to have a Gaussian behavior. The average daily value is obtained from the average monthly values of the minimum and maximum temperatures; daily values are generated using the following standard deviations based on [3.8], [3.9]:

$$\sigma_{T\min} = \max\left(0.5, \left(\frac{5.2 - 0.13 \cdot \overline{T_{\min}}}{2}\right)\right) \tag{3.37}$$

$$\sigma_{T\max} = \max\left(0.5, \left(\frac{5.8 - 0.09 \cdot \overline{T_{\max}}}{2}\right)\right) \tag{3.38}$$

Calculation of Hourly Temperatures

Hourly temperature values are obtained from the maximum and minimum temperature values for day of operation. The day is divided into three segments and the calculations use the temperature values of the previous and the subsequent day [3.10]:

- Midnight to sunrise + 2 h

$$T_a(h) = T_L - S \cdot \left(h + 24 - h_{s(n-1)}\right) \tag{3.39}$$

where

$$\tau = \frac{\pi\left(h_{s(n-1)} - h_{r(n-1)} - 2\right)}{h_{s(n-1)} - h_{r(n-1)}} \tag{3.40}$$

$$T_L = T_{\min(n-1)} + \left(T_{\max(n-1)} - T_{\min(n-1)}\right)\sin(\tau) \tag{3.41}$$

$$S = \frac{T_L - T_{\min(n)}}{24 - h_{s(n-1)} + h_{r(n)} + 2} \tag{3.42}$$

- Sunset to midnight

$$T_a(h) = T_L - S \cdot \left(h - h_{s(n)}\right) \tag{3.43}$$

where

$$\tau = \frac{\pi\left(h_{s(n)} - h_{r(n)} - 2\right)}{h_{s(n)} - h_{r(n)}} \tag{3.44}$$

$$T_L = T_{\min(n)} + \left(T_{\max(n)} - T_{\min(n)}\right)\sin(\tau) \tag{3.45}$$

$$S = \frac{T_L - T_{\min(n+1)}}{24 - h_{s(n)} + h_{r(n+1)} + 2} \tag{3.46}$$

- Daylight hours

$$T_a(h) = T_{\min(n)} + \left(T_{\max(n)} - T_{\min(n)}\right) \cdot \sin(\tau) \tag{3.47}$$

where

$$\tau = \frac{\pi\left(h - h_{r(n)} - 2\right)}{h_{s(n)} - h_{r(n)}} \tag{3.48}$$

$T_a(h)$ is the temperature at hour h, n is the current day of the year, h_s is the time of sunset, h_r is the time of the sunrise, and $T_{\min}$ and T_{max} are temperature limits.

Calculation of Average Panel Temperature

The panel operation temperature is obtained by means of the following equation [3.11]:

$$T_{panel} = T_a + \frac{T_n - 20}{800} G_T \tag{3.49}$$

where T_a is the ambient temperature, obtained according to (3.39), (3.43), and (3.47); G_T is the irradiance and T_n is the *normal operating cell temperature*.

3.3. Wind Generation Curves

Wind generation curves are obtained from wind speed curves. Wind speed curves may be synthesized by adding a deterministic component, which defines the general annual trend, and a stochastic component, responsible for introducing a random element in hour-to-hour values. The resulting wind speed values are adjusted to match statistical properties of the evaluation site. In addition, wind speed values must be corrected to match the actual height of the wind turbine. The power generated by the turbine/generator is calculated using the wind-power curves. Finally, the turbine power is adjusted to take into account the actual air density.

The general procedure implemented to obtain the yearly wind speed variation is based on the method proposed in [3.12]. The main steps are:

1. Calculate deterministic curve of wind speed values.
2. Generate wind curve's stochastic component.
3. Sum of deterministic and stochastic components.
4. Final probability density function (PDF) transformation.
5. Height correction.
6. Calculation of generated power.
7. Air density correction.

3.3.1. Calculate Deterministic Curve of Wind Speed Values

The deterministic curve will dictate wind speed's general behavior during the year. The deterministic curve will be based on the site's monthly average values and the equation that describes the curve's hourly values. The steps followed to calculate the deterministic curve are:

1. Make the daily average value of wind speed the same as the monthly average value.
2. Add Gaussian noise to daily average values.
3. Calculate hourly wind speed values using the equation:

$$v(h) = v_d \cdot \left(1 + i_d \cdot \cos\left(\frac{2\pi}{24} \cdot (h - h_p)\right)\right) \tag{3.50}$$

$$h = [1,\ 8760] \tag{3.51}$$

where v_d is the daily average wind speed value, i_d is the ratio of cosine function's amplitude to daily average wind speed value, and h_p is the wind speed peak hour.

3.3.2. Generate Wind Curve's Stochastic Component

Wind curve's stochastic component will be generated using the following equation:

$$r(h) = a \cdot r(h-1) + g(h) \tag{3.52}$$

where a is the auto-regression coefficient and g is the Gaussian noise with zero mean and unity standard deviation.

3.3.3. Sum of Deterministic and Stochastic Components

The deterministic and stochastic components do not follow the same PDF; therefore it's necessary to perform a PDF transformation on one of the components, so they can be summed without problems. The procedure for summing both components is [3.2]:

1. Perform a PDF transformation on *v(h)*, so it follows the same PDF as *r(h)*. The cumulative distribution function (CDF) value of every *v(h)* element must be mapped on *r(h)*'s CDF to find the corresponding value.

$$v(h) \rightarrow v_{norm}(h) \tag{3.53}$$

2. Directly sum the stochastic and deterministic components.

$$v'_{norm} = v_{norm} + r \tag{3.54}$$

3.3.4. Final Probability Density Function (PDF) Transformation

It is widely accepted that the best fit for wind speed values is the Weibull distribution. The Weibull distribution is defined by the following equation:

$$f(v) = \frac{k}{c} \cdot \left(\frac{v}{c}\right)^{k-1} \exp\left[-\left(\frac{v}{c}\right)^{k}\right] \tag{3.55}$$

$$\bar{v} = c \cdot \Gamma\left(\frac{1}{k} + 1\right) \tag{3.56}$$

where $f(v)$ is the probability of v, k is the shape factor, c is the scale factor, and Γ is a Gamma function.

Using the same principle previously explained v'_{norm} will be transformed to follow a Weibull distribution.

$$v'_{norm} \rightarrow v_{weibull} \tag{3.57}$$

3.3.5. Height Correction

Wind speed must be corrected to match the height of the wind turbine. The height correction will be done using the following equation [3.2]:

$$v = v_{ref} \frac{\ln\left(\frac{z}{z_0}\right)}{\ln\left(\frac{z_{ref}}{z_0}\right)} \tag{3.58}$$

where v is the wind speed at height z [m/s], z is the height above ground [m], v_{ref} is the wind speed at height z_{ref} [m/s], z_{ref} is the reference height above ground [m], and z_0 is the roughness length in wind direction [m].

3.3.6. Calculation of Generated Power

The power produced by the turbine/generator can be calculated using the wind-power curves. The corrected wind speed values are evaluated in the curve in order to obtain the corresponding power values [3.2]. Wind-power curves are formed using a set of reference wind speeds values and the matching generated powers (see Figure 3.2). Each corrected wind speed value is mapped in the corresponding wind-power curve (according to the turbine's rated power) and the actual generated power is estimated by means of a simple interpolation method.

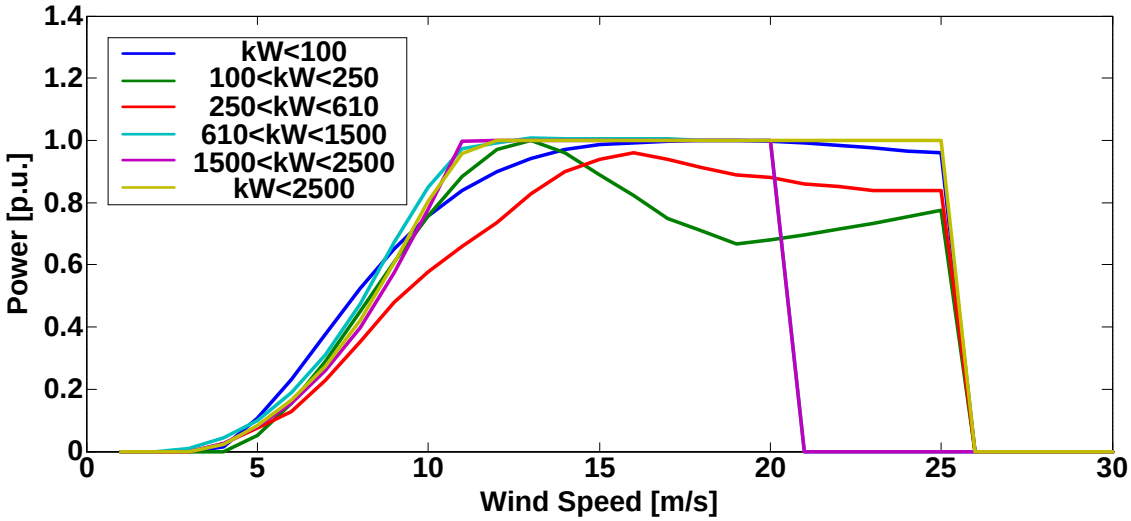

Figure 3.2. Wind turbine power vs. wind speed.

3.3.7. Air Density Correction

Wind-power curves are calculated under standard conditions; the power obtained after evaluating the corrected wind speed must be adjusted to take into account the variation of air density. Air density correction will be done using the following equations [3.2]:

$$\frac{\rho}{\rho_0} = \left(1 - \frac{0.0065 \cdot H}{288.16}\right)^{\frac{9.81}{287 \times 0.0065}} \left(\frac{288.16}{T_a}\right) \tag{3.59}$$

$$P_{WT} = \frac{\rho}{\rho_0} \cdot P_{WT\_STD} \tag{3.60}$$

where ρ is the air density [kg/m^3], ρ_0 is the air density at standard conditions [kg/m^3], H is the site altitude over sea level [m], and T is the ambient temperature [K].

3.3.8. Estimation of Curve Generation Parameters

Certain parameters used for the generation of wind speed curves need to be estimated for every specific site under study, since they are usually not available in any database. The parameters to be estimated are: i_d, h_p, a and k. A genetic algorithm can be used to estimate all parameters [3.12]; the objective will be to minimize the Euclidian distance between the generated mean monthly values and the real monthly values.

$$OF = \sqrt{\sum_{i=i}^{N} \left(f_i - f_i^{\,0}\right)^2} \tag{3.61}$$

where f_i is the real monthly mean value and $f_i^{\,0}$ is the generated monthly mean value.

Table 3.1 summarizes the range of variability for the different optimization parameters.

Parameter	Lower boundary	Upper boundary
i_d	0.0	0.3
h_p	12	18
a	0.6	0.9
k	1.0	2.5

Table 3.1. Range of optimization parameter variability.

3.4. Node Load Profiles

Load profiles describe hourly behavior of system node demands. They are generated using realistic base load curves, including the combination of different types of curves. Base load curves represent typical behavior of different types of customers.

In this study load curve information was taken from [3.13]. They have been classified into several categories according to tariff:

- Residential: residential tariff is available for service through one meter to individual residential customers.
- Small loads: tariff applied to loads with a peak demand less than 10 kW.
- Low power factor: Low power factor tariff is applied to customers with peak demand equal or greater than 10 kW.
- High and medium power factor: This tariff is available for customers with peak demand equal or greater than 50 kW.
- Large loads: Large load tariff is applied to loads connected to the company's transmission or subtransmission system and have a peak demand greater than 1000 KVA.

3.4.1. Synthetic Generation of Load Curves

Base curves presented have been obtained through measurements of real customers. However, when performing studies with power distribution systems it is necessary to have at disposal different sets of curves, since it is not logical to assume that all clients, even those within the same category, will follow the same pattern. New load curves will be synthetically generated to have different sample curves that follow the same general pattern but present differences in hour-to-hour values. The base load curves will serve as starting point to ensure the new curves reflect the behavior of real costumers.
The procedure for the creation of load curves [3.14] is as follows:

1. Choose a base load curve.
2. Determine yearly trend using Fourier series.
3. Define weekly cycles using average values.
4. Reconstruct daily average cycles.
5. Generate an approximate curve overlaying the effect of yearly trend, weekly cycles and daily average cycles.
6. Calculate the error of the approximate curve.
7. Estimate the error PDF for every hour and month of the year.
8. Generate random error values using the error PDF.
9. Aggregate generated errors to the approximate curve.

Choose a Base Load Curve

In this first step the user must choose one of the presented base load curves. This curve will be analyzed and serve as base for the new synthetic curve. Base curve will be referred to as l_S.

Determine Yearly Trend Using Fourier Series

Base load curve hourly values are analyzed using the Fast Fourier Transform. A yearly trend is constructed using up to the fourth harmonic.

$$l_{S1} = \frac{a_0}{2} + \sum_{i=1}^{4} a_n \cos(i \cdot w \cdot h + \phi_n) \tag{3.62}$$

where

$$w = \frac{2\pi}{8760} \tag{3.63}$$

$$h = [1,8760] \tag{3.64}$$

being l_{S1} the y early trend curve.

Define Weekly Cycles Using Average Values

Load demands present day-to-day variations; therefore, one should expect different levels of consumption for each day of the week. In order to incorporate this trend into the new curve, the annual daily average must be calculated after eliminating the yearly trend. The steps used to define weekly cycles are as follows:

1. Calculate new curve eliminating yearly trend.

$$l_{SY} = l_S - l_{S1} \tag{3.65}$$

2. Obtain average value for a day of the week.

$$\overline{l_{SY-Day}} = \frac{1}{N_{Day}} \sum_{j=1}^{N_{Day}} l_{LS-Day}(j) \tag{3.66}$$

   where N_{Day} is the number of yearly hours for the day under consideration, and $l_{SY\text{-}Day}$ is the curve values corresponding to yearly hours for the day under consideration.

3. Add daily average value to the yearly trend curve.

$$l_{S2-Day} = l_{S1-Day} + \overline{l_{SY-Day}} \tag{3.67}$$

where l_{S2} is the curve including yearly trend and weekly cycles and $l_{S2\text{-}Day}$ is the curve values corresponding to yearly hours for the day under consideration.

4. Repeat steps (2) and (3) for every day of the week.

Reconstruct Daily Average Cycles

Load demands also present hour-to-hour variations during the day. Those variations are not entirely random; instead they follow a pattern that repeats over time. Daily cycles are reconstructed using Fourier series. First, yearly trend and weekly cycles are eliminated; then hourly averages for weekdays and weekends are calculated. The next steps are followed for all months of the year:

1. Calculate new curve eliminating yearly trend and weekly cycles.

$$l_{SS} = l_S - l_{S2} \tag{3.68}$$

2. Determine all hourly averages for weekdays of a specific month.

$$\overline{l_{SS-W\_h}} = \frac{1}{N_{W\_h}} \sum_{j=1}^{N_{W\_h}} l_{SS-W\_h}(j) \tag{3.69}$$

where $\overline{l_{SS-W\_h}}$ is the average value of hour h for weekdays of the month under consideration, N_{W_h} is the number of hours that correspond to hour h for weekdays of the month under consideration, $l_{SS\text{-}W\_h}$ is the curve values of hour h for weekdays of the month under consideration.
This step must be repeated for every hour of the day.

3. Reconstruct daily cycles using harmonics 1 through 4 from Fourier series.

$$l_{SS\_WEEK} = \frac{a_0}{2} + \sum_{i=1}^{4} a_n \cos(i \cdot w \cdot h + \phi_n) \tag{3.70}$$

$$w = \frac{2\pi}{24} \tag{3.71}$$

$$h = [1, 24] \tag{3.72}$$

4. Determine all hourly averages for weekends of a specific month.

$$\overline{l_{SS-WD\_h}} = \frac{1}{N_{WD\_h}} \sum_{j=1}^{N_{WD\_h}} l_{SS-WD\_h}(j) \tag{3.73}$$

where $\overline{l_{SS-WD\_h}}$ is the average value for hour h for weekends of the month under consideration, N_{WD_h} is the number of hours that correspond to hour h for weekends of the month under consideration, and $l_{SS\text{-}WD\_h}$ is the curve values of hour h for weekends of the month under consideration.
This step must be repeated for every hour of the day.

5. Reconstruct daily cycles using harmonics 1 through 4 from Fourier series.

$$l_{SS\_WND} = \frac{a_0}{2} + \sum_{i=1}^{4} a_n \cos(i \cdot w \cdot h + \phi_n) \tag{3.74}$$

$$w = \frac{2\pi}{24} \tag{3.75}$$

$$h = [1, 24] \tag{3.76}$$

6. Add daily average cycles for weekdays and weekends of the month under consideration.

$$l_{S3-WEEK} = l_{S2-WEEK} + l_{SS\_WEEK} \tag{3.77}$$

$$l_{S3-WND} = l_{S2-WND} + l_{SS\_WND} \tag{3.78}$$

   where *ls3* is the approximate curve including yearly trends, weekly and daily average cycles.
7. Repeat steps (2)-(6) for every month of the year.

Calculate Error of the Approximate Curve

The error is calculated as the difference between the real curve and the approximate curve

$$error = l_S - l_{S3} \tag{3.79}$$

Estimate Error PDF for Every Hour and Month of the Year

Steps to estimate the error PDF for a given hour of a specific month:

1. Filter hourly values to obtain the values corresponding to the hour under consideration.
2. Calculate nonparametric PDF using filtered values.
3. Repeat for every hour of a specific month.

The number of error sample values is not enough to determine the real PDF; however it is assumed that the estimated PDF is good enough for the synthetic generation of load curves.

Generate Random Error Values Using the Error PDF

Error PDF will be used to generate random error values. The steps necessary to generate error values are:

1. Calculate autocorrelation coefficients for lags “1” and “2”.
2. Generate *N* random values using a normal distribution with zero mean and unity standard deviation, being *N* the number of days in the month.
3. Correlate randomly generated values using autocorrelation coefficients.

4. Map autocorrelated values in the estimated PDF and obtain errors
5. Repeat steps (1)-(4) for every for hour and month of the year.

Aggregate Generated Errors to the Approximate Curve

The new load curve will calculated after adding the generated error values to the approximate curve.

$$l_{S4} = l_{S3} + err\_rnd \tag{3.80}$$

where *err_rnd* is the randomly generated error.

3.4.2. Generation of Load Profiles

New load profiles can be generated using the synthetically generated load curves. The steps followed to create new load profiles are:

1. Establish what percentage of nominal power is assigned to each type of customer. Customers are represented by their base load curves.
2. Synthetically generate load curves used for the new load profile.
3. Create the new load profile by calculating the weighed sum of the generated load curves.
4. Define an hourly variation factor.
5. Randomly generate factors for every hour of the year using a uniform distribution.
6. Multiply new load profile's hourly values by randomly generated variation factors.
7. Normalize load profile's values.

Figure 3.3 illustrates the main steps implemented in the development of the three applications presented in this Chapter. Figure 3.4 provides an example of curve shapes derived from the three procedures for a given period of the year.

3.5. Case Study

A case study has been developed in order to demonstrate the usefulness of the previously presented procedures. Figure 3.5 shows the diagram of the test system used in this study. Some important numbers about the system are given below:

- Rated system voltage: 4.16 kV
- Rated power of substation transformer: 5000 kVA
- Number of load nodes: 51
- Initial maximum coincident load measured at the substation: 1700 kVA
- Overall line length: 26.36 km.

Table 3.2 presents the statistics and parameters used to generate the PV and Wind generation curves. Base curves for node load profiles were obtained from [3.13].

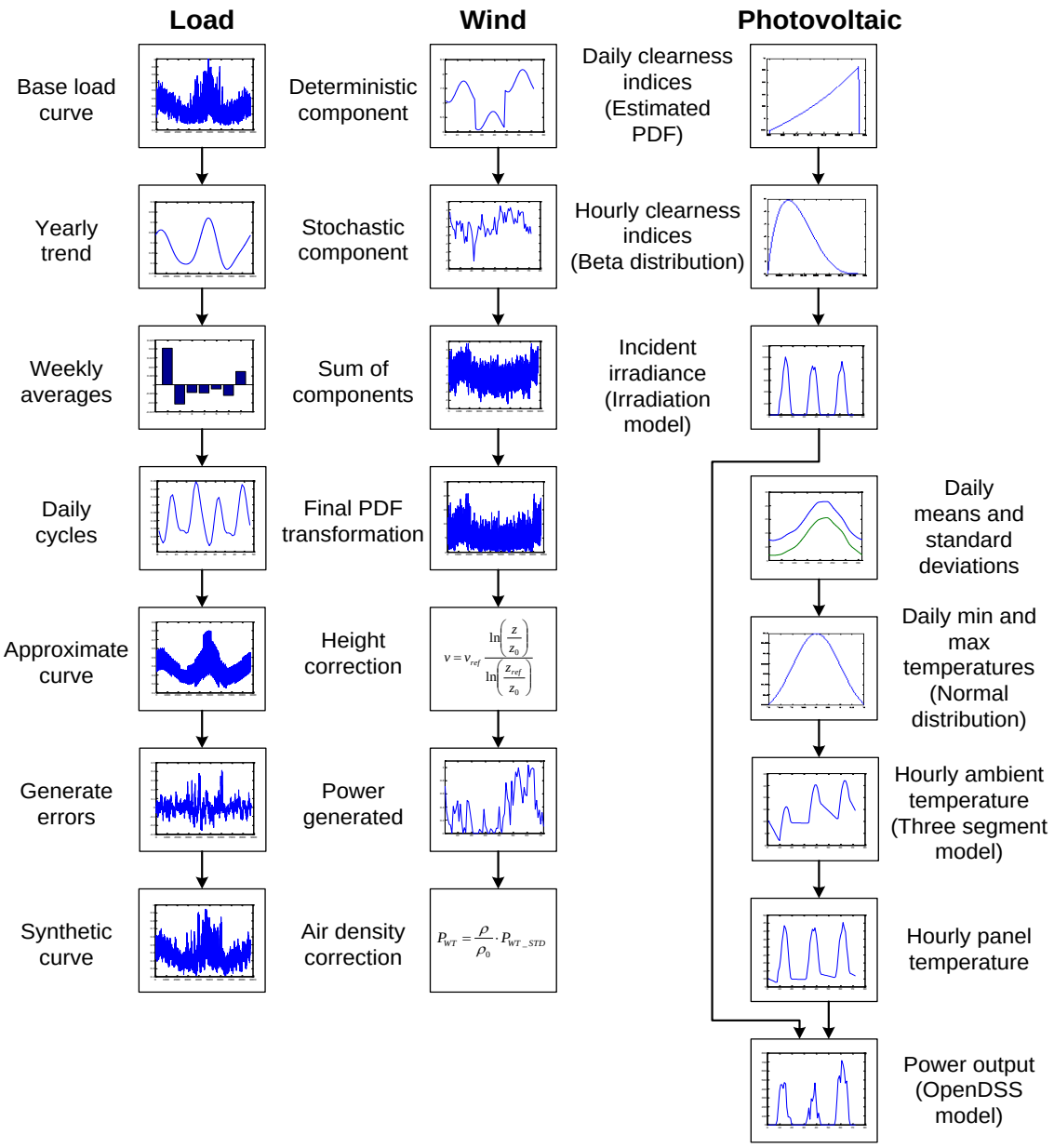

Figure 3.3. Generation of yearly curve shapes for distribution system analysis.

Average monthly clearness index	0.51, 0.56, 0.56, 0.55, 0.54, 0.57, 0.60, 0.57, 0.55, 0.50, 0.48, 0.49
Panel's slope angle	35º
Normal operating cell temperature	45ºC
Average monthly daily minimum temperatures (ºC)	6.77, 6.97, 8.39, 10.0, 13.3, 17.1, 19.9, 20.5, 18.2, 15.3, 10.7, 8.18
Average monthly daily maximum temperatures (ºC)	12.2, 12.7, 14.5, 16.1, 19.5, 23.5, 26.3, 26.4, 23.7, 20.2, 15.7, 13.2
Average monthly wind speed (m/s)	6.64, 7.84, 7.34 5.35, 4.61, 4.76, 4.27, 4.46, 4.53, 6.1, 4.83, 8.16
Wind curve parameters: i_d, h_p, a, k	0.05, 15.04, 0.73, 1.88

Table 3.2. Summary of solar and wind resources.

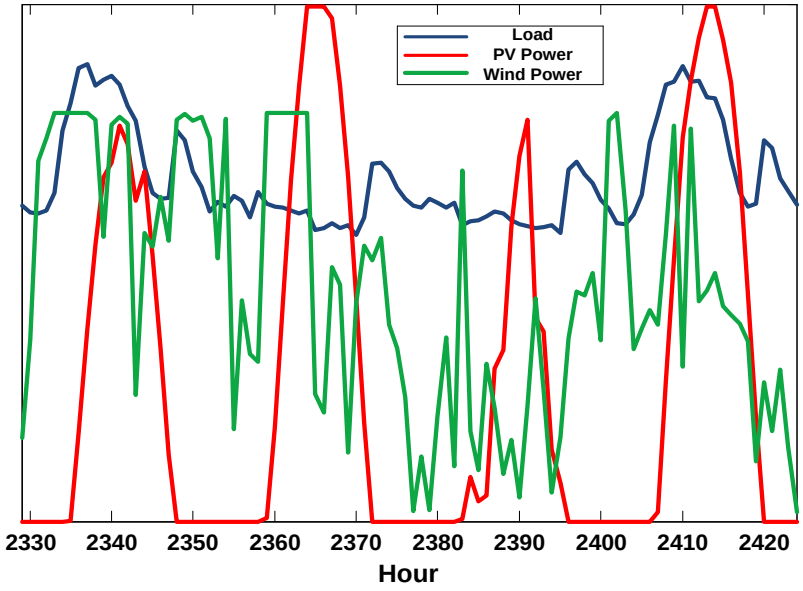

Figure 3.4. Curve shapes for node loads and renewable generation.

The study presented here is aimed at analyzing the long-term impact of the DG on the system performance. That is, knowing the yearly load shapes at all system nodes and assuming a certain yearly variation of the loads, the goal is to estimate the resulting voltage values and energy losses, or the yearly energy that will be demanded from the HV system after connecting DG units. System curves should be updated to avoid repeating identical consumption and generation patterns for every year considered for the study. For this purpose the algorithms presented in the previous section have been modified in order to create different sets of system curves. Load profiles will use the same combination of base load curves to create the new profiles, while PV and wind generation curves will follow the same statistics for their respective resources. The implemented algorithms are applied every year by introducing some randomness that guarantees that all the yearly curves are different.

Given that generation units by independent producers can be randomly located and provided they fulfill the connection rules, the main results of the study can be useful for the utility, which could decide whether the ratings and locations of the generation units are adequate or not.

The study will be carried out for a period of 10 years, and assuming the predicted variation of the load is not the same for all nodes. As for the distributed generators, they will not be simultaneously connected to the system. The ratings of the DG units, their locations and the year of connection are as follows:

- Unit 1: PV, 100 kVA, connected at node A716, year 2
- Unit 2: Wind, 150 kVA, connected at node A728, year 3
- Unit 3: PV, 150 kVA, connected at node A758, year 5
- Unit 4, Wind, 100 kVA, connected at node A766, year 6

It is assumed by default that the connection of each unit is made at the beginning of the corresponding year, and the generators will only inject active power.

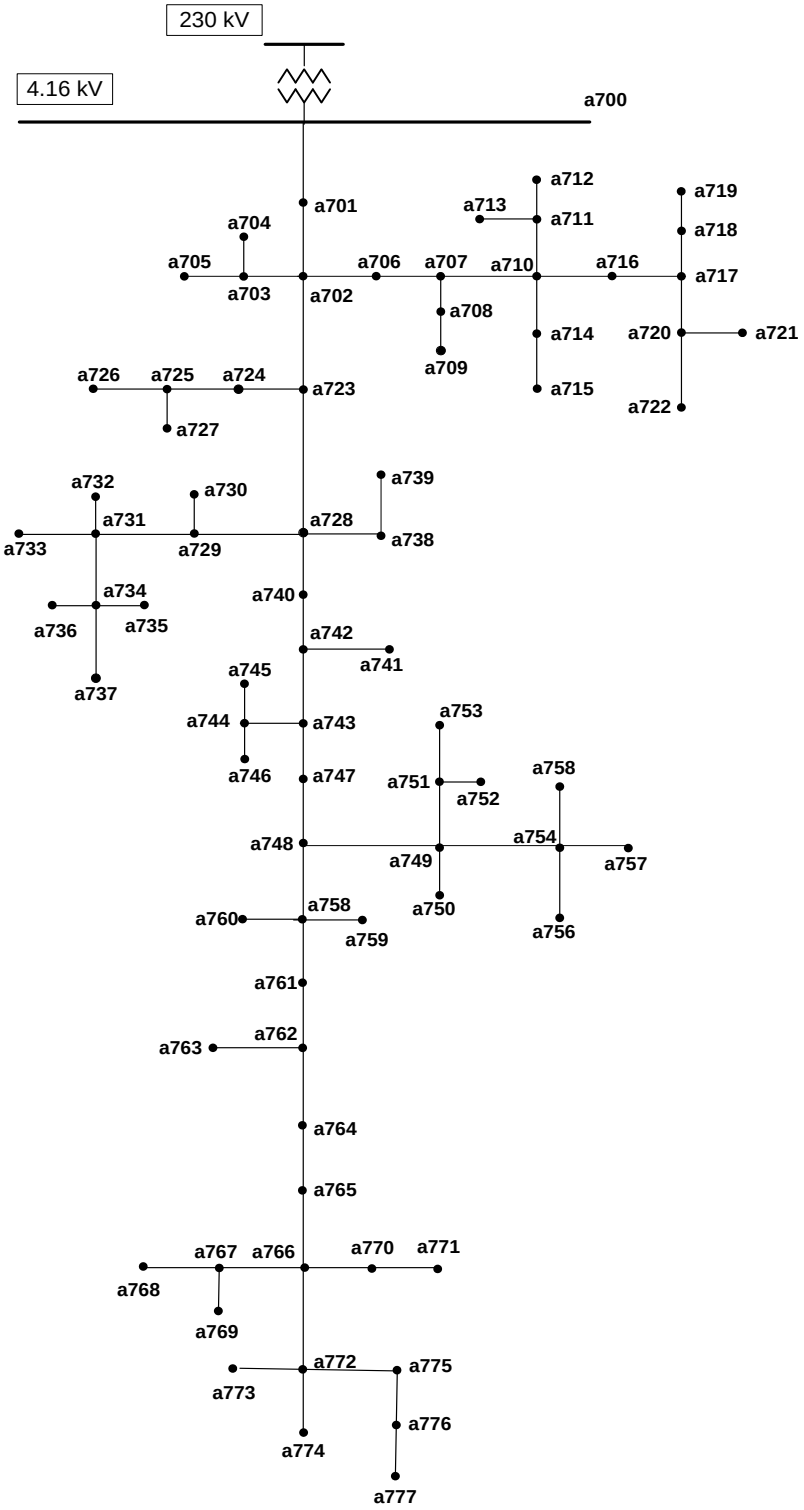

Figure 3.5. Diagram of the test system.

Figure 3.6 through Figure 3.8 show some results of the study when using a constant power model for representing node loads. A simple software application was implemented using MATLAB and OpenDSS to obtain the information presented in these plots. It is obvious from these results that, as expected, there is a positive impact of the DG on the node voltages (although the minimum voltage at certain year is below 0.95 pu even with DG), and a significant reduction in the system losses and in the energy required from the HV system is achieved.

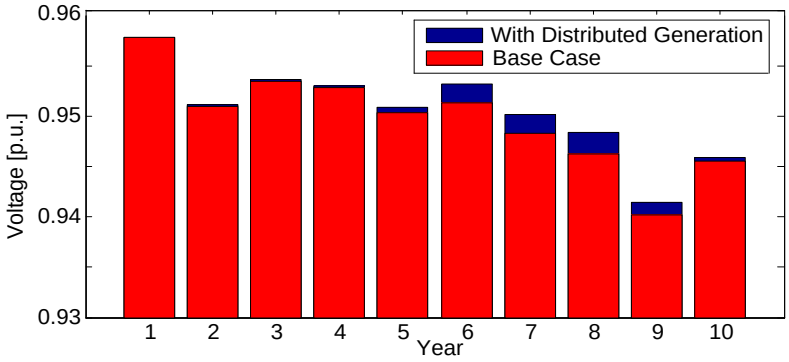

Figure 3.6. Impact of DG on the minimum voltage values.

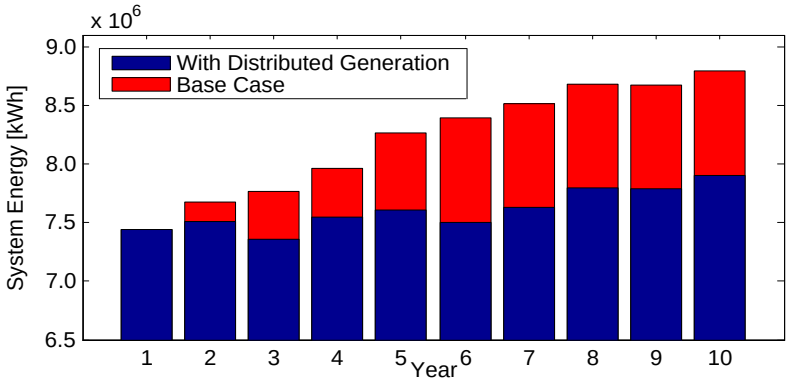

Figure 3.7. Energy required from the HV system (measured at the secondary substation terminals).

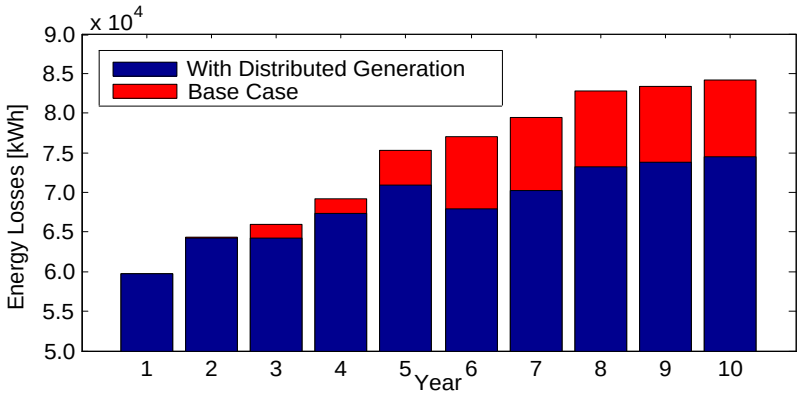

Figure 3.8. Energy losses (without considering substation losses).

Some interesting conclusions can be derived from the results presented in these figures. For instance, randomness in load and generation values is evident from the minimum voltage values obtained for every year. Although the load is larger during the tenth year than the ninth year and no generation is connected after the sixth year, the lowest value of the voltage is obtained during the ninth year. This is obviously due to a (random) coincidence of large load and low generation. On the other hand, it is evident that, in spite of that randomness, the contribution of the generators remains basically constant once that last generator has been connected to the system. From the plots showing energy injection and energy losses one can conclude that, after accounting for the predicted yearly increase of load, both the energy injected and the energy losses remain almost constant during the last three years.

3.6. Conclusions

This Chapter has summarized the main features of some procedures implemented for synthesizing load and renewable generation curve shapes. The procedures have been implemented in MATLAB and used in combination with a MATLAB-OpenDSS link that drives OpenDSS from MATLAB.

The procedures developed are useful for generating load and generation curves with an integration step of one hour. Their usefulness has been proven with the presented case study; it was also demonstrated that the procedures can be adjusted in order to cover evaluation periods greater than one year.

It is important to keep in mind that with a one-hour time step some relevant information and behavior is missed. For instance, the actual impact of a sudden cloudy scenario cannot be analyzed since the time frame required for such a study should be in the range of one minute. It is also important to remember that the load variation when steps of one minute or less are used will not be as smooth as when a one-hour step is used; see for instance [3.15] and [3.16]. Similar conclusions can be drawn regarding wind generation.

3.7. References

[3.1] J.A. Martinez and J. Martin-Arnedo, "Distribution load flow calculations using time driven and probabilistic approaches". *IEEE PES General Meeting*, Detroit, July 2011.

[3.2] HOMER Software, National Renewable Energy Laboratory (NREL), 2003. Available at http://www.nrel.gov/homer.

[3.3] J. Taylor, J.W. Smith, and R. Dugan, "Distribution modeling requirements for integration of PV, PEV, and storage in a smart grid environment," *IEEE PES General Meeting*, Detroit, July 2011.

[3.4] J.W. Smith, R. Dugan, and W. Sunderman, "Distribution modeling and analysis of high penetration PV," IEEE PES General Meeting, Detroit, July 2011.

[3.5] J.F. Manwell, A. Rogers, G. Hayman, C.T. Avelar, and J.G. McGowan, "Hybrid2 – A Hybrid System Simulation Model, Theory Manual", University of Massachusetts, November 1998.

[3.6] URL: https://eosweb.larc.nasa.gov/cgi-bin/sse/grid.cgi?email=skip@larc.nasa.gov

[3.7] V.A. Graham and K.G.T. Hollands, "A method to generate synthetic hourly solar radiation globally," *Solar Energy*, vol. 44, no. 6, pp. 333-341, 1990.

[3.8] J. Schuol and K.C. Abbaspour, "Using monthly weather statistics to generate daily data in a SWAT model application to West Africa," *Ecological Modelling*, vol. 201, pp. 301–311, 2007.

[3.9] A. Soltani and G. Hoogenboom, "A statistical comparison of the stochastic weather generators WGEN and SIMMETEO." *Climate Research*, vol. 24, pp. 215-230, September 2003.

[3.10] D.C. Reicosky, L.J. Winkelman, J.M. Baker, and D.G. Baker, "Accuracy of hourly air temperatures calculated from daily minima and maxima," *Agricultural and Forest Meteorology*, vol. 46, pp. 193-209, 1989.

[3.11] RETScreen International, Clean Energy Decision Support Centre, "Photovoltaic Project Analysis," in *Clean Energy Project Analysis. RETScreen Engineering and Case Textbook*, Minister of Natural Resources Canada, 2005.
[3.12] R. Carapellucci and L. Giordano, "A methodology for the synthetic generation of hourly wind speed time series based on some known aggregate input data," *Applied Energy*, Vol. 101, pp. 541-550, January 2013.
[3.13] URL: https://www.aepohio.com/service/choice/cres/LoadProfiles.aspx.
[3.14] L. Magnano and J.W. Boland, "Generation of synthetic sequences of electricity demand: Application in South Australia," *Energy*, vol. 32, no. 11, pp. 2230-2243, November 2007.
[3.15] A. Wright and S. Firth, "The nature of domestic electricity-loads and effects of time averaging on statistics and on-site generation calculations," *Applied Energy*, vol. 84, no. 4, pp. 389-403, April 2007.
[3.16] A. Wright and S. Firth, "The nature of domestic electricity-loads and effects of time averaging on statistics and on-site generation calculations," *Applied Energy*, vol. 84, no. 4, pp. 389-403, April 2007.

Chapter 4

Optimum Allocation of Distributed Generation

4.1. Introduction

Distributed generation can support voltage, reduce losses, provide backup power, improve local power quality and reliability, provide ancillary services, and defer distribution system upgrade [4.1]-[4.3]. Modeling of renewable generation raises several challenges to distribution load flow calculations since capabilities for representing intermittent generators, voltage-control equipment, or multi-phase unbalanced systems are required. In addition, studies of systems with intermittent non-dispatchable resources will require a probabilistic approach and calculations performed over an arbitrary time period that may range from minutes to years. Load representation is another important issue since voltage-dependent loads with random variation must be also accounted for. These issues complicate the study of power distribution systems since software tools have to combine new analysis capabilities with a high number of models for representing various generation technologies, besides the conventional distribution system components, and include capabilities for time-driven calculations [4.4].

The optimum allocation of distributed generation can be seen from two different perspectives:

- From the independent producer's point of view the goal is to optimize the benefit. Although the utility will usually impose some constraints to the generation units to be connected to its system (e.g. a maximum rated power), it can be assumed by default that the units can be connected to any node of the system. Therefore, the optimization approach will be in general a feasibility study whose main goal is to check the viability of the installation and select the most economical size (irrespectively of the location) and, in case of dispatchable units, the control strategy that will maximize the benefit; see for instance [4.5], [4.6].

- From the utility's point of view the goal is to maximize the positive impact of distributed generation (e.g., voltage support, energy losses, investment deferring) and minimize or avoid those aspects that can negatively affect the system performance (e.g. miscoordination of protective devices, overvoltages during low load periods); see for instance [4.7].

Since DG units are relatively small in size, one of the criteria used to locate DG is to place generation close to load consumption. Several strategies have been proposed to optimally allocate DG; for instance, loss minimization [4.8], minimizing system update [4.9], risk minimization [4.10], or maximizing DG capability [4.11]. A significant activity has been dedicated to this purpose during the last decade; for a summary of the works related to optimum allocation of DG see references [4.12] and [4.13].

Although some works have been performed in this field using probabilistic methods [4.14]-[4.15], not much has been done with a full model; e.g., a model such as that mentioned above for the distribution system, load and DG. The Monte Carlo method is a natural approach when uncertainties are involved and some variables are random/intermittent, although it is evident that its application to a system of actual size when using an advanced representation and considering a multi-objective method is very costly in terms of computer time. However, multicore computers and software that takes advantage of their capabilities (e.g., Parallel MATLAB) can be used to significantly reduce the computing time.

The application of a pure Monte Carlo method can be time consuming for allocating many DG units in large distribution systems. Therefore it is necessary to study different approaches aimed at reducing the number of runs without significantly reducing the accuracy of the solution.

The present Chapter is organized as follows. In Section 4.2 the implemented Monte Carlo method is introduced. Section 4.3 presents the results for the optimum allocation of PV and wind generation in radial feeders; this section also explores a refinement of the Monte Carlo method aimed at reducing total simulation times. In Section 4.4 the usefulness of the Monte Carlo method for the optimum allocation of distributed generation in Multi-feeder systems under a short term evaluation is checked. Section 4.5 presents the application of the Monte Carlo method to the optimum allocation of PV generation units using a long term evaluation and assuming a sequential connection of the generators; additionally, it proposes an alternative methodology based on a "Divide and Conquer" approach. The main conclusions derived from this Chapter are presented in Section 4.6.

4.2. Application of the Monte Carlo Method

4.2.1. Introduction

The goal of the Monte Carlo method is to minimize energy losses; therefore, the developed procedure presented here may be defined as a Parallel Monte Carlo method aimed at estimating the location and size of one or more generation units to minimize the system losses.

System energy losses are computed over an evaluation period that can span over several years. Optimum allocation studies can be categorized according to the length of the evaluation period: (1) short term studies, (2) long term studies. A one-year evaluation period has been considered for short term studies, whereas evaluation periods of 10 or more years are contemplated for long term studies. The approach for the allocation of two or more distributed generators will also depend on the length of the evaluation period. For short term studies generation units will be connected simultaneously; however, the connection of these units will be carried out in a sequential manner for long term evaluations.

Input data include system parameters, and time variation of loads and generations. Random variables to be generated during the application of the Monte Carlo method are locations and sizes of the generation units. Note that this can be rigorously made by considering that the generation pattern depends of the area/node where the generator is located. Generation units are either PV arrays or wind power systems. It is assumed that the solar radiation is the same for each system node, but the wind speed can be different because the altitude over sea level is not the same for each system node. Although DG units can inject both active and reactive power, in this work all generators, irrespectively of their technology, will only inject active power. Note that the procedure can be also applied to allocate capacitor banks by simply changing active by reactive power.

4.2.2. Short Term Evaluation

The goal of short term studies is to select ratings and locations of generation units to minimize the distribution energy losses for an evaluation period of one year, taking into account some operational constraints (e.g., there is a maximum voltage that should not be exceeded; there is a thermal limit for each system line section). All generation units considered for optimum allocation will be connected simultaneously at the start of the evaluation period.

The procedure has been implemented taking into account certain rules when choosing locations and sizes for the generators. The rules as well as the general procedure used in this work for short term (one year) evaluations are detailed below:

1. The generators will only be connected to MV nodes; the user can specify a list of nodes where generators cannot be connected. The locations to which generators will be connected are determined by generating as many random values as units to be allocated and using a uniform distribution.
2. Once the locations (and feeders) are known, the rated power values are determined. Beforehand, the user has to fix the maximum generation power that can be connected to each node. This value is derived from the maximum thermal limit of the line sections connected to the selected node. This step is carried out as follows:
    - When only one generator is to be allocated, the maximum rated power will depend on the selected location. Every time a system node is randomly selected, the maximum rated power for that node is determined according to the following steps: (i) calculate the maximum non-coincident active power (i.e. the active power value that results from adding the active rated power of all load nodes) for the feeder where the node is located; (ii) check

the maximum power that can be carried by the line sections connected to the selected node; (iii) compare the previous power values and choose the minimum one; this will be the maximum rated power a generation unit can be assigned during the Monte Carlo execution. Then generate a random number uniformly distributed between 0 and 1, and multiple it by the above value.

- When two or more units are to be installed on the same feeder, the following changes are introduced in the procedure:
  - ✓ Generate an independent uniformly-distributed random value for the initial rated power of each generation unit using the maximum rated power fixed for every node as the upper endpoint of each uniform distribution.
  - ✓ Compare the maximum rated powers for all the chosen locations and choose the maximum value, P_{DG_MAX}.
  - ✓ Generate the penetration factor as a uniformly distributed random number between 0 and 1. Multiply the maximum value found in the previous step by this penetration factor; the result will be the overall rated power of distributed generators.

$$\sum_{i=1}^{NG} P_{DG\_i} = pf \cdot P_{DG\_MAX} \tag{4.1}$$

    where NG is the number of generation units under evaluation, P_{DG_i} is the rated power of unit i, pf is the penetration factor, and P_{DG_MAX} is the maximum DG rated power found in the previous step.
  - ✓ Calculate the scale factor from the initial rated powers as follows:

$$sf = \frac{pf \cdot P_{DG\_MAX}}{\sum_{i=1}^{NG} P_{DGinit\_i}} \tag{4.2}$$

    where sf is the scale factor and P_{DGinit_i} is the initial rated power for unit i (obtained in the first step).
  - ✓ Obtain generator rated powers by scaling initial rated powers

$$P_{DG\_i} = sf \cdot P_{DGI\_i} \tag{4.3}$$

  Note that the order in which random values for locations and rated powers are generated matters: first, the location nodes; afterwards, the rated powers.

3. Perform the load flow calculation. Neglect the case if one of the following conditions is satisfied: (i) the voltage at one node exceeds the fixed maximum value; (ii) the current through one or more system sections is above the thermal limit.
4. Stop the procedure when the specified number of runs or samples (according to the terminology of the Monte Carlo method) is reached.

The combination of rated powers and locations that produces the minimum energy losses and meets the technical conditions will be selected by the procedure as the optimum solution. The number of executed runs must be large enough to ensure that optimum energy losses are near the global minimum; it is assumed the method has converged when the variations of the target variable (system energy losses) are within a margin of 1%.

4.2.3. Optimum Allocation for Longer Evaluation Periods

Some long term studies, such as feasibility studies, are carried out considering a period that can reach up to 20 or more years [4.5], [4.6]. The Monte Carlo procedure and the load flow calculation have been modified to cope with evaluation periods greater than one year.

The optimum allocation will be carried out in a sequential manner and requires information regarding the number of generation units to be allocated, the year when each unit will be connected to the system and the length of the evaluation period (i.e. number of years). It is assumed that generation units are connected at the beginning of the year and that the length of the evaluation period is the same for all units. Additionally, load growth curves for every node load must be defined.

The new method is called sequential because the generation units will be optimally allocated in a sequence that depends on the year of connection; the procedure for the individual allocation of a single unit will be based on the steps introduced in the previous section. The new procedure is summarized in the following steps:

1. Perform the optimum allocation of the first unit following the same rules as in the short term evaluation but considering the new longer evaluation period. For example, if the first unit is scheduled to be connected during the first year and the evaluation period is 10 years, this first unit will be allocated taking into account the energy losses for the first 10 years (from the beginning of year 1 until the end of year 10).
2. The first optimally placed unit will be incorporated to the test system and will be included in all following load flow calculations.
3. Perform the optimum allocation of the second unit considering that the evaluation period starts when the unit is scheduled to be connected. For instance, if the second unit is to be installed in the second year, the optimization target will be the system energy losses from the beginning of year 2 until the end of year 11.
4. Incorporate the new generation unit to the test system.
5. Repeat steps 3 and 4 for the remaining units to be allocated.

Certain aspects of the original method had to be adjusted in order to better fit the sequential nature and the longer evaluation period of the new procedure. The main aspects are summarized below:

- System curves (load shapes, irradiance and panel temperature curves) are updated for every year of the simulation period. In the case of node loads this is carried out taking into account the expected yearly variation. For solar irradiance and panel temperature of PV generators, the implemented algorithm is applied every year by introducing some randomness that guarantees that all the yearly curves are different.
- The rules for the determination of locations and rated powers are the same that were used for the short term evaluation only for the first unit to be allocated in each feeder. Once some generation has been located in one feeder, the procedure for the second and subsequent units will exhibit some differences: (i) the location node cannot be any of the nodes selected for previously allocated units; (ii) the maximum power of the new unit can be the value that results after subtracting the rated power of the already allocated units from the maximum

non-coincident power of the corresponding feeder loads, but taking into account that the rated power of the selected unit cannot exceed the maximum power that can be connected to the new selected node.

4.2.4. Implementation of the Procedure

The procedure has been implemented in OpenDSS, a simulation tool for electric utility distribution systems, which can be used as both a stand-alone executable program and a COM DLL that can be driven from some software platforms. In this study, the program is driven from MATLAB (see Figure 4.1), which is used to calculate the random variables and control the execution of the procedure. The implementation of the procedure, when using parallel computing, is shown in Figure 4.1, and is valid for any number of cores. MATLAB capabilities are used to distribute Monte Carlo runs between cores.

The implementation of the procedure for any number of cores when using parallel computing is based on the library of MATLAB modules developed by M. Buehren [4.16]. Load and intermittent generation (solar, wind) curves were generated by means of the algorithms detailed in Chapter 3.

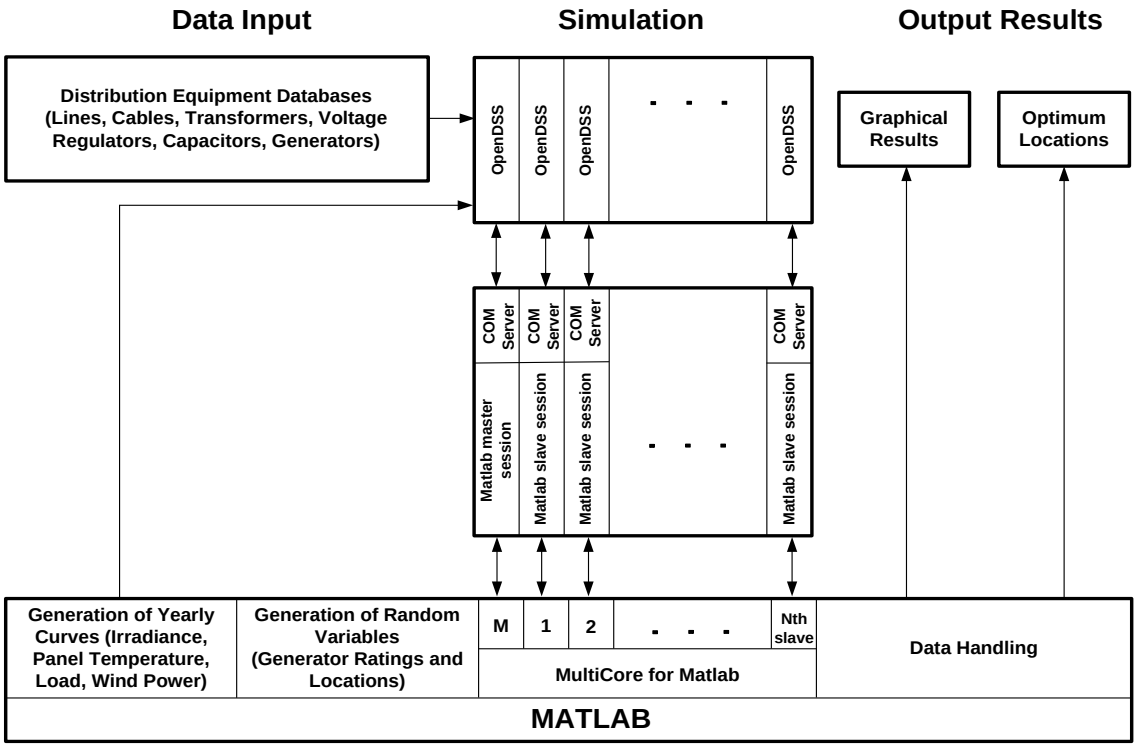

Figure 4.1. Block diagram of the implemented procedure.

4.3. Optimum Allocation of Distributed Generation in Radial Feeders

4.3.1. Introduction

The radial feeder configuration has been chosen because the solution to this problem is well known when the load is constant, voltage independent and uniformly distributed. The optimum allocation of capacitor banks in a distribution feeder with uniformly distributed load has been thoroughly analyzed [4.17]. A similar conclusion is derived when the goal is to minimize losses by installing generation units that only inject active power [4.8]. That is, this test system configuration can be useful for validating test cases whose result is obtained by means of a Monte Carlo method.

The radial feeder configuration will also be used to test the application of parallel computing to the optimum allocation of distributed generation. The results from these studies will help to assess the potential reduction in execution times when compared to the serial execution of the Monte Carlo method using single-core computing. Furthermore, the feasibility of a refined Monte Carlo method aimed at achieving a greater reduction in total simulation times will be examined.

4.3.2. Test System Configuration

Figure 4.2 shows the diagram of the test system. It is a three-phase 60-Hz single-feeder distribution system with a distributed load. The model includes the substation transformer and a simplified representation of the high-voltage system. The phase conductors are in a flat configuration and the normal thermal limit is 400 A, while the emergency limit is 600 A. Three different test systems following the configuration shown in Figure 4.2 will be studied in this Section (*n* is the number of load nodes in the test system). Each test system will have different values of feeder length, number of nodes and system load.

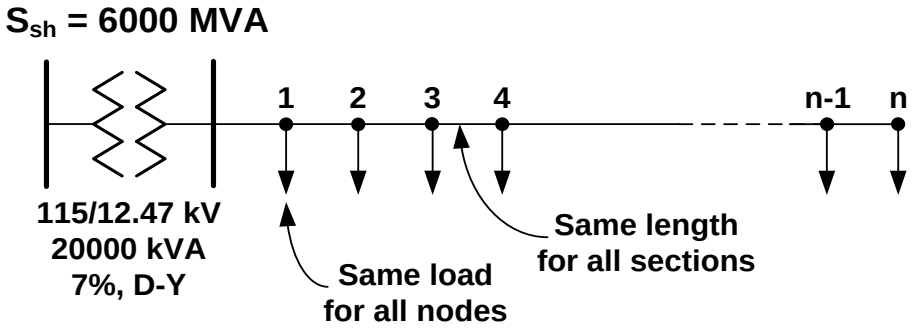

Figure 4.2. Test system configuration and data.

4.3.3. 100-Node System

The system used for this study is a 100-node feeder with the configuration shown in Figure 4.2. The values used in calculations are as follows:

- Total feeder length: 10000 ft.
- Number of nodes: 100 (i.e., section length = 100 ft).
- Nominal node load = 75 kW, pf = 0.9 (lg) (i.e., total load = 7500 kW).

The goal of this study is to apply the Monte Carlo procedure in order to obtain the optimum allocation of Capacitor banks and PV generation. The node load curves and PV generation curves used were generated using the capabilities of HOMER [4.18]. All studies are carried out for an evaluation period of one year, except for the first two studies with capacitor banks.

Optimum Allocation of Capacitor Banks

The Monte Carlo procedure presented in the previous section can be adjusted to perform the optimum allocation of capacitor banks. The main difference is that the capacitor rated power will be determined based on the maximum non-coincident reactive power. The procedure will be used to obtain the optimum allocation of capacitor banks with both constant and time-varying load.

A solution to the optimum allocation of *n* capacitor banks of equal sizes on a distribution feeder with a uniformly distributed load has been known for many years. For a single capacitor bank, the expressions in [4.17] provide the well-known 2/3 rule. For two capacitor banks, the compensation ratio of each capacitor bank is 2/5 of the reactive load, giving a total compensation of 4/5, while the optimum locations for both capacitor banks are respectively 2/5 and 4/5 of the feeder length.

Figure 4.3 shows the results obtained after using the Monte Carlo method for estimating the optimum location of a single capacitor bank on a feeder with a constant load. The minimum of the surface shown in the figure corresponds to a capacitor bank of 2892 kvar located at 6200 ft from the substation. It is important to keep in mind that the theoretical results were derived for a single-phase feeder with some simplifications about voltage drop, and load and line models.

According to the 2/3 rule, the optimum capacitor bank should have a rated power of 2420 kvar and should be located at 6667 ft from the substation. Although the accuracy of a Monte Carlo method can be improved by increasing the number of runs, the accuracy that can be obtained in this study after 1000 runs is in general acceptable. In fact, differences were not significant with more runs. There are some reasons to justify these differences (e.g., there can be some steady-state unbalance and some voltage drop, and line capacitances are included in calculations). Another important reason is the feeder model used to obtain the above expressions, see [4.17].

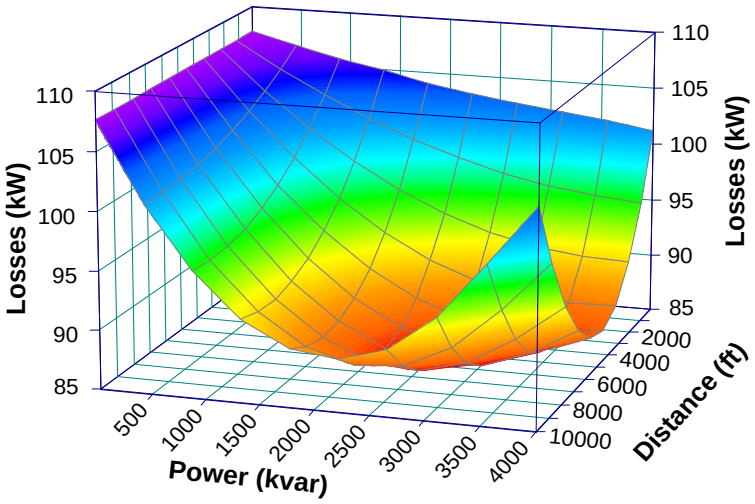

Figure 4.3. Optimum location of one capacitor bank. Test system with 100 nodes; 1000 runs.

Figure 4.4 shows the results obtained after using the method to estimate the location of two capacitor banks of the same size. In this case the random variables are three, the two distances and the reactive power of each capacitor bank. To visualize the results, the procedure has been initially applied with a fixed compensation ratio of the reactive power. The figure shows the results that correspond to a total compensation of 80%, which is the theoretical optimum compensation ratio when installing two capacitors banks. The minimum of the surface shown in Figure 4.4 corresponds to distances of 4300 and 8100 ft. The theoretical values for this compensation ratio are respectively 4000 and 8000 ft.

To estimate the optimum compensation ratio, the procedure was applied with several ratios. The results obtained are summarized in Table 4.1. According to these results, the optimum allocation is closer to a compensation ratio of 100%, although the improvement with respect to the theoretical optimum (i.e., 80% compensation) is very small.

When running the procedure with three random variables (i.e., the compensation ratio is also varied), the optimum after 1000 runs corresponds to a compensation ratio per capacitor bank of 47% and respective locations of 0.30 and 0.76 in per unit of the feeder length.

The last test case in this section assumes a time varying load and is aimed at estimating the optimum allocation of a single capacitor bank but using a yearly load curve. To check the accuracy of the procedure, the yearly shape of each load, as well as that of the capacitor bank, are the same, so the 2/3 rule can be also considered. Figure 4.5 shows the results obtained after using the Monte Carlo procedure. The minimum of this case corresponds to a capacitor bank of 2723 kvar located at 6300 ft from the substation.

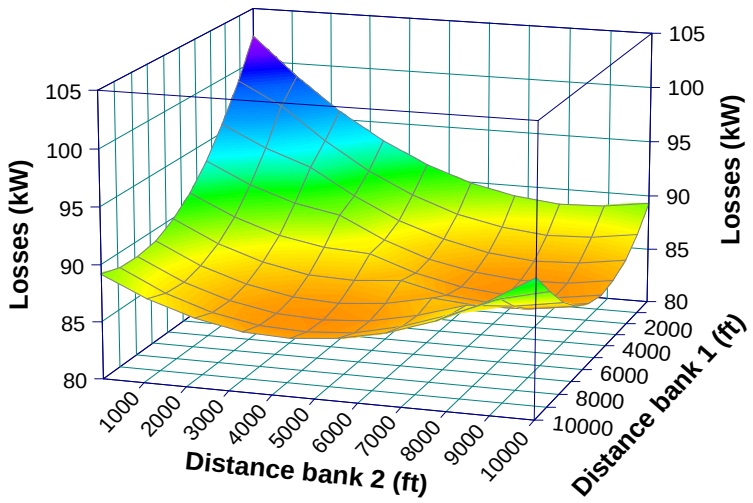

Figure 4.4. Optimum location of two capacitor bank with compensation ratio of 80%. Test system with 100 nodes; 1000 runs.

Compensation ratio	Distance Bank 1 (ft)	Distance Bank 2 (ft)	Losses (kW)
20%	8600	10000	97.39
40%	7200	9100	90.45
60%	5700	8600	86.32
80%	4300	8100	84.33
100%	2900	7600	83.83

Table 4.1. Optimum allocation of two capacitor banks - 100 nodes.

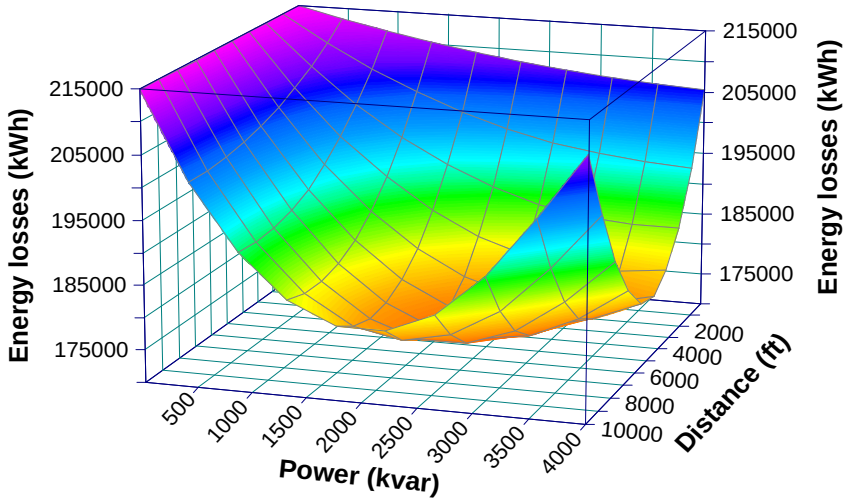

Figure 4.5. Optimum location of a single capacitor bank with a time varying load. Test system with 100 nodes; 1000 runs.

Table 4.2 shows the results obtained with a different number of runs when simulating the test system during a year. Obviously, the more runs, the better the accuracy of the results; however, the results shown in the table do not exhibit any improvement when passing from 300 to 1000 runs.

Runs	Distance (ft)	Size (kvar)
300	6327	2720
600	6344	2712
1000	6322	2723

Table 4.2. Optimum allocation of one capacitor bank with time varying load - 100 nodes.

Optimum Allocation of PV Generation

For this study generation is by default of photovoltaic type. The implemented procedure will be used for obtaining the optimum allocation of PV generation units when considering that the shape of each node load is different (although the patterns will exhibit some similarities; e.g., during the day hours and the week days), the generators only inject active power, their generation patterns are the same and they are previously known.

An important aspect to be considered when running the procedure during a given period of time is that the shapes of the generation curves correspond to those of photovoltaic units and there will be generation during daily hours only, see Figure 4.6. Another important aspect of this study is that there will be constraints for some operating conditions (i.e., all voltages must be between 1.05 and 0.95 pu, the thermal limit of 400 A for line conductors cannot be exceeded), so those combinations of active power and distance for which at least one limit is exceeded are neglected.

Table 4.3 shows the results obtained after applying the procedure with different number of runs when one unit is to be allocated in the 100-node feeder. It is important to remember that the 2/3 rule should not be considered now since the peak of node loads are not coincident.

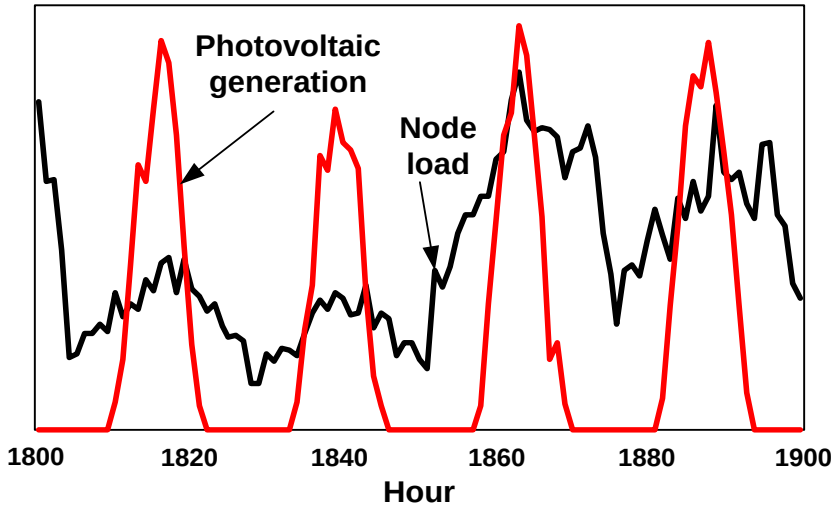

Figure 4.6. Profiles of load and generation (not with the same scale).

The results for a different number of runs show a clear tendency for the rated power and location of the distributed generator. The optimum rated power is about 60% of the total load, whereas the optimum distance is approximately 65% of the total feeder length. Although not too large, it is possible to observe a discrepancy with respect to the 2/3 rule for the distributed generator's rated power. These results reinforce the notion that

the 2/3 rule should not be used for this type of studies. Figure 4.7 shows the results obtained after applying the Monte Carlo method for estimating the optimum location of a single generation unit in the 100-node feeder using 1000 runs.

Runs	Power (kW)	Distance (ft)	Energy Losses (kWh)
200	4733.52	6100	134914.6
500	4386.21	6800	134854.8
1000	4533.57	6700	134763.5

Table 4.3. Optimum allocation of one generation unit - 100 nodes.

Table 4.4 shows the results for a different number of runs when allocating two and four generation units in the 100-node feeder. This time the differences between the results derived from each study are important, and these results clearly prove that the number of runs has to be increased with the number of generation units to be allocated, especially when allocating four generation units.

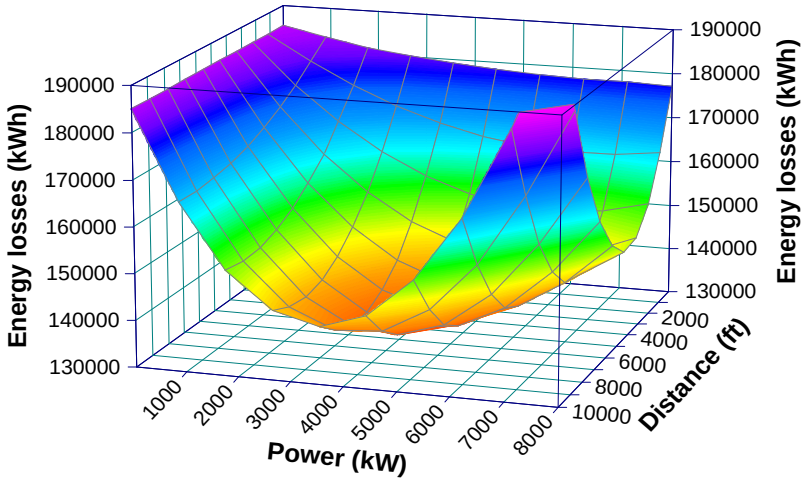

Figure 4.7. Optimum location of a single generation unit. Test system with 100 nodes; 1000 runs.

The results in Table 4.3 and Table 4.4 can be compared to those derived from the theoretical results that correspond to the optimum location of generation units injecting only active power if the load system was constant, see Table 4.5. These results can be obtained from the well-known equations used for allocating capacitor banks (see [4.17]) by sweeping reactive and active power. The optimum distances for two and four generation units are very similar to the values presented in Table 4.4; therefore, it can be expected that for this case the global optimums will be very similar to those calculated values. Individual optimum rated powers for two and four generation units do not present a well-defined trend and can't be compared to the values obtained using theoretical equations. However, the overall active power of the PV generation units shows a more stable tendency. This value is always smaller than the theoretical optimum compensation ratio and it can be used as a reference when looking to minimize energy losses.

Two generation units				
Runs		1000	2000	4000
Unit 1	Power (kW)	3021.29	2803.49	2657.25
	Distance (ft)	4000	3100	3900
Unit 2	Power (kW)	2546.03	3094.43	2815.21
	Distance (ft)	7700	8000	7800
Energy Losses (kWh)		130846.6	130916.7	130736.2
Four generation units				
Runs		2000	4000	8000
Unit 1	Power (kW)	1140.51	2059.86	1829.14
	Distance (ft)	4000	3500	2300
Unit 2	Power (kW)	1638.53	2134.85	1113.11
	Distance (ft)	4300	5000	4400
Unit 3	Power (kW)	1406.45	560.26	1646.99
	Distance (ft)	6900	7300	6800
Unit 4	Power (kW)	1429.05	1290.21	1399.69
	Distance (ft)	9200	9800	9500
Energy Losses (kWh)		130014.3	130316.5	129379.9

Table 4.4. Optimum allocation of generation units - 100 nodes.

Scenario		One Unit	Two Units	Four Units
Unit 1	Power (kW)	5000	3000	1666.7
	Distance (ft)	6666.7	4000	2222.2
Unit 2	Power (kW)	----------	3000	1666.7
	Distance (ft)	----------	8000	4444.4
Unit 3	Power (kW)	----------	----------	1666.7
	Distance (ft)	----------	----------	6666.7
Unit 4	Power (kW)	----------	----------	1666.7
	Distance (ft)	----------	----------	8888.8

Table 4.5. Optimum allocation of generation units – theoretical results in snapshot mode – 100 nodes.

4.3.4. 500-Node System

The 500-node feeder follows the same configuration shown in Figure 4.2. The values used for the 500-node test system are as follows:

- Total feeder length: 30000 ft.
- Number of nodes: 500 (i.e., section length = 60 ft).
- Node load = 9 kW, pf = 0.9 (lg) (i.e., total load = 4500 kW).

As in the previous study, the goal is to optimize the location and rated power of PV generations for an evaluation period of one year. System curves were generated using HOMER. Figure 4.8 shows the results corresponding to the 500-node test system when the goal is to allocate a single generation unit. The values are different but the shape of the plot surface is similar to that obtained with the 100-node test system.

Table 4.6 summarizes the main results (i.e., locations and rated powers of the PV units) when allocating one, two, and four generation units. The results show clear tendencies for one and two generation units, which indicates that the number of executed runs is enough for these two cases. The values obtained for four units present important

variations from one execution to another; this is an indication that more runs are necessary to identify the correct values or tendencies for the optimum distances and rated powers.

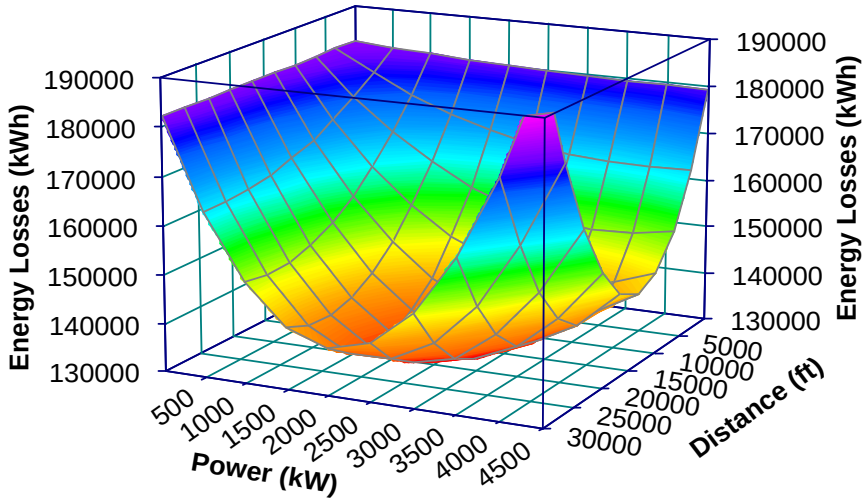

Figure 4.8. Optimum location of a single generation unit. Test system with 500 nodes; 5000 runs.

		One generation unit		
Runs		2500	5000	10000
Unit 1	Power (kW)	2738.2	2717.4	2735.9
	Distance (ft)	19860	19860	19560
Energy Losses (kWh)		132081.2	132076.4	132087.6
		Two generation units		
Runs		5000	10000	15000
Unit 1	Power (kW)	1625.7	1581.8	1717.3
	Distance (ft)	11220	12840	11460
Unit 2	Power (kW)	1727.1	1472.4	1629.1
	Distance (ft)	23880	25560	23460
Energy Losses (kWh)		128185.0	128322.8	128188.0
		Four generation units		
Runs		10000	15000	20000
Unit 1	Power (kW)	640.5	1322.6	646.4
	Distance (ft)	3660	8640	8520
Unit 2	Power (kW)	985.5	784.6	1064.6
	Distance (ft)	11160	17100	14100
Unit 3	Power (kW)	936.4	626.6	884.3
	Distance (ft)	19260	24300	19860
Unit 4	Power (kW)	1059.5	635.4	846.1
	Distance (ft)	24360	26460	26880
Energy Losses (kWh)		126891.4	127053.5	126858.1

Table 4.6. Optimum allocation of generation units - 500 nodes.

4.3.5. 1000-Node System

The 1000-node test system has the same configuration as the 100 and 500-node feeders. The values used for the test system are:

- Total feeder length: 50000 ft.
- Number of nodes: 1000 (i.e., section length = 50 ft).
- Node load = 3 kW, pf = 0.9 (lg) (i.e., total load = 3000 kW).

The procedure will be applied to determine the optimum allocation of one or more PV and wind generation units using a one-year evaluation period. Both studies will be carried out independently (i.e. either only PV generation or wind generation will be considered).

All node load profiles, PV and wind generation curves have been created using the algorithms presented in Chapter 3. Table 4.7 presents the statistics and parameters used to generate the PV and Wind generation curves. Base curves for node load profiles were obtained from [4.19].

Average monthly clearness index	0.51, 0.56, 0.56, 0.55, 0.54, 0.57, 0.60, 0.57, 0.55, 0.50, 0.48, 0.49
Panel's slope angle	35º
Normal operating cell temperature	45ºC
Average monthly daily minimum temperatures (ºC)	6.77, 6.97, 8.39, 10.0, 13.3, 17.1, 19.9, 20.5, 18.2, 15.3, 10.7, 8.18
Average monthly daily maximum temperatures (ºC)	12.2, 12.7, 14.5, 16.1, 19.5, 23.5, 26.3, 26.4, 23.7, 20.2, 15.7, 13.2
Average monthly wind speed (m/s)	6.64, 7.84, 7.34 5.35, 4.61, 4.76, 4.27, 4.46, 4.53, 6.1, 4.83, 8.16
Wind curve parameters: i_d, h_p, a, k	0.05, 15.04, 0.73, 1.88

Table 4.7. Summary of solar and wind resources.

Optimum Allocation of PV Generation

The Monte Carlo procedure was applied using different number of runs for one, two, four, and eight PV generation units. Figure 4.9 shows the results when the goal is to allocate a single PV generation unit. The surface drawn resembles the ones obtained for the 100 and 500-node feeders; therefore, one could expect a similar behavior for any type of radial feeder when allocating one single PV generation unit.

The complete results for this study are shown in Table 4.8. These results clearly prove that the number of runs has to be increased with the number of generation units to be allocated. The same behavior as in the previous studies can be identified; the results for one and two generation units show clear tendencies but when allocating more units the results are not conclusive and require a larger number of runs.

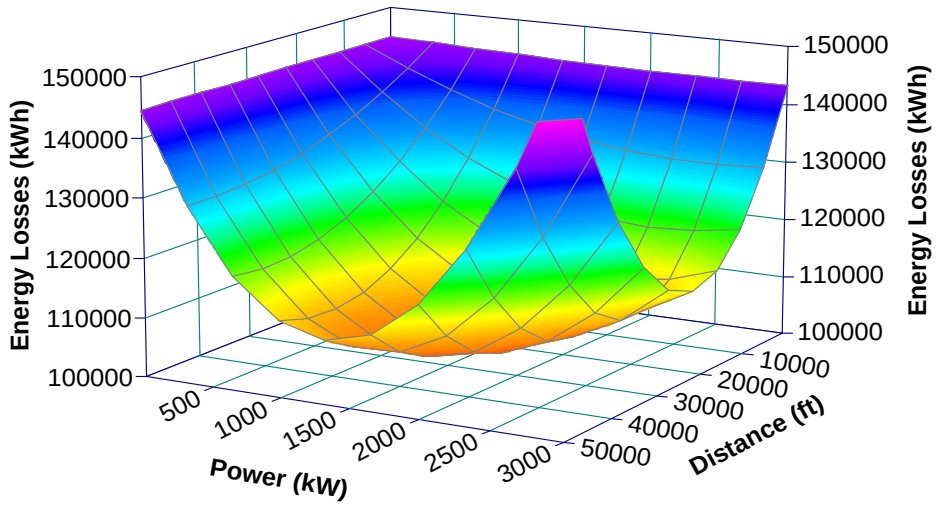

Figure 4.9. Optimum location of a single PV generation unit. Test system with 1000 nodes; 10000 runs.

Optimum Allocation of Wind Generation

The same procedure was applied to the 1000-node feeder for the allocation of one, two, four, and eight wind generation units. Figure 4.10 shows the results from the allocation of one wind generation unit. Note that the resulting surface is very similar to the surface found for the allocation of PV generation, but the optimum values are different. The surface appears to be less smooth; this is due to the fact that several heights over sea level were considered for the nodes in the feeder.

Table 4.9 shows the results for a different number of runs. The results show some significant differences between the values found when the generation is of photovoltaic type or wind type, and that the required ratings of the wind power generation units are smaller than those required for solar power generation. This conclusion can also be easily understood by looking at the curves for solar and wind generation; since the generation patterns are very different, see Figure 4.11, the optimum values will also be different.

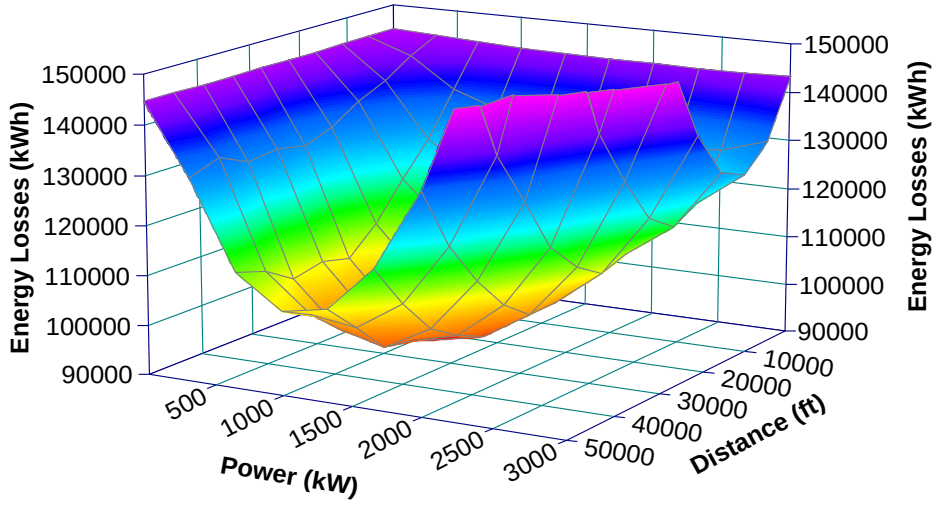

Figure 4.10. Optimum location of a single wind generation unit. Test system with 1000 nodes; 10000 runs.

One important aspect to consider is the energy losses obtained for the execution with different numbers of runs; the differences in energy losses are very small and in some cases negligible (always within the 1% margin). Therefore, it can be expected that global minimum won't present a significant variation with respect to the values found with the procedure. It has been discussed that more runs are required to establish a well-defined tendency for more than two generation units. However, one must consider if the increment in computational time is justified when assessing the improvement in energy losses obtained with a larger number of runs.

		One Generation Unit		
Runs		5000	10000	20000
Unit 1	Power (kW)	1801.5	1792.08	1776.87
	Distance (ft)	32900	33250	33400
Energy Losses (kWh)		104452.4	104447.8	104447.1
		Two Generation Units		
Runs		10000	20000	40000
Unit 1	Power (kW)	1309.76	1081.21	1023.82
	Distance (ft)	19550	18500	18450
Unit 2	Power (kW)	967.51	1119.06	1130.2
	Distance (ft)	39450	39750	41200
Energy Losses (kWh)		101485.1	101278.6	101365.4
		Four Generation Units		
Runs		20000	40000	80000
Unit 1	Power (kW)	774.66	605.28	538.94
	Distance (ft)	12850	12950	11150
Unit 2	Power (kW)	618.62	615.88	726.17
	Distance (ft)	23550	22950	22200
Unit 3	Power (kW)	391.24	459.91	735.68
	Distance (ft)	36700	30950	34250
Unit 4	Power (kW)	558.38	699.32	412.93
	Distance (ft)	47050	45500	45950
Energy Losses (kWh)		100263.3	100197.3	100139.4
		Eight Generation Units		
Runs		40000	80000	160000
Unit 1	Power (kW)	246.13	265.91	96.03
	Distance (ft)	2550	1100	1650
Unit 2	Power (kW)	299.13	424.88	385.24
	Distance (ft)	14400	8800	7400
Unit 3	Power (kW)	283.59	453.44	389.27
	Distance (ft)	16050	15250	13900
Unit 4	Power (kW)	319.48	509.56	344.8
	Distance (ft)	22850	25500	20200
Unit 5	Power (kW)	380.83	169.66	119.94
	Distance (ft)	29850	29900	21700
Unit 6	Power (kW)	259.11	308.29	461.31
	Distance (ft)	34800	37350	30850
Unit 7	Power (kW)	340.23	333.58	426.57
	Distance (ft)	40300	41700	37750
Unit 8	Power (kW)	307.93	299.64	367.79
	Distance (ft)	46250	47950	47350
Energy Losses (kWh)		99779.0	99798.2	99747.2

Table 4.8. Optimum allocation of PV generation units.

One Generation Unit				
Runs		5000	10000	20000
Unit 1	Power (kW)	1371.16	1420.68	1455.31
	Distance (ft)	29900	29950	29750
Energy Losses (kWh)		92137.5	92034.1	92089.6
Two Generation Units				
Runs		10000	20000	40000
Unit 1	Power (kW)	921.03	934.97	872.08
	Distance (ft)	22250	21600	23500
Unit 2	Power (kW)	655.47	724.17	763.19
	Distance (ft)	39400	38400	39600
Energy Losses (kWh)		89622.9	89580.9	89545.7
Four Generation Units				
Runs		20000	40000	80000
Unit 1	Power (kW)	668.92	447.87	158.62
	Distance (ft)	3600	1850	10450
Unit 2	Power (kW)	254.63	679.33	250.85
	Distance (ft)	14700	7700	16400
Unit 3	Power (kW)	663.58	708.12	685.47
	Distance (ft)	23450	27750	26900
Unit 4	Power (kW)	781.07	633.71	671.78
	Distance (ft)	38600	39450	39100
Energy Losses (kWh)		89499.1	89331.5	89447.0
Eight Generation Units				
Runs		40000	80000	160000
Unit 1	Power (kW)	255.7	570.58	435.34
	Distance (ft)	2800	1400	2550
Unit 2	Power (kW)	305.14	353.11	71.44
	Distance (ft)	3850	1600	3100
Unit 3	Power (kW)	52.14	27.14	534.94
	Distance (ft)	8900	13500	5600
Unit 4	Power (kW)	44.47	291.97	108.08
	Distance (ft)	16550	17200	14150
Unit 5	Power (kW)	55.95	59.09	40.74
	Distance (ft)	17100	17700	19700
Unit 6	Power (kW)	857.68	37.19	208.59
	Distance (ft)	22500	22600	21100
Unit 7	Power (kW)	70.75	737.44	711.18
	Distance (ft)	36050	25950	26650
Unit 8	Power (kW)	735.32	731.63	638.5
	Distance (ft)	42250	37900	39700
Energy Losses (kWh)		91218.5	90164.9	90197.1

Table 4.9. Optimum allocation of wind generation units.

4.3.6. Monte Carlo Method Using Multi Core Computing

A very important aspect to consider is the reduction of time that can be achieved when using parallel computing. Table 4.10 provides the computing times that were required for simulating the 100 and 500-node test systems, as well as the corresponding energy losses, using single- and multicore computations. Note that the 500-node test system was not simulated using a single core environment when more than one PV generation unit had to be allocated.

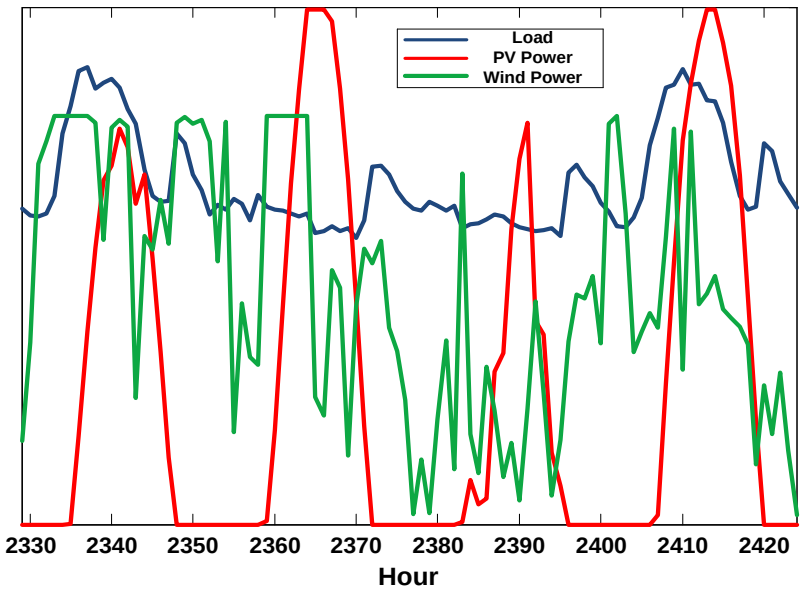

Figure 4.11. Profiles of load and generation.

100-Node Test System			
Scenario	Single Core	Multicore Computing	
		30 cores	60 cores
One photovoltaic generator (1000 runs)	134736 kWh 6211 s	134758 kWh 246 s	134763 kWh 124 s
Two photovoltaic generators (2000 runs)	130874 kWh 12729 s	130895 kWh 467 s	130916 kWh 231 s
Four photovoltaic generators (4000 runs)	129797 kWh 26009 s	129587 kWh 914 s	130316 kWh 481 s
500-Node Test System			
Scenario	Single Core	Multicore Computing	
		30 cores	60 cores
One photovoltaic generator (5000 runs)	132076 kWh 118846 s	132078 kWh 5566 s	132076 kWh 2653 s
Two photovoltaic generators (10000 runs)	---------	128304 kWh 11227 s	128322 kWh 5335 s
Four photovoltaic generators (20000 runs)	---------	126965 kWh 22630 s	126858 kWh 10567 s

Table 4.10. Simulation results using multicore computing.

As expected, the achieved reduction of simulation time is significant and almost proportional to the number of cores. Although the simulation times are still too high, mainly for the larger test system, the conclusion of the study is that, as expected, the simulation time can be reduced by just increasing the number of cores involved in computations.

The application of a parallel distributed computing environment is becoming a usual practice and it is foreseen that large multicore systems will be soon available at an affordable cost. In addition, a similar procedure could be implemented in a larger computer cluster (i.e., using grid computing), so a not-too long simulation time could be achieved without significantly increasing the cost.

4.3.7. Refinement of the Monte Carlo Method

Figure 4.12 is aimed at illustrating the way in which the Monte Carlo method can be applied to this particular study when only one generation unit has to be connected. Every cross within the square is a combination of the two random numbers that are generated for each run: the distance, in feet, with respect to the origin of the feeder at which the capacitor bank or the generation unit is to be installed, and the corresponding rated power (in kW). The result that is of concern for the present study is the energy loss obtained for each combination of values; see, for instance, the plot of Figure 4.8.

Not much difference between results should be expected when the combination of the two random values gives a point that is closely located to a previously obtained and simulated point. Therefore, during the generation of random values, these cases do not need to be simulated. There are, then, two options:

1. Skip the simulation of such cases, reducing in turn the final number of runs.
2. Repeat the generation of random values when the case to be simulated is one of those mentioned above, and keep the number of runs.

The option followed in this work is the first one. The goal is to check how much accuracy is lost and how much reduction of time is achieved by neglecting some runs. The approach is basically the same when more than one generation unit has to be connected. In such case all combinations located within a Euclidean distance equal or shorter than R are discarded.

Assume that some Monte Caro runs have been already computed and simulated. The combination of random values corresponding to run k is not simulated when the following condition is fulfilled:

$$\sqrt{x_{j-k}^2 + p_{j-k}^2} \leq R \tag{4.4}$$

where n is the number of generation units to be connected, $x_{ij\text{-}ik}$ is the distance in percentage between the location of the unit i corresponding to runs j (previously simulated) and k, respectively, and $p_{ij\text{-}ik}$ is the distance in percentage between the rated powers of the unit i corresponding to runs j and k. R in this work will be 5%.

However, obtaining the minimum Euclidean distance between the combinations of random values corresponding to two different runs is not obvious, since the order in which generation units are numbered does not have to be same when comparing two different runs. In addition, expression (4.4) has to be checked with respect to any previous combination, which can be time consuming.

Consider Figure 4.13 in which the random values of four units at run *k* have to be paired with the random values already used in run *j* in order to obtain the minimum distance between the two runs. The figure is aimed at illustrating the difficulty of such task since the number of combinations, taking into account the two values associated to each PV generation unit, that have to be checked will significantly increase as the number of units to be allocated increases.

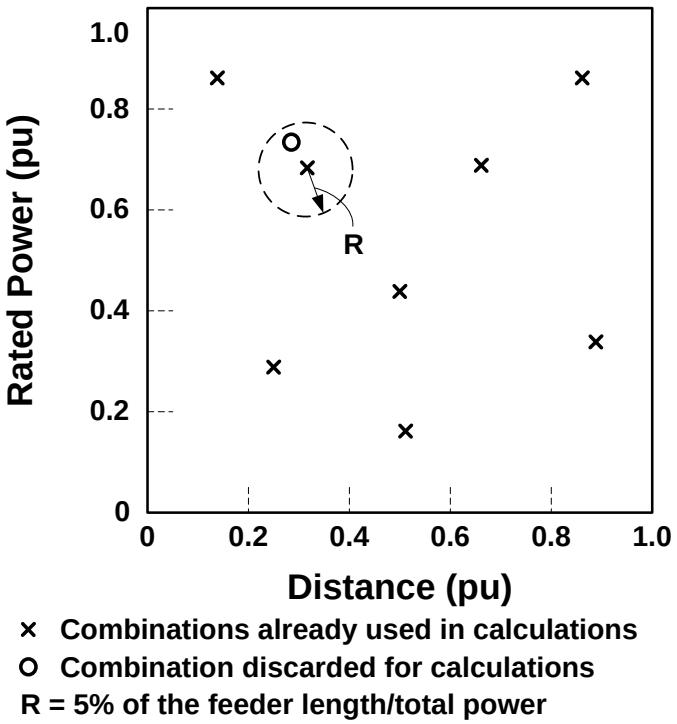

Figure 4.12. Generation of random values for energy loss calculations – One generation unit.

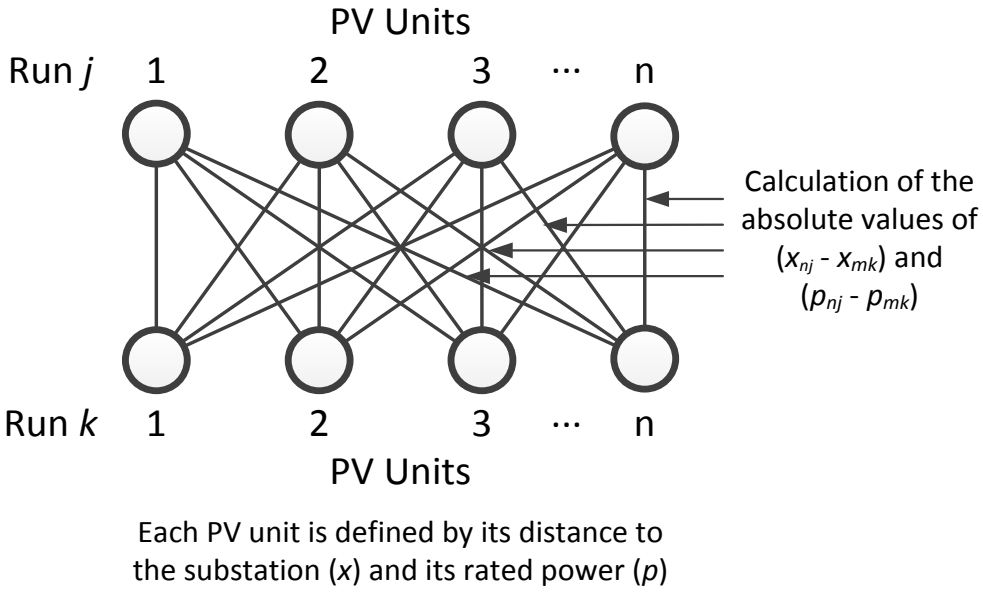

Figure 4.13. Pairing of n PV generation units in the Monte Carlo method to obtain the minimum distance between random values.

The criterion used in this work is a simplified one and it is based on pairing units considering their location. Figure 4.14 illustrates this aspect. The procedure corresponding to runs *j* and *k* begins with unit 1 which is paired to the closer unit in run *j*, continues with unit 2 which is paired to the closer unit selected between the remaining units, and so on. Figure 4.14a shows the result of pairing units according to this criterion. That is, units are paired as (1-3), (2-4), (3-1) and (4-2), being the first number corresponding to run *k*. Note that pairing generation units as indicated in Figure 4.14a is equal to order units taking into account their distance to the substation (i.e., shorter distances first). Therefore, pairing generation units is straightforward if they are ordered in such a manner after generating random numbers. However, this procedure is not too rigorous since some additional checking might be required, as illustrated in Figure 4.14b. As shown in this second case, pairs are (1-2), (2-4), (3-4) and (4-3), and they might result in a shorter overall distance.

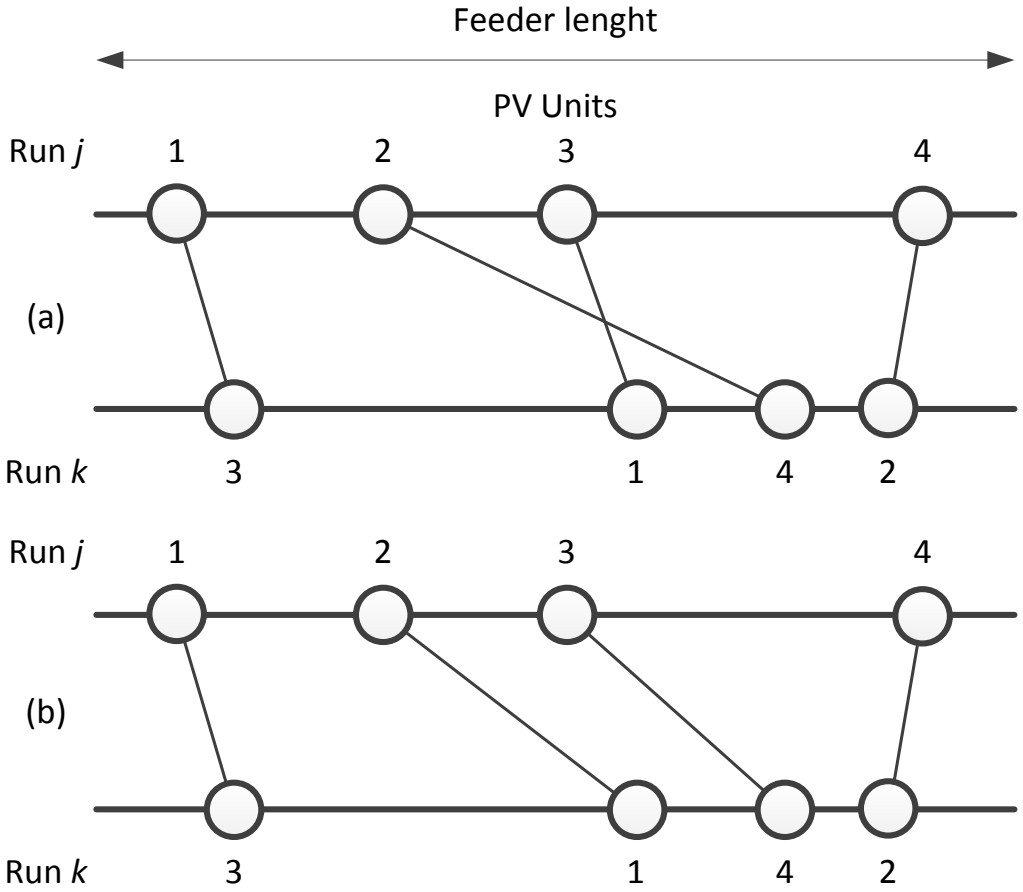

Figure 4.14. Pairing of PV generation units to obtain the distance between two Monte Carlo runs.

Since the goal is to reduce the number of runs, the criterion illustrated in Figure 4.14a will be applied in this work. Note that the random values obtained in the two runs for the rated powers are irrelevant to pair units when applying this criterion. Another important aspect is the minimum distance between two adjacent generation units. The combination of random numbers will be discarded before any checking with previous runs if at least one of these distances is shorter than the minimum distance *MinD*, see (4.5).

$$MinD = \frac{4 \cdot R}{n} \cdot F_L \tag{4.5}$$

where n is the number of generation units to be connected, R is the minimum Euclidean distance between two different runs, and F_L is the total feeder length.

Assume that n PV generation units have to be allocated and p runs have been already simulated; the procedure to decide whether the combination of random values (p+1) will be simulated or not can be summarized as follows:

1. Start the application of the criterion detailed above (see Figure 4.14a) to pair units by comparing the values of run (p+1) to the values of run 1, and obtain the 2n differences between random values.
2. Discard the run if at least one physical distance between two contiguous generation units is shorter than *MinD*.
3. Check if at least one difference exceeds the tolerance R (see Figure 4.13); otherwise, calculate the Euclidean distance using (2). Use flag "1" if at least one value from both checks is above R; otherwise use flag "0".
4. Repeat the two previous steps to compare run (p+1) to any previous run.
5. Simulate the run if the p flags are "1".
6. Continue the procedure until the last run previously scheduled.

Table 4.11 through Table 4.13 show a summary of results obtained for the 500 and 1000-node test systems by applying this procedure. All the results shown in the table were obtained by using parallel computing and 60 cores. It is worth mentioning that the computing time spent to perform the additional calculations with respect to the original method is less than 5 seconds when four units have to be allocated in the 500-node test system.

Scenario		Original Method	Refined Method
One photovoltaic generator Scheduled number of runs = 5000	Generation locations (ft)	19860	18840
	Rated powers (kW)	2717.4	2768.8
	Energy losses (kWh)	132076	132184
	Simulation time (s)	2653	176
Two photovoltaic generators Scheduled number of runs = 10000	Generation location (ft)	12840 - 25560	11880 – 23580
	Rated powers (kW)	1581.8 - 1472.4	1402.4 – 1744.4
	Energy losses (kWh)	128322	128221
	Simulation time (s)	5335	2708
Four photovoltaic generators Scheduled number of runs = 20000	Generation location (ft)	8520 - 14100 - 19860 - 26880	10140 - 15720 - 22020 - 27180
	Rated powers (kW)	646.4 - 1064.6 - 884.3 - 846.1	679.6 - 1021.0 - 674.2 - 830.2
	Energy losses (kWh)	126858	127018
	Simulation time (s)	10567	2746

Table 4.11. Simulation results using a refined Monte Carlo method – 500-node test system.

The tables prove that a significant reduction in computing time can be achieved; however, the accuracy of the new approach decreases as the number of generation units increases. This is an expected result, and it is evident that the accuracy can be improved by checking the differences between rated powers, not only between distances to the substation. Although some differences between location and power values between the two approaches are very significant, the energy losses obtained when applying the Monte Carlo method with the new rules are basically the same that were obtained whit the original method. These differences can be justified by looking at the energy losses obtained when a single generation unit is to be allocated, see Figure 4.8. The surface shown in those figures is very smooth, mainly around the optimum, so the difference between energy losses for non-small deviation with respect to the optimum will not be very significant.

Scenario		Original Method	Refined Method
One generator Scheduled number of runs = 10000	Generation locations (ft)	33250	32750
	Rated powers (kW)	1792.1	1831.5
	Energy losses (kWh)	104447.8	104469.2
	Simulation time (s)	11431	369
Two generators Scheduled number of runs = 40000	Generation location (ft)	18450 - 41200	19550 - 39200
	Rated powers (kW)	1023.8 - 1130.2	1168.9 - 1010.4
	Energy losses (kWh)	101365.5	101321.7
	Simulation time (s)	46966	12051
Four generators Scheduled number of runs = 80000	Generation location (ft)	11150 - 22200 - 34250 - 45950	9950 - 24650 - 36550 - 44000
	Rated powers (kW)	538.9 - 726.2 - 735.7 - 412.9	693.1 - 704.4 - 510.2 - 487
	Energy losses (kWh)	100139.4	100114.8
	Simulation time (s)	92757	47871
Eight generators Scheduled number of runs = 160000	Generation location (ft)	1650 - 7400 - 13900 - 20200 - 21700 - 30850 - 37750 - 47350	5950 - 9200 - 15400 - 22400 - 27800 - 34050 - 41850 - 49250
	Rated powers (kW)	96 - 385.2 - 389.3 - 344.8 - 119.9 - 461.3 - 426.6 - 367.8	281.5 - 359.5 - 262 - 238 - 245.1 - 548.7 - 344.1 - 287
	Energy losses (kWh)	99747.2	99773.3
	Simulation time (s)	189062	41208

Table 4.12. Simulation results using a refined Monte Carlo method – 1000-node test system – PV generation.

Scenario		Original Method	Refined Method
One generator Scheduled number of runs = 10000	Generation locations (ft)	29950	28600
	Rated powers (kW)	1420.7	1288.1
	Energy losses (kWh)	92034.2	93126.5
	Simulation time (s)	12660	423
Two generators Scheduled number of runs = 40000	Generation location (ft)	23500 - 39600	20550 - 38750
	Rated powers (kW)	872.1 - 763.2	761.4 - 901.3
	Energy losses (kWh)	89545.8	88802.1
	Simulation time (s)	47376	11901
Four generators Scheduled number of runs = 80000	Generation location (ft)	10450 - 16400 - 26900 - 39100	3850 - 20500 - 26850 - 34550
	Rated powers (kW)	158.6 - 250.8 - 685.5 - 671.8	610.9 - 707.1 - 67.5 - 722.5
	Energy losses (kWh)	89447	88516.1
	Simulation time (s)	99338	47594
Eight generators Scheduled number of runs = 160000	Generation location (ft)	2550 - 3100 - 5600 - 14150 - 19700 - 21100 - 26650 - 39700	100 - 3000 - 14050 - 20950 - 22250 - 25050 - 33850 - 37100
	Rated powers (kW)	435.3 - 71.4 - 534.9 - 108.1 - 40.7 - 208.6 - 711.2 - 638.5	172.6 - 121.24- 659.6 - 181.9 - 90.6 - 194.9 – 72 - 798.7
	Energy losses (kWh)	90197.1	89209.3
	Simulation time (s)	195259	41392

Table 4.13. Simulation results using a refined Monte Carlo method – 1000-node test system – Wind generation.

4.4. Optimum Allocation of Distributed Generation in Multi-feeder Systems

4.4.1. Introduction

The previous section introduced the application of the Monte Carlo method for the optimum allocation of distributed generation in radial feeders. Although the studies that were carried out provided much useful information, the conclusions drawn from those studies are limited because the radial feeder configuration is not a realistic one. Therefore, it is necessary to test the procedure using a test system that better represents the characteristics of real power distribution systems.

The studies presented in this Section are carried out for an evaluation period of one year (i.e. short term evaluation). These studies will help validate the Monte Carlo approach when working with Multi-feeder systems; furthermore, the results from this Section will be used to estimate the number of required executions of the Monte Carlo method in order to achieve the desired accuracy according to the number of generation units to be connected.

4.4.2. Test System

Figure 4.15 shows the diagram for the test system. It is a three-phase overhead system serving three feeders with different topologies and load characteristics. The system is based on IEEE test feeders [4.20], and has been created on purpose for this study. The model includes a simplified representation of the high-voltage system. Some of the main characteristics of the substation transformer are given below:

- High-voltage rating: 230 kV
- Low-voltage rating: 4.16 kV
- Rated power of substation transformer: 10000 kVA

System curves have been generated using the procedures presented in the previous Chapter. Table 4.14 presents basic information for the three feeders of the test system and Table 4.15 summarizes the information used to obtain sun power generation curves. For the present study a PV generator is connected to the system through a step-up interconnection transformer, see Figure 4.16. The rated power of the interconnection transformer is chosen once the rated power of the PV plant has been selected; it is rounded in steps of 50 kVA. By default, the short circuit impedance is 6%.

Feeder	Total active power (kW)	Total reactive power (kvar)	Number of loads	Lengths (km)
A	1700	930.72	51	26.36
B	2045	992.69	31	18.52
C	2290	899.38	19	11.81

Table 4.14. Test system information.

Average monthly clearness index	0.51, 0.56, 0.56, 0.55, 0.54, 0.57, 0.60, 0.57, 0.55, 0.50, 0.48, 0.49
Panel's slope angle	35º
Normal operating cell temperature	45ºC
Average monthly daily minimum temperatures	6.77, 6.97, 8.39, 10.0, 13.3, 17.1, 19.9, 20.5, 18.2, 15.3, 10.7, 8.18
Average monthly daily maximum temperatures	12.2, 12.7, 14.5, 16.1, 19.5, 23.5, 26.3, 26.4, 23.7, 20.2, 15.7, 13.2

Table 4.15. Summary of solar resources.

4.4.3. Short Term Evaluation

The evaluation period for this first study will be one year. The study is performed without including substation transformer losses in the optimization process. The number of runs is always chosen as a multiple of the number of core nodes (60 cores in this work) to obtain a homogeneously distributed burden among processing units.

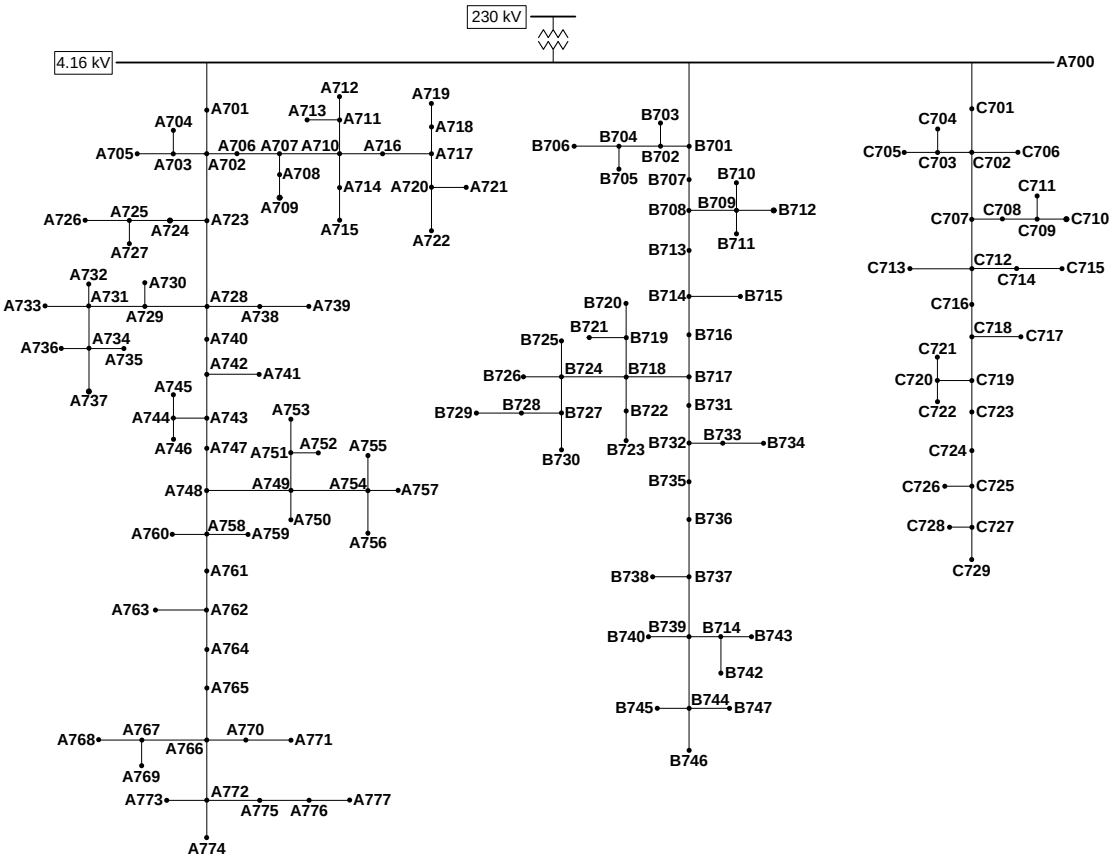

Figure 4.15. Test system configuration.

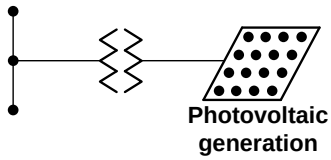

Figure 4.16. Configuration of a PV generator.

Table 4.16 provides some information about the system behavior considering three different load models and before connecting distributed generation. The ZIP load model is defined as a combination of constant power, constant current and constant impedance load models [4.21]; each load representation is assigned weighting factors for active and reactive powers, being the sum of all weighting factors equal to unity for both active and reactive powers. For the present study each part of the model has been assigned a weighting factor equal to 1/3 for both active and reactive powers; this means that 1/3 of the load behaves respectively as a constant power, constant current and constant impedance load.

	Constant power load model	Constant impedance load model	ZIP load model
Feeder A	62924.8 kWh	62645.1 kWh	62768.9 kWh
Feeder B	56683.4 kWh	55593.9 kWh	56102.2 kWh
Feeder C	153289.3 kWh	148248.6 kWh	150643.1 kWh
Total feeders	272897.6 kWh	266487.6 kWh	269514.2 kWh

Table 4.16. Short term evaluation (1 year) – Energy losses without distributed generation.

Optimum Allocation of One PV Generation Unit				
Runs		1560	2400	3120
Unit 1	Node	C724	C723	C723
	Power (kW)	1045.5	1236.2	1277.1
Energy losses (kWh)		256694.4	256486.0	256460.9
Optimum Allocation of Two PV Generation Units				
Runs		9600	14400	19200
Unit 1	Node	A770	A772	A773
	Power (kW)	196.3	246.5	279.9
Unit 2	Node	C719	C719	C724
	Power (kW)	1244.3	1088.2	1188.1
Energy losses (kWh)		253445.5	253714.9	253105.8
Optimum Allocation of Four PV Generation Units				
Runs		33600	50400	67200
Unit 1	Node	A766	A769	A766
	Power (kW)	343.0	360.3	284.6
Unit 2	Node	B740	B714	B721
	Power (kW)	195.79	233.9	34.75
Unit 3	Node	B747	B736	B744
	Power (kW)	292.2	366.0	320.4
Unit 4	Node	C723	C719	C725
	Power (kW)	1109.8	1140.0	1110.5
Energy losses (kWh)		250175.5	250491.9	249938.3

Table 4.17. Short term evaluation (1 year) – Optimum allocation of PV generation units (constant power).

Table 4.17 presents the results obtained after applying the procedure with different number of units and runs, and assuming the load behaves according to the constant power model. This first study will be used to fix the number of runs of the Monte Carlo method when one, two or four generation units are to be connected. The required number of runs depends on the variance of the target variable, the energy losses measured at the substation terminals, and the desired accuracy [4.22]. In this study the 1% margin for the variations of the target variable is used as the convergence criterion.

Note that the results in Table 4.17 for any number of units and obtained with different number of runs show that although the combinations of rated powers are different from each other, the resulting energy losses are rather similar; at the end, the differences between the energy losses are within 1%. This behavior proves that only small variations in the energy losses are achieved when the evaluation point is close to the actual optimum solution and suggests that the ultimate goal could be reaching a quasi-optimum result if a significant reduction in the simulation time can be achieved.

Table 4.18 through Table 4.20 summarize the results upon the application of both the conventional and the refined Monte Carlo methods (introduced in the previous Section of this Chapter) to the optimum allocation of one, two, and four generation units with a different number of runs and different load models. Note that when two or more units are to be allocated they have been ordered beginning with the largest one.

The results in Table 4.18 through Table 4.20 show that as expected, the more units to be connected, the larger the energy loss reduction. It is also evident that although the results with different load models exhibit variations of the optimum rated power values

and connection nodes, and they depend on the number of runs, the energy loss values resulting from combinations with the same number of units are very similar and differences between results from different models are rather low. Finally, the discrepancies between the results obtained with four units suggest that more runs are required.

Scenario		Original method	Refined method
One PV generator Runs = 3120	Node	C723	C723
	Rated power (kW)	1277.1	1211.1
	Energy losses (kWh)	256460.9	256671.6
	Simulation time (s)	783.8	276.2
Two PV generators Runs = 19200	Nodes	C724 - A773	C724 - A765
	Rated powers (kW)	1188.1 - 279.9	1364.4 - 429.5
	Energy losses (kWh)	253105.8	253387.8
	Simulation time (s)	4818.9	4501.9
Four PV generators Runs = 67200	Nodes	C725 - B744 - A766 - B721	C723 - B731 - A762 - B742
	Rated powers (kW)	1110.5 - 320.4 - 284.6 - 34.7	1291.4 - 454.6 - 383.8- 195.5
	Energy losses (kWh)	249938.3	249663.1
	Simulation time (s)	17009.6	15762.6

Table 4.18. Short term evaluation (1 year) – Comparison of simulation results - Constant Power Load Model - 60 cores.

Scenario		Original method	Refined method
One PV generator Runs = 3120	Node	C723	C724
	Rated power (kW)	1182.2	1141.1
	Energy losses (kWh)	252166.2	252239.5
	Simulation time (s)	733.4	267.6
Two PV generators Runs = 19200	Nodes	C723 - A767	C723 - A772
	Rated powers (kW)	1089.2 - 200.2	1161.5 - 299.7
	Energy losses (kWh)	249436.9	249003.6
	Simulation time (s)	4488.1	4277.8
Four PV generators Runs = 67200	Nodes	C724 - C719 - A763 - B747	C720 - C725 - B744 - A773
	Rated powers (kW)	747.4 - 378.3 - 326.8 - 191.9	595.3 - 427.5 - 333.4 - 140.3
	Energy losses (kWh)	247096.5	245883.5
	Simulation time (s)	16074.7	15141.1

Table 4.19. Short term evaluation (1 year) – Comparison of simulation results - Constant Impedance Model - 60 cores.

Table 4.21 provides a summary of the main results derived from the three load models when using the conventional Monte Carlo method. Note that in most scenarios the highest rated power generation corresponds to the ZIP model but the maximum energy loss reduction is achieved when assuming constant power load models. As for the

Monte Carlo approaches, it can be concluded that, except when only one unit is to be allocated, not much simulation time reduction (actually less than 20%) has been achieved with the refined method. In addition, it is very obvious that only when using a multicore environment the simulation times are affordable.

Scenario		Original method	Refined method
One PV generator Runs = 3120	Node	C723	C723
	Rated power (kW)	1232.9	1318.2
	Energy losses (kWh)	254228.5	254298.3
	Simulation time (s)	820.8	297.3
Two PV generators Runs = 19200	Nodes	C719 - A767	C723 - A765
	Rated powers (kW)	1140.0 - 282.7	1349.3 - 381.0
	Energy losses (kWh)	250820.0	251098.9
	Simulation time (s)	5013.8	4678.8
Four PV generators Runs = 67200	Nodes	C723 - B747 - A775 - A756	C724 - B731 - C728 - A759
	Rated powers (kW)	1140.3 - 289.1 - 228.4 - 120.9	624.6 - 598.3 - 460.7 - 282.4
	Energy losses (kWh)	247948.0	248701.0
	Simulation time (s)	17912.8	17268.3

Table 4.20. Short term evaluation (1 year) – Comparison of simulation results - ZIP Model - 60 cores.

Number of Units	Load Model	Total Generation (kW)	Loss Reduction (%)
1 Unit	Constant power	1277.1	6.02
	Constant impedance	1182.2	5.37
	ZIP	1232.9	5.67
2 Units	Constant power	1468.1	7.25
	Constant impedance	1289.5	6.39
	ZIP	1422.7	6.93
4 Units	Constant power	1750.3	8.41
	Constant impedance	1644.5	7.27
	ZIP	1778.8	8.00

Table 4.21. Short term evaluation (1 year) – Energy loss reduction – Conventional Monte Carlo method.

One can observe from the results presented in Table 4.18 trough Table 4.21 that when one unit is allocated the energy loss reduction is no more than 6.0%, depending on the load models, but when two units are connected the energy loss reduction increases not much more 1% and a similar increment is achieved when four units are connected. In case of a sequential connection, this would mean that it is with the first unit with which the largest energy loss reduction is achieved, and that unit should be connected to the feeder with the largest potential energy loss reduction (feeder C in this study). However, the second and subsequent unit would be connected taking into account not only the potential reduction that can be achieved in each feeder, but also the number of units already connected to each feeder.

4.5. Optimum Allocation of Distributed Generation Using Long Term Evaluation

4.5.1. Introduction

This section presents the results derived from a long term study aimed at estimating the optimum size and location of PV generators when the target is to minimize the energy losses and the generating units are sequentially connected. The objective is to apply the procedure for the sequential allocation of generation units with a longer evaluation period (i.e. larger than one year) presented in Section 4.2.3.

4.5.2. Long-term evaluation

Figure 4.17 shows the variation assumed for all loads of a given feeder during the evaluation period. Note that negative variations have also been assumed. Table 4.22 shows the year of connection for each PV generation unit. Table 4.23 gives the energy losses that would correspond to the entire period of evaluation (i.e., 17 years) without distributed generation and considering the three types of load models.

The main aspects of the study are:

- Up to 8 PV generation units will be connected to the three feeders of the test system.
- The optimization period, every time a PV unit is added to the system, is 10 years. That is, the target upon which the locations and rated powers of the units are selected is the optimization of energy losses during 10 years. According to this, if a unit is connected at the beginning of year 6, the energy losses to be accounted for are those caused from the beginning of year 6 till the end of year 15 (see Table 4.22).

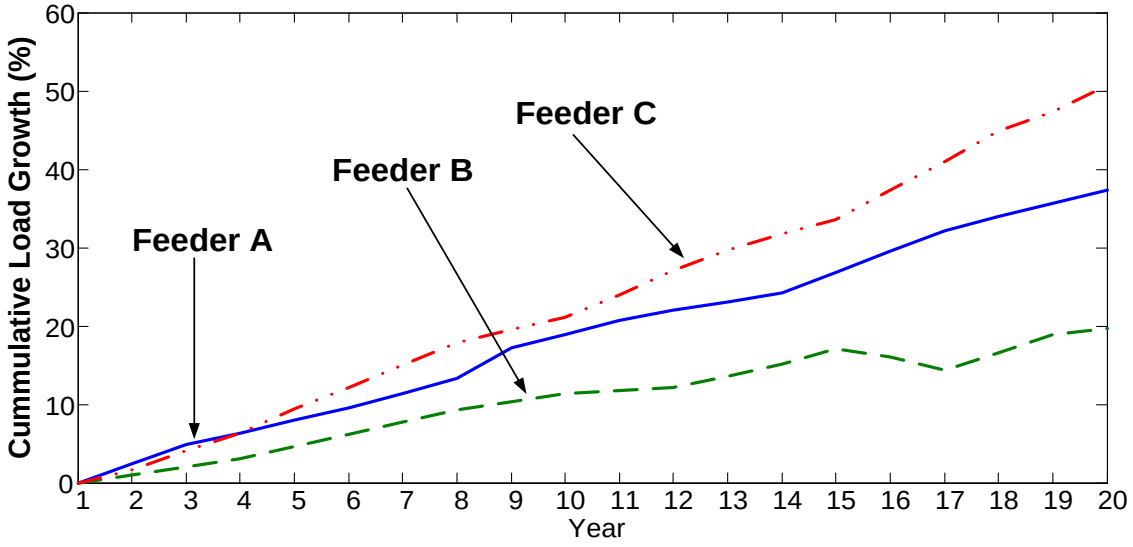

Figure 4.17. Load growth.

PV Unit	Year 1	2	3	4	5	6	7	8	9	10	11	12	13	14	15	16	17
1	•	X	X	X	X	X	X	X	X	X	–	–	–	–	–	–	–
2		•	X	X	X	X	X	X	X	X	X	–	–	–	–	–	–
3			•	X	X	X	X	X	X	X	X	X	–	–	–	–	–
4				•	X	X	X	X	X	X	X	X	X	–	–	–	–
5					•	X	X	X	X	X	X	X	X	X	–	–	–
6						•	X	X	X	X	X	X	X	X	X	–	–
7							•	X	X	X	X	X	X	X	X	X	–
8								•	X	X	X	X	X	X	X	X	X

Notes: • = Year of connection, X = Considered for optimization; – = Not considered for optimization

Table 4.22. Scenario for long term evaluation.

	Constant power load model	Constant impedance load model	ZIP load model
Feeder A	1498994.5 kWh	1457234.6 kWh	1476761.4 kWh
Feeder B	1180259.1 kWh	1135125.5 kWh	1156116.3 kWh
Feeder C	3786100.3 kWh	3543363.1 kWh	3656742.1 kWh
Total feeders	6465354.0 kWh	6135723.3 kWh	6289620.0 kWh

Table 4.23. Long Term Evaluation (17 years) – Energy losses without distributed generation.

Table 4.24 shows the results obtained upon the application of both the conventional Monte Carlo method and the refined method during the period of evaluation (17 years). The number of runs to be used every year PV generation is connected is based on the experience obtained with the previous study. As shown in Table 4.17 through Table 4.20, when one generator is to be connected 3120 runs will usually suffice. Table 4.25 summarizes the main results corresponding to each load model.

The maximum coincident active power measured at the substation terminals for each load model during the period of study is as follows: (1) constant power model = 5938.1 kW, (2) constant impedance model = 5547.7 kW; (3) ZIP model = 5727.1 kW. After connecting eight generation units, the total rated power of all the generation units is less than 60% of the maximum coincident power of the system at the end of the period. From the results presented in Table 4.24 one can observe that the maximum rated power of a generation unit is below 1500 kW with all load models. This maximum can be accepted according to the interconnection policies adopted by many utilities. However, it can exceed the limit adopted by other utilities, see for instance [4.23]; in such case, the procedure should be modified to include that limit in calculations.

Figure 4.18 shows the rated power of the generation units to be connected every year and the corresponding feeder to which they must be connected when using the conventional Monte Carlo method. The plots also show the cumulative reduction of energy losses, not the yearly reduction.

As expected, the larger values of the rated powers correspond to the first units to be allocated; that is, the rated powers of the unit to be connected at the beginning of year 1 are larger than the rated powers of any unit to be connected in subsequent years, irrespectively of the load model. However, due to the yearly variation of loads, when a unit is to be connected to a feeder in which other generation units have been previously connected, the optimum rated power of the new PV generation unit will not be always

smaller than any other PV generator in operation because the energy losses to be compensated for a certain 10-year term could be larger than for a previous term; for instance, rated powers to be connected at the beginning of year 5 are larger than those to be connected at the beginning of year 4. As with the short term evaluation, the highest reduction of energy losses corresponds again to the constant power load model, while the lowest generation is required when the load is represented as constant impedance. Observe that when comparing the results presented in Table 4.24 with those provided in Table 4.18 through Table 4.20, the resulting rated power values are different; this is basically due to the fact that in Table 4.24 the location and rated power of the PV generation unit have been derived from considering a long term evaluation (i.e. 10 years) which can justify the larger values.

Generation unit		Constant power load model Conventional - Refined method	Constant impedance load model Conventional - Refined method	ZIP load model Conventional - Refined method
Unit 1	Node	C723 - C724	C724 - C724	C724 - C724
	Rated power (kW)	1415.2 - 1334.4	1228.4 - 1277.7	1414.1 - 1301.4
Unit 2	Node	A766 - A765	A767 - A766	A765 - A766
	Rated power (kW)	375.2 - 415.6	373.7 - 414.4	367.8 - 344.1
Unit 3	Node	B739 – B739	B735 - B736	B737 - B739
	Rated power (kW)	501.9 - 505.5	556.2 - 473.9	521.9 - 511.6
Unit 4	Node	C729 - C715	C715 - C709	C711 - C709
	Rated power (kW)	279.2 - 288.3	195.8 - 321.7	227.7 - 328.1
Unit 5	Node	C709 - C709	C709 - C715	C715 - C715
	Rated power (kW)	237.4 - 245.6	325.1 - 193.2	144.7 - 203.7
Unit 6	Node	C715 - C729	C729 - C729	C722 - C729
	Rated power (kW)	163.2 - 156.7	142.0 - 154.3	191.1 - 229.8
Unit 7	Node	A754 - B727	A749 - B726	A749 - A749
	Rated power (kW)	236.6 - 184.3	272.8 - 104.5	187.0 - 143.0
Unit 8	Node	B724 - C722	C722 - C722	B724 - B727
	Rated power (kW)	185.0 - 237.2	187.5 - 141.3	136.4 - 143.9
Energy losses (kWh)		5766679.8 - 5777333.0	5547082.9 - 5551270.4	5660782.4 - 5659358.8
Simulation time (s)		65365.1 - 21390.1	63091.8 - 20131.5	70679.4 - 22565.9

Table 4.24. Long Term Evaluation – Comparison of simulation results.

Load Model	Total Generation (kW) (Conventional – Refined)	Cumulative Energy Loss Reduction (%) (Conventional – Refined)
Constant power	3393.9 - 3368.1	10.80 - 10.64
Constant impedance	3281.7 - 3081.5	9.59 - 9.52
ZIP	3191.1 - 3206.0	9.99 - 10.02

Table 4.25. Long Term Evaluation – Total generation and energy loss reduction.

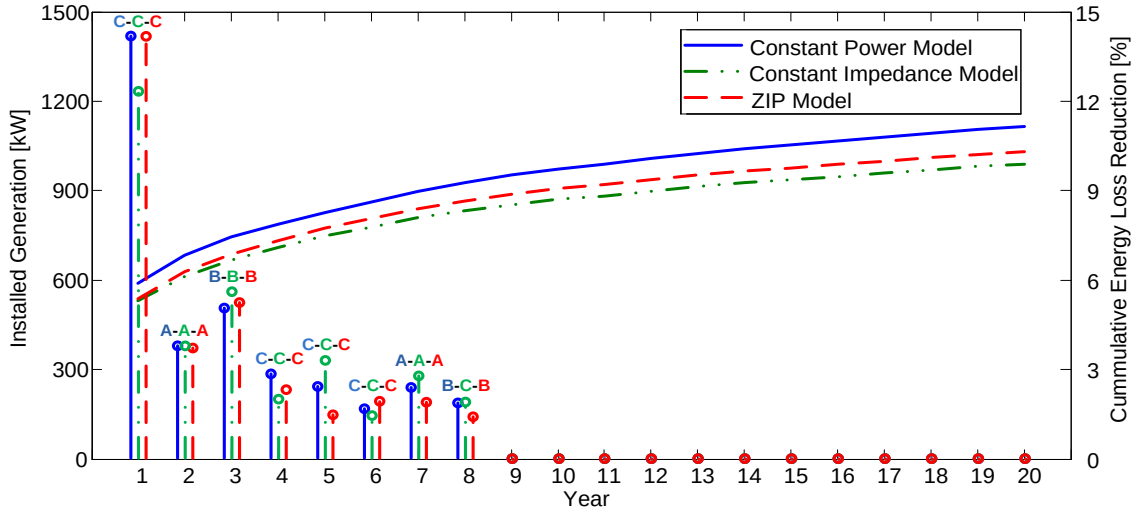

Figure 4.18. Sequential connection of optimum rated PV generators – Conventional Monte Carlo method.

The total power to be allocated is similar with the three load models: differences between load models are less than 2% with either the conventional Monte Carlo method or the refined one (see Table 4.25). As for the reduction of energy losses, the resulting values are different for each load model, but differences are again not too large. In addition, the resulting energy losses are basically the same with the two Monte Carlo approaches. This supports the conclusion that a quasi-optimum solution can be reached by considering different combinations of locations and rated powers because the optimum reduction of energy losses is not very sensitive with respect to rated powers and locations of generators. From the simulation times required in the case studies presented in Table 4.24 it is evident that a significant reduction in the CPU time can be achieved by using the refined approach only when units are connected one by one.

The behavior of the energy loss reduction factor deserves some special attention. The curves of Figure 4.18 show the energy loss reductions that are obtained at the end of a given year considering all the energy losses caused from the beginning of the period. One can note that the total reduction at the end of the studied period is not too large; less than 11%. There are several causes that justify this quantity. For example, consider the reduction achieved during the first year (about 6%); such small reduction is a consequence that only losses obtained in Feeder C, to which the first unit is connected, are compensated by the connected PV generation unit (although the substation transformer couples the three feeders and loads can be voltage dependent, the effect of the coupling is very small on the other two feeders). Moreover, since PV generators inject only active power, energy losses caused by the reactive component of load currents are not compensated. The nature of the solar resource causes that the connected PV generators will not inject power during many hours of the day and the injected power during other hours will be below or far below the maximum value they can inject. Finally, since the optimization period is 10 years and the load at the feeder to which the generator will be connected will be higher at the end of this period, the selected rated power will be such that the unit will overcompensate active load during the first years and undercompensate during the last years.

One can also observe that the reduction of energy losses continues after the last PV generation unit has been connected. Remember that the last unit is connected at the beginning of the 8th year, and its rated power is selected to minimize losses until the end of the 17th year. However, one can also observe that the cumulative energy loss reduction factor continues to increase after the optimization period (i.e. after the year 17). The cumulative energy loss reduction factor one year after the optimization period will exceed the cumulative energy loss reduction factor at the end of the optimization period if the energy loss reduction factor of that year exceeds the cumulative energy loss reduction factor at the end of the period. To understand this behavior assume the energy losses caused without and with distributed generation during a given year *i* are ΔE_i and $\Delta E_i'$, respectively. The energy loss reduction factor for that year is defined as follows:

$$r_i = \frac{\Delta E_i - \Delta E_i'}{\Delta E_i} \tag{4.6}$$

This expression can be rewritten to obtain

$$r_i = 1 - \frac{\Delta E_i'}{\Delta E_i} = 1 - f_i \tag{4.7}$$

where f_i is the ratio between energy losses with and without distributed generation, respectively, for year *i*.

Note that once a generation unit has been connected the energy losses during any period subsequent to the connection are smaller than they would be without the generation unit. Since the first unit in this study is connected at the beginning of year 1, this means that $1 > f_i > 0$ for any year *i*.

The cumulative energy loss reduction factor for a period of *n* years is defined as:

$$R_n = \frac{\sum_{i=1}^{n} \Delta E_i - \sum_{i=1}^{n} \Delta E_i'}{\sum_{i=1}^{n} \Delta E_i} \tag{4.8}$$

For an optimization period of *n* years (in Table 4.22 is 17 years), the goal is to determine the condition that has to be fulfilled to obtain the cumulative energy loss reduction factor at year (*n*+1) larger than that at year *n*; that is, the condition to have $R_{n+1} > R_n$.

This can be easily determined by using the following result. Given two fractions (*a*/*b*) and (*x*/*y*), in which *a*, *b*, *x* and *y* are real and positive numbers, if follows that:

$$\begin{aligned} &\frac{a+x}{b+y} > \frac{a}{b} \quad \text{if} \quad \frac{a}{b} < \frac{x}{y} \\ &\frac{a+x}{b+y} < \frac{a}{b} \quad \text{if} \quad \frac{a}{b} > \frac{x}{y} \end{aligned} \tag{4.9}$$

Equation (4.7) can be rewritten as follows:

$$R_n = 1 - \frac{\sum_{i=1}^{n} \Delta E_i'}{\sum_{i=1}^{n} \Delta E_i} = 1 - F_n \tag{4.10}$$

where

$$F_n = \frac{\sum_{i=1}^{n} \Delta E_i'}{\sum_{i=1}^{n} \Delta E_i} \tag{4.11}$$

Therefore, the condition to be obtained ($R_{n+1} > R_n$) will then occur if

$$F_{n+1} < F_n \tag{4.12}$$

The factor F at the end of year ($n + 1$) can be written as:

$$F_{n+1} = \frac{\sum_{i=1}^{n+1} \Delta E_i'}{\sum_{i=1}^{n+1} \Delta E_i} = \frac{\sum_{i=1}^{n} \Delta E_i' + \Delta E_{n+1}'}{\sum_{i=1}^{n} \Delta E_i + \Delta E_{n+1}} \tag{4.13}$$

According to second inequality of (4.9), condition (4.12) will be fulfilled if

$$\frac{\sum_{i=1}^{n} \Delta E_i'}{\sum_{i=1}^{n} \Delta E_i} > \frac{\Delta E_{n+1}'}{\Delta E_{n+1}} \tag{4.14}$$

which can be rewritten as $F_n > f_{n+1}$

This result is equivalent to the following one:

$$1 - F_n = R_n < r_{n+1} = 1 - f_{n+1} \tag{4.15}$$

This result means that the value of the cumulative energy loss reduction factor corresponding to the end of a given year, R_{n+1}, will exceed the value corresponding to the end of the previous year, R_n, if the energy loss reduction factor of year n+1, r_{n+1}, exceeds the cumulative energy loss reduction factor at the end of the previous year, R_n; that is, the cumulative factor will continue increasing while the energy loss reduction factor of one year is larger than the cumulative factor at the end of the previous year.
The cumulative energy loss reduction factor at the end of the optimization period is less than 11% with a constant power load model (see Figure 4.18) while the energy loss reduction factor during the subsequent years is above 11.5%; therefore, if no more generation units are connected, the trend will continue until the year at which the cumulative energy loss reduction factor exceeds the energy loss reduction factor

corresponding to that year. It is to be expected that the reduction of energy losses could be larger if the number of units to be connected were higher. However, the present study is not aimed at estimating the number of units that could achieve the maximum reduction of energy losses.

Figure 4.19 shows some results derived from this study with the ZIP model only. It is obvious from these results that DG has a positive impact on node voltages (Figure 4.19a shows how the voltages are increased after distributed generation is connected), and some important reductions of the energy required from the HV system and in the distribution test system losses are achieved.

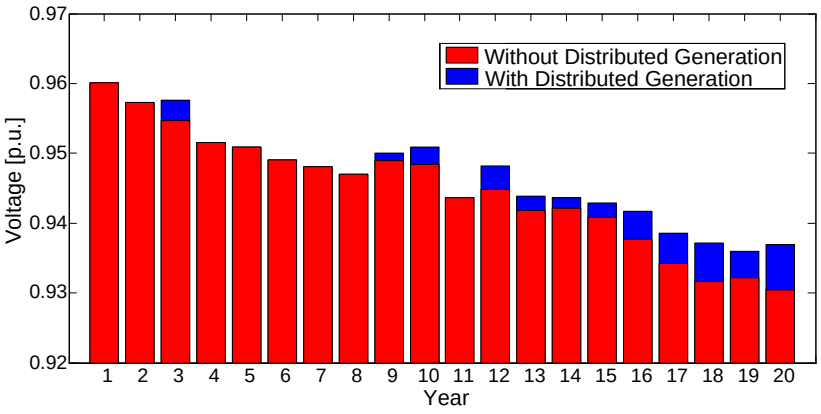

a) Impact of DG on the minimum voltage values.

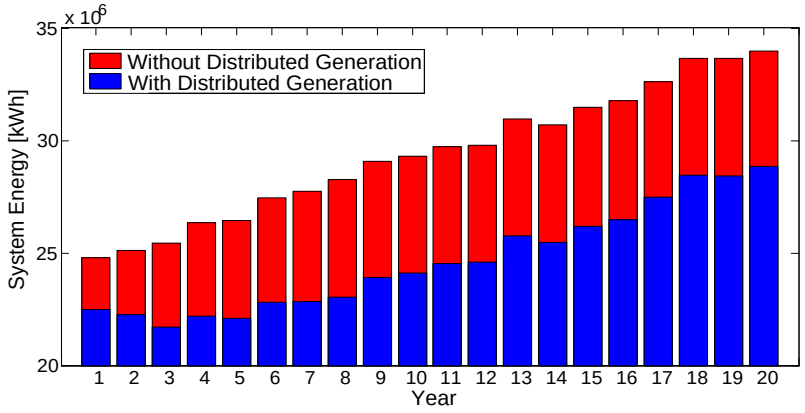

b) Energy required from the HV system (measured at the secondary substation terminals).

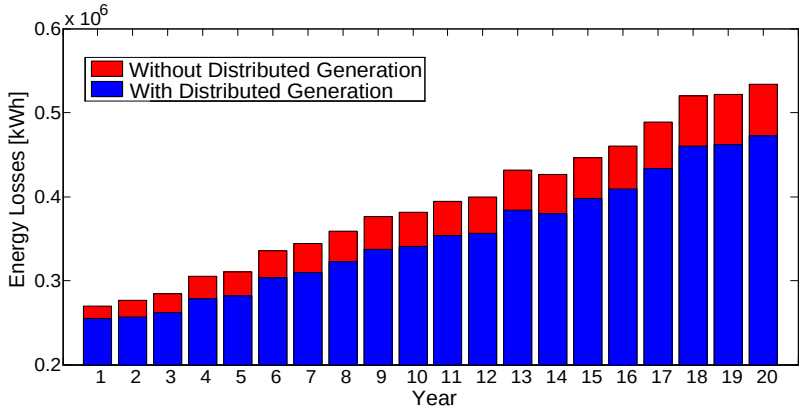

c) Energy losses (without considering substation losses)

Figure 4.19. Simulation results – Conventional Monte Carlo method – ZIP Model.

Some interesting observations can also be derived from the results presented in these figures. For instance, randomness in load and generation values is evident from the minimum voltage values obtained for every year: although the loads are larger at the end of the 9th year than at the end of the 8th year in all feeders and no generation is connected after the 8th year, the impact on the minimum voltage obtained during the 9th year is larger. This is due to a (random) coincidence of large load and low generation at the time the lowest voltage was achieved for the 8th year. On the other hand, it is evident that, in spite of that randomness, from the plots showing energy injection and energy losses one can conclude that, after the last unit has been connected, the energy not required from the HV system remain basically constant during the last years (remember that loads vary with time). Note also that the load reduction assumed for some year is clearly reflected in Figure 4.19.

4.5.3. "Divide and Conquer" Approach

The results presented in the previous section show that the first three generation units are connected to the three feeders (one per feeder) and the order in which they are connected goes from the feeder with the highest energy losses (Feeder C) to the feeder with the lowest energy losses (Feeder B). Take into account that this order C-A-B does not correspond to the feeder loads (since the highest load is in Feeder C and the lowest one is in Feeder A, the order is then C-B-A). From the fourth year on, the feeders to which optimally rated units are to be connected depend on the remaining energy losses and the number of units already connected to each feeder; both quantities can vary with the load model.

These observations suggest that the optimum allocation might be carried out using a different procedure that could be summarized as follows:

1. For every generation unit that has to be allocated estimate the feeder in which a higher energy loss reduction can be achieved for the period of study (in this work 10 years).
2. Proceed to estimate the optimum location and rated power by scanning only the feeder at which the unit will be located.

Note that if the Monte Carlo method is going to be applied considering only one feeder, the number of runs could be much lower, and the simulation time can be significantly reduced by using the refined method.

However, the selection of the feeder to which a generation unit will be connected every time a new unit has to be allocated cannot be based only on the energy losses that would have resulted before connecting the generation unit during the period of evaluation (e.g. 10 years). As detected from the results presented in Table 4.18 through Table 4.20, the maximum energy loss reduction that can be achieved after connecting an optimum generator depends not only on the feeder losses to be reduced but also on the number of generation units already connected to every feeder.

Table 4.26 provides the additional maximum percentage of energy loss reduction that can be achieved during one year in each feeder (not in the entire system) with the three load models every time a new generation unit is connected. The table shows the factors that result for the first four units.

The reduction percentages have been calculated with respect to the energy losses of the corresponding feeder. According to the table, the maximum reduction corresponds always to the first unit. Note that the additional reduction that can be achieved with subsequent units is rather small; in addition, the reduction factors depend on the feeder and the load model, and for every feeder all of them decrease as the number of units connected to the feeder increases. Note also that the maximum energy loss reduction factor that can be achieved with the first unit is different for every feeder. This is a consequence of the profiles of loads and losses in feeders. As an example, Figure 4.20 compares the hourly losses for Feeders B and C during the first year before connecting any unit; one can observe that if the PV generation is going to be larger during summer time, then the impact will be comparatively higher in Feeder C than in Feeder B for a test system located on the northern hemisphere.

Constant Power Load Model						
	Feeder A		Feeder B		Feeder C	
Unit	Losses (kWh)	Reduction (%)	Losses (kWh)	Reduction (%)	Losses (kWh)	Reduction (%)
0	62924.80	-----	56683.40	-----	153289.30	-----
1	58955.75	6.31	53269.15	6.02	136934.08	10.67
2	58667.95	0.49	52783.95	0.91	135737.67	0.87
3	58596.23	0.12	52661.60	0.23	134896.12	0.62
4	58535.42	0.10	52595.28	0.13	134330.47	0.42
Constant Impedance Load Model						
	Feeder A		Feeder B		Feeder C	
Unit	Losses (kWh)	Reduction (%)	Losses (kWh)	Losses (kWh)	Reduction (%)	Losses (kWh)
0	62645.10	-----	55593.90	-----	148248.60	-----
1	59028.84	5.77	52484.16	5.59	133951.72	9.64
2	58685.15	0.58	52133.23	0.67	133065.36	0.66
3	58506.99	0.30	51958.05	0.34	132350.99	0.54
4	58402.53	0.18	51854.18	0.20	131772.04	0.44
ZIP Load Model						
	Feeder A		Feeder B		Feeder C	
Unit	Losses (kWh)	Reduction (%)	Losses (kWh)	Reduction (%)	Losses (kWh)	Reduction (%)
0	62768.90	-----	56102.20	-----	150643.10	-----
1	59013.21	5.98	52812.49	5.86	135429.76	10.10
2	58579.31	0.74	52333.56	0.97	134610.63	0.60
3	58454.01	0.21	52108.37	0.43	133921.26	0.51
4	58328.39	0.21	51951.19	0.30	133531.09	0.29

Table 4.26. Short Term Evaluation (1 year) – Additional reduction of energy losses.

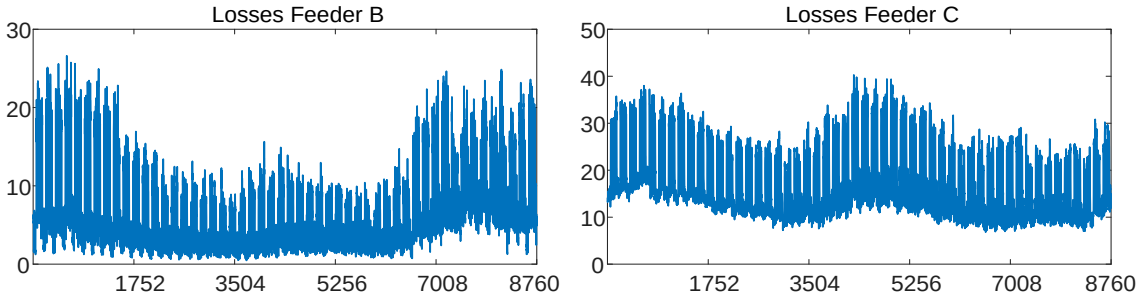

Figure 4.20. Power losses – First year.

The reduction factors provided in Table 4.26 will be used to select the feeder to which the optimum generation units will be connected using the following heuristic approach:

- When the first unit has to be allocated, the feeder to be selected is that with the largest potential energy loss reduction during the period of study (i.e. 10 years).
- When one or more generation units have already been allocated in the distribution system, the selection of the next feeder to which a unit will be connected is made by estimating the potential reduction of energy losses that the next unit can cause. The reduction percentages that a new unit can cause have been estimated from the previous studies and are shown in Table 4.27.

To better understand the way in which this procedure must be applied, assume that the first unit has already been allocated. According to all results previously presented, it should have been connected to Feeder C. For each load model, the location of the second unit should be selected from the maximum potential energy loss reduction that resulted from using the percentage (taken from Table 4.27) corresponding to Unit 2 for Feeder C and Unit 1 for feeders A and B.

Constant Power					
Feeder	U1	U2	U3	U4	U5
A	6.5	0.50	0.15	0.10	0.05
B	6.0	0.90	0.25	0.15	0.05
C	10.5	0.85	0.6	0.4	0.1
Constant Impedance					
Feeder	U1	U2	U3	U4	U5
A	6.0	0.60	0.30	0.20	0.10
B	5.5	0.70	0.35	0.20	0.10
C	9.5	0.65	0.55	0.45	0.15
ZIP					
Feeder	U1	U2	U3	U4	U5
A	6.0	0.75	0.20	0.20	0.19
B	6.0	1.0	0.45	0.30	0.05
C	10.0	0.60	0.50	0.30	0.25

Table 4.27. Long Term Evaluation – Percentage reduction of energy losses (%).

Note that the quantities specified in Table 4.27 are slightly different from those presented in Table 4.26. The new numbers have been rounded because they do not have to be very accurate and the values provided in Table 4.27 were estimated from a short term study. It is then obvious than the percentages specified in Table 4.27 can only provide good results for long term evaluations if the profiles of losses in each feeder exhibit a similar yearly pattern along the whole evaluation period, as in this study.

The new approach (which will be referred to as “Divide and Conquer”) for long term evaluations is as follows:

1. Estimate the energy loss reduction factors for every feeder of the system using a one-year evaluation, as shown in Table 4.26.
2. Estimate the feeders to which the first and subsequent units will be connected using a table similar to Table 4.27.
3. Obtain the energy loss reduction for the evaluation period (10 years in this study) every time a generation unit is to be connected.

Table 4.28 shows the results obtained when the new "Divide and Conquer" methodology and the two Monte Carlo methods are applied. The Monte Carlo runs every time a new unit had to be allocated were 1560, irrespectively of the selected feeder. It is evident that, although there are some differences with respect to the results presented in Table 4.24, the patterns of connections are basically the same and the energy losses at the end of the period are very similar for all the load models and the two Monte Carlo methods. However, the simulation time required with the new methodology is now three times shorter when the refined method is applied. Table 4.29 summarizes the main results corresponding to each load model.

Generation unit		Constant power load model Conventional - Refined method	Constant impedance load model Conventional - Refined method	ZIP load model Conventional - Refined method
Unit 1	Node	C724 - C724	C723 - C723	C724 - C723
	Rated power (kW)	1366.6 - 1363.7	1321.9 - 1298.8	1330.2 - 1341.4
Unit 2	Node	A766 - A765	A766 - A766	A766 - A766
	Rated power (kW)	423.5 - 379.3	380.5 - 434.7	376.8 - 277.8
Unit 3	Node	B737 - B737	B739 - B739	B739 - B739
	Rated power (kW)	502.2 - 462.6	457.4 - 469.9	410.7 - 424.7
Unit 4	Node	C715 - C711	C728 - C729	C715 - C728
	Rated power (kW)	230.4 - 325.9	280.4 - 290.1	182.1 - 291.7
Unit 5	Node	C711 - C715	C711 - C715	C711 - C715
	Rated power (kW)	273.3 - 223.8	229.2 - 143.4	276.3 - 191.5
Unit 6	Node	C729 - C729	C715 - C711	B724 - B719
	Rated power (kW)	185.5 - 108.4	137.9 - 206.5	277.7 - 188.6
Unit 7	Node	B724 - B726	A749 - A757	A749 - A758
	Rated power (kW)	230.0 - 146.6	194.7 - 93.7	192.7 - 188.1
Unit 8	Node	A754 - A748	B727 - B727	C729 - C711
	Rated power (kW)	188.4 - 231.5	189.9 - 100.4	232.1 - 202.2
Energy losses (kWh)		5767106.5 - 5779733.9	5542878.1 - 5554953.7	5647596.8 - 5654882.4
Simulation time (s)		32865.5 - 7290.9	30942.7 - 7067.5	34387.4 - 7916.3

Table 4.28. Long Term Evaluation – "Divide and Conquer" procedure.

Load Model	Total Generation (kW) (Conventional – Refined)	Cumulative Energy Loss Reduction (%) (Conventional – Refined)
Constant power	3400.2 - 3242.2	10.79 - 10.60
Constant impedance	3192.3 - 3037.9	9.66 - 9.46
ZIP	3278.9 - 3106.4	10.20 - 10.09

Table 4.29. Long Term Evaluation – Summary of results with "Divide and Conquer" procedure.

As mentioned above, this is not a rigorous procedure because feeders are actually coupled through the substation transformer, so the loss reduction achieved after connecting a generation unit will impact on the substation terminal voltage. However, one can confidently assume that the calculations will provide accurate enough results when the differences between the estimated energy losses in different feeders are rather

large. In addition, the margin for reducing losses in a given feeder after connecting two units will be very small, and estimating the correct feeder to which the next unit has to be connected will be more difficult. Although the procedure makes the approach dependent of the system under study (i.e. system configuration and feeder load patterns), the results presented in the previous sections support the fact that the reduction of energy losses is not very sensitive to changes of locations and rated powers once the solution is not far from the optimum. That is, a quasi-optimum solution can provide very similar results to that corresponding to the optimum, and in turn it can be obtained by significantly reducing the computation effort.

The main results obtained prove that the total power of the PV generation to be allocated exhibits some dependency with respect the load model, but the differences between the resulting energy losses derived from different load models are not too large. Finally, these results indicate that if the connection of units is sequential, as assumed in this work, all the steps can be confidently based on the refined Monte Carlo method, irrespectively of the system configuration, the number of units to be allocated and the duration of the evaluation period.

4.6. Conclusions

This Chapter has presented a procedure based on a Monte Carlo method for optimum allocation of distributed generation using multicore computing. The procedure has been developed to cope with short and long term evaluation periods (i.e. greater than one year). Moreover, the method can be applied to any system regardless of its topology. The present procedure is single-objective, but it can be expanded to include other objectives (e.g., minimization of the cost of energy or the cost of interruptions, system upgrading) when optimizing the allocation of generation units.

Advantages and disadvantages of Monte Carlo-based procedures are well known: they are rather simple and can be usually based on complete/advanced models; in turn, they usually require a high number of runs, and consequently, a long CPU time. The introduction of parallel computation in this work has achieved a significant reduction of the simulation time. However it is evident from the obtained results that the application of a conventional Monte Carlo method to very large distribution systems (i.e. with several thousands of nodes) to which several dozens of DG units are to be connected might not be carried out in an affordable time even if a large multicore installation (i.e. with several hundreds of cores) was used. This can be very obvious when a long term evaluation is carried out.

The results derived from short term evaluation of radial feeders show that the energy loss surface is very smooth near the global optimum. The most interesting conclusion is that a quasi-optimum value can be obtained by means of several combinations (i.e. combinations of node location and rated power of PV generators); that is, values very close to the global optimum (with differences below 1%) can be reached by considering several results; these findings are the foundation of the Refined Monte Carlo approach. Through the application of the 5% criterion (it is assumed the energy loss corresponding to two solutions will not be very different unless the Euclidean distance between those solutions is greater than 5%) the number of run/samples used for the Monte Carlo method can be significantly reduced without the loss of accuracy.

The Chapter has also proved that an alternative "Divide and Conquer" procedure can be considered with large multi-feeder systems. A quasi-optimum solution can be obtained without having to include the entire distribution system in the optimization procedure: if generators are to be allocated one by one during a given period, the study can be carried out by analyzing only the feeder in which the highest energy loss reduction can be achieved; then the refined approach can be advantageously used to significantly reduce the simulation time.

The allocation of distributed generators in deregulated systems is not made following a sequential connection of generation units with which the optimum reduction of energy losses is achieved by connecting the largest generation unit at the beginning of the period with little room for more energy loss reduction in subsequent years. The usefulness of this study is in the insight it provides about the impact that the connection of PV generation can have on the system energy losses; that is, utilities can obtain from this or similar studies important information about the maximum loss reduction they should expect.

4.7. References

[4.1] F.A. Farret and M. Godoy Simões, *Integration of Alternative Sources of Energy*, John Wiley, Hoboken, USA. 2006.

[4.2] T. Ackerman, G. Andersson, and L. Söder, "Distributed generation: A definition," *Electric Power Systems Research*, vol. 57, no. 3, pp. 195-204. April 2001.

[4.3] H. Lee Willis and W.G. Scott, *Distributed Power Generation. Planning and Evaluation*, Marcel Dekker. New York, USA. 2000.

[4.4] R.C. Dugan, R.F. Arritt, T.E. McDermott, S.M. Brahma, and K. Schneider, "Distribution system analysis to support the smart grid," *IEEE PES General Meeting*, Minneapolis, USA, July 2010.

[4.5] T. Lambert, P. Gilman, and P. Lilienthal, "Micropower System Modeling with HOMER," Chapter 15 of *Integration of Alternative Sources of Energy*, by F.A. Farret and M. Godoy Simões. John Wiley. Hoboken, USA. 2006.

[4.6] J.A. Martinez and J. Martin-Arnedo, "Tools for analysis and design of distributed resources - Part I: Tools for feasibility studies", *IEEE Trans. on Power Delivery*, vol. 26, no. 3, pp. 1643-1652, July 2011.

[4.7] R.A. Walling, R. Saint, R.C. Dugan, J. Burke, and L.A. Kojovic, "Summary of distributed resources impact on power delivery systems," *IEEE Trans. on Power Delivery*, vol. 23, no. 3, pp. 1636-1644, July, 2008.

[4.8] C. Wang, and M.H. Nehrir, "Analytical approaches for optimal placement of distributed generation resources in power systems," *IEEE Trans. on Power Systems*, vol. 19, no. 4, pp. 2068-2076, November 2004.

[4.9] G. Celli, E. Ghaiani, S. Mocci, and F. Pilo, "A multiobjective evolutionary algorithm for the sizing and siting of distributed generation," *IEEE Trans. on Power Systems*, vol. 20, no. 2, pp. 47-55, May 2005.

[4.10] G. Carpinelli, G. Celli, S. Mocci, F. Pilo, and A. Russo, "Optimization of embedded generation sizing and sitting by using a double trade-off method," *IEE Proc., Gener. Trans. Distrib.*, vol. 152, no. 4, pp. 503-513, July 2005.

[4.11] A. Keane and M. O'Malley, "Optimal allocation of embedded generation on distribution networks," *IEEE Trans. on Power Systems*, vol. 20, no. 3, pp. 1640-1646, August 2005.

[4.12] P.S. Georgilakis and N.D. Hatziargyriou, "Optimal distributed generation placement in power distribution networks: Models, methods, and future research," *IEEE Trans. on Power Systems*, vol. 28, no. 3, pp. 3420-3428, August 2013.

[4.13] A. Hadian, M.R. Haghifam, J. Zohrevand, and E. Akhavan-Rezai, "Probabilistic approach for renewable DG placement in distribution systems with uncertain and time varying loads," *IEEE PES General Meeting*, Calgary, July 2009.

[4.14] Y.G. Hegazy, M.M.A. Salama, A.Y. Chikhani, "Adequacy assessment of distributed generation systems using Monte Carlo simulation," *IEEE Trans. on Power Systems*, vol. 18, no. 1, pp. 48-52, February 2003.

[4.15] Y.M. Atwa, and E.F. El-Saadany, "Probabilistic approach for optimal allocation of wind-based distributed generation in distribution systems," *IET Renewable Power Generation*, vol. 5, no. 1, pp. 79-88, January 2011.

[4.16] M. Buehren, *MATLAB Library for Parallel Processing on Multiple Cores*, Copyright 2007. Available from http://www.mathworks.com.

[4.17] T. Gönen, *Electric Power Distribution System Engineering*, 2nd Edition, CRC Press, 2008.

[4.18] HOMER Software, National Renewable Energy Laboratory (NREL), 2003. Available at http://www.nrel.gov/homer.

[4.19] URL: https://www.aepohio.com/service/choice/cres/LoadProfiles.aspx.

[4.20] IEEE Distribution Planning WG, "Radial distribution test feeders," *IEEE Trans. on Power Systems*, vol. 6, no. 3, pp. 975-985, August 1991.

[4.21] D.P. Chassin, Electrical Load Modeling and Simulation, Chapter 10 of *High Performance Computing in Power and Energy Systems*, S. Kumar Khaitan and Anshul Gupta (Eds.). Springer. Berlin. Germany. 2013.

[4.22] G.J. Anders, *Probability Concepts in Electric Power Systems*, John Wiley, 1990.

[4.23] The Regulatory Assistance Project, "Interconnection of Distributed Generation to Utility Systems," *RAP report (Main author: P. Sheaffer)*, September 2011. Available at www.raponline.org.

Chapter 5

Reliability Assessment of Distribution Systems

5.1. Introduction

Reliability analysis is a fundamental piece of distribution system planning and design. Reliability models and studies can be useful, among other aspects, to identify design limitations, quantify equipment improvements or determine the impact of system expansion [5.1], [5.2]. The importance of reliability assessment is increasing with the advent of the smart grid. The future distribution system offers a potential of improved reliability by implementing rapid fault location and isolation, and service restoration [5.3], [5.4].

It is widely accepted that distributed generation (DG) can have a positive impact on the distribution system since it can support voltage, reduce losses, provide backup power, provide ancillary services, or defer distribution system upgrade [5.5], [5.6]. However, the connection of generation to the distribution system can cause miscoordination of protection devices and, if not properly handled, reduce reliability and power quality. Although distributed generation is often presented as a solution for reliability improvement, the fact is that such assumption is not widely accepted, see for instance [5.7].

Two main modes of DG connection can be distinguished: (1) operating as a backup source within a microgrid; (2) operating in parallel with the distribution system. In the first case, the generation units are locally operated and can be allowed to inject power to the system; if they are correctly controlled, they can have a positive impact on distribution system reliability [5.8]. A generation unit operating in parallel to the system can be forced to be disconnected in case of system fault, and the benefit to the system reliability is not so obvious and can be negative [5.7], [5.8].

The reliability of distribution systems with distributed generation has already been analyzed in a significant number of works; see, for instance, references [5.1]-[5.16]. A summary of the methods proposed until 2009 was presented in [5.17].

The present Chapter has been organized as follows. In Section 5.2 the Monte Carlo method implemented for reliability analysis is introduced; the main aspects, scenarios, and special considerations are explained in detail. Section 5.3 presents the test system, while a case study aimed at illustrating the main aspects of the develop approach is detailed in Section 5.4. The main results from the reliability analysis of the test system with and without distributed generation are provided in Section 5.5. Finally, the main conclusions derived from the study and the application of the Monte Carlo method for reliability analysis of distribution systems are presented in Section 5.6.

5.2. Reliability Analysis Using the Monte Carlo Method

5.2.1. Principles of the Method

The procedure developed for this purpose may be defined as a parallel Monte Carlo method aimed at estimating the probability density functions of reliability indices related to frequency of interruptions, duration of interruptions and non-supplied energy. It can be applied to distribution systems (either overhead or underground) with or without distributed generation.

Input data include system parameters (i.e., network topology, component parameters, including setting of protection devices) and yearly variation of loads and generations. A failure is caused by a fault, a term to which several random variables are related: location, time of occurrence, duration, type. Random variables to be generated during the application of the Monte Carlo method implemented for this work are those related to failures rates, fault characterization and reconfiguration times. The use of a power flow simulator will allow the estimation of the non-supplied energy.

The procedure may be summarized as follows:

1. Run the test system during one year using time-driven simulation and a constant time step (e.g., 1 hour). This run, known in this work as base case, will provide basic information (e.g., energy values) that will be used for later calculations. The simulation can be carried out, depending on the system under study, with or without distributed generation
2. Estimate in advance all the random values related to the faults/failures to be simulated (location/component, time of occurrence, duration, type) for one year.
3. Run the test system again but considering now the possibility of equipment failure. Regardless of the location, type and duration of the fault, a protective device will always operate. Reliability indices are updated once this sequence of events is finished.
4. Repeat the procedure from step 2 as many times as required to obtain accurate information for reliability index calculation.

The stopping criterion used for assessing convergence is the coefficient of variation (CV) [5.18], which helps to determine if enough executions have been performed in

order to estimate a variable's probability density function (PDF). The Monte Carlo method is assumed to have converged when the CV of all calculated indices is below 5%. Reliability indices are calculated as recommended by IEEE Std 1366 [5.19].

5.2.2. Scenarios

Three different scenarios have been considered to calculate reliability indices with and without distributed generation:

1. A first scenario assumes that only protective devices operate; that is, a protection device locks out after a permanent fault, and service is not restored until the faulted component is repaired.
2. The second scenario considers switching operations aimed at isolating the faulted section. This design may restore service only to load nodes upstream the failed component.
3. The third scenario includes also transfer switches between feeders, so system reconfiguration may be used to restore service also to some load nodes downstream the faulted section, depending on the system design.

The specific steps taken by the procedure when a fault occurs depend on the scenario considered.

First Scenario

1. System is simulated until time reaches the moment when a fault occurs, time-step is one hour.
2. The fault is simulated by placing a short-circuit at the element considered for failure.
3. Simulation time-step is reduced to allow the correct response of protection devices.
4. Simulation time-step is increased to continue with the simulation and perform switching actions; new time-step is 5 minutes.
5. Reconnect DG units disconnected during the fault but can be placed back in service immediately.
6. After repair is finished, return operated protection device to its original closed position, restoring service to all loads.
7. Reconnect DG units that were disconnected.
8. Continue simulation until the time for the next fault is reached. Time-step is increased to one hour.

If a one-phase fault occurs on a distribution line protected by a fuse, two cases can be considered:

- Voltage at load point above 0.9 p.u.: the repair will be carried out in a normal manner; loads will not experience any interruptions.
- Voltage at load point below 0.9 p.u.: the remaining phases will be opened, isolating all elements downstream from the operated fuse.

If a two-phase fault occurs on a distribution line protected by a fuse, the remaining phase must be opened to disconnect all voltage sources from the failed zone.

Second Scenario

1. System is simulated until time reaches the moment when a fault occurs, time-step is one hour.
2. The fault is simulated by placing a short-circuit at the element considered for failure.
3. Simulation time-step is reduced to allow the correct response of protection devices.
4. Simulation time-step is increased to continue with the simulation and perform switching actions; new time-step is 5 minutes.
5. Reconnect DG units disconnected during the fault but can be placed back in service immediately.
6. Failed element is disconnected.
7. If possible, the operated protection device is returned to its original closed position. This action will return service to all loads upstream from the failed element.
8. Reconnect DG units that were disconnected and are located upstream from the failed element.
9. After repair is finished, perform switching actions in order to return the system to its original stated.
10. Reconnect DG units that could not be previously put back in operation.
11. Continue simulation until the time for the next fault is reached. Time-step is increased to one hour.

If a one-phase fault occurs on a distribution line protected by a fuse, two cases can be considered:

- Voltage at load point above 0.9 p.u.: the repair will be carried out without disconnecting the failed element; loads will not experience any interruptions.
- Voltage at load point below 0.9 p.u.: the procedure will follow the steps presented above.

Third Scenario

1. System is simulated until time reaches the moment when a fault occurs, time-step is one hour.
2. The fault is simulated by placing a short-circuit at the element considered for failure.
3. Simulation time-step is reduced to allow the correct response of protection devices.
4. Simulation time-step is increased to continue with the simulation and perform switching actions; new time-step is 5 minutes.
5. Reconnect DG units disconnected during the fault but can be placed back in service immediately.
6. Failed element is disconnected.
7. If possible, the operated protection device is returned to its original closed position. This action will return service to all loads upstream from the failed element.
8. Reconnect DG units that were disconnected and are located upstream from the failed element.

9. Check for availability of back-up feeder.
10. If there is an available back-up feeder, load is transferred.
11. If load is transferred, reconnect DG units that were disconnected and are located downstream from the failed element.
12. After repair is finished, perform switching actions in order to return the system to its original stated.
13. Reconnect DG units that could not be previously put back in operation.

If a one-phase fault occurs on a distribution line protected by a fuse, two cases can be considered.

- Voltage at load point above 0.9 p.u.: the repair will be carried out without disconnecting the failed element and no load transfer will be performed; loads will not experience any interruptions.
- Voltage at load point below 0.9 p.u.: the procedure will follow the steps presented above.

All switching actions aimed at returning the system to its original state are performed simultaneously by the procedure; therefore all possible effects on loads and generators are neglected.

Figure 5.1 shows the simplified sequence of events and time step size for every interval when switching devices can be used to isolate the faulted device and when additional switches are available to reconfigure the system and transfer some load between feeders.

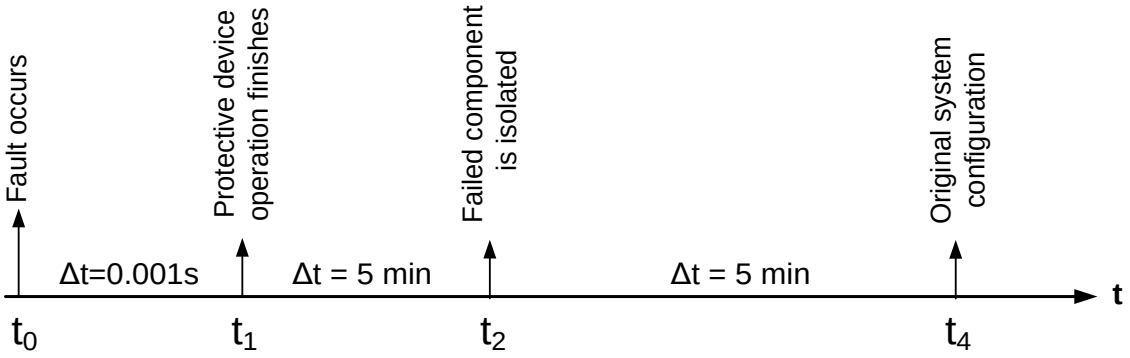

a) Sequence of events to isolate the faulted section

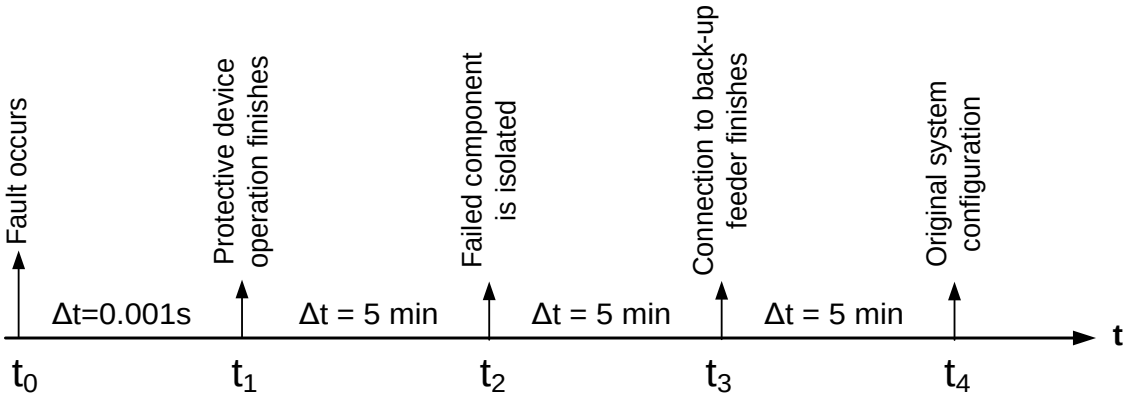

b) Sequence of events to reconfigure the system

Figure 5.1. Sequence of events after a failure.

The operation of the protective device finishes at t_1 and may include some reclosing operations. If the protective device that isolates the fault/failure is a fuse, then its replacement must be made after the fault location is isolated. The service is restored to loads upstream from the point of failure at t_2. If possible, the connection of the back-up feeder will be performed at t_3. Finally, the system will return to its original state after the faulted element has been repaired/replaced at t_4.

5.2.3. Parameters for Reliability Analysis

The application of the implemented Monte Carlo method requires the generation of random variables related to faults and switching and reconfiguration times. A fault is fully defined by specifying the faulted component (line, voltage regulator, or capacitor bank), the occurrence time, the duration, and the fault type.

Failed Elements

The system elements to be considered for failure are: distribution lines, voltage regulators, capacitor banks, distribution transformers, PV generator interconnection transformers, and PV plant modules.

Frequency of failures

The system is divided into zones, with different statistics for line sections. In all cases, it is assumed that the number of failures for each zone follows a normal probability density distribution (characterized by a mean and a standard deviation) while the location is assume to be uniformly distributed within the zone. These assumptions may not be fully correct; in fact, many works assume a constant failure rate, which is similar to assuming that failure rates follow a Poisson distribution. For other elements the failure rate will be assumed constant and the number of yearly faults will follow a Poisson distribution [5.4]. The failure of a distribution transformer or a voltage regulator is always sustained and interrupts the service to all customers located downstream, while the failure of a capacitor bank will not interrupt the service of any costumer, although it can affect some node voltages.

Duration

Line failures are classified as momentary and sustained, with a percentage for each type. Although a distinction is made between momentary and sustained, no duration is assigned to any type. By default sustained interruptions are assumed to be caused by permanent fault, while momentary interruptions are caused by temporary faults shorter than 5 minutes and that are isolated by the affected protective devices in less than 5 minutes. Failures of PV plant modules, transformers, voltage regulators and capacitor banks are assumed by default sustained. The design of distribution transformer protection is a relatively complex task since several technical choices may provide a correct protection [5.20]. In this work an internal distribution transformer failure forces the operation of an overcurrent protection located at the primary MV side of the transformer. In the case of voltage regulators, this operation will separate the component

from the upstream components; continue with a confirmation of the regulator failure and by its separation from the downstream components. Capacitor banks are protected by fuses. As for PV generation plants, the interconnection protection will detect abnormal voltage values caused by a fault in the proximities of the plant.

Type of fault

Faults causing failures may be one-phase (type 1), two-phase (type 2), and three-phase (type 3) [5.2]. This distinction is only used for overhead lines, because in case of fuse blowing the number of phases affected will depend on the type of fault. Failures of distribution transformers, voltage regulators and capacitor banks are three-phase.

Time of occurrence

Monthly and daily statistics will be used to determine the month, day and hour when a fault will occur on distribution lines. Time of occurrence for voltage regulators, capacitor banks, distribution transformers, PV generator interconnection transformers, and PV plant modules will be generated using a uniform distribution. No coincident faults will be considered.

Switching Times

The sequence of events, after a protective device has isolated the fault, may include fault location, isolation of the failed component, and some switching operations to reconfigure the system (e.g., load transfer between feeders). Depending on the system design, switching may be used for:

- Isolating only the faulted section after the protective device has operated.
- System reconfiguration by using transfer switches.
- Restoring the original system configuration after the failed equipment has been repaired.

The times to be used for these operations may correspond to manually or remotely controlled switches. Switching times are defined as a constant average for every element and follow an exponential distribution [5.4]; time values are varied to reflect automation improvements, and will also depend on the failed component location. In this work, the switching time required for isolating the failed section or component includes also the time required for locating the fault.

Repair Times

Repair times are randomly generated using an exponential distribution and depend on the fault characteristics [5.4]; for line sections they depend on the system zone. The repair time values include several operations (protective device lockout, fault location, isolation of the faulted line section, reconfiguration of the system to restore service as quick as possible to as many customers as possible, equipment repair, and switching required to recover the original system configuration). Repair times are also used to fix

the moment at which the normal operation of the whole system is restored, taking as a reference the moment at which the failure occurs.

Replacement Times

They must be considered when the fault causes a fuse operation. During calculations for sustained interruptions, this time is included in the time required for repairing the failed component. Fuse replacement depends on the number of faulted phases; a base time has been established and extra time is added for every phase to be replaced.

Load Transfer Times

The load transfer will depend on the time needed to disconnect the failed element and the time required to connect the back-up feeder. The latter will also be randomly generated and follow an exponential distribution. Two cases have been considered:

- Back-up feeder connection time is lower than time needed to disconnect the failed element and close the operated device: in this case the procedure will perform both actions simultaneously, using the greater time as the reference.
- Back-up feeder connection time is greater than time needed to disconnect the failed element and close the operated device: for this condition the procedure will perform both actions independently at their specified times.

PV Plant Availability Model

The reliability model of a PV plant is rather complex; see, for instance, [5.8], [5.21]-[5.23]. Implementing and applying an accurate model is out of the scope of this work; instead a simplified reliability model is used. All PV generators consist of one or more 100 kW modules characterized by the same failure rate and repair time. Therefore, the parameters of each generator to be defined for reliability assessment are the rated power (i.e. the number of 100 kW modules), the failure rate and the mean repair time. A PV plant can reduce partially or totally the power it injects into the distribution when either the interconnection transformer or a PV module fails. The reliability parameters for the interconnection transformer are those used for any other distribution transformer. The number of PV module failures in a year will be randomly generated using the failure rate and following a Poisson distribution; it is assumed that in average one module will fail in every event. The average repair time will be calculated multiplying the module's mean repair time and the number of failed modules. The actual repair time will be randomly calculated using an exponential distribution.

5.2.4. Reliability Indices

Customer Indices

System reliability will be quantified by means of the customer interruption indices. The following indices are calculated at the end of every execution of the Monte Carlo method and according to [5.19].

System average interruption frequency index:

$$SAIFI = \frac{\sum_{i=1}^{n} N_i}{N_T} \quad (5.1)$$

System average interruption duration index:

$$SAIDI = \frac{\sum_{i=1}^{n} N_i \cdot H_i}{N_T} \quad (5.2)$$

Customer average interruption duration index:

$$CAIDI = \frac{\sum_{i=1}^{n} N_i \cdot H_i}{\sum_{i=1}^{n} N_i} = \frac{SAIDI}{SAIFI} \quad (5.3)$$

Where k is the number of interruptions, N_i is the number of customer interrupted by a fault, N_T is the total number of customers in the system, and H_i is the duration of interruption to customers interrupted by a fault.

An additional reliability index referred to as Actual Energy not Supplied (AENS) is defined as the difference between the energy served without faults (i.e. base case) and the energy supplied when considering system failure, see Figure 5.2.

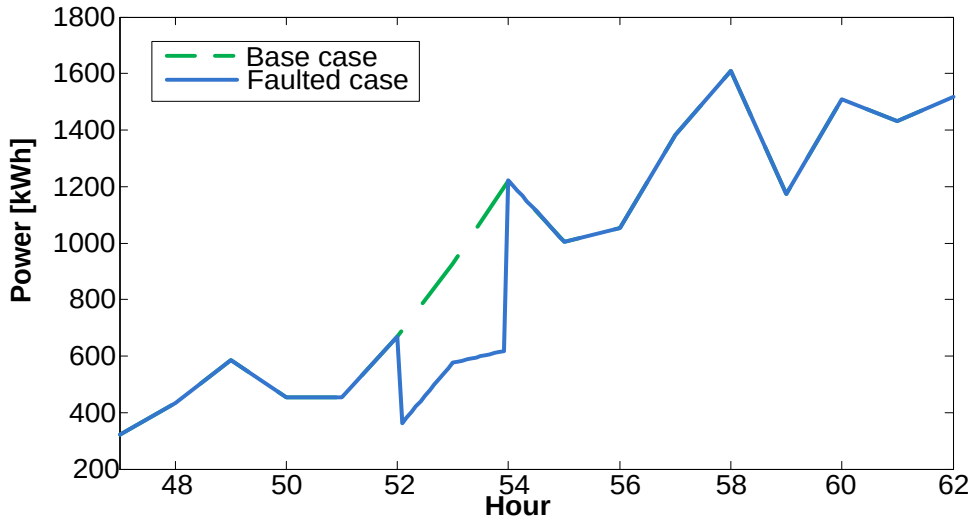

Figure 5.2. Actual energy not supplied during an event.

DG Reliability Indices

In order to assess the impact of system failure on distributed generation, the following two indices related to power generation, and named according to reference [5.9], have been defined.

Average Number of DG Interruptions ($SAIFI_{DG}$):

$$SAIFI_{DG} = \frac{\sum_{i=1}^{k} PG_i}{PG_T} \quad (5.4)$$

Average Duration of DG Interruptions ($SAIDI_{DG}$):

$$SAIDI_{DG} = \frac{\sum_{i=1}^{k} PG_i \cdot H_i}{PG_T} \quad (5.5)$$

where k is the number of interruptions, PG_i is the connected kW of generators interrupted by a fault, PG_T is the total connected generation in kW, and H_i is the duration of interruption to generators interrupted by a fault.

A third index is the Actual Energy not Produced (AENP). It is the difference between the actual energy produced when the system is simulated without any fault and that resulting when faults can occur.

5.2.5. Special Considerations

It is important to remark some important aspects and rules that have been considered during the implementation of the procedure.

Reverse Power Flow through Voltage Regulators

Network reconfiguration and surplus in PV generation can cause reverse power flow through voltage regulators. Reverse power flow can interfere with voltage regulator control and cause unacceptable operating conditions; therefore, it has been established that voltage regulator control will be disabled during reverse power flow.

DG Operation and Protection

In this work the generation is of renewable nature (i.e. photovoltaic) and represented by means of the model available in OpenDSS. It is assumed that DG units are operating in parallel to the distribution system and there are no microgrids in the distribution network. By default PV generators can only inject active power.

All protective devices located between the generator and substation must be three-phase. The interconnection protection of each generator has over-/undervoltage and overcurrent protection. After an interruption a generator will be reconnected when normal voltage values at the point of common coupling (PCC) are confirmed (> 0.9 p.u.). On the other hand, it is assumed that PV generators do not suffer any damage during a fault and can be put back in operation as soon as possible.

A fault in a line section close to the substation will cause a voltage dip at the nodes of the adjacent feeder, and this could cause the operation of the undervoltage protection of some PV generation. Protective devices have been coordinated to avoid these consequences; that is, the overcurrent relay installed to protect the faulted feeder will be faster that the undervoltage protection of PV generators connected to the adjacent feeder.

Load Transfer

Load transfer will be carried out only when normal operating conditions are ensured. The procedure follows the next steps when load transfer is considered:

1. Check for availability of back-up feeder.
2. If there is an available back-up feeder, load is transferred without restrictions.
3. During the simulation, voltages at load points and phase currents through lines and voltage regulators are monitored.
4. When the simulation is finished, the procedure checks for the technical restrictions (all load point voltages are above 0.9 p.u.; phase current through distribution lines and voltage regulators do not exceed 110% of nominal rating).
5. If one of the previous restrictions is not satisfied the procedure will deem the load transfer not successful and will repeat the simulation without considering load transfer.

Repair and switching times are randomly generated, and although certain rules have been defined, it is possible to face special situations for independent actions. One of these situations can occur when load transfer is possible. Assume two maintenance crews are involved: one will take of the repair and associated operations, the other one will take care of the transfer maneuver. Given the random values to be estimated for each crew and that both actions are considered independent from each other, the second crew could take longer for the switching transfer than the first one for isolating the failed component and repair it. As a rule of thumb load transfer can only be performed when the estimated repair time is at least 15 minutes longer than the estimated time for back-up feeder connection. This situation will not be considered if remote control of the transfer maneuver is possible and a very short time is actually required.

Determining Reconfiguration Switches

The procedure to determine the switches that need to be operated for system reconfiguration and load transfer between feeders after a failure may be summarized as follows:

1. Find the line sections that can be used for load transfer between feeders. They have been previously classified.
2. Create a list of nodes to which these line sections are connected. A list of nodes to which system components are connected is previously available.
3. Create an $m \times n$ system matrix in which m is the number of system components normally operating (i.e., without including line sections for load transfer) and n is the number of buses. Each row of this matrix corresponds to a system component, so each column indicates the nodes to which this component is connected; that is, "1" for connection nodes, "0" for the others.
4. Create a new $n \times n$ connectivity matrix, in which n is again the number of system nodes. This matrix describes the way in which system nodes are connected to each other. That is, each row corresponds to a system node and each column indicates the nodes to which that node is connected (i.e., "1" if there is a connection, "0" when there is no connection).
5. After a sustained interruption, determine the nodes to which the failed component is connected to and create two new lists: (i) "oldlist" includes the indices of the two connection buses, (ii) "busqlist" includes only the index of the node downstream the failed component.
6. Run the search algorithm based on the connectivity matrix and check whether there is or not a transfer section available.
7. If there is a transfer section available, its name is store in the variable "linefeederaux". Otherwise, this variable is empty.

5.2.6. Implementation of the Procedure

The procedure presented has been implemented in MATLAB, which is used to calculate the random variables and control the execution of power flow calculations performed by OpenDSS. Figure 5.3 shows a diagram with the connections between the different tools used for this work, as well as the information inputted to and generated by each tool. Notice that all the required information is generated by means of custom-made applications if they cannot rely on OpenDSS capabilities. For instance, the load and PV generation curves are generated using the algorithms implemented in MATLAB (introduced in Chapter 3), and can be obtained at the time the reliability study is carried out.

To obtain a probability density function of the reliability indices the procedure is simultaneously run in a multicore computing environment. The procedure schematized in Figure 5.3 is valid for any number of cores. The system simulated in every core is the same but the number of faults and the characteristics of each fault are different and randomly calculated for each core. MATLAB capabilities can be used to distribute the different runs between cores [5.24]- [5.26]. This work is based on the library developed by M. Buehren and available at the MathWorks web site [5.27].

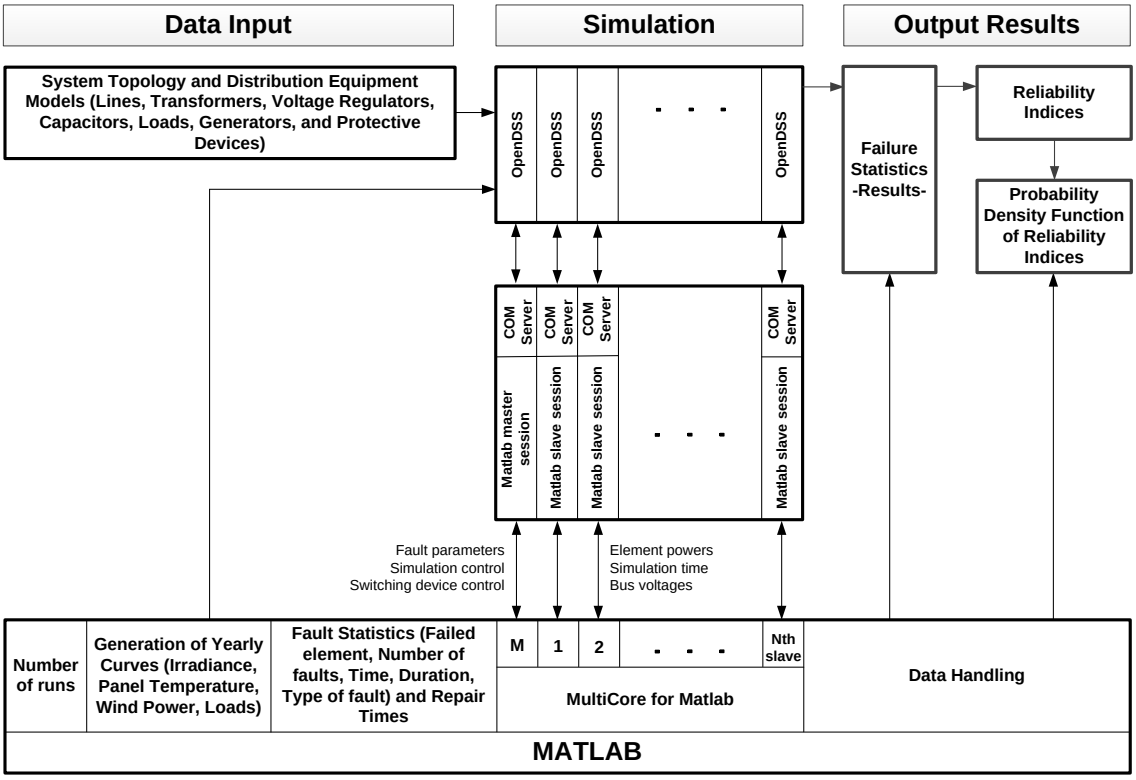

Figure 5.3. Block diagram of the implemented procedure.

5.3. Test System

Figure 5.4 depicts the diagram of the test system. It is a 60-Hz three-phase overhead distribution system based on IEEE test feeders [5.28]. Table 5.1 summarizes the information used to obtain sun power generation curves. The figure shows the location of the protective devices and transfer switches that can be used for system reconfiguration and restoration of power. The model includes a simplified representation of the high-voltage system, the substation transformer and all distribution MV/LV transformers. All loads are supplied from the LV terminals of distribution transformers and are voltage-independent. As indicated in the figure, all line sections have switching devices at both terminals. These switches are used to isolate the faulted section and, depending on the automation level in the test system, may be operated either manually or remotely. Note that a zone classification has been used; which is required to obtain fault isolation and repair times of line sections.

Some important numbers about the test system are given below:

- Rated voltage: 4.16 kV.
- Rated power of substation transformer: 10000 kVA.
- Rated PV generation power (peak value): 1800 kW.
- Number of load nodes: 107.
- Overall number of customers: 713.
- Average rated power per load node: 74.77 kVA.
- Overall line length: 52.1 km.

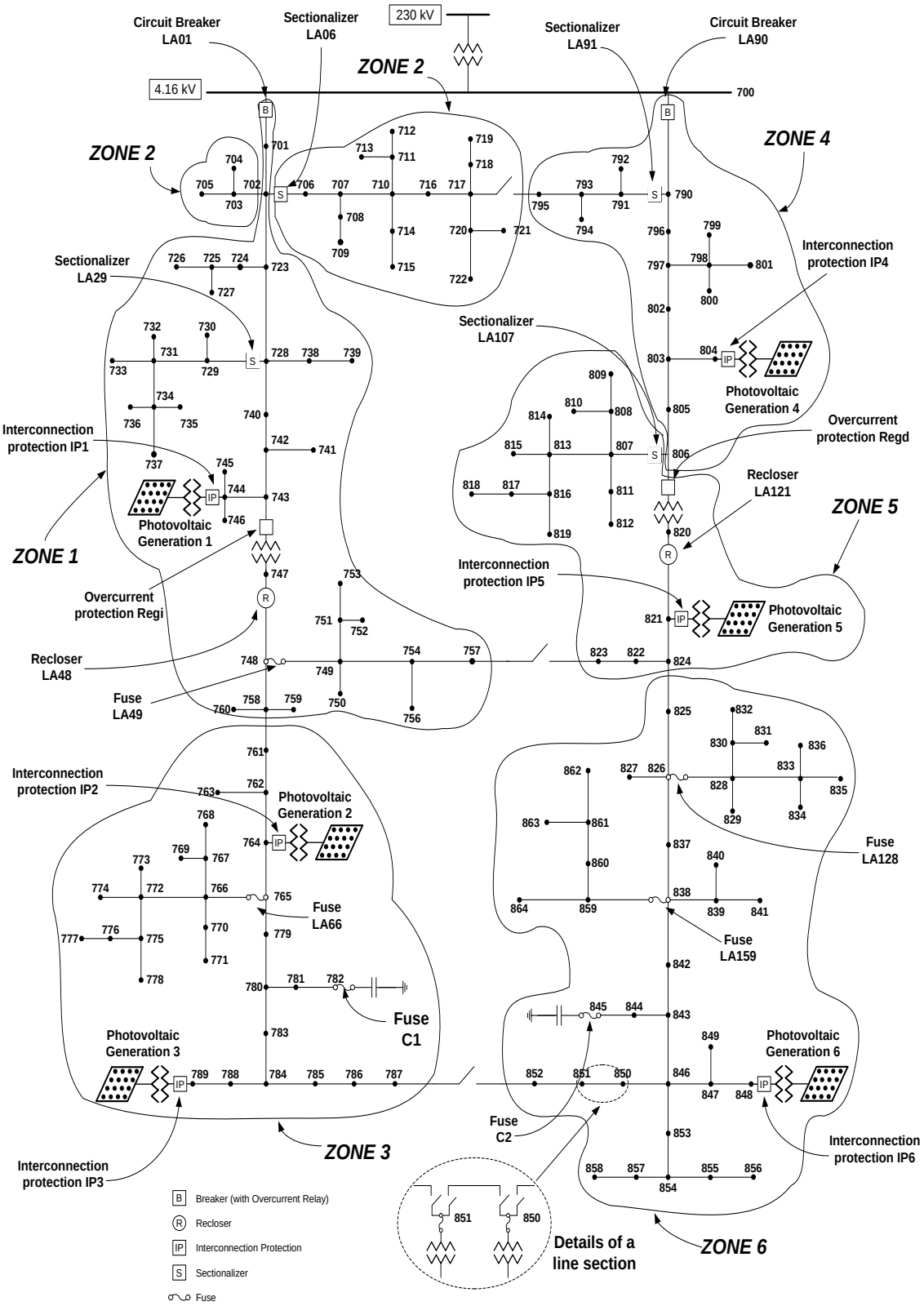

Figure 5.4. Test system configuration.

Average monthly clearness index	0.41 , 0.43, 0.44, 0.47, 0.45, 0.5, 0.51, 0.5, 0.51, 0.5, 0.42, 0.4
Panel's slope angle	35º
Normal operating cell temperature	45ºC
Average monthly daily minimum temperatures	-5.92, -3.9, -0.21, 5.09, 9.89, 14.9, 17.1, 16.6, 12.6, 6.95, 1.97, -3.76
Average monthly daily maximum temperatures	2.58, 5.5, 11.1, 18.9, 25.1, 29.9, 31.6, 30.7, 26.7, 19.8, 11.2, 4.13

Table 5.1. Summary of solar resources.

The average switching time may vary between 10 and 60 minutes when the failed component is an overhead line section, and is assumed 30 minutes for a voltage regulator. The average time required to reconfigure the system and transfer loads between feeders is also 30 minutes.

Table 5.2 and Table 5.3 provide some information about the protective devices and the components they protect. Take into account that reclosers can perform up to 3 opening operations, two of which use the faster characteristic. In all devices with automatic reclosing capabilities, the assumed dead times are 10 and 20 seconds. Except the sectionalizer model, which is a custom-made model, the models used to represent protective devices are those available in OpenDSS. The characteristic time-current curves of the protection devices are shown in Figure 5.5.

Protective Device	Current (A)	TC Curve	
		Fast	Slow
Relay.la01	1000	Fast2	-----
Relay.la90	640	Fast4	-----
Recloser.la48	440	Fast1	Slow1
Recloser.la121	370	Fast3	Slow3
Overcurrent protection *regi*	490	Regi	-----
Overcurrent protection *regd*	390	Regd	-----
Fuse.la49(1)	140	Tlink	-----
Fuse.la66(1)	140	Klink	-----
Fuse.la128(1)	100	Tlink	-----
Fuse.la159(1)	140	Klink	-----
Fuse.c1(1)	30	Klink	-----
Fuse.c2(1)	50	Klink	-----
Sectionalizer.la06(2)	115	-----	-----
Sectionalizer.la29(2)	60	-----	-----
Sectionalizer.la91(2)	25	-----	-----
Sectionalizer.la107(2)	80	-----	-----

(1) Fuse was coordinated using a *fuse saving* scheme
(2) Sectionalizer counts up to 2 operations before performing opening action

Table 5.2. Characteristics of protective devices.

According to IEEE Std 1366-2012 there exist a distinction between momentary and sustained interruptions [5.19]. A momentary interruption is shorter than 5 minutes, and its effects are not computed when calculating reliability indices; that is, only the effects of sustained interruptions are computed for reliability index calculation. However, the

coordination and performance between protective devices can always be tested, whether the failure is momentary or sustained.

Protected Plant	Over/Undervoltage Protection		Overcurrent protection	
	Protective Device	Rated Voltage (kV)	Protective Device	Pick-up Current (A)
Plant1	Relay.LV1	4.16	Relay.PV1	65
Plant2	Relay.LV2	4.16	Relay.PV2	110
Plant3	Relay.LV3	4.16	Relay.PV3	130
Plant4	Relay.LV4	4.16	Relay.PV4	65
Plant5	Relay.LV5	4.16	Relay.PV5	110
Plant6	Relay.LV6	4.16	Relay.PV6	130

Table 5.3. Interconnection protection of PV plants.

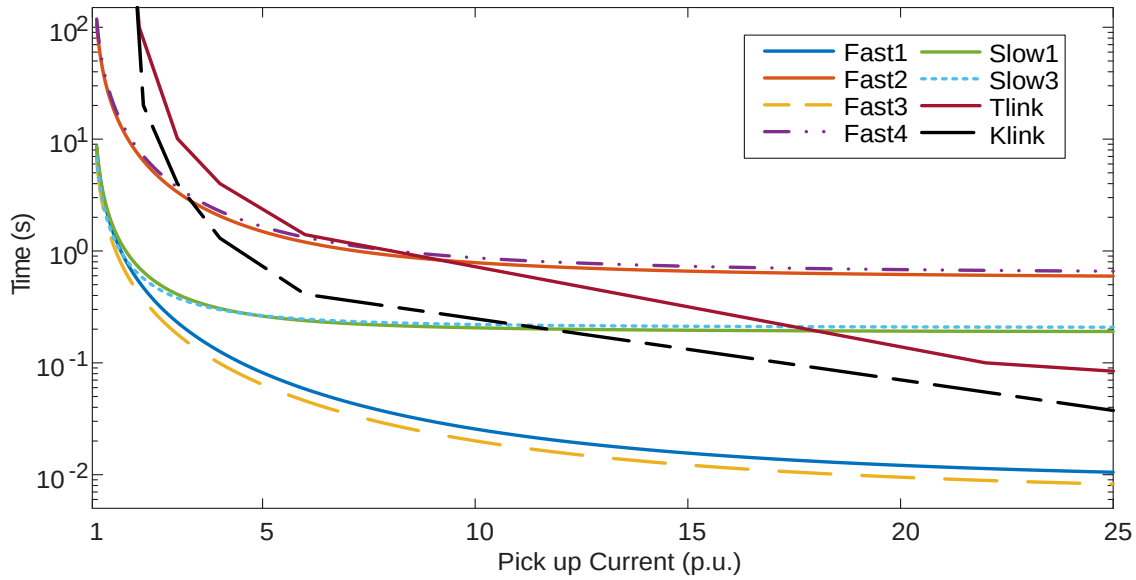

Figure 5.5. Time-current curves of protective devices.

System faults/failures may be classified as temporary or permanent. Although temporary distribution faults rarely exceed 5 minutes, depending on the grounding system design, it is possible to find temporary faults longer than 5 minutes. Therefore, momentary interruption (i.e., less than 5 minutes) should not be always seen as equivalent of temporary fault/failure (i.e., more than 5 minutes). Although there is a distinction between fault and failure, both concepts are indistinctly used. A failure in an overhead line may be temporary or permanent, while a failure in any other component will be by default permanent. Finally, all faults are assumed by default bolted.

Table 5.4 and Table 5.5 show the statistics assumed in this work for the random generation of element failure. Note that the failure statistics for overhead line sections are presented according to the zone classification. The values presented in Table 5.5 are individual averages; in the case of failure rate, this value must be multiplied by the total number of elements in order to obtain the system failure rate for each element.

Time of Occurrence		
Month and Hour		Probability (%)
Month	January	4
	February	5
	March	8
	April	7
	May	8
	June	8
	July	11
	August	15
	September	13
	October	9
	November	7
	December	5
Hour interval	1-6	30
	7-12	20
	13-18	30
	19-24	20

Duration	
Type	Probability (%)
Momentary	75
Sustained	25

Type	
Number of phases	Probability (%)
One-phase - 1	70
Two-Phase - 2	25
Three-Phase - 3	5

Failures			
Zone	Average number (per 100 km)	Standard deviation (per 100 km)	Repair time (hours)
1	50	12	2
2	20	7.5	3
3	30	10	3
4	45	10	2.5
5	25	7.5	2.5
6	20	5	3

Table 5.4. Failure statistics for overhead line sections.

Distribution Transformers	
Failures per year	Repair time (hours)
0.100	10

Voltage Regulators	
Failures per year	Repair time (hours)
0.125	10

Capacitor Banks	
Failures per year	Repair time (hours)
0.250	4

PV Generation Modules		
Module Size (kW)	Failures per year	Repair time (hours)
100	0.100	10

Table 5.5. Failure statistics for system elements.

5.4. An Illustrative Case Study

The occurrence of a fault or a component failure will cause a sequence of events that may imply protective devices, isolation switches, a system reconfiguration when it is possible and advisable, the repair of the failed component, and the recovery of the original system configuration. This case study is aimed at illustrating the sequences that can be produced after the occurrence of a fault/failure, the calculations to be made, depending on the system response, as well as the results that can be required for a later estimation of system reliability indices.

5.4.1. Case Study Characteristics

The characteristics of the case are according to the following information:

- Location: Line section L793, between load nodes 791 and 793, see Figure 5.6.
- Time of occurrence: 2750 hour.
- Type of fault: Phase-to-phase (two-phase fault).
- Faulted phases: A and B.
- Duration: Sustained.
- Line section repair time: 6 hours and 20 minutes.
- Failed element disconnection time: 1 hour and 25 minutes.
- Back-up feeder connection time: 1 hour and 30 minutes.
- Scenario: Disconnection and repair of the failed element with load transfer between feeders.

5.4.2. Sequence of Events

The detailed event sequence during fault simulation is summarized as follows:

1. Fault occurs at designated hour.
2. Circuit Breaker LA90 performs first opening action.
3. Interconnection protection IP4, IP5, and IP6 operate.
4. Circuit Breaker LA90 carries out automatic reclose.
5. Circuit Breaker LA90 performs second opening action.
6. Sectionalizer LA91 reaches operation count limit and opens terminals.
7. Circuit Breaker LA90 closes.
8. PV generators PVplant4, PVplant5, and PVplant6 are placed back in operation
9. Line LA93 is disconnected and sectionalizer LA91 is returned to its original closed position.
10. Line repair starts.
11. Back-up feeder FA01 is connected.
12. Repair of Line LA93 is finished.
13. Line LA93 is reconnected and back-up feeder FA01 is disconnected, returning the system to its original configuration.

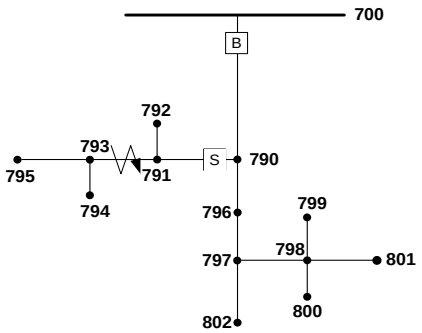

Figure 5.6. Faulted element location.

Event log generated by OpenDSS:

Hour=2750, Sec=0.246, ControlIter=1, Element=Relay.la90, Action=OPENED
Hour=2750, Sec=0.246, ControlIter=1, Element= , Action=PHASE TARGET
Hour=2750, Sec=0.502, ControlIter=1, Element=Relay.lv6, Action=OPENED ON UV & LOCKED OUT
Hour=2750, Sec=0.502, ControlIter=1, Element=Relay.lv5, Action=OPENED ON UV & LOCKED OUT
Hour=2750, Sec=0.502, ControlIter=1, Element=Relay.lv4, Action=OPENED ON UV & LOCKED OUT
Hour=2750, Sec=10.246, ControlIter=1, Element=Relay.la90, Action=CLOSED
Hour=2750, Sec=10.49, ControlIter=1, Element=Relay.la90, Action=OPENED
*Hour=2750, Sec=10.49, ControlIter=1, Element=Sectionalizer.la91, Action=OPENED
Hour=2750, Sec=10.49, ControlIter=1, Element= , Action=PHASE TARGET
Hour=2750, Sec=40.49, ControlIter=1, Element=Relay.la90, Action=CLOSED
*Manually added

Figure 5.7 shows how the configuration of the system changes during the sequence of events caused by the analysed fault and the status of the various protective devices and switches/disconnectors involved in this case. Remember that, once the fault occurs, the first steps in the sequence of events are caused by the design and settings of the protection system, while the last steps will depend on the performance of the maintenance crew.

Figure 5.8 provides a sequence of events with the time of occurrence of each one. As mentioned above, some of the values required to obtain this sequence are derived from the operation of the protective devices and are of deterministic nature, while others due to the performance of the maintenance crew are of random nature and generated according to the estimated probability distributions.

Figure 5.9 shows a diagram with the status (e.g. opened/closed) of the protective devices and switches/disconnectors involved in the simulation of this case.

5.4.3. Simulation Results

Figure 5.10 through Figure 5.13 present some results derived from the simulation of the case study. The various plots in the figures show the active power measured at the MV terminals of the substation, the power injected by the affected generators into the network, and the active power measured at some load nodes. Note that, except for Figure 5.10, the time scales are in hours and all the plots compare the power curves that result without the fault with those that are a consequence of the fault; they also incorporate some information about the operation of protective devices and switching operations.

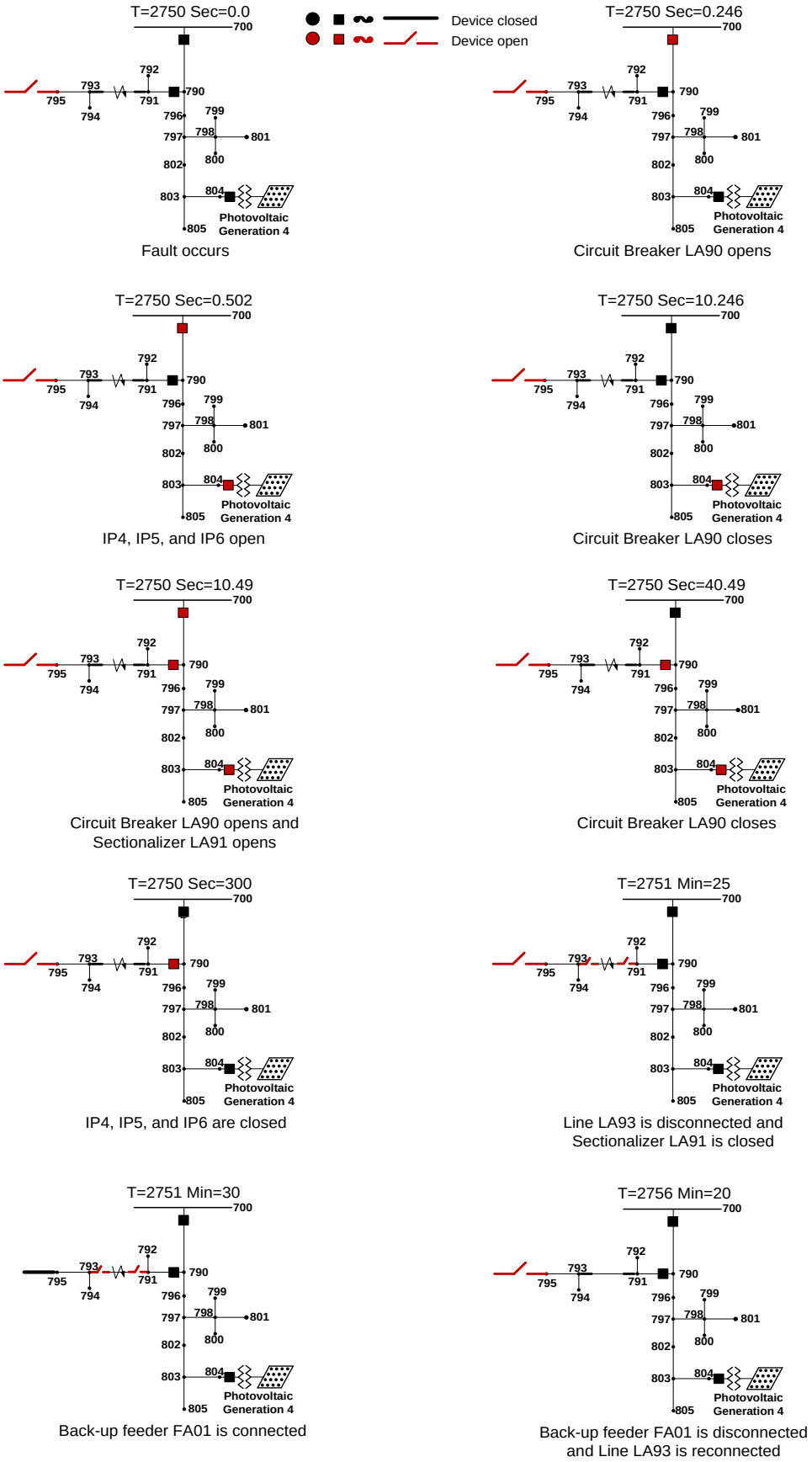

Figure 5.7. Sequence of the system configurations after the occurrence of the fault.

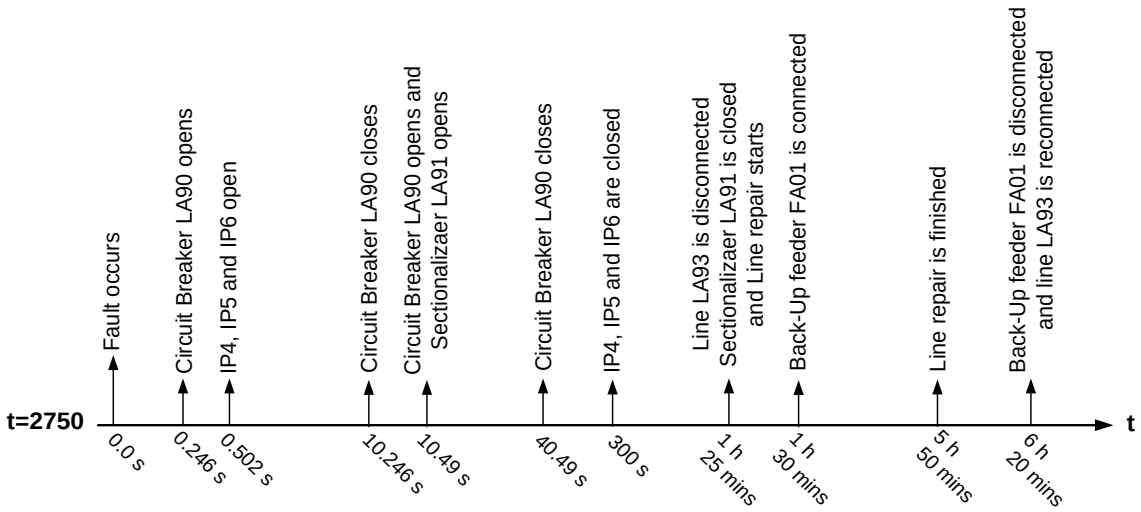

Figure 5.8. Sequence of events after the occurrence of the fault.

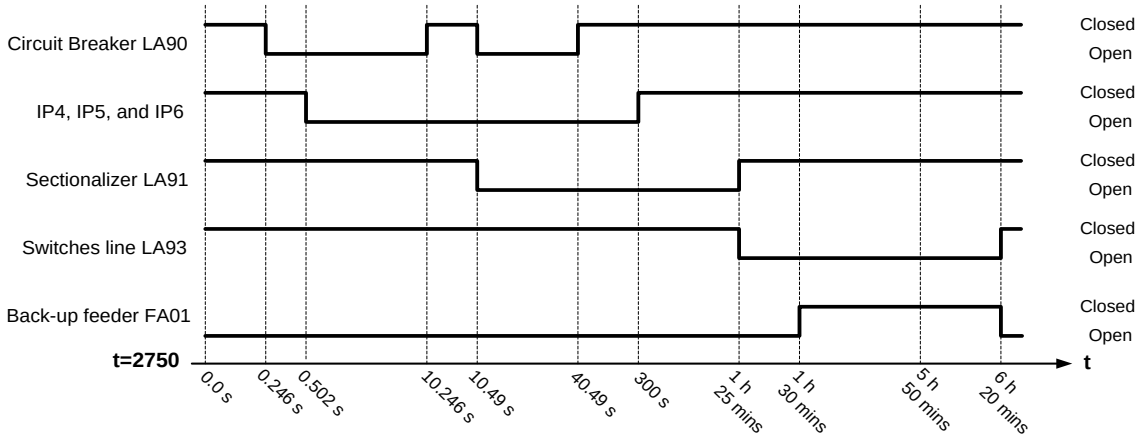

Figure 5.9. Status of protective devices and switches after the occurrence of the fault.

Power Supplied by HV System

Figure 5.10 presents the power provided by the HV system during the operation of the protection system. Power values show a sudden increase when the fault occurs and they remain approximately constant until circuit breaker LA90 performs the first opening action. Generators' interconnection protection IP4, IP5, and IP6 trip due to low voltage at their point of common coupling (PCC); power values are not affected by this action since the entire feeder was previously isolated by circuit breaker LA90. The remaining value corresponds to the loads connected to the unfaulted feeder. After the relay's dead time has passed, circuit breaker LA90 recloses. The fault is still present and forces a second operation. This operation also causes the sectionalizer LA91 to reach its count limit and open. When the circuit breaker performs a second reclosing action, it will not sense any fault currents because the fault was isolated by the operation of sectionalizer. The rest of the system will remain under normal operation. After a normal voltage value has been confirmed at the generators' PCC, they will be reconnected to the system. This action will cause a decrease in the power supplied by the HV system.

Figure 5.11 presents the power supplied by the HV system during the complete simulation process; the effect caused by the fault has been neglected since the differences in scale would not allow observing the changes produced by the switching actions. After the protection system has finished its operation sequence and the PV generators have been reconnected, a small decrease in power can be observed when compared to pre-fault values. This small decrease is a consequence of the loads disconnected by the operation of sectionalizer LA91. The procedure takes into account the time needed for the maintenance crew to reach the faulted line, isolate it, and return the sectionalizer to its original closed position. This sequence allows restoring service to all loads located upstream from the faulted line. The procedure also takes into account the time needed to perform load transfer, if possible. For the present case, service can be restored to all loads downstream from the faulted line through the connection of back-up feeder FA01. Figure 5.11 shows how after these two actions have been completed, service is restored to all loads in the system. Switching actions aimed at returning the system to its original state (i.e. reconnecting Line LA93 and disconnecting back-up feeder FA01) are performed simultaneously and their effect on the system is neglected.

PV Generators

The affected generators (i.e. PVplant4, PVplant5, and PVplant6) are separated from the system by their interconnection protection due to low voltage at their PCCs. Since no damage to the generators is assumed during the fault, they can be put back in operation as soon as possible; therefore, all tripped generators are reconnected after confirming normal voltage values at their PCCs. For the present case, those PV generators are located outside of the sectionalizer's protection area and can be reconnected after operation of the protection system; as a consequence, their downtime is deemed negligible, and the interruption is considered momentary. Figure 5.12 presents PVplant4 generation curve.

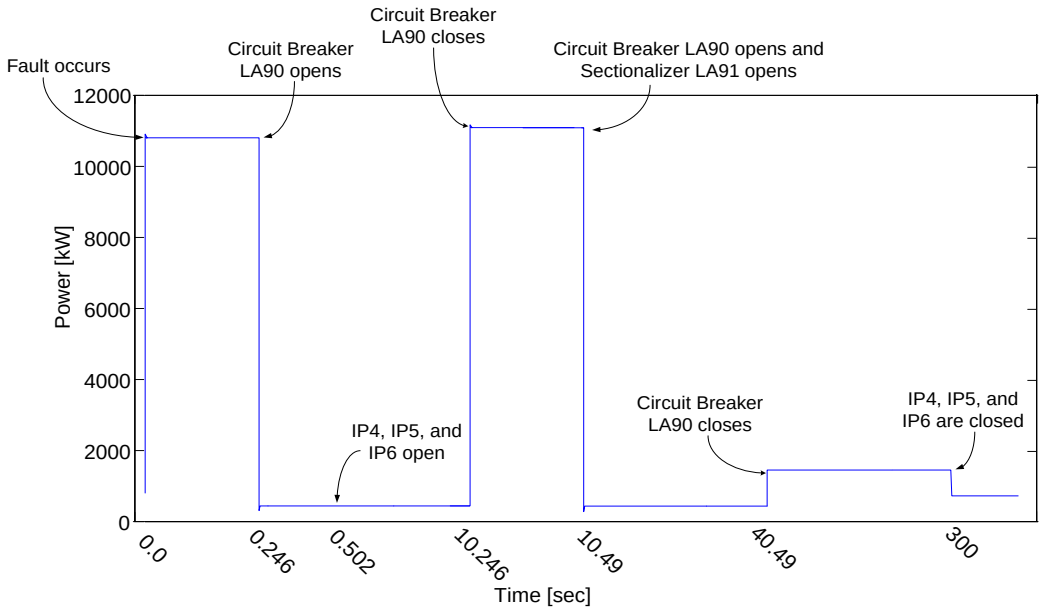

Figure 5.10. Power measured at the substation terminals during protection system operation.

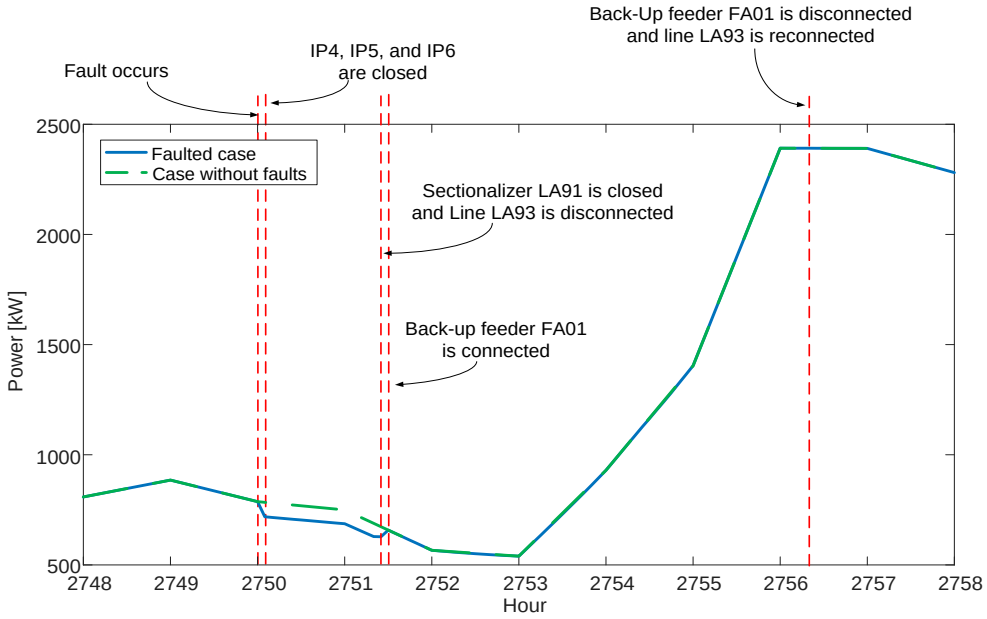

Figure 5.11. Power measured at the substation terminals during complete simulation.

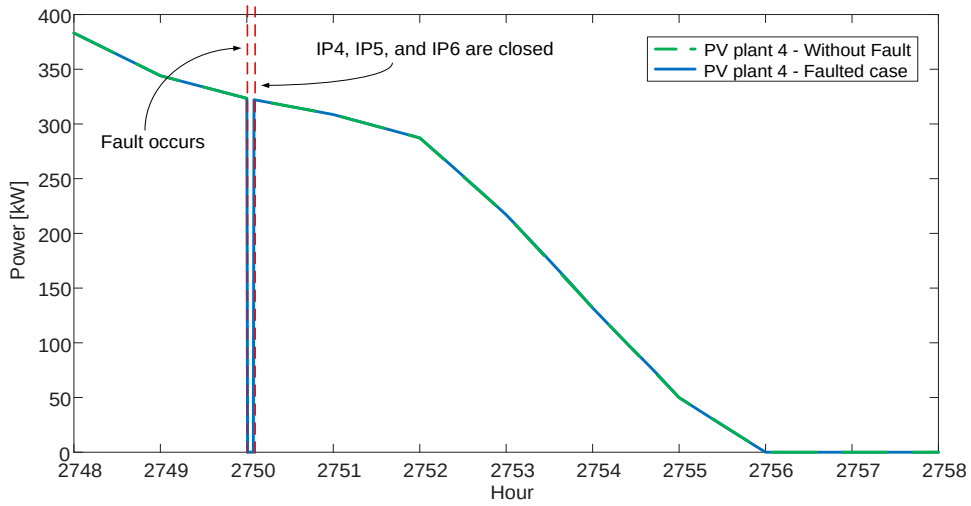

Figure 5.12. Power injected by the PV generation units.

Affected Loads

As a consequence of the sectionalizer operation, only loads SA792, SA794, and SA795 will suffer a sustained interruption. Load SA792 is located upstream from Line LA93 and its service can be restored after isolating the faulted line and closing sectionalizer, whereas loads SA794 and SA795 will remain without service until back-up feeder FA01 is connected. Figure 5.13 shows the power supplied to SA792 and SA794.

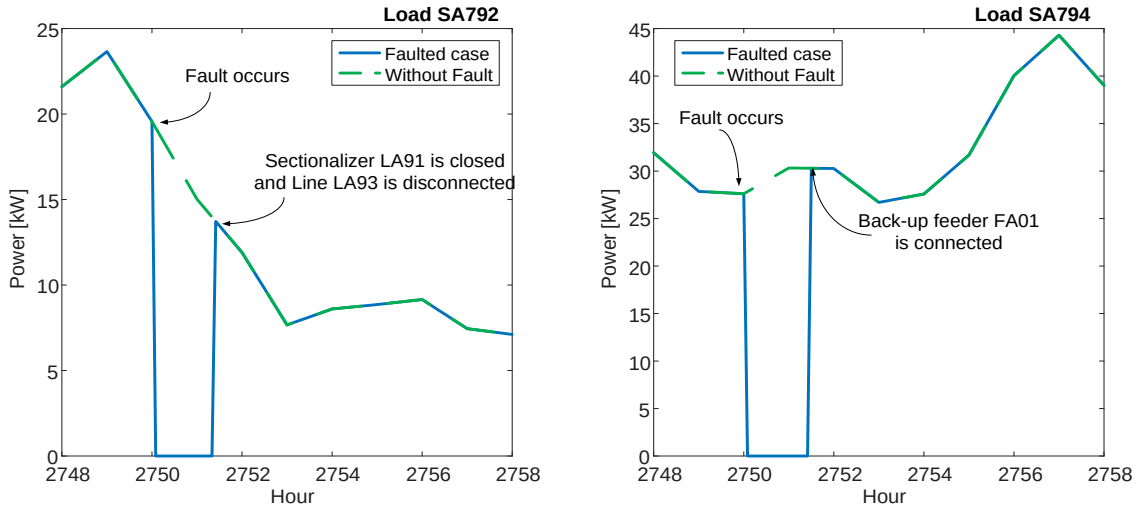

Figure 5.13. Power consumed from some affected load nodes.

5.5. Reliability Analysis of the Test System

5.5.1. Simulation Results

The objective of this study is to obtain the probability density functions of the reliability indices for the test system. To assess the impact of DG on the indices the study has been carried out considering the three scenarios (which depend on the level of automation assumed for the test system) with and without generation; however, for a better assessment the indices when PV generation units are connected to the test system have also been calculated assuming that the equipment related to generation (i.e. PV modules and interconnection transformers) will never fail. All calculations are made using a distributed computing environment with 60 cores, see Figure 5.3.

Table 5.6 shows the values obtained for some reliability indices derived after 360 and 420 runs, and considering only Scenario 3. The table shows that 360 runs are enough to estimate all load related reliability indices with enough accuracy, but the CV value after 360 runs is more than 5% for those indices related to generation; the main reason is the low number of generation units that are affected by a fault. Therefore, the number of executions must be increased to 420 in order to have all coefficients of variation under the 5% threshold.

Table 5.7 through Table 5.9 show the results obtained for the three scenarios. Given the results presented in Table 5.6, the number of runs considered without and with DG has been 420. The computing time required for the various scenarios considered in this work are summarized in Table 5.10 and the probability density functions for some reliability indices are shown in Figure 5.14. Table 5.7 through Table 5.9 present a summary of the probability distributions of these indices.

		Without DG	With DG (DG equipment does not fail)		With DG (DG equipment can fail)	
		360 runs	360 runs	420 runs	360 runs	420 runs
SAIFI (int)	Mean	1.2029	1.2029	1.1727	1.1970	1.1634
	Deviation	0.6116	0.6116	0.6536	0.6069	0.6126
	CV (%)	2.6796	2.6796	2.7197	2.6725	2.5693
SAIDI (h/yr)	Mean	2.7032	2.6406	2.5965	2.6757	2.5867
	Deviation	1.3752	1.2846	1.2803	1.4263	1.3729
	CV (%)	2.6812	2.5640	2.4060	2.8095	2.5898
CAIDI (h/int)	Mean	2.6830	2.6376	2.8094	2.6987	2.6281
	Deviation	1.7113	1.6957	1.8960	1.8194	1.5373
	CV (%)	3.3617	3.3883	3.2931	3.5533	2.8543
AENS (kWh/yr)	Mean	8592.57	8365.62	8266.28	8565.58	8186.95
	Deviation	4730.40	4354.32	4475.88	4976.61	4668.52
	CV (%)	2.9015	2.7432	2.6420	3.0621	2.7824
$SAIFI_{DG}$ (int)	Mean		1.1077	1.0779	1.3608	1.3272
	Deviation	----	0.6577	0.6973	0.6958	0.6840
	CV (%)		3.1296	3.1567	2.6950	2.5147
$SAIDI_{DG}$ (h/yr)	Mean		1.6593	1.6342	6.2117	6.0574
	Deviation	----	1.4997	1.5714	5.9842	5.2398
	CV (%)		4.7634	4.6921	5.0774	4.2208
AENP (kWh/yr)	Mean		489.37	486.33	1837.30	1883.8
	Deviation	----	593.21	613.49	2092.35	1908.67
	CV (%)		6.3887	6.1552	6.002	4.9438

Table 5.6. Reliability indices - Sensitivity study.

Note that the results to be obtained for the first scenario do not depend on the times required to isolate the failed component or to reconfigure the system, since it is assumed that service is restored (to nodes downstream of the protective device that opens) after the failed equipment is repaired. When service is restored after some switching operations and the times required for these operations are shorter than repair times, some reliability indices significantly improve, being the performance better when service may be restored both downstream and upstream of the faulted section.

	Scenario 1		Scenario 2		Scenario 3	
	Mean	Deviation	Mean	Deviation	Mean	Deviation
SAIFI (int)	1.2045	0.6521	1.1762	0.6542	1.1727	0.6536
SAIDI (h/yr)	5.5215	3.1703	3.7785	2.3958	2.6541	1.3162
CAIDI (h/int)	5.0740	2.3073	3.8095	2.4414	2.8613	1.9095
AENS (kWh/yr)	17529.16	10179.57	11698.20	7232.81	8475.17	4631.51
$SAIFI_{DG}$ (int)	----	----	----	----	----	----
$SAIDI_{DG}$ (h/yr)	----	----	----	----	----	----
AENP (kWh/yr)	----	----	----	----	----	----

Table 5.7. Probability distributions of reliability indices – Without DG – 420 runs.

	Scenario 1		Scenario 2		Scenario 3	
	Mean	Deviation	Mean	Deviation	Mean	Deviation
SAIFI (int)	1.2045	0.6521	1.1762	0.6542	1.1727	0.6536
SAIDI (h/yr)	5.5215	3.1703	3.7785	2.3958	2.5965	1.2803
CAIDI (h/int)	5.0740	2.3073	3.8095	2.4414	2.8094	1.8960
AENS (kWh/yr)	17529.11	10179.56	11698.17	7232.79	8266.28	4475.88
$SAIFI_{DG}$ (int)	1.0779	0.6973	1.0779	0.6973	1.0779	0.6973
$SAIDI_{DG}$ (h/yr)	4.6399	3.9465	3.2561	3.3192	1.6342	1.5714
AENP (kWh/yr)	1464.10	1713.74	1043.20	1375.36	486.33	613.49

Table 5.8. Probability distributions of reliability indices – With DG (DG equipment does not fail) – 420 runs.

	Scenario 1		Scenario 2		Scenario 3	
	Mean	Deviation	Mean	Deviation	Mean	Deviation
SAIFI (int)	1.1998	0.6120	1.1672	0.6128	1.1634	0.6126
SAIDI (h/yr)	5.6888	3.3017	3.9361	2.5686	2.5867	1.3729
CAIDI (h/int)	5.0066	2.1887	3.7412	2.2158	2.6281	1.5373
AENS (kWh/yr)	17887.71	10456.71	12121.98	7722.25	8186.95	4668.52
$SAIFI_{DG}$ (int)	1.3272	0.6840	1.3272	0.6840	1.3272	0.6840
$SAIDI_{DG}$ (h/yr)	9.3247	6.2455	7.9004	5.8615	6.0574	5.2398
AENP (kWh/yr)	2971.89	2620.42	2486.91	2310.80	1883.84	1908.67

Table 5.9. Probability distributions of reliability indices – With DG (DG equipment can fail) – 420 runs.

		1 core	60 cores
Base case with Distributed Generation	1 run	191 s	----------
Without Distributed Generation	1 run	5256 s	----------
	360 runs	----------	38237 s
With Distributed Generation (DG equipment does not fail)	1 run	5375 s	----------
	420 runs	----------	45405 s
With Distributed Generation (DG equipment can fail)	1 run	5427 s	
	420 runs	----------	46154 s

Table 5.10. Simulation times – Scenario 3.

Load Indices

The restrictions upon the formation of islands causes load indices to present similar probability distributions with and without PV generation. Note that the SAIFI index, which depends only on failure rates, is similar but not the same in all studies. This is basically due to single-phase faults. When a single-phase fault provokes a fuse operation, affected loads may suffer a voltage drop instead of an interruption. When load transfer is not possible, the loads downstream the fault will suffer the sustained interruption that is caused by the isolation of the faulted line; however, if load transfer is possible and the transfer is fast enough, those loads might only suffer the momentary interruption caused by the switching operations needed to make the transfer. This is the reason why for some runs the SAIFI index is lower when load transfer is possible than that resulting when the transfer is not possible. Scenario 1 presents higher values for this

index: as previously explained, every time one-phase fault occurs the system checks the minimum voltage at load terminals; if the minimum voltage is below 0.9 p.u., the procedure will open the remaining phases, causing an interruption to all loads downstream from the operated fuse. Finally, Scenario 2 presents values slightly higher than Scenario 3 but lower than Scenario 1; one-phase faults protected by fuses are again responsible for this behavior. As in Scenario 1, the procedure checks the minimum voltage at load terminals and if the minimum voltage is below 0.9 p.u., the procedure then will isolate the failed line and replace the operated fuse; under these circumstances only load downstream from the failed line will suffer a sustained interruption. If transferring load through a back-up feeder is possible (i.e. Scenario 3) and the connection time is lower that the time required to isolate the failed line and replace the operated fuse, the procedure will perform both actions simultaneously; as a consequence loads located downstream from the failed line will not experience any sustained interruption.

The differences between SAIDI values for Scenarios 1 and 2 and two are clear: the possibility of isolating the failed element and closing the operated protection device reduces the interruption time experienced by loads upstream from the failed element, having this decrease an impact on the global SAIDI value. Moreover, the possibility of load transfers (i.e. Scenario 3), which allows quickly restoring service to those loads located downstream from the failed element, will further reduce the index. As for AENS, the conclusions are similar to those drawn for SAIDI.

DG Indices

The results provided in Table 5.8 and Table 5.9 show that $SAIFI_{DG}$ values are the same for all 3 scenarios, while $SAIDI_{DG}$ values depend on the level of automation (i.e. the scenario under study). These results are reasonable since all protective devices between PV generators and the substation transformer are three-phase and the number of interruptions does not depend on the automation incorporated to the system. However, the $SAIDI_{DG}$ reduction is less important when compared to load indices because the failure of DG equipment is independent from network automation level and normal operation can only be resumed after all repairs have been finished. As for AENP, its variation is similar to that obtained for $SAIDI_{DG}$.

Simulation Times

The minimum simulation time required for reliability assessment with the approach presented in this work would be approximately the time required for a single run if the number of runs and the number of cores are equal. Given the system tested in this work, both the simulation time and the required number of cores have been affordable. However, both values would be much higher if the procedure had to be applied to a more realistic-size system (e.g., several hundreds of nodes) with shorter time steps and a detailed sequence of events was actually needed. Therefore, the procedure proposed in this Chapter has to be seen as a first step for accurate reliability assessment using a power flow simulator. Some refinements aimed at reducing the number of runs and a more powerful system simulator, using for instance internal parallel processing, should be then considered. The computing times presented in Table 5.10 correspond to the complete simulation of the test system during a year.

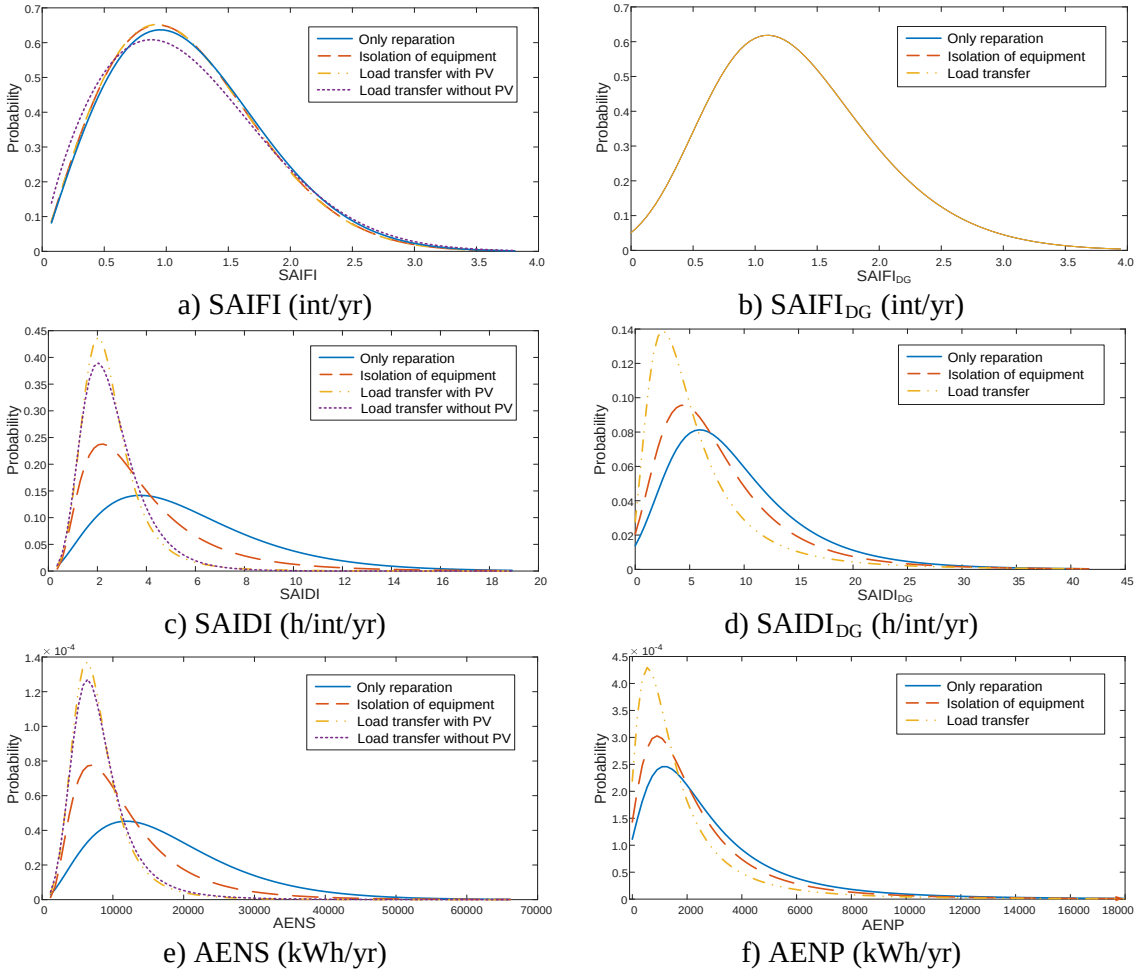

a) SAIFI (int/yr)

b) $SAIFI_{DG}$ (int/yr)

c) SAIDI (h/int/yr)

d) $SAIDI_{DG}$ (h/int/yr)

e) AENS (kWh/yr)

f) AENP (kWh/yr)

Figure 5.14. Reliability indices – Probability density functions.

5.5.2. Reduction of the Simulation Time

Several aspects may be considered when analyzing any of the three scenarios. For instance, (i) is it necessary simulating the system during a whole year to obtain reliability indices? (ii) how many runs are required to obtain accurate reliability indices (i.e., probability density functions of the reliability indices)?

When assessing the reliability of the test system during one year, in addition to the simulation of the whole year including switching events caused by both sustained and momentary interruptions, the following options can be considered:

- Since the effects of momentary interruptions are not included in reliability evaluation [5.19], an option for reliability index calculation is not to simulate the sequence of events caused by temporary faults with duration shorter than 5 minutes. Remember that failures of distribution transformers, voltage regulators, capacitor banks, and PV plants are by default sustained.
- Additional computing time can be saved when simulation results do not depend on history. Such circumstance could be taken into account for systems without energy storage devices. Without this dependency, only the values corresponding to interruptions longer than 5 minutes are of concern. That is, instead of simulating the whole year only the sequence of events corresponding to

sustained interruptions (i.e., protective device operation, fault location, isolation of the faulted section, service restoration, equipment repair, and original system reconfiguration) need to be simulated.

The results corresponding to the discussed options after one run are provided in Table 5.11. Note that all values for a given index are the same, regardless of the selected option.

	Complete Simulation	Without momentary interruptions	Only sustained interruptions
SAIFI (int)	0.9116	0.9116	0.9116
SAIDI (h/yr)	2.0809	2.0809	2.0809
CAIDI (h/int)	2.2826	2.2826	2.2826
AENS (kWh/yr)	7416.63	7416.63	7416.63
$SAIFI_{DG}$ (int)	0.9444	0.9444	0.9444
$SAIDI_{DG}$ (h/yr)	1.3101	1.3101	1.3101
AENP (kWh/yr)	340.60	340.60	340.60

Table 5.11. Reliability indices without switching operations (Scenario 3) – With Distributed generation (DG equipment can fail) – 1 Run.

	1 run 1 core	360 runs 60 cores	420 runs 60 cores
Complete simulation	5427 s	39676 s	47268 s
Without momentary interruptions	2051 s	23691 s	26275 s
Only sustained interruptions	2030 s	22971 s	25588 s

Table 5.12. Simulation times – With Distributed generation (DG equipment can fail) – Scenario 3.

The interest of this comparison is in the reduction that can be achieved for the simulation time; the resulting times in Table 5.12 prove that a significantly shorter simulation time is required when the calculation of reliability indices is based only on the simulation of sustained interruptions without a loss of accuracy. The differences are due to the fact that when performing reliability calculations, in addition to the reduction of the time-step size during a faulted condition, some variables (e.g., node voltages) are permanently monitored and this type of tasks slows down the procedure.

5.5.3. Assessing DG Impact on System Reliability

The results presented in Table 5.6 through Table 5.9 correspond to the study of the test system under certain load and generation conditions. Therefore, the conclusions derived from those results should be used with care. Although the differences obtained for load indices are not too significant with and without DG, concluding that DG will not significantly impact reliability when islanding conditions (i.e. microgrids) are not allowed can be wrong. The following discussion with some simulation results will clarify this. First, remember that PV generation can only help during day time hours when solar radiation is non-zero; this means that under some operating conditions its impact during that period of the day can be significant. Second, restrictions in operating conditions are considered in order to determine whether load transfer is possible or not.

Comparative Case With and Without DG

The present case shows the consequences a failure can have with and without PV generation. The characteristics of the case are according to the following information:

- Failed element: Voltage Regulator Regi, located between nodes 743 and 747; see Figure 5.15.
- Time of occurrence: 492 hour.
- Type of fault: Three-phase.
- Faulted phases: A, B, and C.
- Duration: Sustained.
- Repair time: 22 hours and 5 minutes.
- Failed element disconnection time: 40 minutes.
- Back-up feeder connection time: 40 minutes.
- Scenario: Disconnection and repair of the failed element with load transfer between feeders.

Detailed event sequence during fault simulation according to presence of DG is:

With PV

1. Fault occurs at designated hour.
2. Overcurrent protection Regi performs opening action and locks out.
3. PCC protection IP2 and IP3 operate.
4. Voltage regulator Regi is isolated and Back-up Feeder FA02 is connected.
5. Voltage regulator repair starts
6. PV generators PVplant2 and PVplant3 are placed back in operation.
7. Repair is finished.
8. Voltage regulator Regi is reconnected and Back-up Feeder FA02 is disconnected.

Without PV

1. Fault occurs at designated hour.
2. Overcurrent protection Regi performs opening action and locks out.
3. Voltage regulator Regi is isolated and Back-up Feeder FA02 is connected.
4. Voltage regulator repair starts.
5. Repair is finished.
6. Voltage regulator is reconnected and Back-up Feeder FA02 is disconnected.

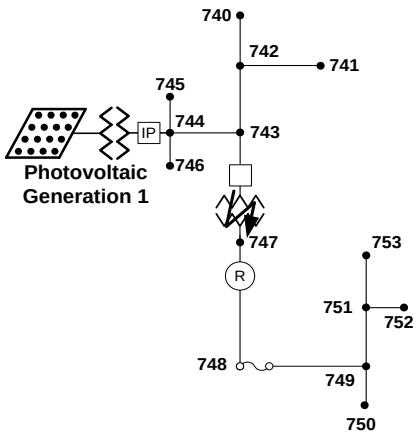

Figure 5.15. Location of failed element.

Given the location of the failed component, a load transfer using the intermediate switch transfer could be possible. However, since the failure occurs at noon of a January's day, the presence of PV generators has a significant impact: without these generators, there would be an overload of the voltage regulator located on the right feeder, and load transfer is not made. As a consequence, service cannot be restored to all load nodes (about 3 MW of rated power)

The procedure monitors system conditions, i.e. voltages and currents, in order to ensure that load transfer is possible. After the operating conditions for load transfer have been checked (see Table 5.13), the procedure must decide whether load transfer has been successful or not. Using the previously defined rules, minimum voltage of 0.9 p.u. and maximum overload of 110%, it can be observed that without PV generation the load transfer is considered unsuccessful.

With PV			
Load with minimum voltage	Minimum Voltage (p.u.)	Maximum overloaded element	Overload (%)
SA814	0.9314	Voltage regulator Regd	99.65
Without PV			
Load with minimum voltage	Minimum Voltage (p.u.)	Maximum overloaded element	Overload (%)
SA814	0.9240	Voltage regulator Regd	112.22

Table 5.13. Operating conditions with and without PV generation.

An unsuccessful load transfer forces the procedure to repeat the simulation but neglecting the possibility of transferring load. If possible, the procedure performs the disconnection of the failed element and returns the operated protection device to its original closed position. This action is not possible when a voltage regulator fails; therefore, all customers will remain without service until the repair has been completed. Original repair time included Back-up Feeder switching times; under the new circumstances a new repair time must be calculated, this time without Back-up Feeder switching times.

As a consequence of the unsuccessful load transfer the energy not supplied during service interruption reaches a value close to 23 MWh. Table 5.14 presents numbers related to reliability indices, they are different for both cases due to the impossibility of performing load transfer without PV generation.

	With PV	Without PV
Number of customers interrupted	206	206
Nominal power interrupted (kW)	2140	2140
Actual energy not supplied (kWh)	750.94	23680.27
Generation power interrupted (kW)	700	----
Actual energy not produced (kWh)	207.76	----

Table 5.14. Simulation results with and without PV generation.

The new sequence of events during fault simulation is:

With PV

1. Fault occurs at designated hour.
2. Overcurrent protection Regi performs opening action and locks out.
3. PCC protection IP2 and IP3 operate.
4. Voltage regulator Regi is isolated and Back-up Feeder FA02 is connected.
5. Voltage regulator repair starts.
6. PV generators PVplant2 and PVplant3 are placed back in operation.
7. Repair is finished.
8. Voltage regulator Regi is reconnected and Back-up Feeder FA02 is disconnected.

Without PV

1. Fault occurs at designated hour.
2. Overcurrent protection Regi performs opening action and locks out.
3. Voltage regulator Regi is isolated.
4. Voltage regulator repair starts.
5. Repair is finished.
6. Voltage regulator is reconnected.

Figure 5.16 presents the power demanded by all system loads during the fault simulation. The presence of PV generation will impact the system operating conditions; however, loads have been modeled as constant power loads and the actual power absorbed will remain the same with and without PV generation. It can be observed that with PV generation the service is restored to all customers through network reconfiguration, whereas without PV generation the system returns to its original state after the failed voltage regulator has been reconnected.

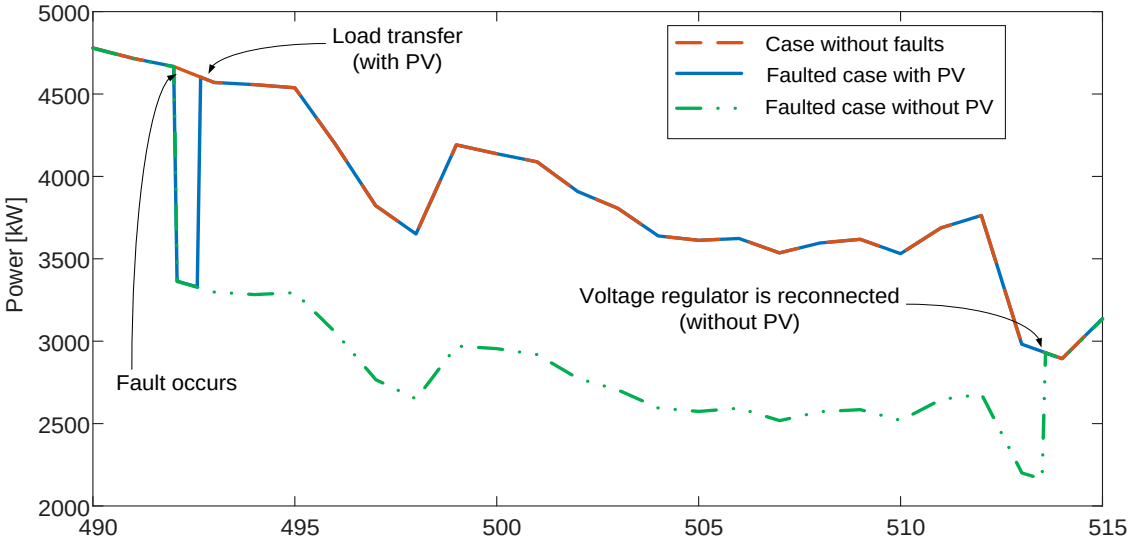

Figure 5.16. Failure of the voltage regulator located within the left-side feeder – Total load power.

New Load Conditions

An important observation can be derived from the previous case: if the load level was higher than that assumed in the previous study, the impact of PV generation would have been more significant than reflected in Table 5.6 through Table 5.9. Figure 5.17 and Table 5.15 show the reliability indices that result when considering Scenario 3 and new operating conditions in which load profiles have been modified in order to produce a load increment during day-time hours without increasing load nominal powers. The table and the figure compare the indices that result from the initial and the new operating conditions. Under the new conditions, system reliability becomes more sensitive to PV generation and those indices related to interruption duration (SAIDI, CAIDI, and AENS) increase. However, when comparing cases with and without PV generation it can be observed that the reduction of said indices is more significant than the reduction achieved with the initial operating conditions. Since PV generation can only provide support during day-time hours, PV generation can have a significant impact on system reliability if system loads are predominantly diurnal. Note that this impact can be easily quantified and/or analysed because the reliability analysis is based on the use of a power flow simulator.

	Without DG		With DG (DG equipment does not fail)		With DG (DG equipment can fail)	
Index	Mean	Deviation	Mean	Deviation	Mean	Deviation
SAIFI (int)	1.1727	0.6536	1.1727	0.6536	1.1634	0.6126
SAIDI (h/yr)	2.9701	1.7845	2.7205	1.4178	2.7956	1.6120
CAIDI (h/int)	3.1515	2.2033	2.9257	2.0272	2.8034	1.6546
AENS (kWh/yr)	10281.67	6423.42	9408.71	5378.14	9643.40	6023.54
$SAIFI_{DG}$ (int)	-----	-----	1.0779	0.6973	1.3272	0.6840
$SAIDI_{DG}$ (h/yr)	-----	-----	1.8010	1.7857	6.3436	5.2832
AENP (kWh/yr)	-----	-----	571.70	701.76	1907.45	1802.72

Table 5.15. Comparison of Reliability Indices (Scenario 3) – New Operating Conditions – 420 Runs.

5.6. Conclusions

This Chapter has presented a procedure based on a Monte Carlo method for reliability assessment of overhead distribution systems with or without distributed generation using a multicore computing environment. The procedure uses a power simulator running in time-driven mode. The implemented approach offers some important advantages:

- The model can be realistic and detailed, and results can be very accurate.
- Simulation results provide a significant amount of information that can be used for other purposes (e.g., optimum location of DG units).
- The information can also be used for estimating other performance indices than those presented here.

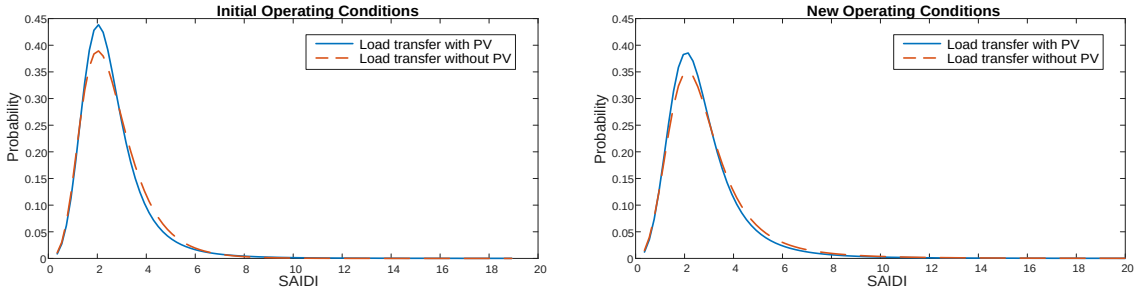

a) SAIDI

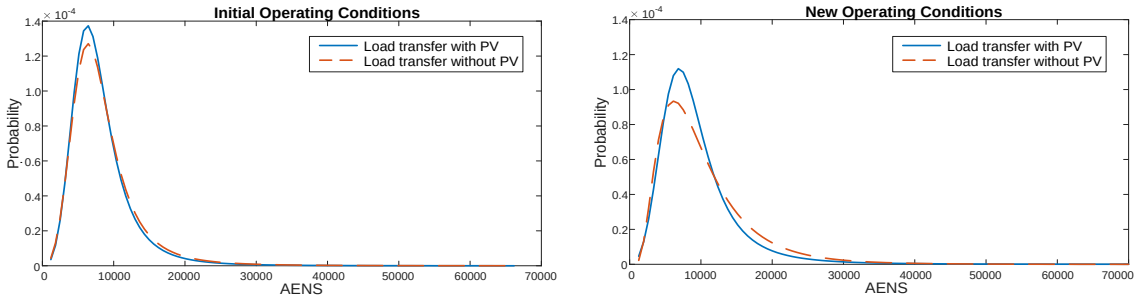

b) AENS

Figure 5.17. Reliability indices – Probability density functions.

This work has illustrated how parallel computing can circumvent an important disadvantage of the procedure; that is, the application of a time-consuming Monte Carlo method. Its application can reduce the simulation time to approximately that corresponding to a single run if the number of available cores is equal to the number of runs evaluated; this is not possible for big systems unless several thousands of cores were available.

The Chapter has also shown that under some circumstances computing time can be significantly reduced by simulating the system only when a sustained interruption is caused. The results show no difference for the index values obtained with all three options.

Although the main goal is to present a procedure for reliability analysis, the results presented prove that, depending on the operating conditions, distributed generation can improve the reliability of distribution systems, mainly due to the overload that could occur in a faulted system without the presence of embedded generation; this is especially important when load transfer between feeders is possible in the system under study.

5.7. References

[5.1] R.E. Brown, *Electric Power Distribution Reliability*, 2nd Edition, CRC Press, 2009.

[5.2] A.A. Chowdhury and D.O. Koval, *Power Distribution System Reliability. Practical Methods and Applications*, John Wiley, 2009.

[5.3] K. Moslehi and R. Kumar, "A reliability perspective of the smart grid," *IEEE Trans. on Smart Grids*, 2010, 1, (1), pp. 57-64.

[5.4] D. Haughton and G.T. Heydt, '"Smart distribution system design: Automatic reconfiguration for improved reliability," *IEEE PES General Meeting*, Minneapolis, July 2010.

[5.5] T. Ackerman, G. Andersson, and L. Söder, "Distributed generation: A definition," *Electric Power Systems Research*., 2001, 57, (3), pp. 195-204.

[5.6] H.L. Willis and W.G. Scott, *Distributed Power Generation. Planning and Evaluation*, Marcel Dekker, 2000.

[5.7] F. de Leon, R. Salcedo, X. Ran, and J.A.Martinez-Velasco, 'Time-Domain Analysis of the Smart Grid Technologies: Possibilities and Challenges', in Martinez-Velasco J.A. (Ed.), *Transient Analysis of Power Systems: Solution Techniques, Tools and Applications*, John Wiley, 2015.

[5.8] C.L.T. Borges: "An overview of reliability models and methods for distribution systems with renewable energy distributed generation," *Renewable and Sustainable Energy Reviews*, 2012, 16, (6), pp. 4008-4015.

[5.9] G. Celli, E. Ghiani, F. Pilo, and G.G. Soma; "Reliability assessment in smart distribution networks," *Electric Power Systems Research*, 2013, 104, pp. 164–175.

[5.10] M. Al-Muhaini and G.T. Heydt, "Evaluating future power distribution system reliability including distributed generation," *IEEE Trans. on Power Delivery*, 2013, 28, (4), pp. 2264-2272.

[5.11] A.M. Leite da Silva, L.C, Nascimento, M.A. da Rosa, D. Issicaba, and J.A. Pecas Lopes, "Distributed energy resources impact on distribution system reliability under load transfer restrictions," *IEEE Trans. on Smart Grid*, 2012, 3, (4), pp. 2048–2055.

[5.12] X. Zhang, Z. Bie, and G. Li, "Reliability assessment of distribution networks with distributed generations using Monte Carlo method," *Energy Procedia*, 2011, 12, pp. 278-286.

[5.13] H. Ge and S. Asgarpoor, "Parallel Monte Carlo simulation for reliability and cost evaluation of equipment and systems," *Electric Power Systems Research*, 2011, 81, (2), pp. 347-356.

[5.14] L. Jikeng, W. Xudong, Q. Ling, "Reliability evaluation for the distribution system with distributed generation," *Euro. Trans. Electr. Power*, 2011, 21, (1), pp. 895-909.

[5.15] J. Park, W. Liang, J. Choi, A.A. El-Keib, M. Shahidehpour, and R. Billinton, "A probabilistic reliability evaluation of a power system including solar/photovoltaic cell generator," *IEEE PES General Meeting*, Calgary (Canada), July 2009.

[5.16] I.S. Bae and J.O. Kim, "Reliability evaluation of distributed generation based on operation mode," *IEEE Trans. on Power Systems*, 2007, 22, (2), pp. 785-790.

[5.17] H. Ferreira, H. Faas, G. Fulli, W.L. Kling, and J. Peças Lopes, "Reliability analyses on distribution networks with dispersed generation: a review of the state of the art," Joint Research Centre – Institute for Energy and Transport, 2010.

[5.18] M.V.F. Pereira and N. Balu, "Composite generation and transmission reliability evaluation," *IEEE Proc*., 1992, 80, (4), pp. 470-491.

[5.19] IEEE 1366: 'IEEE Guide for Electric Power Distribution Reliability Indices', 2012.

[5.20] D. Fulchiron, *Protection of MV/LV substation transformers*, Cahier Technique No. 192; Schneider, 1998.

[5.21] M.A. Eltawil and Z. Zhao, "Grid-connected photovoltaic power systems: Technical and potential problems—A review," *Renewable and Sustainable Energy Reviews*, 2010, 14, (1), pp. 112-129.

[5.22] P. Zhang, W. Li, S. Li, Y. Wang, and W. Xiao, "Reliability assessment of photovoltaic power systems: Review of current status and future perspectives," *Applied Energy*, 2013, 104, pp. 822-833.

[5.23] E. Collins, M. Dvorack, J. Mahn, M. Mundt, and M. Quintana M, "Reliability and availability analysis of a fielded photovoltaic system," *34th IEEE Photovoltaic Specialists Conference (PVSC)*, Philadelphia (PA, USA), June 2009.

[5.24] J. Kepner, *Parallel MATLAB for Multicore and Multinode Computers*, SIAM, 2009.

[5.25] C. Moler, *Parallel MATLAB: Multiple processors and multiple cores*, TheMathWorksNews & Notes, 2007.

[5.26] P. Luszczek P, "Enhancing multicore system performance using parallel computing with MATLAB," *MATLAB Digest*, 2008.

[5.27] M. Buehren, *MATLAB Library for Parallel Processing on Multiple Cores*, Copyright 2007. Available from http://www.mathworks.com.

[5.28] IEEE Distribution Planning WG: 'Radial distribution test feeders', *IEEE Trans. on Power Systems*, 1991, 6, (3), pp. 975-985.

Chapter 6

General Conclusions

This doctoral Thesis presents a contribution to three main topics related to power distribution studies. The generation of system curves (i.e. load and renewable generation curves) to be used in other studies was introduced in Chapter 3, while Chapters 4 and 5 presented procedures developed for optimum reduction of distribution losses by allocating distributed generation and reliability assessment of power distribution systems with distributed generation.

The tools used for application development are MATLAB and OpenDSS. OpenDSS is the tool chosen for carrying out the simulation of distribution systems. An optimized solution algorithm along with a large number of system element models makes OpenDSS a powerful simulator for power distribution systems. Although OpenDSS is a highly efficient and flexible software tool, it lacks the capabilities of a programming language; however this drawback can be circumvented by taking advantage of the COM server DLL. The COM server DLL allows the user to link OpenDSS with other software tools (e.g. MATLAB). MATLAB is a high-level programming language with great capabilities and many built-in functions, and can be used to control the execution of simulations performed by OpenDSS, handle data generated by OpenDSS, and produce graphical outputs. User can take full advantage of the combination of these tools and their features to create custom-made applications that can be adapted to a wide range of studies.

Many studies, such as those based on the Monte Carlo method, require a large number of executions in order to achieve the desired accuracy. Although individual execution times can be affordable, total simulation times can become prohibitive. Parallel computing is a natural approach when the objective is to reduce the total execution time of problems with an embarrassingly parallel nature (such as the Monte Carlo method). The use of a multicore environment allows users to distribute task executions among available CPUs, thus reducing total simulation times.

Therefore, the procedures for optimum allocation of distributed generation and reliability assessment of power distribution systems have been developed taking advantage of parallel computing, namely they were conceived as parallel Monte Carlo methods. It can be expected that parallel computing will become a common practice in power distribution studies, especially when working with detailed models and large realistic systems.

The generation of system curves (which include load consumption and photovoltaic and wind generation) represents a key element in studies that include time variation of loads and generation. The main reason behind the implemented algorithms is to not depend on external tools (e.g. HOMER) in order to generate this information, allowing more flexibility and control over the generation process. A clear example is represented by load and generation curves used for long-term studies; with an evaluation period of up to 20 years, it would have been an extremely difficult and tedious task to generate these curves using a tool like HOMER, whereas the implemented algorithms were able to generate these curves without much effort. The procedure usefulness has been proven throughout the studies performed for this Thesis; however the one-hour time step can be a restriction, since some studies may require shorter time steps (e.g. 1 minute or less). This requirement implies that the present algorithms must be improved in order to provide curve-shapes with shorter time steps.

The optimum allocation of distributed generation has been the objective of many studies in recent years; the procedure presented in this Thesis is aimed at minimizing system energy losses for short and long term evaluation periods (a sequential connection of generating units is assumed for long term periods). Although reaching the global optimum using a Monte Carlo approach can be a time consuming task even when a multicore installation is used, the results obtained have proven that the procedure is capable of finding a quasi-optimum solution. Furthermore, two new approaches (i.e. the so-called Refined method and a “Divide and Conquer” approach) were presented; their application has permitted an important reduction of simulation times without a significant loss in accuracy.

More effort must still be put into further reducing simulation times, especially when considering long-term evaluation of large distribution systems.

Optimum allocation methods face an important drawback; in deregulated markets the connection of distributed generators is not made following the results of any optimization technique, from the independent producer’s point of view the goal is to optimize the benefit. However these methods should not be seen as just an academic exercise; the information generated as a result of the Monte Carlo method can be useful to have a clear vision on the maximum energy loss reduction that can be expected when connecting new distributed generation units. Moreover, the results can also be used to define areas where distributed generation can have a greater impact on system energy losses (without necessarily being the optimal energy losses) and also determine location and rated power combinations that meet utility requirements for the connection of DG.

Reliability analysis is a fundamental piece of distribution system planning and design, the developed procedure is mostly aimed at replicating the random nature of system and power components failure. It calculates the system reliability indices through consecutive power flow executions of the test system. The obtained results show that

the method is able to estimate the probability density function of the different reliability indices with the desired accuracy for systems with and without distributed generation. Additional reliability indices related to distributed generation have been introduced ($SAIFI_{DG}$ and $SAIDI_{DG}$); these new indices help assessing the impact of system failure on DG. Furthermore, the use of a power flow simulator allows an easy and accurate calculation of the Actual Energy Not Supplied (AENS) and Actual Energy Not Produced (AENP) indices, the latter related to distributed generation.

Although the results obtained are satisfactory, there is still a lot of work to be done. The main aspects to be considered for future work are: improvement of the availability model of distributed generation, reliability analysis including microgrids, and a more detailed sequence of switching actions. Simulation of microgrids deserves special attention, since a detailed generator model for island-operation must be implemented. The goal must be to incorporate these aspects into the reliability evaluation of distribution systems.

Finally, the work presented in this Thesis must be seen as an initial effort for developing a set of simulation-based applications for the analysis and study of power distribution systems. Future work must be aimed at improving these applications, implement more detailed DG models, and develop new techniques for reducing total simulation times, a requirement especially important when simulating large realistic distribution systems. Additional work must be put into implementing algorithms that can generate load and generation curves with short or very short time steps (e.g. with a resolution of 1 minute or less).

Appendix A

OpenDSS

A.1. Introduction

OpenDSS (Open Distribution System Simulator) is a power distribution system simulator released by EPRI (Electrical Power Research Institute) and developed for over 15 years. The result of this effort is a frequency-domain simulation engine with many characteristics found in other commercial simulation tools, as well as many new features aimed at supporting ongoing research efforts on distribution system simulation. Originally conceived as an analysis tool for the interconnection of distributed generation, its continuous development has provided it with capabilities that can be used for studies that range from harmonic analysis to energy efficiency [A.1].

Namely, OpenDSS can be used for:

- distribution planning and analysis,
- general multi-phase ac circuit analysis,
- analysis of distributed generation interconnection,
- annual load and generation simulations,
- wind plant simulations,
- storage modeling,
- harmonic and inter-harmonic distortion analysis,
- distribution state estimation,
- others.

The program includes different solution modes, such as:

- power flow (snapshot and time-driven),
- harmonics,
- dynamics,
- fault study,
- Monte Carlo study,
- others.

Due to its frequency-domain nature, it is not capable of carrying out electromagnetic (time-domain) transients simulations; however, it does perform electromechanical transients or dynamics analysis. This same nature makes the program different from the typical power flow program since it gives the tool great modeling flexibility, particularly for accommodating all sorts of load models and unusual circuit configurations.

OpenDSS was designed to receive instructions via scripts, allowing greater flexibility to the user. The program can be accessed through a stand-alone executable version and the COM interface implemented on the in-process server DLL. The stand-alone version provides a text scripting interface, which allows a complete interaction with the program. OpenDSS can be linked to other software platforms (such as MATLAB, Python, C#, and other languages) using the COM interface; this gives the user the possibility to implement custom-made features, models, and solutions, in addition to providing greater data handling capabilities. Figure A.1 shows how the different internal modules interact within the program structure.

In this Appendix the main features as well as some of the most important capabilities of OpenDSS are presented. Section A.2 presents the program's solution method and some of the available element models. Section A.3 introduces the Stand-Alone version of OpenDSS; a small example is developed to demonstrate its basic functionalities. In Section A.4 the link between MATLAB and OpenDSS is explained; the Section also presents a MATLAB script used to solve the test system presented in Chapter 3 and some plots that were generated using the information collected during the simulation.

A.2. Basic Solution Methods and Models

A.2.1. Solution Algorithm

OpenDSS represents distribution circuits through their nodal admittance equations. System elements are modeled by means of their primitive admittance matrix, or primitive Y [A.2]. Each primitive admittance matrix is added to the system matrix, allowing the formation of the system nodal admittance matrix for the main solution.

OpenDSS models non-linear behavior by current source injections, also referred to as "compensation" currents (see Figure A.2). In this manner, the lineal current produced by the primitive admittance matrix is compensated by an external current source; the correct current value will be obtained through an iterative process.

The default solution algorithm is shown in Figure A.3 [A.2]. This algorithm requires that an equation be formed by populating the current vector with compensation currents from *power conversion* elements (e.g. loads, generators, etc.). The compensation current is the difference between the current drawn by the nonlinear power conversion element and the portion of the element that is embedded in the system Y matrix. The following conditions must be ensured:

1. The initial guess at the voltages must be close to the final solution.
2. The series impedance of the power delivery elements must be less than the equivalent shunt impedance of load devices.

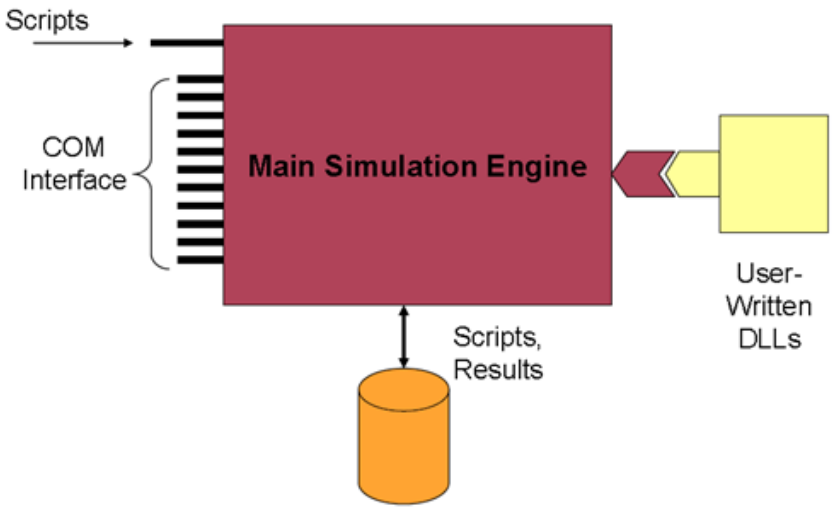

Figure A.1. OpenDSS structure [A.1].

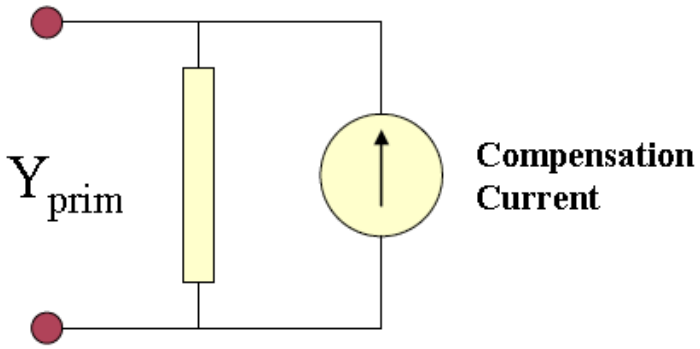

Figure A.2. OpenDSS element model [A.1].

The initial guess is obtained by performing a non-iterative solution of the system without including compensation currents, except for voltage and current sources. The subsequent solutions are calculated using the iteration loop; the process finishes when voltage values meet the specified tolerance. For time-driven power flow solutions, one should not expect big changes in voltage values between consecutive solutions; therefore, the previous solutions are used as the initial guess for the new simulation step, which helps to speed up the solution process.

A.2.2. Element Models

A great number of element models are available in OpenDSS; among those models the user can find power conversion elements, power delivery elements, protection devices, and control models. All element objects are initialized with a default set of parameter values; when a new instance of an element is created, the default values are overwritten by those specified in the new instance definition. Due to the default parameter initialization, it is not necessary to define all parameter values for a new element, only those that are necessary. Some of the most important elements and their main parameters are summarized in this Section [A.1].

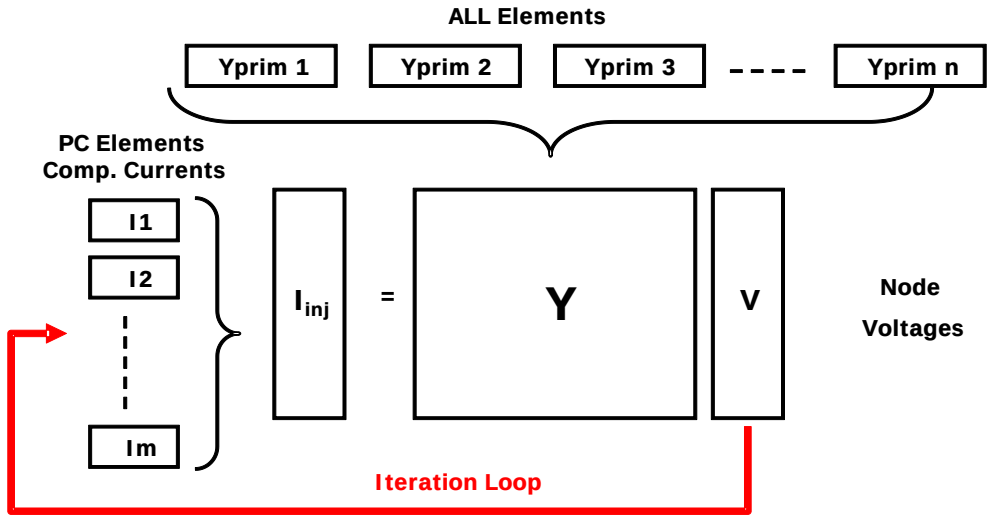

Figure A.3. Default solution loop [A.2].

Load

A Load is a power conversion element that represents the power consumption of distribution system customers. It is defined by its nominal kW and PF or its kW and kvar. Nominal power values may be modified by a number of multipliers, including the global circuit load multiplier, yearly load shape, daily load shape, and a dutycycle load shape. Loads are assumed balanced for the number of phases specified. For unbalanced loads, it is necessary to define separate single-phase loads. The main parameters are presented in Table A.1.

Property	Description
bus1	Bus to which the load is connected (it may include node specification)
conn	Connection type (Wye or Delta)
kv	Nominal rated (1.0 per unit) voltage for load
kw	Total base kW for the load
pf	Load power factor (use negative value for leading power factor)
model	Integer code for the model to use for load variation with voltage
phases	Number of phases
yearly	Loadshape object to use for yearly simulations

Table A.1. Load object properties.

Generator

A Generator is a power conversion element similar to a Load object. Its rating is defined by its nominal kW and PF or its kW and kvar. Rated power values may be modified by a number of multipliers, including the global circuit load multiplier, yearly load shape, daily load shape, and a dutycycle load shape. For power flow studies, the generator is usually modeled as a negative load that can be dispatched. The main parameters are presented in Table A.2.

Property	Description
bus1	Bus to which the load is connected (it may include node specification)
conn	Connection type (Wye or Delta)
kv	Nominal rated (1.0 per unit) voltage for load
kw	Total base kW for the load
pf	Load power factor (use negative value for leading power factor)
model	Integer code for the model to use for load variation with voltage
phases	Number of phases
yearly	Loadshape object to use for yearly simulations

Table A.2. Generator object properties.

Line

The Line element is used to model most multi-phase, two-port lines or cables; it is a power delivery element described by its impedance using a Pi-model with shunt capacitance. Impedances may be specified by symmetrical component values or by matrix values. Alternatively, the user may refer to an existing LineCode object from which the impedance values will be copied. Furthermore, line impedances can be computed from an existing Geometry object. The main parameters are presented in Table A.3.

Property	Description
bus1	Name of bus to which first terminal is connected
bus2	Name of bus to which 2nd terminal is connected
length	Length of line
phases	Number of phases
linecode	Name of linecode object describing line impedances
geometry	Geometry code for LineGeometry Object (use instead of linecode)

Table A.3. Line object properties.

Transformer

The Transformer is implemented as a multi-terminal power delivery element; it consists of two or more windings, each defined by one of the available connections (Wye or Delta). Transformers have one or more phases; the number of conductors per terminal is always one more than the number of phases. For wye-connected windings, the extra conductor is the neutral point. For delta-connected windings, the extra terminal is open internally. The main parameters are presented in Table A.4.

Property	Description
buses	Specifies all bus connections at once using an array
conns	Specifies all Winding connections at once using an array
kVs	Specifies all kV ratings of all windings at once using an array
kVAs	Specifies all kVA ratings of all windings at once using an array
phases	Number of phases
windings	Number of windings
Xhl	Percent reactance, H-L (winding 1 to winding 2)
%Rs	Specifies all winding %resistances using an array

Table A.4. Transformer object properties.

Capacitor

The capacitor model is implemented as a two-terminal power delivery element. However, if a connection for the second bus is not specified, it will default to the ground reference of the same bus to which the first terminal is connected. That is, it defaults to a grounded wye shunt capacitor bank. If the connection is specified to be Delta, then the second terminal is eliminated. The main parameters are presented in Table A.5.

Property	Description
bus1	Bus to which the capacitor is connected
conn	Connection type (Wye or Delta)
kV	Nominal rated (1.0 per unit) voltage
kvar	Total kvar
phases	Number of phases

Table A.5. Capacitor object properties.

PVSystem

PVSystem is a power conversion element that aims to replicate the behavior of a photovoltaic generator. The model output will depend on the solar irradiance, panel temperature, and panel and inverter efficiency. Nominal irradiance and panel temperature values may be may be modified by a number of multipliers, including the yearly load shape, daily load shape, and a dutycycle load shape. The main parameters are presented in Table A.6.

Property	Description
bus1	Bus to which the PVSystem element is connected (it may include node specification)
conn	Connection type (Wye or Delta)
irradiance	present irradiance value in [kW/m^2] (used as base value for shape multiplier)
kV	Nominal rated (1.0 per unit) voltage for PVSystem element
kVA	kVA rating of inverter
Pmpp	rated maximum power of the PV array in [kW]
pf	power factor for the output power
yearly	Dispatch shape to use for yearly simulations
Tyearly	Temperature shape to use for yearly simulations

Table A.6. PVSystem object properties.

Vsource

A Vsource object is a two-terminal, multi-phase Thevenin equivalent. The data are specified as it would commonly be for a power system source equivalent: Line-line voltage (kV) and short circuit MVA. Voltage sources are used to initialize the power flow solution with all other injection sources set to zero. The main parameters are presented in Table A.7.

Property	Description
angle	Phase angle in degrees of first phase
basekv	Base Source kV (usually phase-phase)
bus1	Name of bus to which the main terminal is connected
frequency	Source frequency
phases	Number of phases
pu	Actual per unit operating voltage
MVAsc1	MVA Short Circuit for one-phase fault
MVAsc3	MVA Short circuit for three-phase fault

Table A.7. Vsource object properties.

Fuse

The Fuse object is a protective device that is connected to one terminal of a circuit element. All circuit elements have switches on each of its terminals, the Fuse object controls the terminal switches according to the current flowing through the monitored element. The monitored and switched circuit element must be explicitly defined, even if they refer to the same circuit element. The main parameters are presented in Table A.8.

Property	Description
FuseCurve	Name of the TCC Curve object that determines the fuse blowing
RatedCurrent	Multiplier or actual phase amps for the phase TCC curve
MonitoredObj	Full object name of the circuit element to which the Fuse is connected
MonitoredTerm	Number of the terminal of the circuit element to which the Fuse is connected
SwitchedObj	Name of circuit element switch that the Fuse controls
SwitchedTerm	Number of the terminal of the controlled element in which the switch is controlled by the Fuse

Table A.8. Fuse object properties.

Relay

The Relay object (like the Fuse object) is a protective device that is connected to one terminal of a circuit element; it can monitor currents and voltages at the terminal to which it is connected. The Relay object can use the current and voltage values to operate the terminal switches of the switched circuit element; it also has the capability to perform reclosing actions. As in the Fuse object, the monitored and switched element must be defined explicitly; moreover, for reclosing actions, the total number of opening actions and reclosing intervals must be specified. The main parameters are presented in Table A.9.

Recloser

The Recloser object is a protection device similar to the Relay and Fuse object. It controls the terminal switches of the switched element according to the current flowing through the monitored element. The Recloser object also has the capability to perform reclosing actions; furthermore, two different time-current curves can be defined (one

fast and one slow/delayed); these can be used to implement a fuse-saving scheme. The main parameters are presented in Table A.10.

Loadshape

A LoadShape object consists of a series of multipliers (typically ranging from 0.0 to 1.0) that are applied to the base kW values of the load to represent variation of the load over some time period. Load shapes are generally fixed interval, but may also be variable interval. For the latter, both the time and the multiplier must be specified. The main parameters are presented in Table A.11.

Property	Description
kvbase	Voltage base (kV) for the relay
MonitoredObj	Full object name of the circuit element to which the relay's PT and/or CT are connected
MonitoredTerm	Number of the terminal of the circuit element to which the Relay is connected
Phasecurve	Name of the TCC Curve object that determines the phase trip
PhaseTrip	Multiplier or actual phase amps for the phase TCC curve
RecloseIntervals	Array of reclose intervals
Shots	Number of shots to lockout
SwitchedObj	Name of circuit element switch that the Relay controls
SwitchedTerm	Number of the terminal of the controlled element in which the switch is controlled by the Relay
Type	Relay type
Overvoltcurve	TCC Curve object to use for overvoltage relay
Undervoltcurve	TCC Curve object to use for undervoltage relay

Table A.9. Relay object properties.

Property	Description
Numfast	Number of Fast (fuse saving) operations
MonitoredObj	Full object name of the circuit element to which the Recloser's PT and/or CT are connected
MonitoredTerm	Number of the terminal of the circuit element to which the Recloser is connected
SwitchedObj	Name of circuit element switch that the Recloser controls
SwitchedTerm	Number of the terminal of the controlled element in which the switch is controlled by the Recloser
PhaseTrip	Multiplier or actual phase amps for the phase TCC curve
RecloseIntervals	Array of reclose intervals
Shots	Total Number of fast and delayed shots to lockout
PhaseFast	Name of the TCC Curve object that determines the Phase Fast trip
PhaseDelayed	Name of the TCC Curve object that determines the Phase Delayed trip

Table A.10. Recloser object properties.

Property	Description
mult	Array of multiplier values for active power (P) or other key
mpts	Max number of points to expect in load shape vectors
interval	Time interval for fixed interval data
hour	Array of hourly values
UseActual	If true, signifies to circuit element objects to use the return value as the actual kW, kvar, kV, or other value rather than a multiplier

Table A.11. Loadshape object properties.

A.3. OpenDSS as Stand-Alone Executable

The stand-alone version of OpenDSS is accessed through the *OpenDSS.exe* file. This file will call the program's user interface (see Figure A.4). Different commands and scripts can be forwarded to the program using this interface; it also provides access to a *Help* section, which contains quick references to DSS commands and element properties.

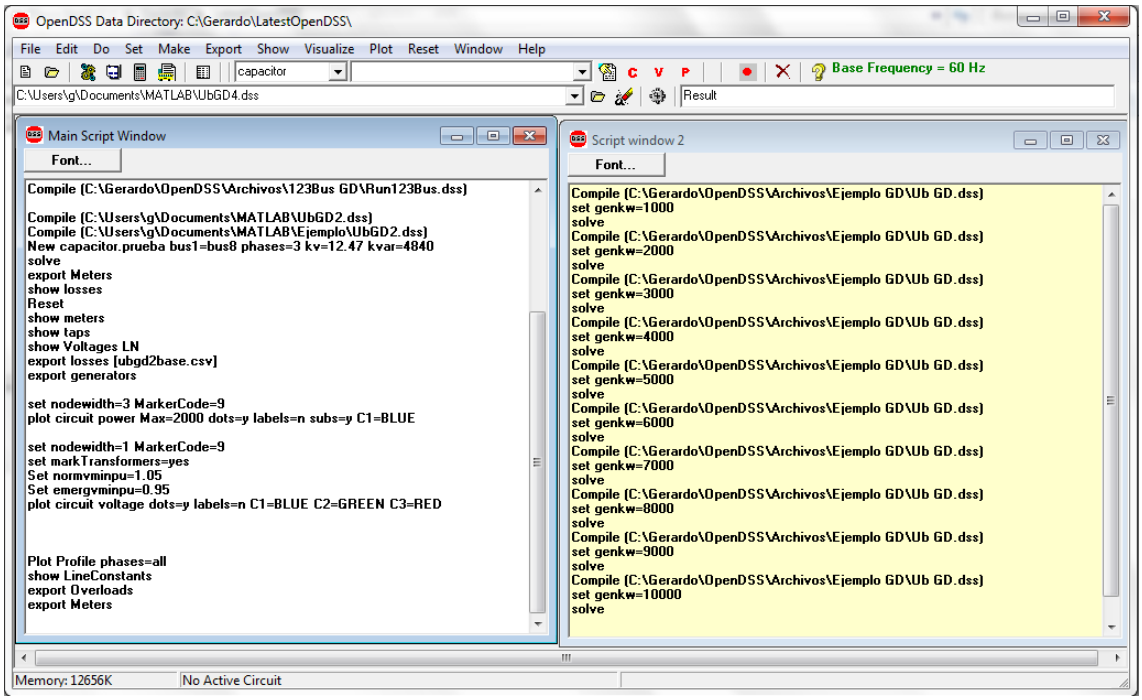

Figure A.4. OpenDSS user interface.

A.3.1. Quick Command Reference

This section introduces some of the most important commands used in OpenDSS, and provides a short explanation about each one [A.1].

Compile

The *Compile* command redirects the command interpreter to take input directly from a text file rather than from the Command property of the COM Text interface (the default

method of communicating with the DSS) or the text form of the EXE version. The *Compile* command resets the current directory to that of the file being compiled. In DSS convention, use Compile when defining a new circuit.

Redirect

Redirects the OpenDSS input stream to the designated file that is expected to contain DSS commands. It processes them as if they were entered directly into the command line. Similar to *Compile* but it leaves current directory where it was when *Redirect* command was invoked. It will temporarily change to subdirectories if there are nested *Redirect* commands that change to other folders.

Clear

The *Clear* command deletes all circuit element definitions from the DSS. This statement is recommended at the beginning of all Master files for defining DSS circuits.

New

Adds an element described on the remainder of the line to the active circuit. The first parameter (*Object=…*) is required for the *New* command. "*Object=*" may be omitted and often is for aesthetics. The remainder of the command line is processed by the editing function of the specified element type.

Edit

Edits the object specified. The object Class and Name fields are required and must designate a valid object (previously instantiated by a *New* command) in the problem. The edit string is passed on to the object named to process. The DSS main program does not attempt to interpret property values for circuit element classes.

More

The *More* command continues editing the active object last selected by a *New*, *Edit*, or *Select* command. It simply passes the edit string to the object's editing function. The *More* command may be abbreviated with simply *M* or *~*.

Disable

Disables object in active circuit. All objects are enabled when first defined. Use this command to temporarily remove an object from the active circuit.

Enable

It cancels a previous *Disable* command. All objects are automatically enabled when first defined. Therefore, the use of this command is unnecessary until an object has been first disabled.

CalcVoltageBases

Estimates the voltage base for each bus based on the array of voltage bases defined with a "*Set Voltagebases=...*" command. When used, it performs a zero-current power flow considering only the series power-delivery elements of the system. The voltage base for each bus is then set to the nearest voltage base specified in the voltage base array.

Set

The *Set* command sets various global variables and options related to solution modes, user interface issues, etc.

Solve

It executes the solution mode specified by the "*Set Mode =…*" command. It may execute a single solution or hundreds of solutions. The Solution is a DSS object associated with the active circuit. It has several properties the user may set to define which solution mode will be performed next. This command invokes the Solve method of the Solution object, which proceeds to execute the designated mode.

CloseDI

Close all Demand Interval (DI) files. This must be issued at the end of the final yearly solution in a Yearly or Daily mode run where DI files are left open while changes are made to the circuit. DI files remain open once the yearly simulation begins to allow for changes and interactions from outside programs during the simulation. They must be closed before viewing the results; otherwise computer system I/O errors may result.

Show

The *Show* command writes a text file report of the specified quantity for the most recent solution and opens the default Editor (e.g. Notepad) to display the file.

Export

The *Export* command writes a text file (.CSV) of the specified quantity for the most recent solution. The purpose of this command is to produce a file that is readily readable by other programs such as MATLAB, spreadsheet programs, or database programs.

Plot

Plot is a rather complex command that displays a variety of results in a variety of graphical manners. Most of the information generated during the solution can be graphically presented using this command.

Buscoords

Define physical coordinates for buses (x,y). Execute after *Solve* or *MakeBusList* command is executed so that bus lists are defined.

Dump

Writes a text file showing all the properties of the circuit object and displays it with the DSS text editor. One would use this command to check the definition of elements. It is also printed in a format that would allow it to be fed back into the DSS with minor editing. If the *Dump* command is used without an object reference, all elements in the active circuit are dumped to a file.

A.3.2. System Simulation using the Stand-Alone Executable

An example case is included to illustrate the application of the stand-alone executable version of OpenDSS to the simulation of power distribution systems. Figure A.5 shows the test system diagram; it is a radial feeder serving five loads distributed along the feeder.

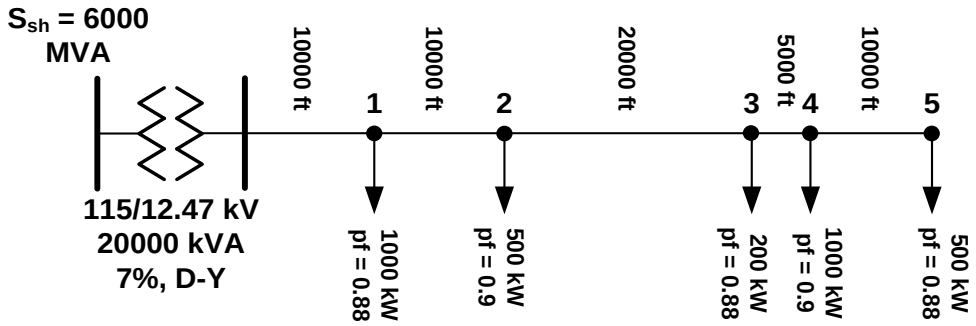

Figure A.5. Test system diagram.

The command lines shown in Figure A.6 were used to define the test system in OpenDSS. They can be directly written into the user interface or saved as a file with *.dss* extension; the present code has been saved as a file under the name *master.dss*.

List.dss file contains information regarding the physical location of system buses; this information is needed as input for some of the graphical tools. The file content is presented in Figure A.7.

```
Clear
new object=circuit.DSSLLibtestckt
~ BasekV=115 pu=1.01 ISC3=30000 ISC1=25000

! Line parameters
new linecode.336matrix nphases=3
more rmatrix=(0.08684 |  0.02983 0.08879 | 0.02888 0.02983  0.08684)
more xmatrix=(0.20254 |  0.08472 0.19614 | 0.07191 0.08472  0.20254)
more cmatrix=(2.74 | -0.70 2.96| -0.34 -0.71 2.74)
more Normamps = 400  Emergamps=600

! Transformer
new transformer.sub phases=3 windings=2 buses=(SourceBus subbus)
more conns='delta wye' kvs="115 12.47 " kvas="20000 20000" XHL=7
more NumTaps=21 MaxTap=1.15 MinTap=0.85 tap=1

! Lines
new line.line1 subbus   loadbus1 linecode=336matrix length=10
new line.line2 loadbus1 loadbus2 336matrix 10
new line.line3 Loadbus2 loadbus3 336matrix 20
new line.line4 Loadbus3 loadbus4 336matrix 5
new line.line5 Loadbus4 loadbus5 336matrix 10

! Loads
new load.load1 bus1=loadbus1 phases=3 kv=12.47 kw=1000.0
more pf=0.88 model=1 class=1 conn=delta
new load.load2 bus1=loadbus2 phases=3 kv=12.47 kw=500.0
more pf=0.90 model=1 class=1 conn=delta
new load.load3 bus1=loadbus3 phases=3 kv=12.47 kw=200.0 pf=0.88
more model=1 class=1 conn=delta
new load.load4 bus1=loadbus4 phases=3 kv=12.47 kw=1000.0
more pf=0.90 model=1 class=1 conn=delta
new load.load5 bus1=loadbus5 phases=3 kv=12.47 kw=500.0
more pf=0.88 model=1 class=1 conn=delta

! Meters
New EnergyMeter.Feeder Line.line1 1

! Define voltage bases so voltage reports come out in per unit
Set voltagebases="115 12.47 .48"
CalcVoltageBases

! Bus coordinates
Buscoords  List.dss
```

Figure A.6. *Master.dss* file.

After the system has been completely defined, OpenDSS can be used to carry out different types of studies. The command lines in Figure A.8 can be used to run a simple snapshot power flow using the previously defined test system.

```
! Bus coordinates
SourceBus, 900, 1000
Subbus, 1000, 1000
LoadBus1, 11000, 1000
LoadBus2, 21000, 1000
LoadBus3, 41000, 1000
LoadBus4, 46000, 1000
LoadBus5, 56000, 1000
```

Figure A.7. `List.dss` file.

```
Compile master.dss
set mode=snapshot
solve
```

Figure A.8. Circuit solution commands.

Once these lines have been typed into the user interface, select the option *Do* after right-clicking over the highlighted text (see Figure A.9). After the system has been solved, it will be possible to generate different files and plots with information produced by the solution.

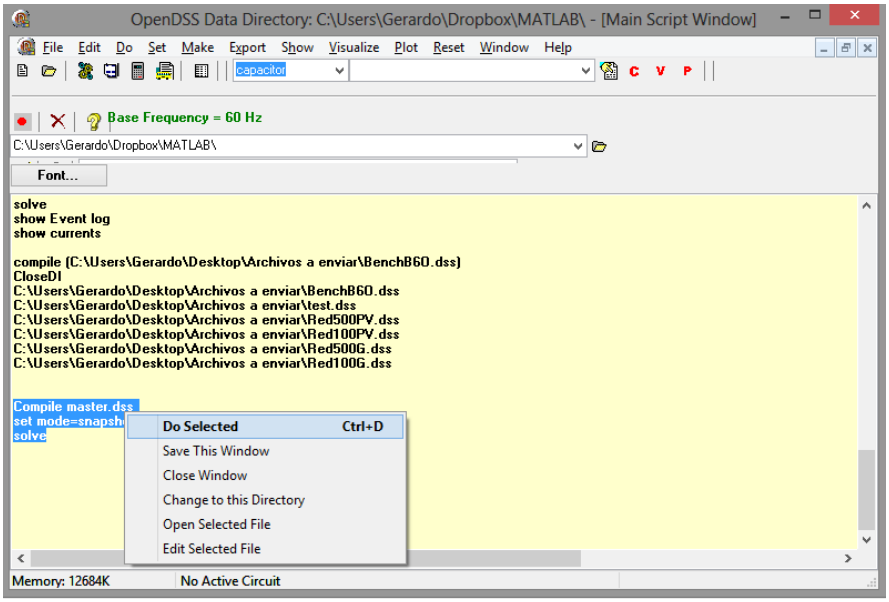

Figure A.9. Run script on user interface.

The *Show* commands in Figure A.10 generate report files containing information related to system losses and power flowing through each system element. The generated files are shown in Figure A.11 and Figure A.12.

```
Show Losses
Show Powers
Plot circuit power Max=1000 dots=y labels=n subs=y C1=BLUE
```

Figure A.10. *Show* and *Plot* examples.

OpenDSS has the capability to generate plots based on the circuit's diagram; different parameters can be displayed using this option. The *Plot* command in Figure A.10 is

used to generate a plot using the test system diagram where line thickness is proportional to the power flowing through each line section. Figure A.13 shows the generated plot.

```
LOSSES REPORT

Power Delivery Element Loss Report

Element                   kW Losses    % of Power   kvar Losses

"Transformer.SUB"       2.71962,      0.08      47.6101
"Line.LINE1"           50.71225,      1.57      102.937
"Line.LINE2"           23.78442,      1.10      47.3182
"Line.LINE3"           28.30848,      1.72      54.9655
"Line.LINE4"            5.48430,      0.38      10.4784
"Line.LINE5"            1.24790,      0.26      0.876467

LINE LOSSES=                         109.5 kW
TRANSFORMER LOSSES=                    2.7 kW

TOTAL LOSSES=                        112.3 kW

TOTAL LOAD POWER =                  3111.1 kW
Percent Losses for Circuit =       3.61 %
```

Figure A.11. `Show Losses` report file.

```
SYMMETRICAL COMPONENT POWERS BY CIRCUIT ELEMENT (first 3 phases)

Element               Term    P1(kW)   Q1(kvar)

"Vsource.SOURCE"       1    -3223.1    -1863.0
"Vsource.SOURCE"       2        0.0        0.0
"Transformer.SUB"      1     3223.1     1863.0
"Transformer.SUB"      2    -3220.4    -1815.4
"Line.LINE1"           1     3220.4     1815.4
"Line.LINE1"           2    -3169.7    -1712.4
"Line.LINE2"           1     2169.8     1172.7
"Line.LINE2"           2    -2146.0    -1125.4
"Line.LINE3"           1     1646.1      883.3
"Line.LINE3"           2    -1617.8     -828.3
"Line.LINE4"           1     1425.5      724.5
"Line.LINE4"           2    -1420.0     -714.1
"Line.LINE5"           1      471.3      254.6
"Line.LINE5"           2     -470.0     -253.7
"Load.LOAD1"           1     1000.0      539.7
"Load.LOAD2"           1      500.0      242.1
"Load.LOAD3"           1      192.3      103.8
"Load.LOAD4"           1      948.8      459.5
"Load.LOAD5"           1      470.0      253.7

Total Circuit Losses =  112.3 +j  264.2
```

Figure A.12. `Show Powers` report file.

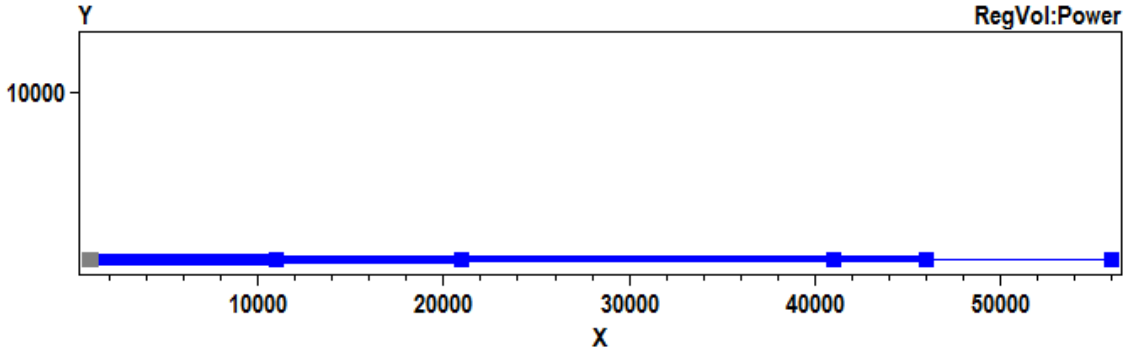

Figure A.13. Output *Plot Circuit Power*.

A.4. OpenDSS – MATLAB Link

OpenDSS can be linked to MATLAB using the COM interface implemented on the in-process server DLL. OpenDSS installation files install both the stand-alone and COM server DLL versions [A.3]; the COM server DLL version is automatically registered in the Windows environment and no other action is needed. MATLAB uses the integrated ActiveX server in order to communicate with the COM server DLL (see Figure A.14). Communication is established using a function created in MATLAB's workspace. The function is defined in Figure A.15.

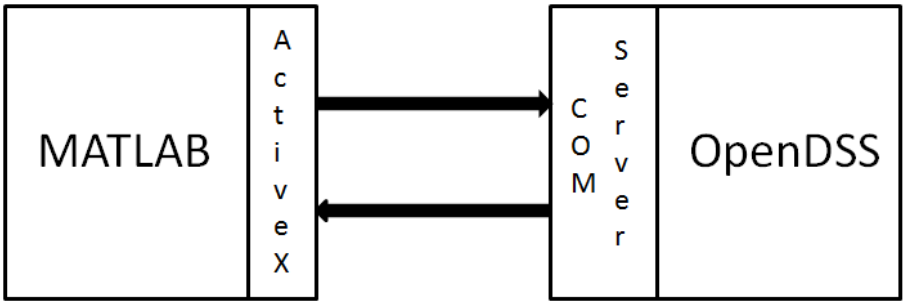

Figure A.14. MATLAB - OpenDSS communication.

```
function [Start,Obj,Text] = DSSStartup()
Obj = actxserver('OpenDSSEngine.DSS');
Start = Obj.Start(0);
Text = Obj.Text;
```

Figure A.15. `DSSStartup` function.

After the communication has been established, the user is able to send instructions to OpenDSS using the text object "`DSS.TextCommand=`". This instruction is equivalent to executing scripts on the user interface. The command lines in Figure A.16 can be used to solve the example case presented in the previous section:

```
DSSStartOK, DSSObj, DSSText] = DSSStartup();
DSSText.Command = 'compile master.dss';
DSSCircuit = DSSObj.ActiveCircuit;
DSSText.Command = 'solve';
```

Figure A.16. Circuit solution command from MATLAB.

A.4.1. COM Server DLL Interface

The COM server DLL provides an interface that allows a much greater flexibility than simply forwarding commands to the program engine. Through object interfaces defined in the MATLAB's workspace the user can send instructions to the program, gather information resulting from solving the circuit, and define or edit system elements. For a complete list of interfaces and interface's methods see [A.4].

Circuit Interface

The circuit interface provides access to the active circuit and allows retrieving information after it has been solved. It is defined as:

```
DSSCircuit = DSSObj.ActiveCircuit;
```

The following commands are useful for retrieving system information after an individual solution:

`DSSCircuit.TotalPower`: Total power delivered by main voltage source in kW.
`DSSCircuit.Losses`: Total system losses in W.
`DSSCircuit.AllBusVmagPu`: All bus voltages in p.u.
`DSSCircuit.Sample`: Forces all meters or monitors to sample.
`DSSCircuit.SystemY`: Retrieves system admittance matrix.

Solution Interface

The solution interface allows defining or modifying parameters related to the circuit solution mode, it can also be used to execute the solution. The interface is defined as follows:

```
DSSSolution=DSSCircuit.Solution;
```

Some of the methods available for the solution interface are:

`DSSSolution.Solve`: Forces the circuit solution.
`DSSSolution.Year`: Sets/gets the year of the solution.
`DSSSolution.dblHour`: Sets/gets the hour of the solution.
`DSSSolution.Converged`: Retrieves whether solution converged or not.
`DSSSolution.Tolerance`: Sets/gets tolerance for voltage values.
`DSSSolution.Number`: Sets/gets number of consecutive solutions.
`DSSSolution.Iterations`: Number of iterations performed for the solution.
`DSSSolution.StepSize`: Sets/gets simulation step size for time-driven power flow.
`DSSSolution.Mode`: Sets/gets simulation mode.

Circuit Element Interface

The circuit element interface helps the user to collect information of a specific element after an individual solution has been performed. It is created in MATLAB's workspace as:

```
DSSElement=DSSCircuit.CktElements;
```

Element information can be accessed as follows:

`DSSElement.Currents`: Element's phase currents in Amps.
`DSSElement.Voltages`: Element's phase voltages in Volts.
`DSSElement.Powers`: Element's phase powers in kW.
`DSSElement.Yprim`: Retrieves element's primitive admittance matrix.

System Elements Interface

The COM server DLL also provides interfaces that allow the user to read or modify parameters of system elements. Some of the available interfaces are:

`DSSCircuit.Loads`: Load interface.
`DSSCircuit.Lines`: Line interface.
`DSSCircuit.Generators`: Generator interface.
`DSSCircuit.Transformers`: Transformer interface.
`DSSCircuit.Meters`: Energy meter interface.
`DSSCircuit.PVSystems`: PV system interface.

A.4.2. System Simulation using the COM Server DLL

A case study has been developed to illustrate how the COM interface can be used to solve a circuit and collect information. The test system will be simulated for a one-year period using the time-driven power flow, all loadshapes are predefined. Figure A.17 shows the test system diagram (more information can be found in Chapter 3).

The MATLAB script presented in Figure A.18 has been implemented to collect information during each simulation step. The code will monitor the power served by the HV system, total system losses, and minimum system voltage in p.u.; additionally it will monitor the power consumed and phase-A voltage of load SA701 (connected to node a701).

The information collected with the MATLAB script has been used to generate different plots that demonstrate the system behavior during the solution. Figure A.19 presents system related information and Figure A.20 shows the information gathered from load SA701. The presented code is rather simple but many other features can be added and if written in an open manner, it can be used to study other systems.

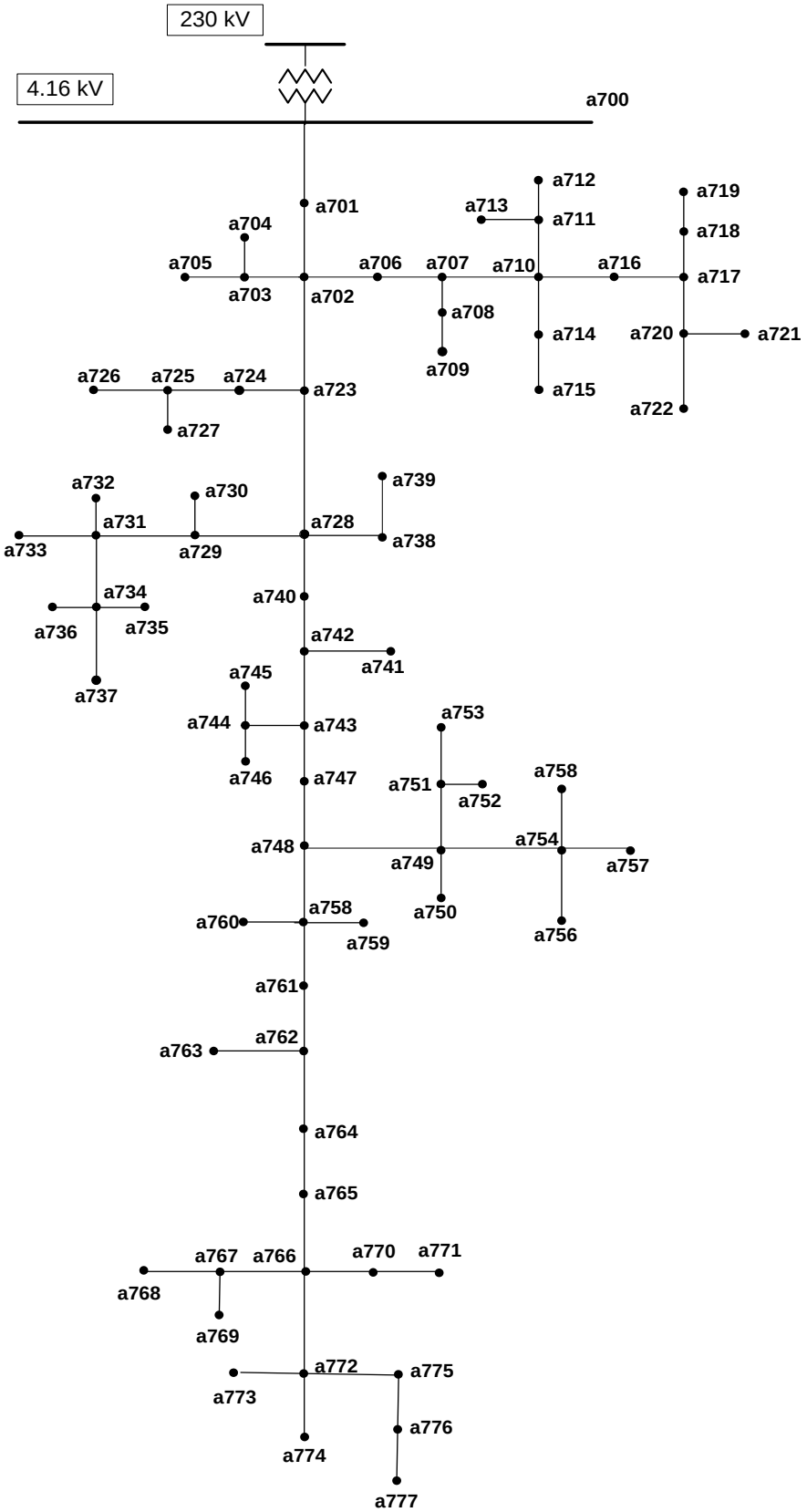

Figure A.17. Test system diagram.

```
DSSStartOK, DSSObj, DSSText] = DSSStartup();
DSSText.Command='Compile Curvessys.dss';
%Circuit Interface
DSSCircuit=DSSObj.ActiveCircuit;
%Solution interface
DSSSolution=DSSCircuit.Solution;
%Loads interface
DSSLoads=DSSCircuit.Loads;
%set solution mode
DSSText.Command='set mode=time LoadshapeClass=yearly';
%set solution step size
DSSSolution.StepSize=3600;
%set number of consecutive solutions
DSSSolution.Number=1;
%set solution tolerance
DSSSolution.Tolerance=1e-4;
%Number of yearly hours
H=8760;
%HV system power
System_power=zeros(H,1);
%System losses
System_losses=zeros(H,1);
%Minimum voltage in p.u.
Minimum_pu=zeros(H,1);
%Load consumed real power
Load_power=zeros(H,1);
%Phase "A" voltage
Load_voltage=zeros(H,1);
for n=1:H
    %Set solution hour
    DSSSolution.dblHour=n;
    %Solve circuit
    DSSSolution.Solve
    %Collect HV system power
    System_power(n)=-DSSCircuit.TotalPower(1);
    %Collect system losses
    System_losses(n)=DSSCircuit.Losses(1)/1000;
    %Collect minimum voltage
    Minimum_pu(n)=min(DSSCircuit.AllBusVmagPu);
    %Circuit element interface
    MyEl=DSSCircuit.CktElements('Load.SA701');
    %Collect load power and phase-A voltage
    Load_power(n)=sum(MyEl.Powers([1 3 4]));
    %Collect load phase-A voltage
    Load_voltage(n)=MyEl.VoltagesMagAng(1);
end
```

Figure A.18. Yearly solution MATLAB script.

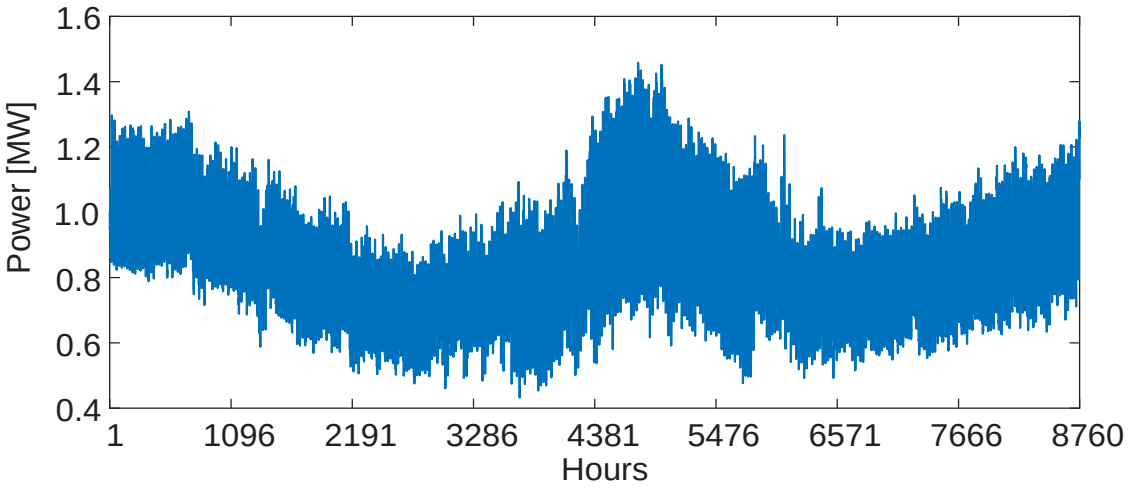

a) HV System energy

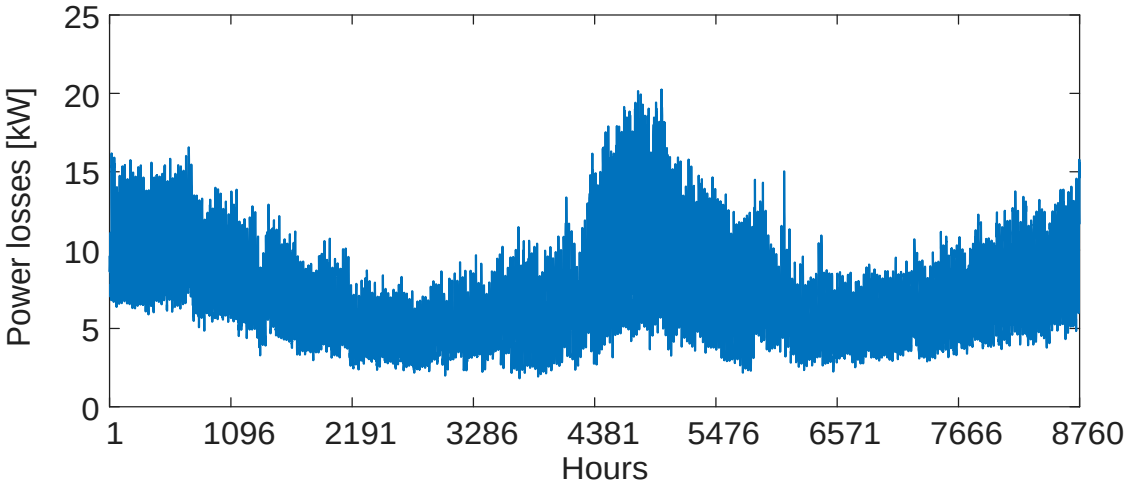

b) System losses

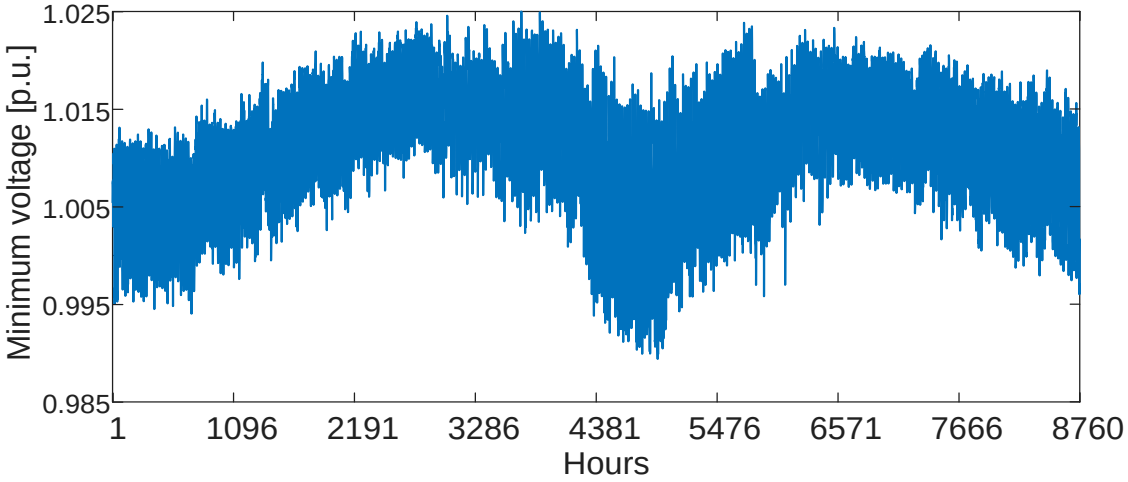

c) Minimum system voltage

Figure A.19. System information plots.

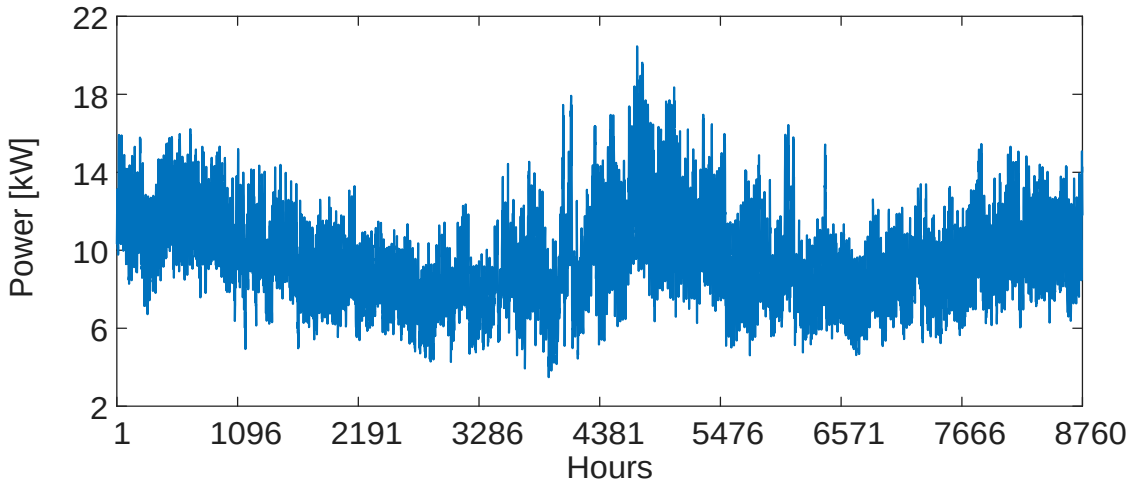

a) Load consumed power

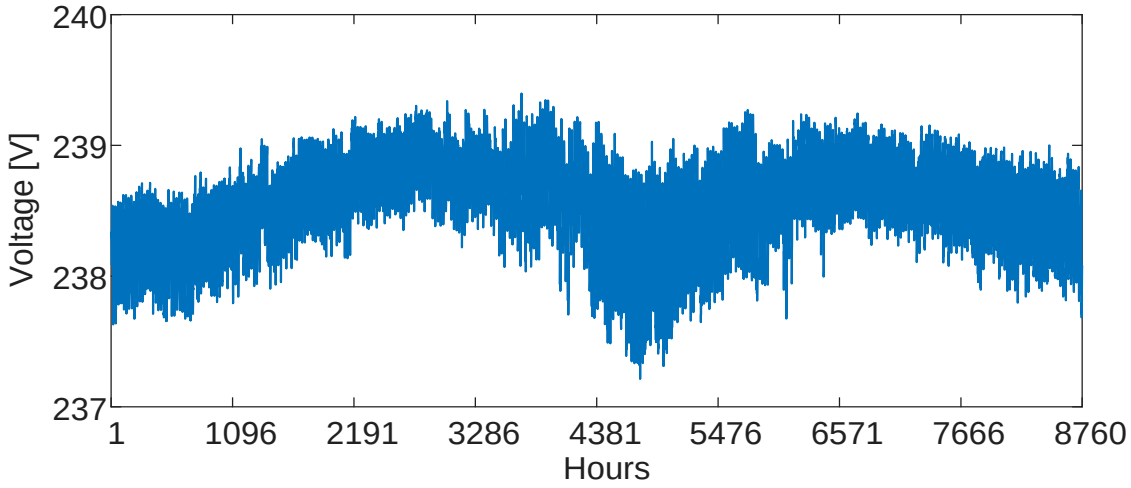

b) Load phase-A voltage

Figure A.20. Load SA701 information plots.

A.5. References

[A.1] Open DSS Reference Guide, Electric Power Research Institute, June 2013.

[A.2] R. Dugan, T.E. McDermott, "An Open Source Platform for Collaborating on Smart Grid Research," IEEE PES General Meeting, Detroit, USA, July 2011.

[A.3] OpenDSS Software, Electric Power Research Institute (EPRI), 2008. Available at http://sourceforge.net/projects/electricdss/

[A.4] URL: http://sourceforge.net/p/electricdss/code/904/tree/trunk/Source/DLL/